Influence of Preparation Techniques on the Fischer-Tropsch Performance of Supported Cobalt Catalysts

Presented by:
Ada Elida Chirinos Maruri
(Chemistry, UNSAAC-Peru)

Submitted to the University of Cape Town in fulfilment of the requirements for the degree of Doctor of Philosophy, PhD

Department of Chemical Engineering
University of Cape Town
Rondebosch
Cape Town
South Africa

July 2003

Acknowlegdments

I would like to express my sincere gratitude to my supervisor, Professor M. E. Dry for his invaluable support throughout my research.

I would like to thank Dr. M. Claeys for his help and courtesy. To my co-supervisor J.C.Q. Fletcher and to Professor E. van Steen for his help, which I really appreciate.

To all the "catalysis members" of the University of Cape Town for their help and the nice atmosphere and to the FRD foundation for their financial support during my PhD studies.

To my husband and my parents for their care and never ending support.

Thank you !

Synopsis

Cobalt based catalysts are generally used for the FT synthesis due to their high activity and selectivity for linear hydrocarbons, low activity for the water gas shift reaction and lower price compared to noble metals [22]. There can, however, be a large effective loss of active metal due to strong metal-support interaction forming complexes that are not reduced at temperatures below 400°C.

In the present study, various modified cobalt catalysts were prepared and investigated. The FT performance and the characterisation of such catalysts were compared with a reference catalyst. The aim of this work was to investigate catalysts obtained by different preparation techniques and using different supports. The silica supported catalysts were prepared with different metal loadings, using different support particle sizes, impregnating the metal salt in 1, 2, 3 or 6 steps, or coating the silica support with 1 or 3 theoretical monolayers of MnO or ZnO prior to the cobalt salt impregnation. The alumina supported catalysts were prepared, using different metal salts dissolved in different solvents, using different calcination conditions, employing different drying procedures different impregnation temperatures and modifying the alumina support.

The investigation started with the study of a catalyst tested in the FT reactor several times to demonstrate satisfactory reproducibility.

The deposition of 10, 20 and 30 g of cobalt on the silica support was studied. As expected the catalysts' activities were not only dependent on the amount of cobalt metal loaded in the FT reactor, but they were also dependent on the metal dispersion.

Catalysts with different particle sizes were investigated. The resulting catalysts were ground in order to get different catalyst particle sizes. No marked difference in FT activity was observed. The FT reaction was performed on calcined and uncalcined catalysts. It was found that the dispersion on the calcined catalyst was somewhat higher than the uncalcined one.

Multiple impregnation of the cobalt salt onto the silica support appeared to result in a better dispersion of the cobalt compared to impregnating the support in a single operation. The differences in activity, however, were not marked.

The deposition of Mn and Zn oxides on the SiO_2 support prior the deposition of the metal salt was investigated. The coverage with 1 or 3 theoretical monolayers of these oxides lowered the BET surface areas of the catalysts. The FT activities were markedly decreased presumably by the interaction of the Mn or Zn oxides with the metal salt and with the silica support.

The preparation of alumina supported catalysts with cobalt nitrate, acetate or acetyl acetonate calcined in N_2 showed higher FT activities than those ones calcined in air. Using cobalt acetate produced a catalyst with the highest initial activity but over a long time on stream the catalysts prepared from the nitrate gave a somewhat better FT performance. The acetyl acetonate preparations yielded poor catalysts despite apparent high metal dispersions when calcined in air.

Some alumina supported catalysts were dried by microwaves prior to calcination in N_2. The activity of the one dried by exposure to microwaves gave a higher metal dispersion than the reference catalyst dried by conventional heat. The FT activities of these catalysts, however, were lower than the reference catalyst.

The impregnation of the cobalt salt onto the alumina at approximately 80°C was also studied. The metal dispersions of these catalysts were somewhat higher than that of the reference catalyst but in this case the metal surface areas and the activities did not correlate.

Modification of the alumina support, prior to cobalt impregnation, was also investigated. The catalyst supported on cobalt aluminate was the most active catalyst at any TOS. Silinizing the alumina did not change the catalyst's performance and the KOH impregnated alumina resulted in a catalyst with a very low FT activity.

Overall alumina supported catalysts were more active than silica supported catalysts despite the fact that a large percentage of the cobalt interacted with the alumina to form non-reducible complexes.

Table of contents

List of figures

List of tables

Chapter I

1 Introduction

1.1 The Fischer-Tropsch Synthesis

The Fischer-Tropsch (FT) synthesis is the reaction of carbon monoxide and hydrogen yielding a broad range of hydrocarbons and oxygenated compounds. This reaction readily occurs over Fe, Co, Ni and Ru catalysts at temperatures and pressures typically ranging from about 170 to 350°C and, to about 50 bar respectively.

1.1.1 The Fischer-Tropsch Synthesis History

The Fischer-Tropsch reaction was developed in Germany during the early 1900s. Franz Fischer and Hans Tropsch reported that carbon monoxide and hydrogen react in the presence of iron, nickel and cobalt catalysts to produce gaseous, liquid and solid aliphatic hydrocarbons. Measurable amounts of liquid product were obtained by recycling carbon monoxide over alkalised iron fillings at 400-450°C and 101-152 bar. The product consisted mainly of oxygen containing compounds. However when the operation was carried out at 1bar pressure hydrocarbons appeared in small amounts. However, the further development of iron catalyst was delayed. By 1937, the Fischer-Tropsch process was in commercial operation with cobalt catalysts [1].

Right after the second war world the Fischer-Tropsch research continued especially in the USA where a FT plant was constructed by Carthage Hydrocol in Brownsville, Texas (1950). A fluidised catalyst bed reactor was used to convert syngas produced from methane over a Fe catalyst at 300°C and 20bar. The FT plant closed down due to the low price of petroleum crude oil.

With the discovery of large deposits of crude oil in the Middle East (1950), interest in the FT research waned but nevertheless a few years later (1973) the world experienced a critical oil crisis, which resulted in the resurgence of the interest in the FT process and research.

In 1955 a Sasol plant based on coal came on stream, in Sasolburg, South Africa. This plant named as "Sasol One" operated with both fixed bed multi-tubular FT reactors operating at about 230°C and with circulating fluidised bed (CFB) reactors at 300°C and 20bar. The latter reactors were designed by Kellog in the USA. After some improvements by Sasol the fluidised bed reactors were re-named the "Synthol" reactors. After 25 years of operation, at Sasolburg, Sasol constructed another plant, "Sasol Two" with Synthol reactors with higher capacity and improved heat exchangers. The plant came on stream in 1980 and produces mainly gasoline and diesel fuel [15]. A similar plant, "Sasol Three" was built and came on line in 1982 [10]. By 1999 all the Synthol reactors at Secunda were replaced by fixed fluidised bed (FFB) reactors of higher capacity. The total production capacity of the three plants of Sasol is about 7500x 10^3 tons per annum [16].

During 1992 the "Mossgas" plant came in operation in Mosselbay, South Africa. The plant produces gasoline and diesel fuel. Syngas is produced from natural gas. Multi-tubular and autothermal reformers are employed to reform CH_4. Circulating fluidised bed (CFB) reactors are used to perform the Fischer-Tropsch synthesis over iron based catalyst. The FT products such C_3/C_4-alkenes are oligomerized over zeolites to produce gasoline and diesel fuel. The Mossgas total fuel production is about 1020x10^3 tons per annum [16].

The SMDS (Shell Middle Distillate Synthesis) plant came on line in 1993 in Bintuli, Malaysia. In the Shell gasification process syngas is obtained by non-catalytic partial oxidation of natural gas at 1400°C and high pressures. The plant was implemented with multi-tubular FT reactors operating at 200-230°C and about 30bar. The products obtained are mainly high molecular mass products. The annual production capacity is roughly 500x10^3 tons per year [16].

Presently the Fischer-Tropsch synthesis enjoys great attention as an option for the production of synthetic fuels and for the production of chemicals [2].

1.1.2 The Fischer-Tropsch Reactor Development

Various types of reactors have been designed for the Fischer-Tropsch synthesis; among them are the fixed-bed reactor (FBR), the slurry-bed reactor (SBR) and the fluidised-bed reactor (FBR).

1.1.2.1 Fixed-Bed Reactor (FBR)

In a conventional fixed-bed, the reactor vessel is filled with catalyst particles having sizes in the range of 1-3mm [3]. Gas flows through this bed in the downward direction [3].
The fixed-bed reactors have two advantages; they are simple to operate and there is no problem to separate the catalysts from the wax product [4, 5]. Among the disadvantages are; a high-pressure drop over the reactor, high temperature gradient (compared to other reactors) and tedious replacement of the decayed catalyst [4].
In general, fixed-bed reactors are suited for low temperature Fischer-Tropsch synthesis (200-240°C) and also for the production of high average molecular weight products [2].

In 1935 the first industrial Ruhrchemie "atmospheric" fixed bed reactor was designed and consisted of a box divided into sections by vertical metal plates and horizontal cooling tubes crossing the sheets [2]. The catalyst was loaded between the plates and cooling water flowed through the tubes. The "medium" pressure reactor consisted of double walled tubes and the catalyst was placed in the 2mm annular section. Cooling water surrounded the tubes. Both reactors used cobalt based catalysts [4].

The companies Ruhrchemie and Lurgi developed the ARGE reactors. The first commercial fixed-bed reactors were commissioned at Sasol in 1955 and are still in operation (Figure 1.1.1). Each reactor consists of 2050 vertical tubes of 5cm x 12m. The tubes are filled with iron based catalysts [4]. Heat removal from the highly exothermic synthesis reaction is achieved by generation of steam on the shell side of the reactor [5].

A 5000 tube reactor was designed by Sasol (1987) but was never implemented because of the development of the slurry bed reactor (SBR) [5].

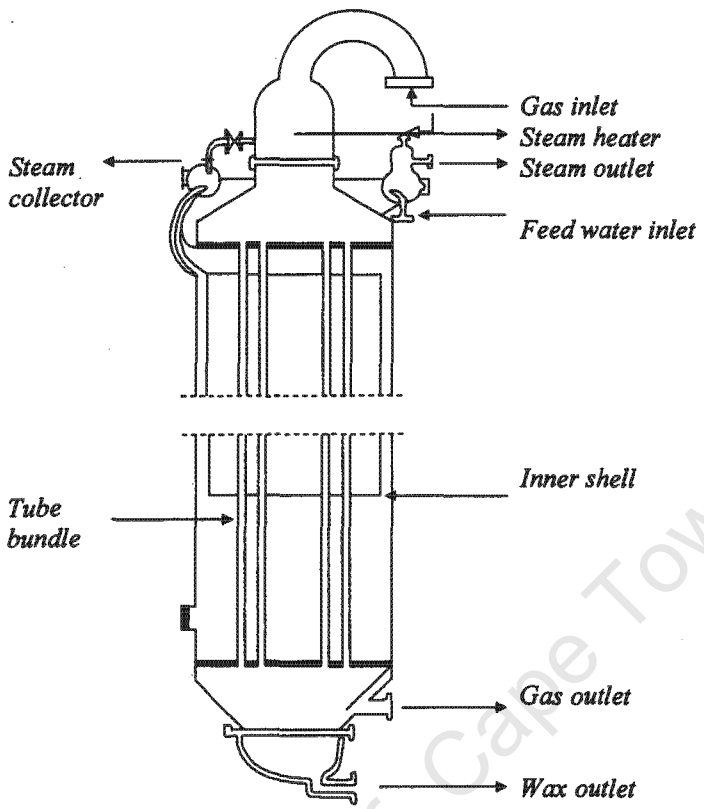

Figure 1.1.1: Tubular fixed bed (ARGE) reactor (FBR)[5].

1.1.2.2 Slurry-Bed Reactor (SBR)

In a slurry-bed reactor, the catalyst is present as finely divided particles, usually in the range of 1-200μm. The gas flow itself provides the agitation power required to keep the catalytic particles in suspension. This type of reactor presents several advantages over the FBR such as; lower catalyst utilization, simple control of temperature, ease of catalyst replacement. There are however, a number of problems associated with handling fine particles like the separation of these fine particles from the wax product, and this was usually troublesome [3] until 1990 when a separating device was tested successfully [4].

Going back to the past. The first Fischer-Tropsch experiment with particles immersed in oil was performed by Fischer and a few years later a pilot plant scale reactor was developed by Köbel at the Reinpreussen Company in 1958 [2, 6].

Presently, the low temperature slurry bed reactor is regarded by many authors as the most efficient process for the Fischer-Tropsch clean diesel fuel production [2].

Sasol developed a slurry reactor (see figure 1.1.2) to convert syngas to liquid fuels and waxes. It consists of a shell fitted with cooling coils in which steam is generated. Hydrogen and carbon monoxide are distributed at the bottom and rise through the slurry. Iron or cobalt catalyst particles are suspended in wax, which is in the liquid phase at reaction conditions. The separation of the catalysts from the product wax is not a major problem since Sasol developed a proprietary solids separation technique [5].

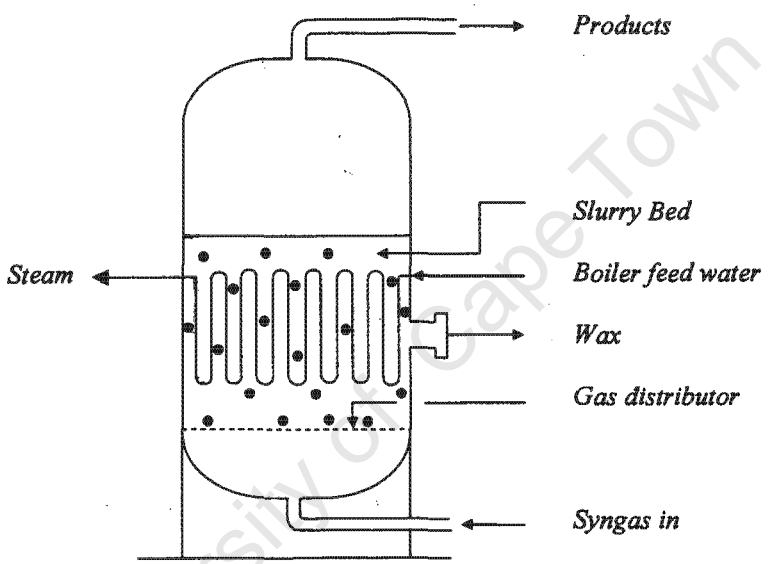

Figure 1.1.2: Slurry bed reactor (SBR) [5].

1.1.2.3 Fluidised-Bed Reactors (FBR)

There are two types of fluidised-bed reactors; the circulating fluidised-bed (CFB) reactor and the fixed fluidised-bed (FFB) reactor (see figures 1.1.3a and 1.1.3b).

In the circulating fluidised-bed the catalysts particles (40-150μm) [6] flows down to the standpipe as a dense phase aerated powder. The catalyst is picked up by the high velocity of the incoming gas stream. The heat of reaction is removed from the reactor by cooling coils generating steam. The catalyst re-enters the hopper with the gas and it is separated by means of cyclones [7]. The gas linear velocities in CFB reactors are three to four times higher than in FFB reactors [16]. The circulating fluidised process was originally developed by Kellogg and further improved by Sasol as the "Synthol" process.

The fixed fluidised bed (FFB) reactor is designed to operate between 20 to 40 bar and it usually operates at 340°C [7]. The reactor consists of a fluidised bed containing the catalyst, which is not transported in the system, a gas distributor, cooling coils in the bed and cyclones to separate the catalyst from the gas product [7]. This reactor shows advantages over CFB reactors, at first it is physically smaller than the CFB reactor, although both reactors have the same production capacity; it is less costly to construct, scale up is easier and it is simple to operate [10].

The main factor, which determines the relative conversion performance of the two types of reactors (CFB and FFB) is the quantity of catalyst, which is loaded into the reactor. In the CFB reactor less than half of the catalyst is in the reaction zone. While in the case of the FFB reactor all the catalyst is in the reaction zone [7].

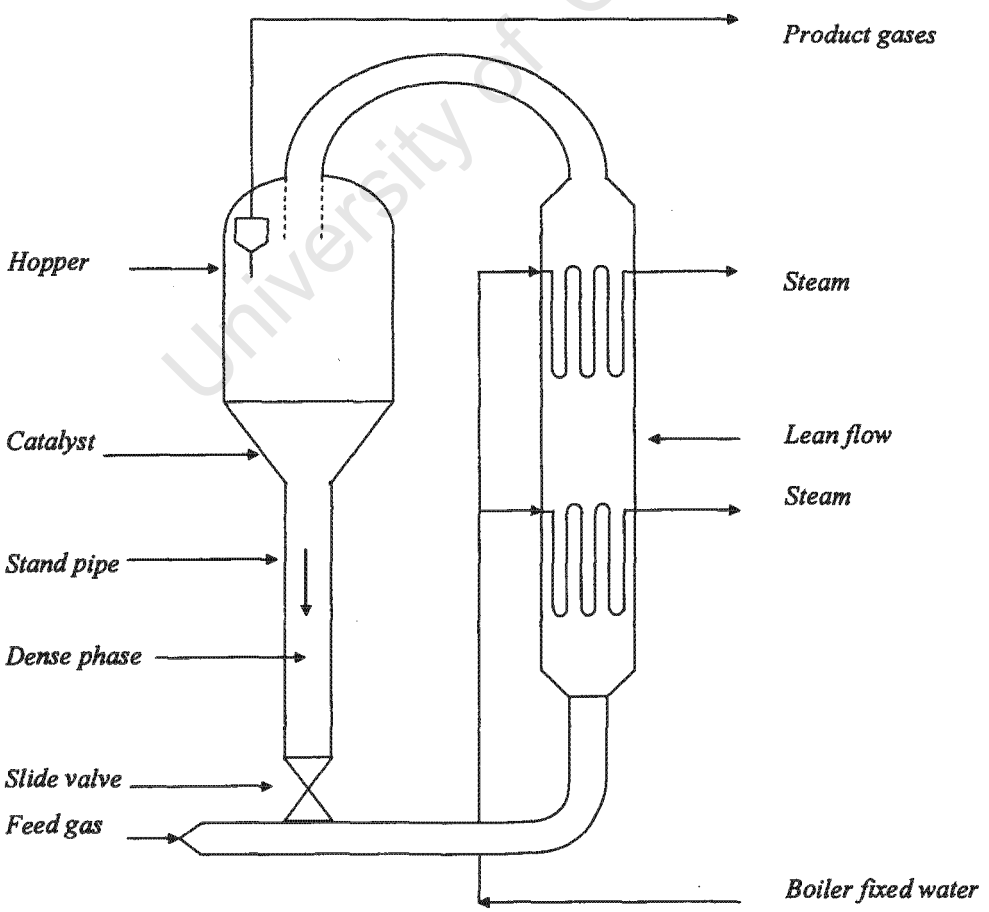

Figure 1.1.3 a: Circulating fluidised bed reactor (CFB) [15].

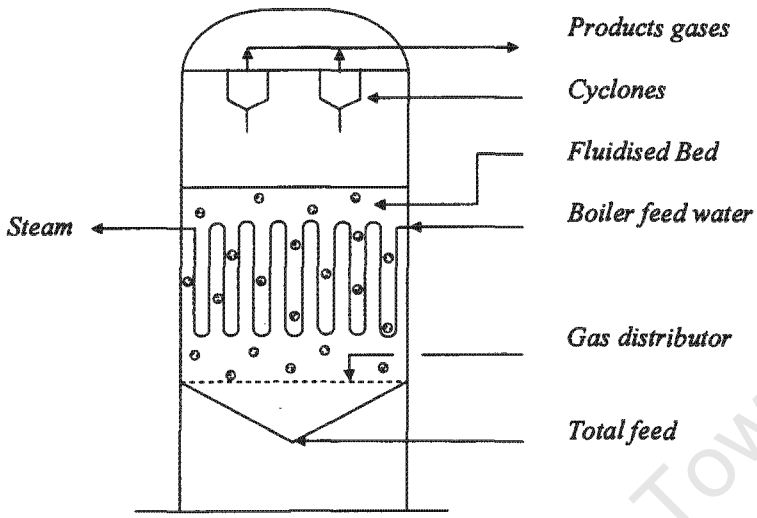

Figure 1.1.3b: Fixed fluidised bed reactor (FFB) [15].

1.1.3 The Fischer-Tropsch Reaction

The Fischer-Tropsch (FT) reaction being the heterogeneously catalysed conversion of syngas (CO and H_2) is an industrial and academic process of interest. During the Fischer-Tropsch synthesis, syngas is passed over a heated, supported or unsupported metal catalyst at atmospheric pressure or higher. The primary products formed are 1-alkenes that undergo isomerisation and/or hydrogenation reactions to yield a mixture of hydrocarbons, predominantly linear alkenes and alkanes. Oxygenated products are also formed [9].

The following equations represent the formation of alkenes (equations 1, 2), alkanes (equations 3, 4) [1] and alcohols (equation 5) [10].

$$2nH_2 + nCO \longrightarrow C_nH_{2n} + nH_2O \quad (1)$$

$$nH_2 + 2nCO \longrightarrow C_nH_{2n} + nCO_2 \quad (2)$$

$$(2n+1)H_2 + nCO \longrightarrow C_nH_{2n+2} + nH_2O \quad (3)$$

$$(n+1)H_2 + 2nCO \longrightarrow C_nH_{2n+2} + nCO_2 \quad (4)$$

$$2nH_2 + nCO \longrightarrow C_nH_{2n+1}OH + (n-1)H_2O \quad (5)$$

Equations 2 and 4 could also be the result of the FT reaction coupled with the water gas shift reaction (WGS), *e.g.*,

$$\begin{array}{lrcrcrcrl} \text{FT}: & 2nH_2 & + & nCO & \longrightarrow & C_nH_{2n} & + & nH_2O & (6) \\ \text{WGS}: & nH_2O & + & nCO & \longrightarrow & nCO_2 & + & nH_2 & (7) \\ \hline & nH_2 & + & 2nCO & \longrightarrow & C_nH_{2n} & + & nCO_2 & (2, 4) \end{array}$$

The reactions above are exothermic. The heat released by these reactions is of high magnitude and its removal is of great interest [1]. The heat released per unit weight corresponds to a theoretical adiabatic temperature rise of about 1600K at complete conversion [6].

The primary products are formed during a single sojourn of a reactive intermediate on a FT synthesis site. The secondary products are formed via hydrogenation, oligomerization, cracking and carbonylation of olefins, and the hydrogenolisis of linear paraffins. The following (figure 1.1.4) explains the formation of primary and secondary products by desorption from a chain growth site [12].

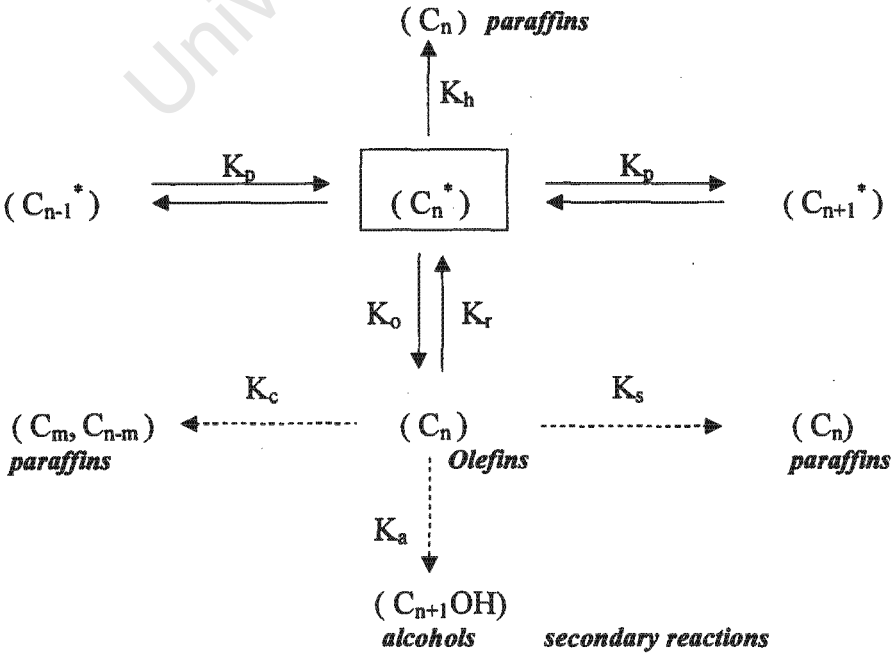

Figure 1.1.4: Chain growth, termination and secondary reactions in Fischer-Tropsch synthesis on Co and Ru catalysts [12].

Where:

n	=	Carbon number.
C_n	=	Olefin and paraffin concentration.
C_n^*	=	Surface concentration of growing hydrocarbon chain.
K_a	=	Hydroformylation rate constant.
K_c	=	Cracking rate constant.
K_h	=	Hydrogenation rate constant.
K_o	=	Hydrogen abstraction rate constant.
K_p	=	Propagation rate constant.
K_r	=	Readsorption rate constant.
K_s	=	Secondary olefin hydrogenation rate constant.

1.1.4 Fischer-Tropsch Product Selectivity

Irrespective of the operating conditions, the FT selectivity always yields olefins, paraffins, alcohols, aldehydes, acids and ketones [16]. The FT product selectivity is influenced by the temperature, gas composition, pressure, type of catalyst and promoters [16].

1.1.4.1 Influence of temperature

For all types of FT catalysts an increase of the operating temperature results in the production of more hydrogenated products and the product selectivity shifts towards lower molecular mass hydrocarbons [16]. For example, using precipitated iron catalysts the hard wax selectivity (boiling point above 500°C) decreases from 47 to 17% when the temperature is increased from 213 to 247°C [16]. Keeping the pressure at 1 bar and raising the temperature from 170 to 180°C using Co/Al_2O_3 (15wt% Co), a slight increase in the production of light hydrocarbons was observed [59]. The selectivity of the $C_1 - C_4$ fraction increased from 20.7 to 25.7% and the $C_5 - C_9$ from 29.0 to 32.9% while the $C_{10} - C_{20}$ fraction decreased from 50.03 to 41.4% [59]. The FT performance of Co/SiO_2 catalysts was tested at 260 and 290°C. The results indicated that the CO conversion increased when the temperature was raised. It was also seen that raising the temperature shorter hydrocarbon chains were formed [56]. Cobalt is more hydrogenating than iron catalysts and when increasing the operating temperature the CH_4 selectivity increases more rapidly than with Fe catalyst [16].

1.1.4.2 Effect of gas composition

When operating at low temperatures (about 220°C) the H_2/CO ratio affects the product selectivity. At low H_2/CO ratios of the feed gas the product selectivity shifts to higher average molecular weight hydrocarbons because at high CO partial pressures the coverage of the catalyst surface with chemisorbed CO is higher and consequently the coverage by adsorbed methylene (CH_2) species is higher and thus results in increased chain growth (α). It was also found that the CH_4 selectivity decreases as the H_2/CO ratio is lowered [16]. Using Fe/SiO_2 catalysts promoted with K the fraction of linear α-alkenes in the total alkene product decreases when the H_2/CO ratio is lowered from 1.7 to 0.67 [14]. The operating conditions were 270°C and 18 bar.

For iron catalysts at high temperatures the product selectivity does not only depend on the H_2/CO ratio. The selectivity is not only dependent on the partial pressure of H_2 and of CO but also on the partial pressure of CO_2 and/or H_2O [16].

1.1.4.3 Influence of pressure

For iron catalysts at 225°C, increasing the total partial pressure from 8 to 21bar (keeping the H_2/CO ratio constant) it was observed that the product selectivity was unchanged [16]. For cobalt catalysts however, the wax selectivity increased with pressure up to 40bar [60]. Changes in the product spectrum can be attributed to the partial pressures of the reactants [61]. Increasing the CO partial pressure when Co catalysts promoted with Zr and Ru were used led to lower CO consumption rates, lower methane selectivity and higher chain growth probability [62]. As the objective of the low temperature Fischer-Tropsch process is to maximize the production of hard wax the total pressure should be above 20 bar and the H_2/CO ratio should be about 2 [16].

1.1.4.4 Influence of promoters

There are certain ways of obtaining higher wax selectivity and this is generally achieved via the addition of chemical promoters. In the case of iron catalysts potassium is generally used

[16]. The addition of K as a promoter for cobalt catalysts does not have a marked effect on the catalyst activity but when K is used in larger amounts the catalyst activity decreases notably. See also discussion on promoters in section 1.2.3.

1.1.5 The Fischer-Tropsch Reaction Mechanisms

Several mechanisms have being proposed in order to explain the syngas reaction on the metallic surface of catalysts and how chain growth develops during the Fischer-Tropsch synthesis.

In 1926 the first theory known as the "**carbide theory**" was proposed by Fischer and Tropsch [2]. Their assumption was that CO absorbs dissociatively as a primary step having carbides as intermediates. Through stepwise hydrogenation the carbidic carbon forms CH_2 species as explained below;

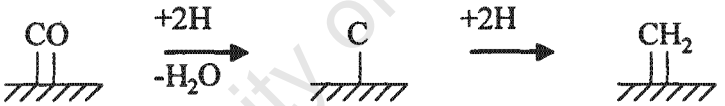

Figure 1.1.5: Dissociative absorption of CO and formation of CH_2 species.

This carbide theory was discarded since cobalt and ruthenium as catalysts do not show bulk carbide phases [2].

In 1951, Storch, Golumbic and Anderson postulated a mechanism where CO is adsorbed onto the catalyst surface and by addition of hydrogen, oxymethylene species are formed [1].

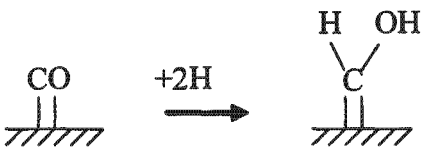

Figure 1.1.6: Formation of oxymethylene species.

These authors also proposed a basic reaction for chain growth, namely that the C-C bonds are formed by a "**condensation reaction**". The primary complex is formed by the reaction of two hydroxymethylene surface intermediates releasing water and a surface oxy species.

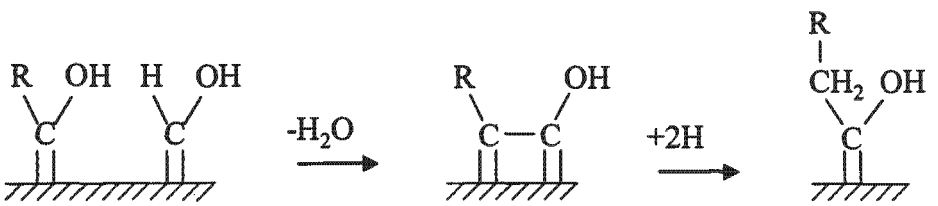

Figure 1.1.7: Condensation mechanism

Another mechanism was developed, the "CO insertion" mechanism, namely the insertion of chemisorbed CO into the metal carbon bond of the alkyl ligand [2].

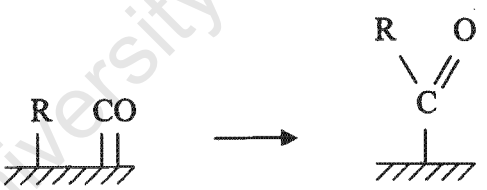

Figure 1.1.8: Insertion mechanism

Via the CO insertion mechanism chain growth takes place through the addition of hydrogen and by subsequent hydrogenolisis, alkyl species are formed.

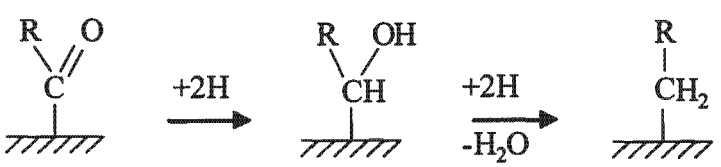

Figure 1.1.9: Chain growth by CO insertion

Schulz visualises the primary paraffin molecule formation by the reaction of an alkyl surface specie with a chemisorbed hydrogen atom [2].

Figure 1.1.10: Paraffin formation.

This reaction is more inhibited than olefin formation because chain prolongation is favoured against chain termination [2].

Figure 1.1.11: Olefin formation via hydrogen abstraction.

A mechanism for FTS on iron catalyst based on Rankin's model is described by 11 elementary steps as described below [13].

1. CO adsorption

$$CO(g) + s \rightarrow CO(a)$$

2. CO dissociation

$$CO(a) + s \rightarrow C(a) + O(a)$$

3. Dissociation of H_2

$$H_2(g) + 2s \rightarrow 2H(a)$$

4. Formation of CH species

$$C(a) + H(a) \rightarrow CH(a) + s$$

5. Formation of CH_2 species

$$CH(a) + H(a) \rightarrow CH_2(a) + s$$

6. Formation of CH_3 species

$$CH_2(a) + H(a) \rightarrow CH_3(a) + s$$

7. Formation of H_2O

$$O(a) + H_2(g) \rightarrow H_2O(g)$$

8. Formation of CO_2

$$O(a) + CO(g) \rightarrow CO_2(g)$$

9. Propagation of hydrocarbons

$$C_{n-1}H_{2n-1}(a) + CH_2(a) \underset{\longleftrightarrow}{rds} C_nH_{2n+1}(a) + s$$

10. Chain Termination

$$C_nH_{2n+1}(a) + H(a) \underset{\longleftrightarrow}{rds} C_nH_{2n+2}(g) + 2s$$

11. α -olefin formation

$$C_nH_{2n+1}(a) + s \underset{\longleftrightarrow}{rds} C_nH_{2n}(g) + H(a) + s$$

Where:

(g)	=	Gas phase.
(a)	=	Adsorbed species.
s	=	Empty surface site.
rds	=	Readsorption.

Rankin assumes that the most abundant surface intermediate is CO absorbed (step 1) and that propagation and termination steps (step 9-11) are slow compared to other steps.

Using iron based catalysts in the Fischer-Tropsch synthesis a wide range of hydrocarbons is produced consisting mainly of alkenes. These alkenes are employed for the manufacture of

chemicals and/or fuels. For the production of polymers and petrochemicals ethene and propene are required as feedstocks. Linear alkenes are produced via the Fischer-Tropsch synthesis and more importantly alkenes containing the double bond in the terminal (or α) position. These linear α-alkenes can be used for the manufacture of chemicals. The C_6 - C_{16} linear α-olefins can be used for the manufacture of detergents and PV plasticizers [14].

Maitlis and co-workers proposed the "**alkenyl mechanism**" in which chain growth is initiated by a vinyl + methylene coupling, proceeds by alkenyl + methylene coupling and terminates via hydrogenation of the alkenyl to yield the 1-alkene [9].

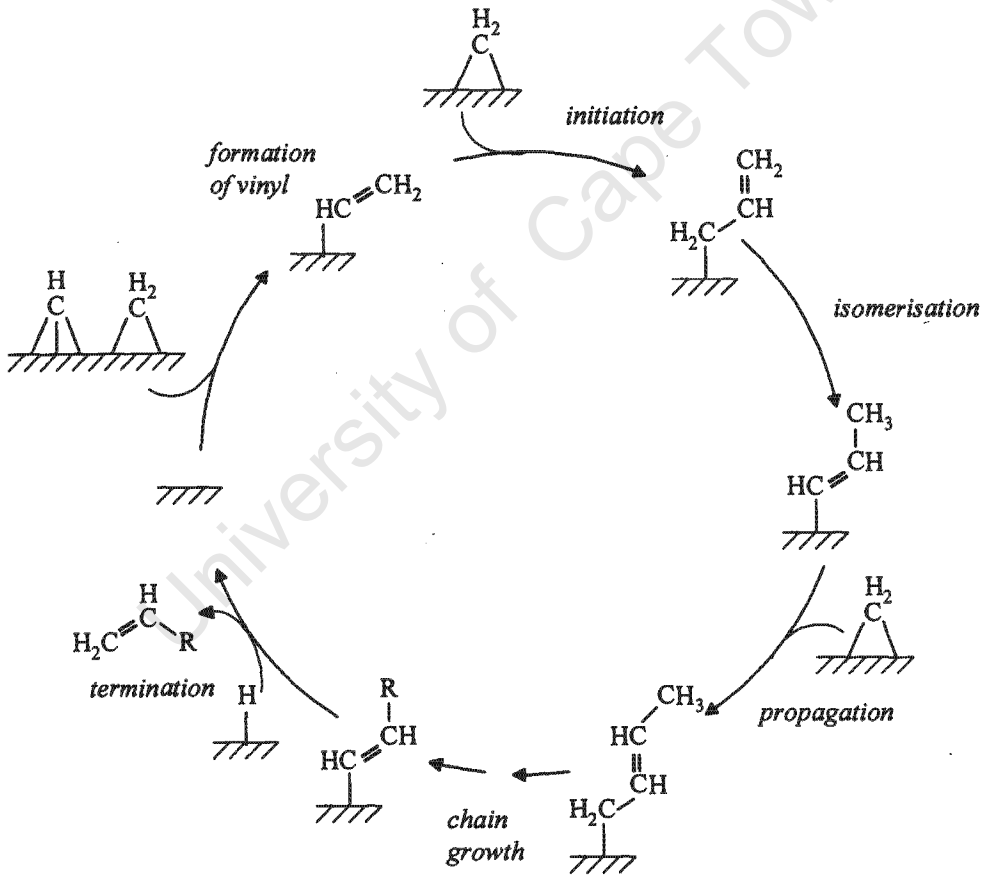

Figure 1.1.12: The alkenyl mechanism for the stepwise polymerisation of methylene in the FT reaction [9].

Schulz investigated olefin secondary reactions creating a kinetic model termed as the "non trivial surface polymerisation". This model is based on the stepwise addition of C_1 species and acknowledges the product desorption as olefins, paraffins, aldehydes and alcohols. This

model indicates that polymerisation reactions of the surface species are faster than the desorption reactions [2].

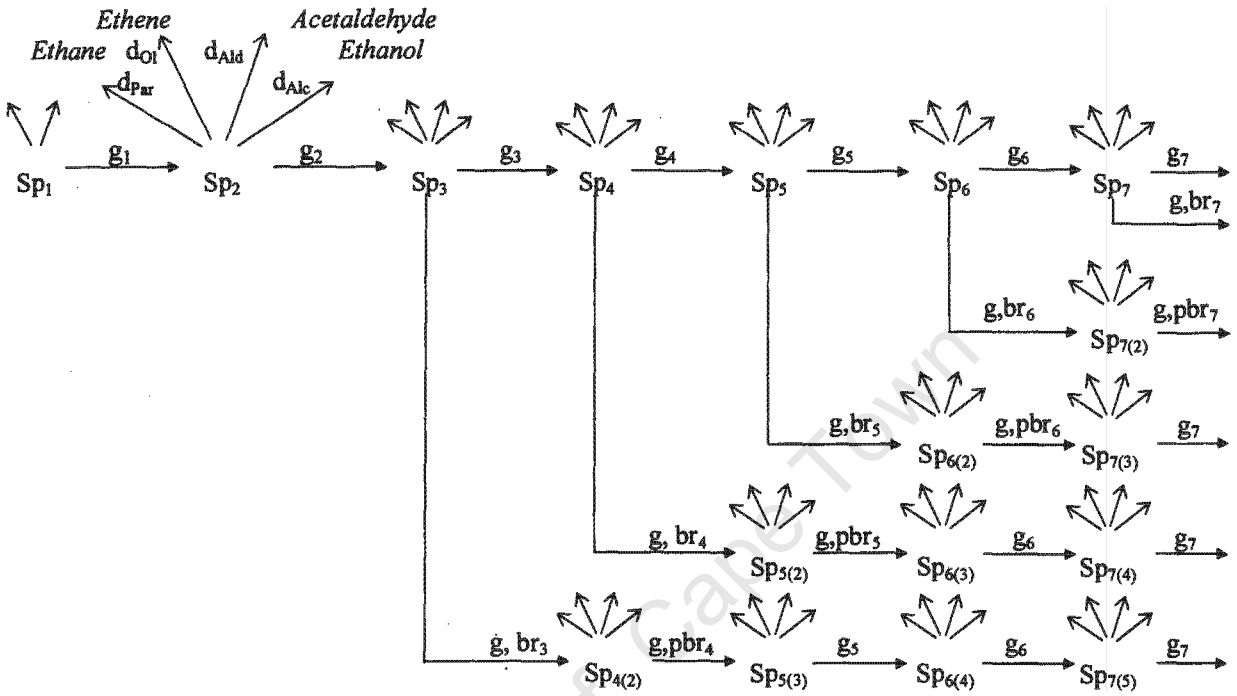

Figure 1.1.13: Kinetic Scheme of "Non-trivial surface polymerisation" for the desorption of olefins, paraffins, alcohols and aldehydes.

With:

$Sp_{n(i)}$	=	Surface species with n carbon atoms and branched in position.
g	=	Linear growth.
d	=	Desorption.
br	=	Formation of a branch.
pbr	=	Step branching (post-branched).

A mechanism over Ru catalysts was proposed recently [63]. The reaction starts with an adsorbed R – CH, which reacts with an adsorbed CH to give R - CH - CH monoradical (vynil like). The latter can be hydrogenated to form adsorbed alkene R - CH $=CH_2$, or can be hydrogenated to R - CH_2 - CH, which is analogue to the initial specie. The initial specie can be hydrogenated and desorbed as R - CH_3, for more details see figure 1.1.14.

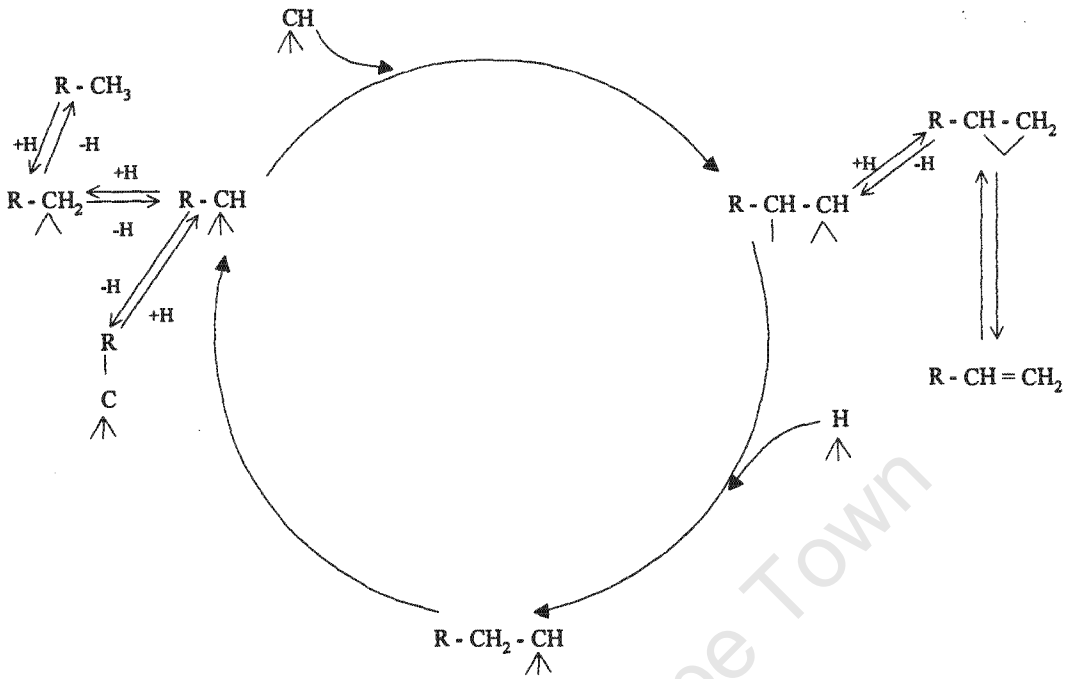

Figure 1.1.14: Fischer-Tropsch mechanism

| Atop adsorption
/\ Bridge adsorption
/\ Three fold site
\/ Di-σ adsorption mode
R = H

1.1.6 The Fischer-Tropsch Product Distribution

The FT product distribution can be explained taking into consideration the following reaction:

$$CO + 2H_2 \longrightarrow -CH_2- + H_2O$$

Initially the CH_2 unit can either react with H_2 to produce CH_4, which can be desorbed as such or can react with another CH_2 unit to yield an adsorbed C_2H_4 unit (figure 1.1.15). This C_2H_4 could have three alternatives; it can be desorbed as ethene or can be hydrogenated to ethane or it can react with another CH_2 unit to yield an adsorbed C_3H_6 unit. The combination of the first two alternatives represents the **"probability of chain termination"** and the third

alternative represents the **"probability of chain growth"**. This principle is followed by a sequence of reactions resulting in long chain products as shown in figure 1.1.15 [16].

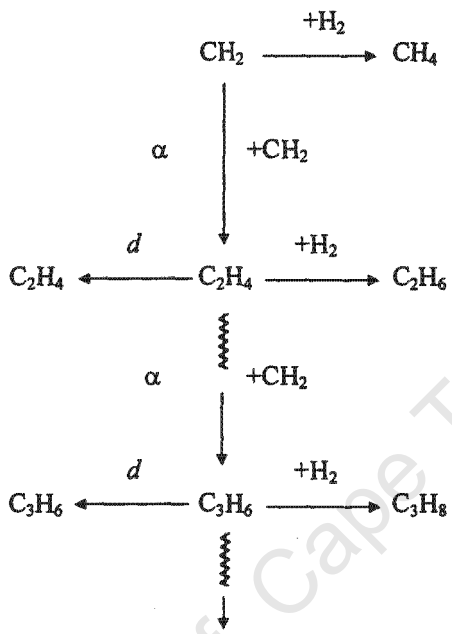

Figure 1.1.15: FT product distribution [16].

d = desorption

At steady state the concentration of each $(CH_2)_n$ specie on the catalyst surface will be constant and if the probability of chain growth is α, then that of termination will be (1-α). Usually, the "Flory product distribution" is used to represent the product distribution. The following equation was applied to describe the polymerisation process during the FT synthesis [12].

$$Fn = n \cdot (1-\alpha)^2 \cdot \alpha^{n-1}$$

$$\log (Fn/n) = n\log\alpha + \log[(1-\alpha)^2/\alpha]$$

Where:

F_n = Fraction of the carbon atoms within chains containing n carbon atoms.

α = Chain growth probability (assuming that α is independent of chain length).

By plotting log(Fn/n) versus n a straight line is obtained. The slope of this line is log α. This way of representing the product spectrum is known as Anderson-Schulz-Flory (ASF)

distribution plots [17]. The existence of two α values may be found with many iron catalysts. On a ASF plot the data fall on two straight lines [17]. Usually the first straight line is obtained from C_3 to about C_{12}. From C_{10} to C_{12} the ASF plot frequently shows a curvature. Consecutively a second straight line of higher alpha value (α_2) is obtained. A possible explanation for this phenomena is that the pores of the catalysts are usually filled with vapour/liquid hydrocarbon emulsions which have longer residence times inside the catalysts particles leading to readsorption of the alkenes to continue further chain growth [17].

1.2 Catalysts for the Fischer-Tropsch Synthesis

The catalytic behaviour of the supported group VIII metals (except for Os) in the hydrogenation of CO was studied by Vannice [19]. The FT conditions in this investigation were, pressure 1 bar, temperatures between 240 – 280°C and various H_2/CO feed ratios. The selectivity for long chain products decreases in the order:

$$Ru > Fe > Co > Rh > Ni > Ir > Pt > Pd$$

The specific activity of the different metals was reported to decrease in the following sequence:

$$Ru > Fe > Ni > Co > Rh > Pd > Pt > Ir$$

(It is however, presently accepted that Ni and Co are more active than Fe).

Of this group, only Fe, Co, Ni and Ru are the commonly used catalysts for the FT synthesis due to their high activities in the hydrogenation of CO [19]. Of the four metals Ru is the most active and gives the highest average molecular weight distribution and the largest C_5^+ fraction [19]. The high cost of Ru compared to the other metals and its insufficient abundance makes the large-scale application unfeasible [15, 16]. Ni produces large quantities of methane [15, 16, 19] and less of the high value alkenes than do Co and Fe catalysts. Under commercial operating conditions Ni carbonyls are formed, which results in loss of the active metal from the FT reactors [16]. The reasons explained above point out to Co and Fe as the only possible catalysts for FT commercial operation.

1.2.1 Iron Catalysts

Sasol uses Fe based catalysts for their commercial operations. Fe catalysts are not only used due to the low price compared to Co and Ru. Fe catalysts have a great advantage in that they produce large quantities of olefins when operated at higher temperatures (300-350°C). Cobalt, being more active (per unit metal area) for hydrogenation reactions than iron produces less olefins. When operating at lower temperatures (200-230°C) both iron and cobalt catalysts can be used to produce high quality diesel by hydrocracking the high molecular weight products [8].

Precipitated Fe catalysts are usually used in fixed-bed and slurry-bed reactors. Using slurry bed the alkene selectivity is higher compared to fixed-bed reactors. The Fe catalyst undergoes physical degradation with the formation of fine particles that plug the fixed-bed reactor, generating pressure gradients [57].

Fe catalysts are also prepared with structural promoters such as SiO_2 or Al_2O_3 to maintain a high surface area and to extend the catalyst life [58].

The Fe catalysts are more versatile than Co catalysts because they produce less methane. The production of alkenes, oxygenates and branched hydrocarbons can be controlled if Fe catalysts are employed but this also depends on the type of promoters and the reaction conditions [58].

The product selectivity of Fe catalysts is generally controlled by the addition of alkalis [1]. Potassium was found to increase wax and alkene selectivity and decrease the methane formation.

Copper has been traditionally added to precipitated Fe catalysts to lower the reduction temperature of Fe oxide to Fe metal [1].

The main factors, which cause activity decline of Fe catalysts in the FT reaction, are loss of active sites due to sintering, fouling and poisoning by sulphur [8].

1.2.2 Cobalt Catalysts

Cobalt catalysts are widely applied in hydrogenation and hydrotreating processes and they are candidates for the production of fuels and chemicals via the FT synthesis [21].

Early studies demonstrated that cobalt based catalysts are highly attractive for FT synthesis due to their high activity, selectivity for linear hydrocarbons, low activity for the water-gas shift reaction (WGS) and lower price compared to noble metals [22, 23].

Cobalt catalysts are well suited to produce a high selectivity in alkanes of high molecular weight, especially when cobalt is supported on silica or on alumina [24]. It is well known that the active phase in FT cobalt catalysts is cobalt metal [23]. Cobalt catalysts show several characteristics in the FT reaction such as; low oxygenate product yield, low selectivity for making CO_2 [25], high stability of the metallic state under operating conditions and a low tendency towards the formation of metal carbides (compared to iron based catalysts) [24].

Cobalt catalysts are usually calcined and then reduced with H_2 prior to FT [23].

Shell's multitubular fixed bed FT plant at Bintuli, Malaysia uses a cobalt-based catalyst and both Exxon and Sasol have employed cobalt based catalysts in their demonstration slurry bed FT units [16].

1.2.2.1 Preparation of cobalt catalysts

Due to the high cost of cobalt it is important to minimize the cobalt content and maximize the cobalt metal surface area. This is achieved by supporting the cobalt on supports of high surface area and with the required pore size distributions [16].

There are at least four principal methods for distributing the metal precursor onto the support surface:

- Precipitation of the catalyst onto the support.
- Co-precipitation of the catalyst and the support.
- Impregnation of the support with a solution of the metal precursor.
- Ion exchange *e.g.,* zeolite with a solution of the metal precursor.

The **co-precipitation** method was the technique used most widely in early studies by Anderson [26]. In co-precipitation the normal procedure is to precipitate a mixture of nitrate solutions (*e.g.,* of Al and Co) with an alkaline solution. The hydrated oxide precipitates and is then filtered, washed, and dried. Many hydrated oxides are voluminous and /or gelatinous, and filtration and washing may be difficult. Precipitated catalysts vary considerably in strength from soft powders to hard glassy gels [1].

A common way of preparing catalysts for the FTS is by the **incipient wetness impregnation method**, which consists on depositing the cobalt salt solution of the appropriate concentration onto the support [16]. During the liquid-phase impregnation the salt solution is transported into the interior of the support via capillary-types forces or by diffusional effects. This, along with the drying procedures, leads to different types of impregnation profiles on the support and to different catalyst performances. Depending on the type of the support incipient wetness or dipping (wet soaking) impregnation may be employed. Incipient wetness is known as a capillary impregnation because it requires an amount of solution just sufficient to fill the pore volume of the support, while by dipping impregnation the material transport occurs solely by diffusion, where there is no intra-pellet flow of the impregnating solution. The dipping impregnation is suitable for precursors, which interact with the support [26].

Various methods for the preparation of cobalt catalysts supported on titania were recently investigated by Baerns. The author introduces a method named **"spreading technique"** similar to the thermal technique in which the cobalt salt is mixed with the support and heated to its melting point and finally heated up to higher temperatures *i.e.*, 400°C in order to decompose the cobalt salt to oxide [27].

The use of microwave drying (heating is internal compared to conventional heating which is external) in the preparation of supported catalysts (Fe/Al_2O_3, $FePd/Al_2O_3$, $PdAl_2O_3$), has shown an increase in the particle size of the metal and that thus the catalyst, $FePd/Al_2O_3$ was found to be resistant to alloy formation as it does when treated with conventional heating [28].

a. Choice of the support

The choice of the support is of great importance in the preparation of supported catalysts for the application in the oil, gas and chemical industries [29]. In the FT reactions the support is dictated by several considerations including basicity, dispersion effect, electronic configuration and strong metal support interaction [26]. The purpose of the support is basically to facilitate preparation of a well dispersed high surface area catalytic phase [29]. Consequently, the most common supports used for the preparation of FT catalysts are inorganic oxides such as; silica, alumina, titania, magnesia and zirconia. Zeolites were also

studied as supports for the preparation of FT catalysts [26]. It would seem that silica is the best support for Fe-base catalysts, at least in terms of activity and wax production [26]. Alumina because of its amphoteric nature presents a variety of interesting characteristics especially in the isomerization of straight chain hydrocarbons. The high surface areas of silica and alumina in an alkali environment suffer significant deterioration. On the other hand, titania supported catalysts are highly hydrogenating due to strong metal support interactions. The formation of carbonaceous material is substantially reduced on magnesia supported catalysts. Magnesia also inhibits sintering. Investigations on MnO supported Fe catalysts confirmed certain inhibition of methane compared to Fe catalysts supported on either alumina or titania and that MnO supported Fe catalysts yield a greater production of $C_2 - C_4$ alkenes [26].

Bartholomew and co-workers found that the specific activity of cobalt for the FT reaction is a function of the support, dispersion, metal loading and catalyst preparation. Based on turnover numbers the decreasing activity at FT conditions of 1 bar and 225°C using catalysts containing 3% Co is [29]:

$$Co/TiO_2 > Co/SiO_2 > Co/Al_2O_3 > Co/C > Co/MgO$$

b. Effect of the support on cobalt catalysts.

The interaction between the metal and the support on cobalt catalysts supported either on silica or on alumina has been widely discussed in several publications [30]. The support is employed to enable the formation of a stable and well dispersed catalytically active phase [30]. In the FT reaction, as well as in hydrogenation reactions, the active phase is metallic cobalt [23]. The metal surface areas can be increased by dispersing the cobalt precursor on high surface area supports [31].

The interaction between the cobalt oxide and the support surface (metal support interaction) has a significant influence in the reduction behaviour [31]. The reducibility of the cobalt catalysts has been shown to be affected by the support, precursor, preparation method, metal loading and by the addition of extra metal ions such as Ru and Pt [21]. The degree of reduction is usually higher on silica than on alumina, especially when the cobalt concentrations are low [21, 25]. It is known that spinel-cobalt aluminates are formed during pre-treatment, reduction and catalytic reaction [23]. These spinel-cobalt aluminates are

The interaction of the metal precursor with the support can be influenced by certain parameters, which are important when the catalysts are prepared by impregnation techniques or by ion exchange: The most important parameters which influence this interaction are the following [33]:

1. Isoelectric point of the oxide support. – The isoelectric point of γ-Al_2O_3 and TiO_2 increase when the temperature of the impregnating solution increases, this is in contrast with that of SiO_2, which appears to decrease.
2. Cationic and anionic metal complexes. - Metal complexes exits in the anionic and cationic form. Nevertheless a neutral state can be found but they will not have an electrostatic interaction with the support.
3. Solution pH. – The pH influences separately or simultaneously the liquid and/or the solid part of the interface. Qualitatively the pH allows finding out the sign of the surface charge. The pH determines the nature and the nuclearity of the complex in liquid phase, and controls the solubility of the support. Qualitatively, the pH determines, the value of the zeta potential of the solid phase related to the concentration of charged surface sites.
4. Ligand nature. – The ligand type affects the nature and the strength of the metal complex surface interaction.
5. Washing. – Washing should be avoided after the deposition of the precursor by impregnation, this could cause in a loss of the active metal salt.

Obtainment of the final catalyst

In order to obtain the desired activity of the catalyst, the metal precursor must be transformed into a suitable compound (*e.g.,* transformation of the oxide to metal). Calcination and reduction are normally the final steps in the preparation of supported catalysts. The reduction is usually called activation, which is defined as the transformation of the solid precursor to the active phase [33]

Prior to calcination and reduction the catalysts are normally dried in order to eliminate the solvent used. Drying usually takes place at low temperatures ranging from 80 to 200°C.

Drying is obviously controlled by the temperature and the flow rate of the drying gas over the catalyst surface.

a. Calcination

The calcination process is very important when the catalysts are prepared with the following oxide supports; Al_2O_3, SiO_2, TiO_2 and ZrO_2. The objective of calcination is the conversion of the metal salt to the oxide. In some cases water is also released in this process, *e.g.,* when cobalt nitrate is used to impregnate the support. The calcination temperature is normally higher than the drying temperature and that of the catalytic reaction. Several changes in the support and the metal oxide can occur during calcination [33]:

1. - **Weak interaction** of the metal oxide and the support.

   - During calcination the metal oxide could detach itself from the support and this could result in the formation of larger aggregates which could result in sintering, *i.e.,* loss of surface area.

2, - **Strong interaction** of the metal oxide and the support.

   - Formation of a monolayer, resulting in high dispersion and consequently in high activity.
   - Extensive formation of new compounds (cobalt aluminates, silicates, titanates, etc.). If these compounds are not reducible, it could mean that less metal is available in the reduced catalyst, which could result in lower activity

They are many ways of controlling the calcination step in order to favour a better dispersion of the precursor. These suggestions are [33]:

1. - Use of the suitable additives to inhibit the interaction of the metal precursor with the support.

2. - Lower the calcination temperature. The calcination temperature may influence several characteristics of the supported precursors such as dispersion, extent of formation of a compound by reaction with the support. High calcination temperatures would lead to sintering.

3. - Modification of the calcination atmosphere (for controlling the oxidation states). When the calcination is carried out under different conditions, *e.g.*, under vacuum or oxidizing atmospheres the nucleation of the oxide could be affected.

An interesting observation was found when catalysts were prepared by incipient wetness impregnation starting with nickel nitrate. One sample was only dried at 120°C and the other one subsequently calcined at 400°C. The dried sample appeared to have a higher dispersion than the calcined sample. From this, it could be suggested that, it is advantageous to start from uncalcined samples [33].

b. Reduction

In most of the cases reduction is the final step in the preparation of catalytic active metals [33]. Reduction is essential to develop the area required for high FT activity [16]. The temperature used in hydrogen reduction depends on the catalytic metal (*e.g.*, Co or Fe) and on the way the catalyst was prepared. The temperatures used range from about 200 to about 400°C. The reduction of unsupported cobalt oxide (Co_3O_4) could occur in two steps [34].

$$Co_3O_4 + H_2 \longrightarrow 3CoO + H_2O$$
$$CoO + H_2 \longrightarrow Co + H_2O$$

The presence of water depresses the rate of reduction and for this reason a high H_2 flow rate is used because it lowers the water partial pressure inside the reactor [16].

Higher temperatures should result in a higher degree of reduction. High reduction temperatures may lead to the so-called strong metal support interaction effect and/or to sintering as previously discussed.

The reduction depends on the nature of the precursor. The degree of reduction varies for different metal precursors. It was shown that catalysts supported on SiO_2 show different reduction characteristics when the precursor is either nitrate or chloride [33].

The hydrogen reduction of cobalt oxide particles may depend on the size of the Co_3O_4 crystallites. The ease of reduction decreased from larger (270-700A°) to smaller particles (60A°) [35].

1.2.3 Promoters

The term promoter is defined as a substance added to catalyst in order to improve its activity and/or selectivity for a specific reaction [1]. Promoters are usually added to a catalyst in small amounts.

These are two types of promoters:

a). - Structural promoters. – These promoters facilitate the formation of a structure of high surface area during preparation or pre-treatment of the catalyst.

b). – Chemical Promoters. – These substances change the chemical nature of the surface and therefore increase the activity or selectivity of the catalysts towards desired products.

A noble metal promoter could affect the catalyst performance in different ways, it increases the reducibility of the cobalt, it preserves the activity by preventing the build up of carbonaceous deposits, it provides a combination of enhanced cobalt reducibility and dispersion [36]. The effect of ruthenium addition prepared by different methods has been widely studied by several researches [22, 36]. The activity and performance of these catalysts changed in the presence of Ru. The activity of Co/SiO_2 and Co/TiO_2 increased and so did the C_5^+ selectivity [36]. Ru promotion facilitated the reduction of catalysts Co/Al_2O_3, Co/SiO_2 and Co/TiO_2, which allows the use of lower reduction temperatures, which in turn minimizes the sintering of the metal produced [36, 37]. It was observed that the number of reduced metal atoms exposed to the surface increased with Ru promotion. Ru appears to inhibit the formation of highly irreducible Co species and promotes their reduction. Co-impregnation of

the metal (Co, Ru) salts appeared to produce catalysts slightly more active for CO hydrogenation [38].

The addition of Ru does not affect the FT synthesis reaction rate order or the activation energy [36, 39].

Ru or Re increases considerably the activity of Co/Al_2O_3 and Co/TiO_2 catalysts. Zr oxide had a similar effect on the activity of Co/SiO_2. While Ru or Re promotion considerably improved the dispersion of Co on the Al_2O_3 support catalysts and to a lesser extent that of Co/TiO_2, addition of Zr oxide had hardly any effect on the properties of the Co/SiO_2 catalyst [40]

Noritatsu and Fujimoto investigated the addition of small amounts of Ru, Pt and Pd to silica supported cobalt catalysts, which were prepared with a mixture of cobalt nitrate and cobalt acetate. The FT activity decreased in the following order:

$$RuCo > PdCo > PtCo > Co$$

The addition of Ru to Co/SiO_2 catalysts resulted in no change in the methane selectivity. The Pt and Pd catalysts however exhibited higher methane selectivities [41].

Rhenium is also a structural promoter of supported cobalt catalysts. Re prevents agglomeration of CoO_x species during calcination treatments or oxidative regeneration. Re improves Co metal dispersion on TiO_2, without influencing the FT synthesis turnover rates [37].

The addition of small amounts of boron to Co/TiO_2 catalysts decreased the Co_3O_4 crystallites size in the oxidized catalyst. It was found that with increasing boron content the reducibility of the catalysts decreased. The FT product spectrum shifted to lower molecular weight hydrocarbons and the CO_2/H_2O ratio increased with increasing boron loading [42].

1.2.4 Catalyst Deactivation

During the FT process the catalyst looses activity. This catalyst deactivation is caused by fouling (blockage of the pores by high molecular weight hydrocarbons, by coke and carbon deposition), sintering (small metal particles grow into larger ones), poisoning by sulphur [48] and oxidation of the metal by water.

1.2.4.1 Fouling

There are generally two types of fouling, physical and chemical fouling. A **"physical fouling"** is caused by the built up of high molecular weight products in the narrow pores of the catalyst, which hampers the diffusion of the reactants through the pores to the active surface sites [8]. A solvent (diesel fuel) was used in order to wash away these high molecular weight products. It was observed that the activity increases drastically for a few minutes, however, fresh wax is again formed and the catalyst pores are rapidly refilled [8].

Fouling by coke deposition is a general concern in petroleum refining [49]. Coke is basically formed by the decomposition or condensation of hydrocarbons. Coke formation is dependant on certain parameters such as operating conditions, nature of the feed and type of catalyst [49, 50]. At temperatures above 350°C polyaromatic or even graphitic compounds are formed. At low temperatures (<200°C) non-polyaromatic products are formed. The formation of these products, known as coke precursors, blocks the catalyst pores making the active sites inaccessible. Fouling can be caused by carbon deposition too. Carbon is formed by the disproportionation of carbon monoxide ($2CO \rightarrow CO_2 + C$ Boudouard reaction) [51, 52]. Enhancement of the carbon deposition rate was observed when catalysts were promoted with alkalis (*e.g.*, K_2O) [8]. Fouling by coke formation or carbon deposition are examples for **"chemical fouling"**.

For iron based catalysts it has been found that carbon deposition is proportional to p_{CO}/p_{H2}^2 (p=partial pressure) at the reactor entrance when the temperature at which the fluidised bed reactor operated was 300°C [8]. The rate of carbon deposition is dependent on the temperature and on the type of catalyst. For example, Fe based catalysts are more sensitive to carbon deposition and hence fixed bed reactors should not be operated at high temperatures, *e.g.*, above 260°C [8].

1.2.4.2 Sintering

Catalyst deactivation is also caused by sintering, which is known as the loss of catalytic surface area due to crystallite growth of either the metal phase (due to pore collapse) or of the support (support collapse) [49, 52]. Sintering usually takes place at high reaction temperatures (*e.g.*, cobalt metal will sinter at temperatures above 500°C) and is generally

accelerated by the presence of water vapour [52]. Two mechanisms have been studied to explain sintering [52];

1.- Crystallite migration. – The crystallites migrate over the support surface and then collide and coalesce.

2.– Atomic migration. – The metal atoms migrate over the support surface and then they are captured by larger crystallites.

Sintering can occur in all stages of the catalyst life. If might occur during catalyst preparation, drying, calcination, reduction, reaction or regeneration (coke burn off) [49].
Sintering depends very strongly on the temperature. At high temperatures the mobility of the atoms increases [49)].
The melting point plays an important role in sintering. The mobility of the atoms becomes faster when the temperature approaches the melting point. Surface migration starts at the so-called Huttig temperature (about $0.25T_M$) and migration in the bulk phase commences at the Tamman temperature (about $0.50T_M$, where T_M is the melting point in Kelvin). The temperature at which the solid state becomes mobile also depends on the texture, size and morphology, *e.g.*, γ-Al_2O_3 (highly porous) is much more sensitive to sintering than α-Al_2O_3 (moderately porous). In practice the mobility is not always undesired. It can be applied to regenerate catalysts, *e.g.*, in the redistribution of Pt on reforming catalysts [49]

1.2.4.3 Effect of dispersion and crystallite size

For cobalt catalysts supported on SiO_2, Al_2O_3 and TiO_2 it was found that the FT activity of the catalysts is proportional to their metal dispersions over the range 0.45 to 9.5% (*i.e.*, for crystal sizes from 100 to 10nm. The FT synthesis rate of the catalysts increases with increasing metal dispersion. The FT synthesis pathways are not affected by the cobalt crystallite size in the range 10 to 210nm [12]. The chain growth probability depends only weakly on the Co dispersion and the type of support [12].
To achieve high Co metal dispersion it is required that the precursor CoO and Co_3O_4 crystallites are small. The formation of these small crystallites requires a strong interaction with the support but this in turn means that a high reduction temperature is required [37].

It appears that the decomposition of cobalt nitrate to CoO and Co_3O_4 during calcination, and also when H_2 reduction is carried out in the presence of high concentrations of H_2O vapour, leads to agglomeration of the particles and to low metal dispersion. The elimination of calcination before reduction increases the cobalt dispersion [37].

Cobalt dispersions above 15-20% (D=5-6nm) are difficult to achieve during synthesis and difficult to maintain during calcination and reduction. The small crystallites are oxidized rapidly in the presence of water vapour and this lowers the FT activity [37].

Silica supported cobalt catalysts starting with cobalt (III) acetyl acetonate have been prepared by the chemical vapour deposition CVD technique. From chemisorption analysis it was deduced that the metallic Co (3.4nm crystals) was well dispersed on samples containing 6wt% Co but the dispersion decreased with increasing Co loading (19.6wt%). The degree of reduction at 550°C was about 30%. The low reducibility might be explained by the formation of cobalt silicates during calcination in air at 450°C. It was also observed that the catalysts prepared with cobalt (II) acetyl acetonate were thermally more stable than the catalysts prepared with cobalt nitrate [53].

Matsuzaki carried out FT experiments using Co/SiO_2 catalysts prepared with metal precursors from different sources, *e.g.*, cobalt nitrate, acetate and chloride. The catalysts were prepared by incipient wetness impregnation, aged for 24hr, dried under vacuum at 100°C and reduced with H_2 at 300°C for 3 hrs. Characterization by extended X-ray adsorption fine structure (EXAFS) (after reduction at 450°C) showed that catalysts prepared from the nitrate and chloride had showed very different dispersions, 4.3 nm was observed for the crystal size prepared with Co nitrate and 20nm for the chloride case. Surprisingly, the catalyst prepared with Co acetate was found to have a particle size smaller than 1nm [54]. In order to achieve greater cobalt dispersions, Co-acetate/SiO_2 catalysts were promoted with Ru, Ir, Rh, Re, Os and Pt. The catalyst preparation followed was as described above. Using EXAFS the Co particles were measured and the results indicated that the dispersion of the Co metal particles was enhanced. The dispersion decreased in the order; Ru, Ir, Rh, Pt and Re [54].

Cobalt catalysts prepared with Co(II) nitrate, Co (II) acetate, Co(II) and Co(III) acetyl acetonate were prepared by sequential incipient wetness impregnation. The Co dispersion for each catalyst containing 12%Co was measured. The following dispersions were obtained 6.1, 7.8, 5.0 and 9.8%. The dispersion and the FT activity appear to correlate. The catalyst prepared with Co(III)-acetyl acetonate showed the highest activity [27].

Supported cobalt on silica catalysts prepared with cobalt carbonyls generally are easy to reduce and show high dispersions resulting in higher activities compared to Co nitrate derived catalysts [55].

1.2.4.4 Effect of sulphur

The activity and selectivity of many supported transition metal catalysts appeared to be influenced by the structure of the catalyst, the dispersion, the degree of reduction of the metal and the strength of adsorption of the reactant molecules on the metal surface [43].
It is known that the addition of small amounts of chemical additives can increase or decrease the activity and selectivity of cobalt catalysed FT reaction [1]. As discussed above an increase in FT activity was shown when Co supported catalysts are promoted with Ru [36, 39]. The opposite effect (deactivation of the catalyst) is known when cobalt based FT catalysts suffer a rapid and substantial loss of activity in the presence of sulphur poisons at ppm levels [44]. For successful commercial FT synthesis with iron based catalysts the S content of the synthesis gas needs to be less than 0.02ppm [16].

1.2.4.5 Effect of water

There is evidence that water vapour produced by the FT reaction results in surface oxidation of the cobalt metal and hence in a drop in the FT activity [45]. Three related aspects may be implicated in this deactivation [16]:

1. – Sintering of the cobalt metal particles.
2. – Oxidation of a portion of the cobalt particles.
3. – Formation of inactive Co – support interactions (cobalt silicates, titanates, aluminates).

When the cobalt crystallites are small the degree of unsaturation of the exposed Co metal atoms is high. And hence these small Co crystallites are more prone to be oxidized [16]. Iglesia has estimated that Co crystallites smaller than 6nm will oxidize under normal FT conditions [37]. Since the formation of cobalt aluminates or silicates requires cobalt to be in

the oxidized state, the presence of water vapour should enhance this reaction [16]. The presence of water during reduction seems to retard the reduction process by increasing Co-alumina interaction and/or forming cobalt aluminates [23].

Hilmen and co-workers studied the effect of water on Co/Al_2O_3 and $CoRe/Al_2O_3$ catalysts by adding water to the synthesis gas feed. They found that the $CoRe/Al_2O_3$ catalyst deactivates when water is added during the FT synthesis [45, 46]. The oxidation increased with increasing H_2O partial pressure and H_2O/H_2 ratio. Bulk deactivation of the cobalt occurs only to a very limited extent [45]. It was suggested that oxidation of highly dispersed phases or surface oxidation are the cause for the observed deactivation. The $CoRe/Al_2O_3$ catalyst was oxidized more easily in $H_2O/H_2/He$ mixtures than the Co/Al_2O_3 catalyst. The ease of this oxidation is probably due to the higher dispersion of the CoRe $/Al_2O_3$ [46]. From TPR studies with H_2O/H_2 or H_2O/He treated catalysts it was observed that a cobalt oxide phase was formed, which had reduction properties very similar to those of Co aluminates [45].

Iglesia and co-workers also carried out some experiments with water addition to a CO/H_2 feed over Ru/TiO_2 and Co/TiO_2 catalysts and proposed that water inhibits the secondary hydrogenation, especially of α-olefins [12]. These authors reported that the effect of water caused an increase in chain growth probability, which can be explained by the inhibiting effect of water on the termination of growing chains by hydrogen addition, which is the predominant irreversible step. Moreover, an increase of olefin selectivity was observed after water treatment [47].

The changes in the catalysts cobalt phases in the presence of water have to be considered carefully, especially when the FT synthesis is carried out in a slurry reactor where the concentration of water as a main oxygenated product is high due to extensive back mixing [47].

Chapter II

2 Experimental

2.1 Catalyst Preparation

2.1.1 Materials

2.1.1.1 Metal salts

The aim of the catalysts preparation of this work was to obtain reduced catalysts containing 30g of cobalt metal on 100g of the support. Obviously the calcined catalysts before reduction had calculated mass of approximately 40.82g Co_3O_4 per 100g SiO_2. Before the catalysts preparation each cobalt salt was dissolved in different solvents in order to determine the grade of solubility of each salt.

2.1.1.2 Solvents

It is known that cobalt nitrate is very soluble in cold water, and is also soluble in methanol. For this reason the cobalt nitrate was dissolved in either water or in methanol prior to the impregnation of the support.

As cobalt acetate is highly soluble in water due to the fact that cobalt acetate is a polar compound, water was used to dissolve cobalt acetate for the preparation of some of the catalysts.

Cobalt acetyl acetonate is a non-polar compound and thus the non-polar dichloro methane was used as solvent.

2.1.1.3 Supports

The support used for this work was silica gel Davisil grade 646 with a BET surface area of 286 m^2, BET pore volume of 1.12 ml/g and a particle size 250-400μm. The other support

used was γ alumina with a BET surface area of 160 m^2/g , BET pore volume of 0.48 ml/g. and an average particle size of 150 μm.

2.1.1.4 Impregnation steps

The number of impregnation steps of the cobalt salts onto the support was dependant on the pore volume of the support and on the solubility of each cobalt salt. For example the cobalt nitrate dissolved in water or in methanol can be impregnated in one step on the silica support and on the alumina in a two step impregnation, whereas the cobalt acetate only can be impregnated onto the alumina in three steps and the cobalt acetyl acetonate in four steps.

2.1.2 Catalysts Supported on Silica

All the catalysts were prepared by the incipient wetness impregnation method using aqueous solutions of cobalt nitrate. Manganese nitrate and zinc nitrate were employed to coat the silica support to minimise interactions of the cobalt with the silica support.

2.1.2.1 Cobalt catalysts with different cobalt levels

- A series of Co/SiO_2 catalysts were prepared in one step. The concentration of the cobalt nitrate was adjusted to obtain cobalt metal loadings of 10, 20 and 30g on 100g of SiO_2. The catalysts are represented in mass ratios as following:

10Co-nit (H_2O)/100 SiO_2 1SCN
20Co-nit (H_2O)/100 SiO_2 1SCN
30Co-nit (H_2O)/100 SiO_2 1SCN

Where,
1S = One step
CN = Calcined under nitrogen

Following impregnation the samples were dried in a dessicator (silica gel) at room temperature for 5 days and then dried at 120°C in air for 24 hrs and subsequently calcined in flowing N_2 (60ml(STP)/min) at 270°C for 6 hrs.

2.1.2.2 Influence of the particle size

- The above obtained sample 30gCo/100gSiO_2, was crushed to pass through a sieve of 120μm grid in order to examine the effect of the catalyst particle size on the FT studies.

30Co-nit (H_2O)/100 SiO_2 1SCN crushed

2.1.2.3 Single and multi-step cobalt addition variation

- In order to determine whether the number of the impregnation steps influences the metal dispersion on the support a sample of 20gCo/100gSiO_2 was prepared adding cobalt nitrate in 2 steps. After the first impregnation the catalyst was aged in a dessicator for 5 days, then it was dried in an oven at 120°C for 24 hrs and calcined under nitrogen at 270°C for 6 hrs. After calcinations the second impregnation was carried out and the same procedure was repeated as explained above.

20Co-nit (H_2O)/100 SiO_2 2SCN

- Another two samples of 30gCo/100gSiO_2 were prepared by sequential incipient wetness impregnation, in three and six steps: The cobalt nitrate was diluted in order to add only 10g or 5g of cobalt metal per 100g of SiO_2 in each step. Between each step the ageing, drying and calcinations procedures were carried out as for the catalysts described above.

30Co-nit (H_2O)/100 SiO_2 3SCN
30Co-nit (H_2O)/100 SiO_2 6SCN

2.1.2.4 Modified catalysts by coating silica

- In the pre-coating cases, $Mn(NO_3)_2.4H_2O$ or $Zn(NO_3)_2.4H_2O$ was added to the silica in one step by incipient wetness impregnation. After drying in a dessicator and afterwards in an oven at 120°C for 24 hrs, the samples were calcined under N_2 (60ml(STP)/min) at 450°C for 6 hrs and then consequently impregnated with $Co(NO_3)_2.6H_2O$ in one step. The dried samples were either used as such or calcined at 270°C. For the pre-coating the amount of Mn and Zn added was estimated to coat the silica with 1 or 3 theoretical monolayers of MnO or ZnO, *e.g*:

30gCo/36gMnO(1 layer)/100gSiO_2, 1SCN

30gCo/108gMnO(3 layers)/100gSiO_2, 1SCN

30gCo/36,4gZnO(1 layer)/100gSiO_2, 1SCN

30gCo/109,3gZnO(3 layers)/100gSiO_2, 1SCN

- Another two catalysts coated with three monolayers of Mn and Zn oxides were prepared adding Mn or Zn nitrate in three steps, each step was equivalent to one monolayer. Both samples were aged for five days in a dessicator, dried at 120°C for 24 hrs and calcined under nitrogen at 270°C for 6 hrs after each impregnation step.

30gCo/108gMnO(3 layers)/100gSiO_2, 3SCN

30gCo/36,4gZnO(3 layer3)/100gSiO_2, 3SCN

It was realised when preparing the pre-coated samples that even though the amounts of the Mn or Zn added were sufficient to coat the SiO_2 completely a perfectly uniform coating was unlikely to be achieved in practice.

2.1.3 Catalysts Supported on Alumina

The catalysts supported on alumina were also prepared by the Incipient Wetness Impregnation Method. The cobalt precursors employed for such preparations were cobalt nitrate, cobalt acetate and cobalt acetyl acetonate. The cobalt nitrate was dissolved in water or in methanol, the cobalt acetate in water and the cobalt acetyl acetonate in dichloromethane.

2.1.3.1 Influence of different solvents and cobalt salts

- Four separate samples were prepared in a four-step impregnation process; two of them were prepared with cobalt nitrate dissolved in water and in methanol. The next catalyst with cobalt acetate dissolved in water and the last catalyst with cobalt acetyl acetonate dissolved in dichloromethane. All the catalysts had loadings of 30g. of cobalt metal on 100g of alumina. The samples were aged in a dessicator for five days, dried in an oven at 120°C and calcined at 270°C under flowing N_2. This procedure was repeated for each impregnation step and the catalysts are represented as follows:

30Co-nit (H_2O)/100 Al_2O_3 4SCN
30Co-nit (CH_3OH)/100 Al_2O_3 4SCN
30Co-ace (H_2O)/100 Al_2O_3 4SCN
30Co-acac (CH_2Cl_2)/100 Al_2O_3 4SCN

2.1.3.2. Calcination variations

- Four additional catalysts samples were studied in order to investigate if the calcining gas influenced the catalysts preparation. These samples were calcined under air instead of under nitrogen at 270°C for 6 hrs. An exception was the catalysts with cobalt acetyl acetonate that were calcined at 300°C and at 350°C because the carbonaceous material could not be decomposed at 270°C (see section 3.6.2 Thermo Gravimetric Analysis).

30Co-nit (H_2O)/100 Al_2O_3, 4SCA
30Co-nit (CH_3OH)/100 Al_2O_3, 4SCA
30Co-ace (H_2O)/100 Al_2O_3, 4SCA
30Co-acac (CH_2Cl_2)/100 Al_2O_3, 4SCA 300°
30Co-acac (CH_2Cl_2)/100 Al_2O_3 4SCA 350°

CA = Calcined under air

2.1.3.3 Drying variations

- The influence of the ageing time in the dessicator was also investigated. After each impregnation the sample was not aged but instead it was dried straight away in an oven at 120°C for 24 hrs and then immediately calcined at 270°C under air for 6 hrs.

30Co-nit (H_2O)/100 Al_2O_3 4SCA Straight away into oven

- On the assumption that drying the catalyst in a microwave oven might result in the more rapid removal of the water and so hopefully result in a better dispersion of the cobalt, two samples were prepared in four steps. One of them was dried straight away in a microwave at medium heat for 10 min after each impregnation. The other sample was aged in a dessicator for five days after each impregnation and then dried in a microwave oven at medium heat for 10 min.

30Co-nit (H_2O/100 Al_2O_3, 4SCA straight away into microwave
30Co-nit (H_2O)/100 Al_2O_3, 4SCA dried in a microwave

- An investigation was carried out to determine to what extent the cobalt interacted with the support during the 270°C calcinations. A sample was prepared in two steps, after each impregnation the sample was aged in dessicator for five days and then dried at 120°C in air. Half of the final batch was used as such and the other half was calcined at 270°C for 6 hrs under nitrogen.

30Co-nit (H_2O)/100 Al_2O_3, 2S uncalcined
30Co-nit (H_2O)/100 Al_2O_3, 2SCN

2.1.3.4 Different impregnation temperatures

- Two catalysts were prepared on the assumption that the temperature of the support during impregnation influences the dispersion of the cobalt. Two samples were prepared impregnating the cobalt nitrate (at ambient temperature) in a two step process on alumina,

which had been pre-heated to 80°C. The samples then were aged in dessicator for five days and then dried in an oven at 120°C for 24 hrs.

30Co-nit (H_2O)/100 Al_2O_3 2S uncalcined, impregnated at 80°C

The second catalyst was calcined at 270°C for 6 hrs under nitrogen between each step.

30Co-nit (H_2O)/100 Al_2O_3 2SCN, Impregnated at 80°C (a)

To further investigate the effect of impregnation temperature a catalyst was prepared adding the cobalt nitrate solution (80°C) onto the support, which was isothermally heated at 80°C in an oil bath. After impregnation the catalyst was aged in a dessicator for five days, then dried at 120°C for 24 hrs and subsequently calcined at 270°C for 6 hrs under flowing nitrogen between each step.

30Co-nit (H_2O)/100 Al_2O_3 2SCN, impregnated at 80°C (b)

2.1.3.5 Modified alumina support

- It was observed that cobalt interacted with the alumina to a much greater extent than with silica during catalyst preparation (see section 3.5.2, TPR studies).

In an attempt to minimise the interaction of the cobalt with alumina a support was prepared by depositing silica on the alumina surface by chemical vapour deposition (CVD). Silica was deposited on alumina using tetraetoxisilane at 100°C for 1 hr in the presence of air (100ml(STP)/min) following by calcination for 4 hrs at 400°C. The amount of silica deposited on the alumina was determined by measuring the weight increase of the alumina support after the CVD operation carried out in 5 cycles.

30Co-nit (H_2O)/100 Al_2O_3 + SiO_2 4SCN, silinized catalyst

It was also conceivable that the silinization of the alumina might create acid sites on the alumina surface.

- To compare the activity of the silinized catalyst with another catalyst having basic surface sites a catalyst was prepared by impregnating 4g. of KOH per 100g of Al_2O_3. After the addition of KOH the cobalt nitrate was added in four steps with ageing, drying and calcination between each step.

30Co-nit (H_2O), 4KOH/ 100Al_2O_3, 4SCN

- In an attempt to obtain a higher dispersion of the metal and hence and a higher catalytic activity a catalyst was prepared from the alumina the surface of which had been converted, at least in part, to a cobalt aluminate species. A standard catalyst, 30Co-nit (H_2O), / 100Al_2O_3, 4SCN was calcined at 700°C in order to form surface cobalt aluminates. After this calcination the cobalt nitrate which corresponds to an additional 30 g. of cobalt metal was added to the new support in four steps. The ageing, drying and calcination were carried out after each impregnation and the catalyst obtained is represented by,

30Co-nit (H_2O)/100 Al_2O_3 (Co_2AlO_4), 4SCN

2.2 Catalyst Characterisation

2.2.1 Atomic Absorption Spectroscopy, AAS

The cobalt concentration of the catalysts was determined using an Atomic Absorption Spectrophotometer Varian 3.0.

The catalysts were calcined prior to analyses. The samples were again dried in order to eliminate water because of the hygroscopic properties of the samples that could lead to a lower concentration of cobalt. Thereafter the samples were ground and dissolved in a mixture of HF/HCl in a ratio of 1:4.

The cobalt concentration was obtained by interpolation using the concentrations of three cobalt solutions as standard. The results were given in ppm (parts per million) and were recalculated as percentage by mass.

2.2.2 X-Ray Diffractometry, XRD

A Philips XRD-6 Diffractometer with CuKα radiation was used to perform X-Ray Diffraction measurements. The spectra were scanned in the 2θ range from 0 to 70° at a rate of 2.0°/min with a step size of 0.1°. The generator voltage was adjusted to 40kV and the current to 20mA.

The X-ray diffraction technique was performed to identify the metal oxide species formed on the support prior to reduction.

2.2.3 Temperature Programmed Reduction, TPR

2.2.3.1 Description of the apparatus

The hydrogen consumption required to reduce the samples was monitored by the thermal conductivity of the effluent gas on a Temperature Programmed Reduction (TPR) Instrument (see figure 2.2.1).

The instrument consisted of a quartz reactor specially designed to handle high temperatures.

Nitrogen was used as a reference gas and a mixture of 6.41% of H_2 in N_2 as reducing gas, calibrated with CuO.

The uptake of hydrogen was measured by the difference in thermal conductivity of the N_2 gas during reduction.

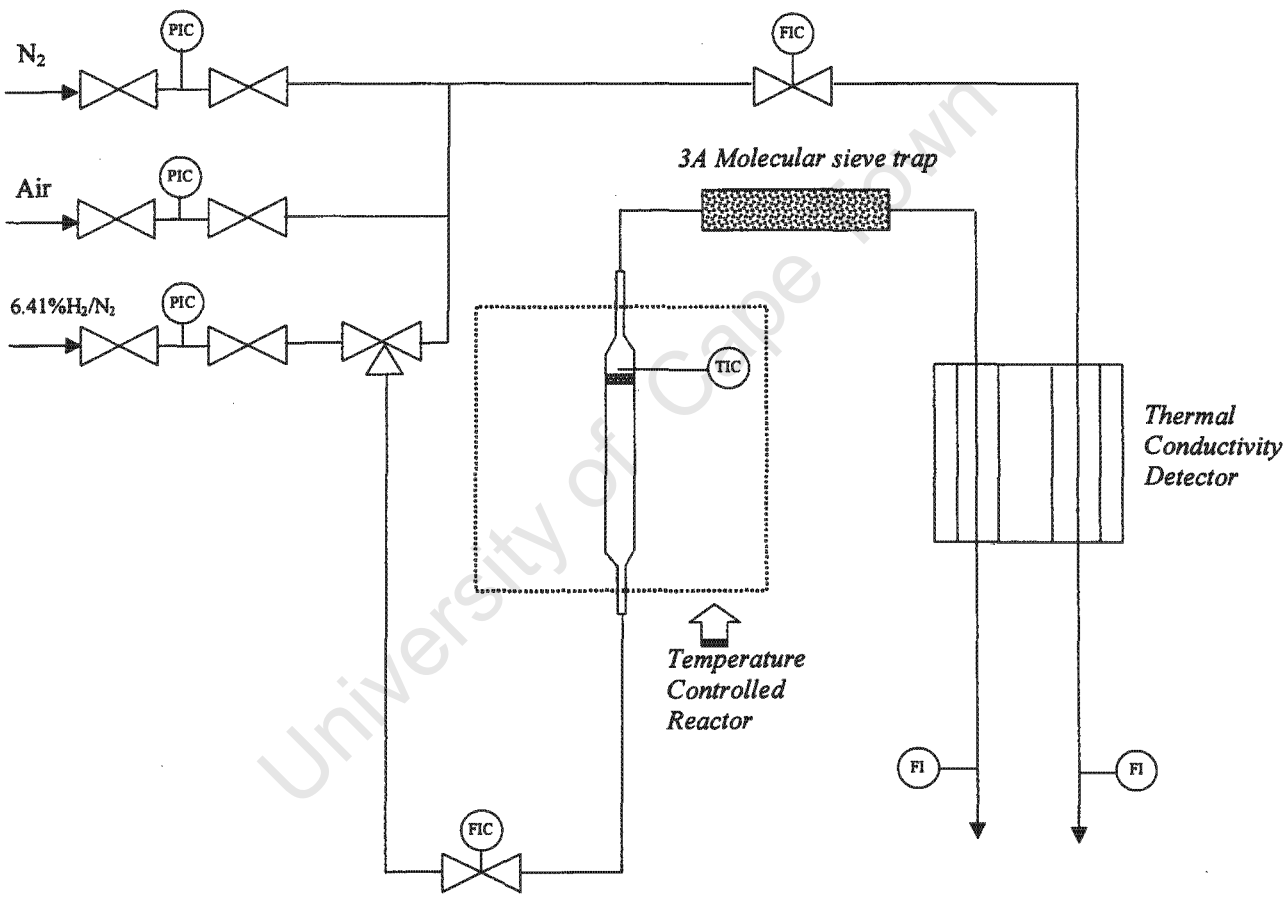

Figure 2.2.1: Temperature Programmed Reduction Apparatus

2.2.3.2 Procedure of the temperature programmed reduction

A mass of 0.0860 g of catalyst was loaded in the quartz cell. After testing for leaks the catalyst was dried under air at 120°C for 1 h (higher temperature was avoided because in several cases the uncalcined catalysts were used as such in the Fischer-Tropsch synthesis). The system was then cooled down to 100°C. Pure nitrogen gas was diverted to the system for at least 10 min. before the thermo conductivity detector was switched on and stabilised at 100°C for 3 hrs. Three reduction procedures were carried out as described below:

a) Standard reduction

The samples were heated at a rate of 10°C /min from 100°C to 1000°C and kept at the latter temperature for 30 min under a reducing gas of 6.41% H_2 in N_2. The flow of the reference and the H_2 / N_2 mixture gases were adjusted to 60ml(STP)/min.

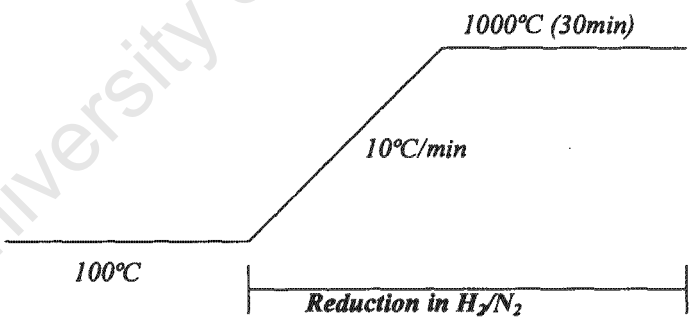

Figure 2.2.2: Standard reduction.

b) Two-ramp reduction

The reduction temperature in the reactor was raised from 100°C to 350°C at 5°C/min under flowing gas of 6.41% H_2 in N_2. The catalyst was maintained at 350°C for 2 hrs and then the second ramp was carried out by elevating the temperature from 350°C to 1000°C in flowing H_2 / N_2 at a rate of 10°C/min.

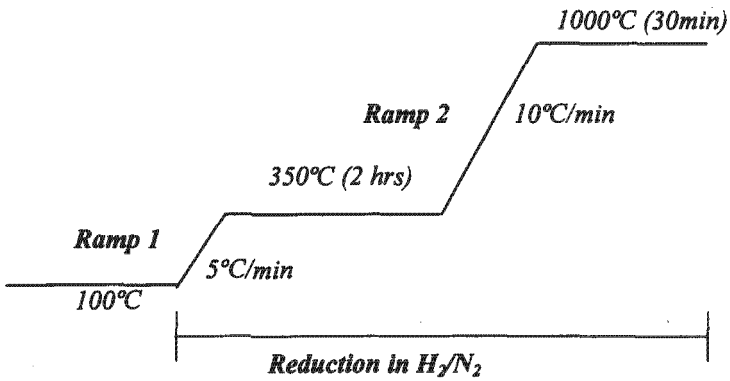

Figure 2.2.3: Two-Ramp Reduction.

c) Two-ramp pre-reduction under pure hydrogen

In order to estimate the reduction behaviour of the catalyst in the FT reactor a sample was reduced in the TPR apparatus at 350°C for 16 hrs after ramping at a rate of 1°C/min in pure hydrogen. Thereafter the TPR was performed elevating the temperature from 350°C to 1000°C at 10°C/min under 6.41% of H_2 in N_2. This procedure was done in order to investigate whether or not the catalyst in the FT reactor is fully reduced at 350°C for 16 hrs.

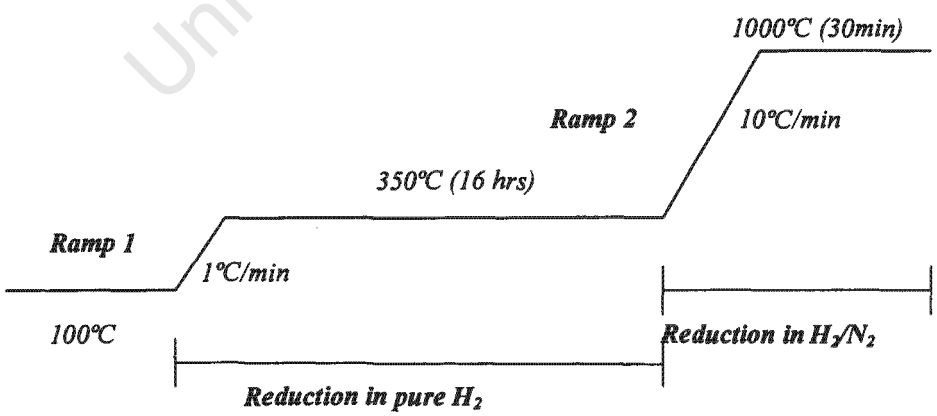

Figure 2.2.4: Two –ramp pre-reduction under pure H_2.

The output from the TCD was recorded on a computer and the hydrogen consumed was quantified by integrating the peak areas of the TPR profiles.

2.2.4 Thermogravimetric Analysis

Thermo gravimetric analysis (TGA) and Differential Thermal Analysis (DTA) measurements were conducted using a Thermal Analyser Staton Redcroff STA 780 (Fig.2.2.5) consisting of an electromagnetic microbalance in a temperature controlled chamber.

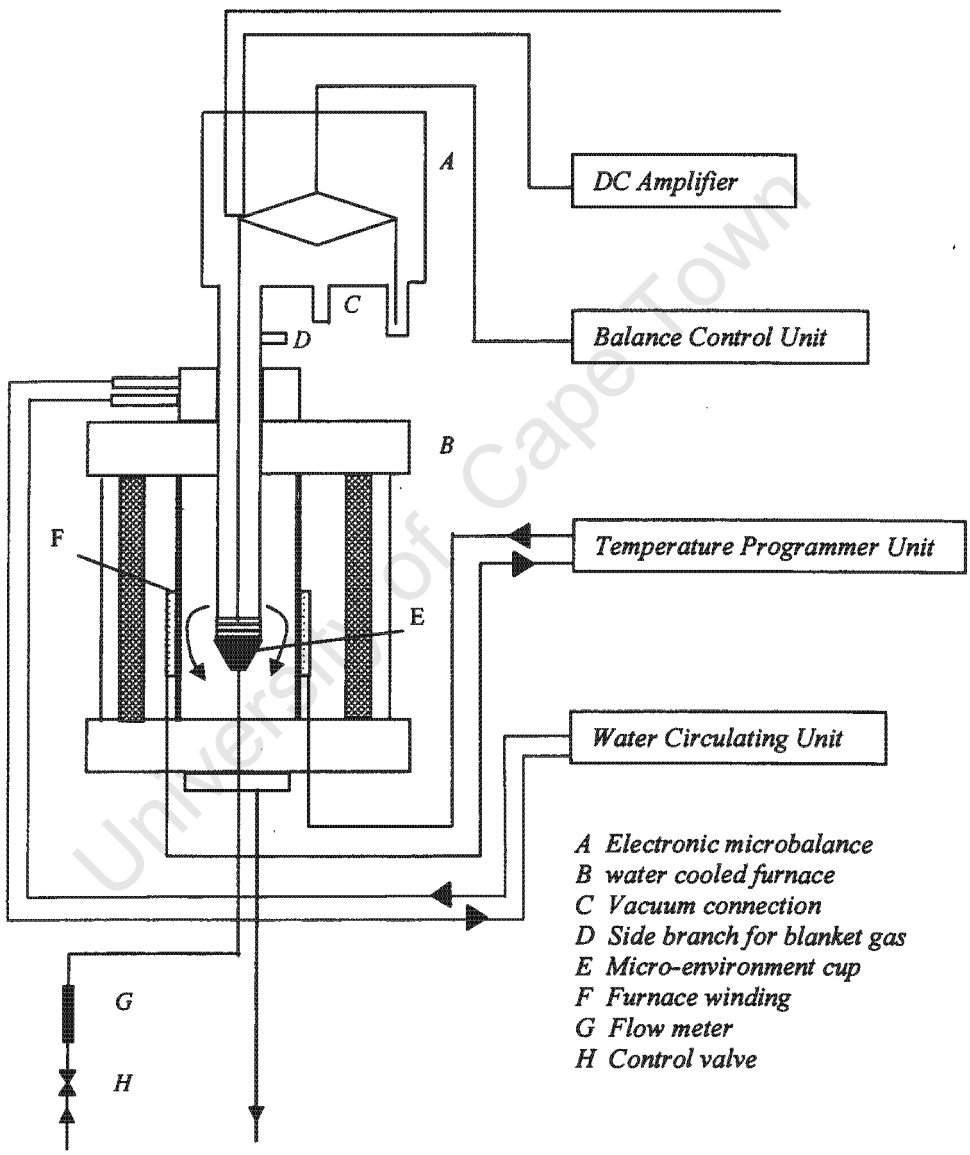

Figure 2.2.5: Schematic of Thermal Analysis System.

A typical sample placed in the microbalance was 25 mg with Al_2O_3 used as a reference. The sample was then linearly heated under either N_2 or under air from ambient temperature to 500°C at 5°C/min, and maintained at this temperature for 2hrs.

The weight loss of the sample was then measured by the difference of the initial and final weight.

2.2.5 Chemisorption

The active metal surface area of the catalysts was estimated by chemisorption of carbon monoxide using a Micromeritics ASAP 2000 Apparatus.

Before adsorption of CO the catalysts were reduced *in-situ* in flowing hydrogen with programming from ambient temperature to 350°C at a rate of 10°C/min and kept at this temperature for 16 hrs. To eliminate any chemisorbed hydrogen the samples were evacuated at 350°C for 120min., at reduction temperature and subsequently cooled down to chemisorption temperature of 30°C. A CO adsorption isotherm was carried out from 50 to 450 mmHg. The sample was degassed for 30minutes and the CO adsorption isotherm repeated. The difference between the two isotherms, *i.e.* the "strong" chemisorption was taken as a measure of the cobalt metal surface area. The "total" chemisorption was obtained by the difference of the first isotherm and the support isotherm as demonstrated in figure 2.2.6a and 2.2.6b.

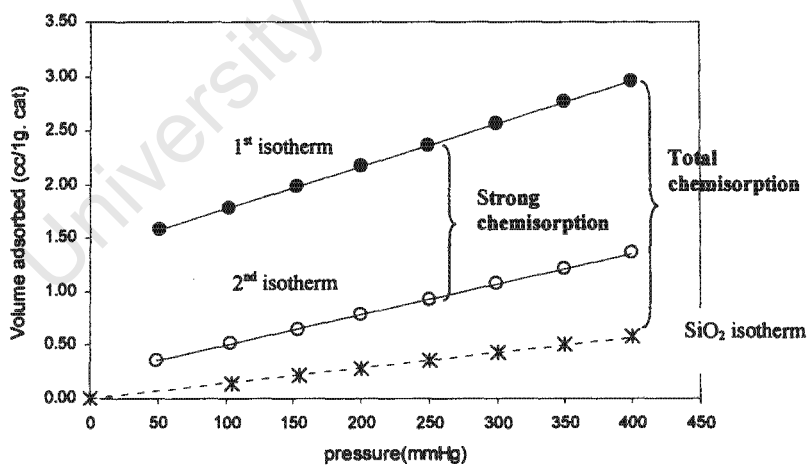

Figure 2.2.6 a: Chemisorption isotherms of the 30gCo/100gSiO_2.

—●— 1st adsorption isotherm of catalyst.

—○— 2nd adsorption isotherm repeated of catalyst after degassing.

—✳— Adsorption isotherm of SiO_2 support (blank).

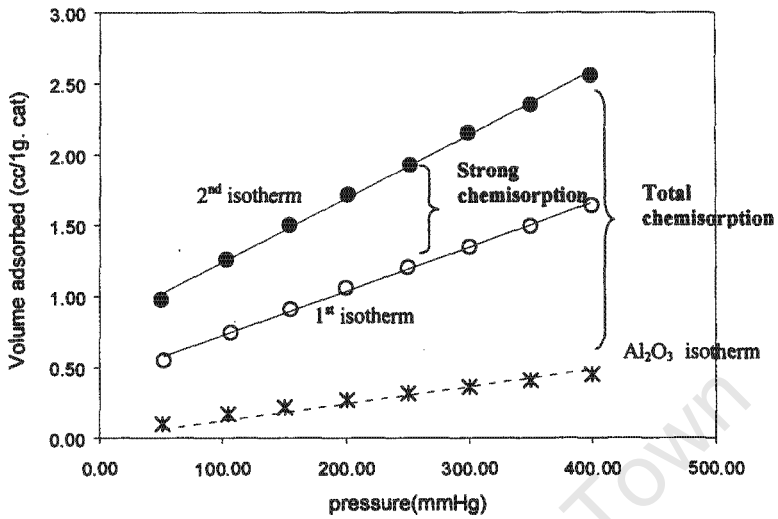

Figure 2.2.6 b: Chemisorption isotherms of the 30gCo/100gAl_2O_3.

—●— 1st adsorption isotherm of catalyst.

—○— 2nd adsorption isotherm repeated of catalyst after degassing.

—✳— Adsorption isotherm of Al_2O_3 support (blank).

Then, the total metallic surface area can be calculated with the following formula:

$$A = \frac{V_m}{22414} \times N \times a_m$$

Where,

A	=	Total metallic surface area (m^2/g.cat.).
V_m	=	Volume of CO chemisorbed (ml/g.cat.)
N	=	Avogadro's number (6.03×10^{-23} molecules/mol).
a_m	=	Cross sectional area occupied by 1 atom of metal ($6.62 \times 10^{-20} m^2$).

The temperature of maximum adsorption on Co catalysts occurs at temperatures ranging 25-200°C [21].

The extent of adsorption at 15°C of CO, O_2 and H_2 on high area silica and alumina support decreases in the order [63].

$$CO > O_2 > H_2$$

The adsorption on the support depends on the metal surface area, metal loading and its dispersion [63].

The **"metal dispersion"** can be directly is obtained from the following equation:

$$D = \frac{V_m}{22414}\frac{M}{wt} \times 100$$

Where,

D	=	Dispersion (%).
V_m	=	Volume of CO chemisorbed (ml(STP)/g.cat.).
M	=	Atomic mass of the metal (g).
wt	=	Mass of metal per 1 g cat(g/g.cat.).

It should be stressed that in this study the metal areas, the dispersions and the crystallite sizes were all calculated from the CO chemisorption results. As the latter is a relative and not necessarily an absolute measure of the available reduced surface cobalt atoms, the calculated areas, dispersions and crystallite sizes are all relative and not absolute values. For comparison purposes the relative values were considered satisfactory.

2.2.6 BET method

The Brunauer-Emmet-Teller method was applied to evaluate the total surface, pore volume and average pore size of the catalysts with nitrogen physisorption using a Micromeritics ASAP 2000 Apparatus.

Before the measurements the samples were dried and degassed under vacuum. Nitrogen was used as the adsorbate at its liquefaction temperature. The isotherms were obtained at constant temperature with a range of relative pressure (p/p_0) from 0 to 1.0. The nitrogen absorbed is plotted as a function of the relative pressure.

$$\frac{p}{n^s(p_0 - p)} = \frac{c-1}{n_m^s c}\frac{p}{p_0} + \frac{1}{n_m^s c}$$

Where,

n^s	=	Quantity of gas adsorbed at an equilibrium pressure p (molecules).
$n_m{}^s$	=	Number of adsorbate molecules at monolayer coverage (molecules).
P	=	Pressure at which a volume V(STP) of gas is adsorbed(atm).
P_0	=	Vapour pressure of the adsorbate in the condensed state at the adsorption temperature (atm).
p/p_0	=	Relative pressure.
c	=	Constant related to the heat of adsorption.

For many practical purposes, the BET equation is generally fitted to the data over the range $p/p_0 = 0.05 - 0.30$ [63].

A straight line results when $\frac{p}{n^s(p_0 - p)}$ is plotted against the relative pressure p/p_0. The value of n_m^s can be also obtained from the slope and the intercept, where;

$$slope = \frac{c-1}{cn_m^s}$$

$$intercept = \frac{1}{n_m^s c}$$

Secondly, the surface area is obtained by;

$$A = n_m^s \times a_m$$

With,

n_m^s	=	Number of adsorbate molecules at monolayer coverage (molecules).
a_m	=	Cross sectional area of the adsorbate (nm^2 /molecule).

Nitrogen, argon and krypton are commonly used as adsorbates [63]. In this thesis the surface areas of the catalysts have being obtained using N_2 as adsorbate gas.

If the pore volume of the adsorbent can be obtained, an average pore diameter d, can be estimated using the following equation proposed by Emmett and Dewitt for cylindrical pores [1];

$$d = \frac{4V}{S}$$

V	=	Volume
S	=	Surface area

2.2.7 Electron microscopy

2.2.7.1 Scanning electron microscopy

The distribution of the cobalt through the catalyst particle was studied using a scanning electron microscope equipped with an energy-dispersed spectrometer (SEM/EDS). The calcined catalysts were molded into methyl methacrylate resin. The moulded samples were hardened by drying the resin and then polished in order to cut the catalysts particles in half.

2.2.7.2 Transmission electron microscopy

The transmission electron microscope photographs were obtained with a JEOL JEM 200CX microscope operated with a voltage of 200kV. The calcined catalysts were finely ground using a mortar. The fine particles were then wetted with distilled water. After drying, the samples were placed on a porous film (copper grids) coated with carbon. The photographs were then taken at a magnification of 100 000 times.

2.3 Fischer-Tropsch Synthesis

2.3.1 Description of the Fischer-Tropsch Apparatus

A flow sheet of the apparatus used to carry out the Fischer-Tropsch Synthesis is shown in Figure 2.3.1.

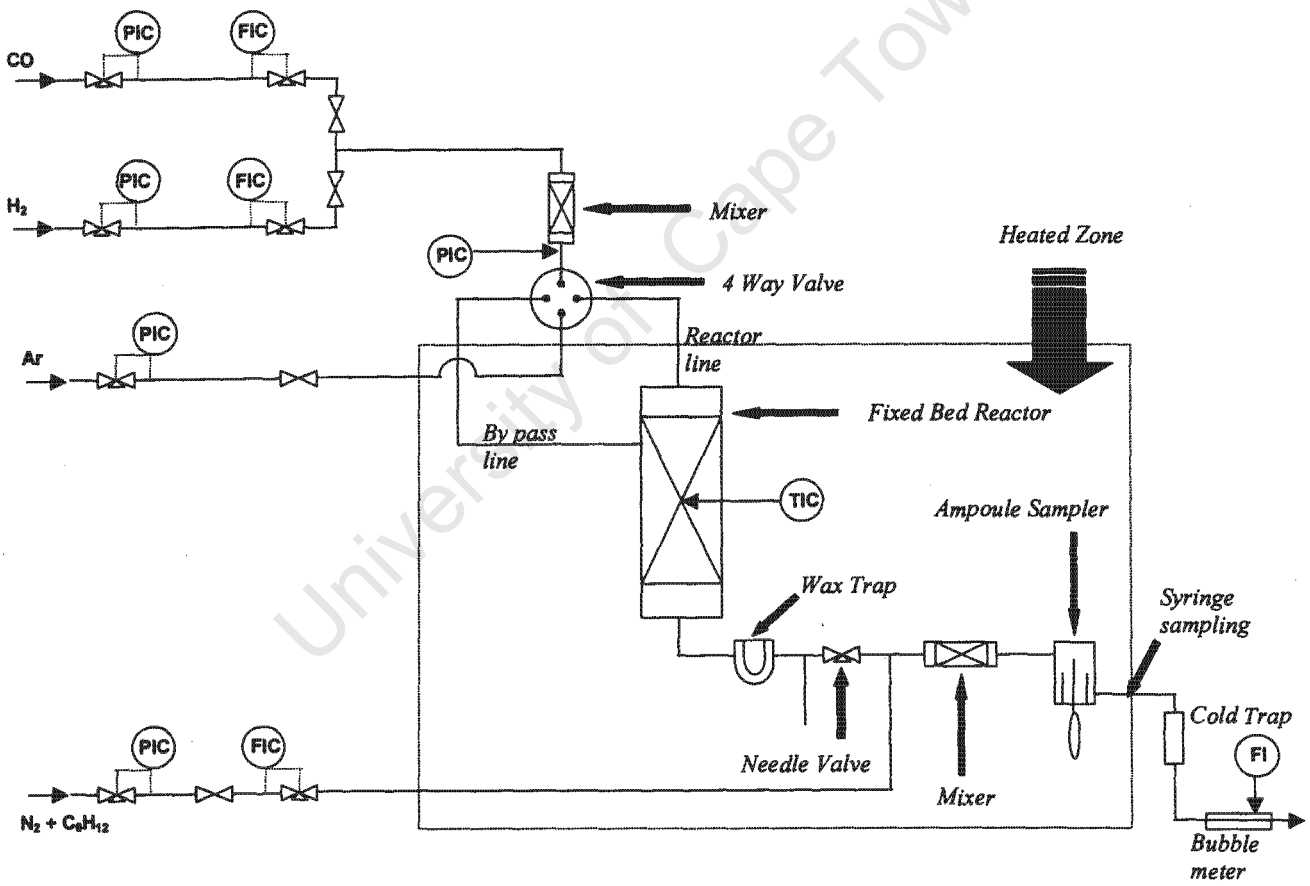

Figure 2.3.1: Flow sheet of fixed bed reactor.

The fixed bed reactor (see figure 2.8) consisted of a glass reactor (ID=10mm) placed with a stainless steel tube (ID= 30mm). The volumetric flow rates of the individual gases (H_2, CO and N_2 + cyclohexane) were controlled with thermal mass flow controllers (Brooks model

5850TR and unit instruments model UCF110061). Depending on the setting of the 4-way valve the two feed gases could either flow through the reactor or through the bypass.

At the exit of the reactor a wax trap is placed, where liquid reaction products are collected to avoid fouling of the needle valve, the mixer and of the exit lines. The reactor pressure can be kept constant by addition of an inert gas. After expansion of the product stream to atmospheric pressure, a reference gas stream (N_2 +C_6H_{12}) is added via a Brooks mass flow controller, and mixed with the product stream. After the needle valve a plug valve is used for pressure tests. The mixer is followed by an ampoule sampler, which allows gas samples to be taken. To maximise condensation of organic products a trap (at room temperature) was located between the ampoule sampler and the bubble meter.

The heating system was split into 3 separate zones the reactor; the wax trap and the exit lines, each of them with an individual temperature controller. The temperature of the catalyst bed was controlled by a thermocouple. For the FT experiments performed in this apparatus the reactor was heated to synthesis temperature of 220°C, the wax and the exit lines were maintained at 180°C and 190°C respectively.

Before commencing the Fischer-Tropsch experiments the apparatus was always pressure tested to verify absence of leaks.

2.3.2 Catalyst Loading in the FT Reactor

A catalyst containing 0.0484 g of cobalt metal was diluted with an inert material (nonporous SiC, Grid n° 46 = 400μm) in a weight ratio of 1:15 to minimise temperature gradients within the catalyst bed. 0.4ml of *iso*-propanol was added to the mixture and stirred in order to have a homogeneous distribution of the catalyst particles and SiC. Then the wet mixture was filled into the glass reactor of internal diameter (ID) = 10mm.

The packed bed was about 6cm, which corresponded to a catalyst bed volume of about 4.7 ml. The bed was placed in the isothermal zone of the reactor.

Glass beads were placed below and on top of the bed to serve as pre-heating zones. To keep the catalyst bed in place plug of silinized glass wool were placed at the bottom and top of the bed. The glass reactor was positioned in its stainless steal container and then in the furnace. The fixed bed reactor is illustrated in figure 2.3.2.

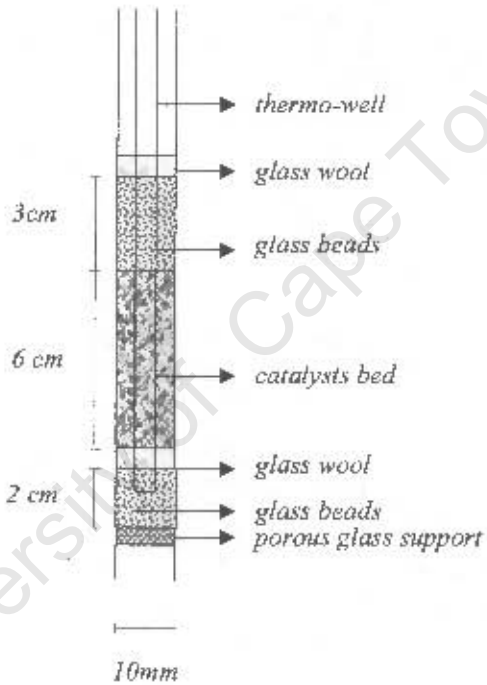

Figure 2.3.2: Fixed bed reactor.

The Temperature in the catalyst bed was measured by a thermocouple as shown in figure 2.3.3.

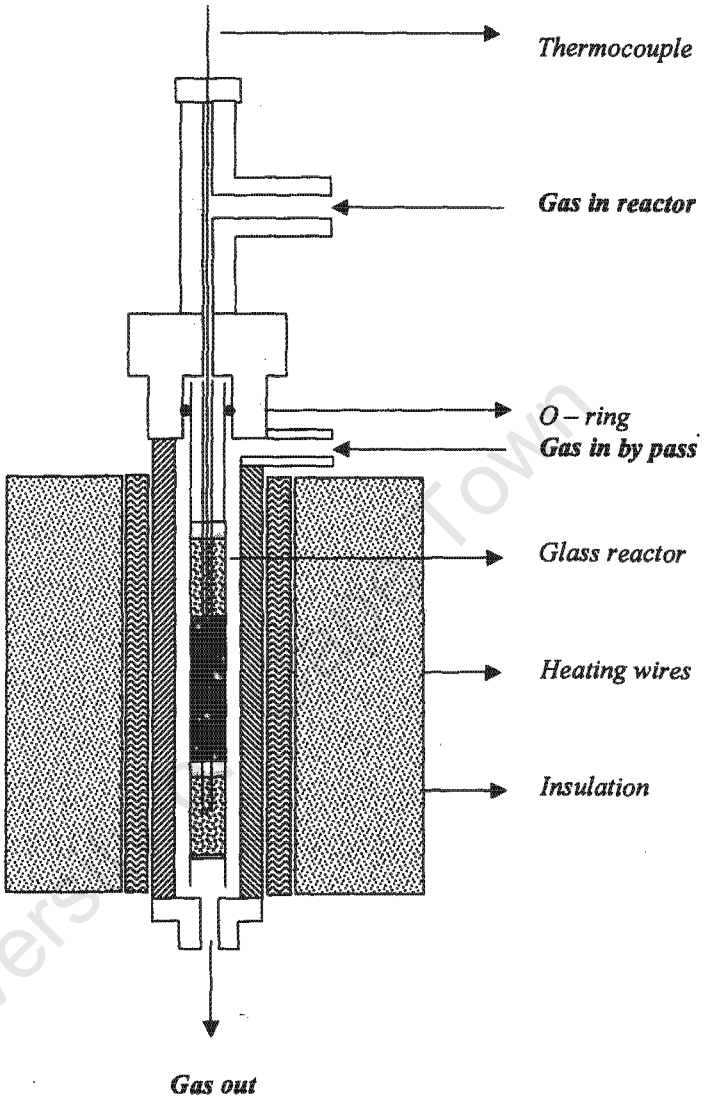

Figure 2.3.3: Reactor.

After the reactor was placed in the furnace the FT apparatus was leak tested pressurising the system to 20 bar with pure hydrogen. The reactor was left at this pressure for about 6hrs to see whether leaks were present.

2.3.3 The Fischer-Tropsch Synthesis Procedure

2.3.3.1 Drying

In order to eliminate the *iso*-propanol and the water present in the mixture (see section 2.3.2) of the catalyst and the SiC the reactor was heated up to 108°C at 2°C/min and held then for a further for 2 hrs under flowing argon of about 80ml(STP)/min.

2.3.2.2 Reduction

Once the catalyst was free of water and iso-propanol the reduction procedure was performed in order to reduce the cobalt oxide species to cobalt metal hydrogen was flowed through the catalyst bed at a rate of about 100ml(STP)/min. The temperature was ramped up to 360°C at 0.8°C/min and then held at 360°C for 14 hrs.

2.3.3.3 Fischer – Tropsch Synthesis

After reduction the reactor was cooled down to reaction temperature (220°C) under H_2. The reactor was then purged with argon (40 ml (STP)/ min) in order to eliminate the excess of H_2 in the reactor. Subsequently, the reactor was pressurised with argon to 15bar g. The flow of argon was controlled with the needle valve and measured with a bubble meter to allow a flow of 45ml (STP)/min

After facing the 4-way valve to the initial bypass synthesis gas was fed containing a flow of 18 ml H_2 (STP)/min and 9 ml CO (STP)/min. Both gases were mixed before they passed through the reactor. When the total flow remained approximately constant a flow of the internal standard (N_2 and cyclohexane) was introduced. Gas sampling took place using a Hamilton gas syringe with a capacity of 500µml. The gas samples were analysed straight away by gas chromatography. Once the desired flow was passing through the by pass the 4-way valve was switched to the glass reactor and the Fischer-Tropsch reaction could start. Gas

samples during the Fischer-Tropsch synthesis were taken at 2, 16, 24, 48 hrs and in some cases at 72hrs time on stream.

The H_2, CO, CH_4 and CO_2 contents of the exit gas were measured with a chromatograph using a TCD (thermal conductivity detector) while the hydrocarbon analyses were determined using FID (flame ionisation detector).

After completion of the experiment the 4-way valve was switched to bypass to recheck the feed gas analysis.
The same Fischer-Tropsch procedure was performed for all the catalysts tested.

2.3.4 Gas sample Analysis

Gas samples were taken using evacuated glass ampoules whose long capillary is pushed through a rubber septum into a guide tube of the ampoule breaker designed specially for this purpose. The ampoule is filled with gas by breaking the capillary tip of the ampoule with a fork, which is situated inside the ampoule sampler. Finally the ampoule is pulled slightly away of the sampler to be flame closed with a butane burner. In this way a representative gas sample at reaction conditions is taken and storable until it is analysed.

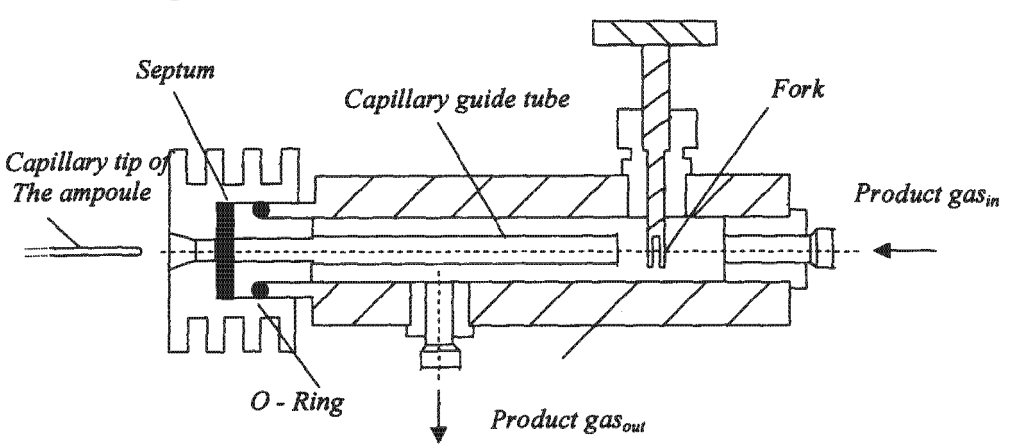

Figure 2.3.4: Ampoule sampler.

2.3.4.1 Analysis of inorganic gases (H_2, CO, N_2, CO_2) and methane

A gas chromatograph (Varian 4400) with a thermal conductivity detector and argon as carrier gas was used to analyse the inorganic gases (H_2, N_2, CO, CO_2) and methane in the synthesis gas and product gas. The sampling was carried out using a gas syringe (Hamilton) with a capacity of 500 μml.

The gas chromatograph was regularly calibrated with a mixture of a reference gas contained:

H_2	14.7%	CH_4	14.7%
CO_2	15.1%	N_2	15.2%
CO	15.5%	Ar	24.8%

The gas analyses were calculated using the correction factors required for quantification of the GC analysis.

Table 2.2.1 GC conditions for the analysis of inorganic gases and methane

Column	Length = 30.5m External diameter = 4.17 mm Material: Stainless steel Packing : Carbosieve S II
Detector	TCD
Carrier gas	Argon
Initial column temp	75°C
Initial column hold time	10.0 min
Injector temperature	150°C
Detector temperature	250 C
TCD A Filament temp.	285°C
TCD A Initial attenuation	8
TCD A Initial range	0.5
Method complete - end time	10.0 min

2.3.4.2 Analysis of organic products.

The organic products of the FT synthesis were analysed with a gas chromatograph Varian 4300 with a flame ionisation detector (FID). The GC was able to detect organic compounds such as paraffins, olefins, alcohols and aldehydes.

The ampoules containing the gas products are placed in the ampoule breaker of the GC, the column was cooled down to –68°C in order to have a satisfactory separation of the C_1, C_2, C_3 and C_4 fractions, thereafter the ampoule was smashed under a N_2 stream and the column consequently heated to 280°C. The organic products are separated in a 50m column with H_2 as the carrier gas and detected with a flame ionisation detector. The gas chromatograph was set-up as shown in table 2.2.2.

Table 2.2.2 GC conditions for the analysis of organic products

Column	Length = 50 m D = 0.25 mm d_{film} = 0.4 μm Packing coating = Dimethyl silicone
Injection gas	N_2
Temperature program	Initial column temp -68 °C Initial column hold time 5.00 min. • Program 1: Final col temp -35 °C. Col rate 15.0 °C/min. Col hold time 100 min. • Program 2: Final col. Temp -5 °C. Col rate 10.0 °C/min. Col hold time 2.5 °C/min. • Program 3: Final col. Temp 25, °C Col rate 2.5 °C/min. Col hold time 0.0 • Program 4: Final col temp 280 °C Col rate 5.0 °C/min Col hold time 60 min
Analysis Duration	120 min.
Detector	FID
Detector temperature	250 °C
Injector temperature	250 °C
Initial attenuation	1
Initial range	12
Initials relays	1234

Chapter III

3 Results and Discussion

3.1 Silica Supported Catalysts with Different Co Loadings

These catalysts with different cobalt loadings were prepared in a single impregnation step as is described in section 2.1.2.1.

3.1.1 Atomic Absorption Spectroscopy (AAS)

AAS was used to measure the catalysts composition with different cobalt levels. The cobalt content of each catalyst is summarized in table 3.1.1. For comparison purposes it was decided to analyse a catalyst provided by industry, named as the "standard" catalyst.

Table 3.1.1 Cobalt content of catalysts

Catalyst	wt(%) Co expected	wt(%) Co measured (AAS)
10gCo/100gSiO_2 1SCN	8.8	8.3
20gCo/100gSiO_2 1SCN	15.7	14.5
30gCo/100gSiO_2 1SCN	21.3	20.7
30gCo/100gSiO_2 (standard)	21.3	20.6

The results are expressed as weight percentage per mass of catalyst. As observed, there was a good agreement of the cobalt content expected and the cobalt content measured by AAS. The measured cobalt content was always somewhat less than expected. This difference can be attributed to the hygroscopic properties of the remaining undecomposed cobalt nitrate present in the catalysts. Cobalt nitrate absorbs water from the atmosphere at room temperature and this effect could result in lower cobalt content per mass of catalyst.

3.1.2 Temperature Programmed Reduction (TPR)

Figure 3.1.1 shows the TPR spectra for the catalysts 10, 20 and 30gCo/100gSiO_2. The TPR spectra are expressed by the percentage of H_2 converted as a function of temperature. The 10Co/100SiO_2 exhibited a small peak at 205°C, two peaks at 300 and 362°C and a flat reduction feature between 600 and 770°C. The presence of the small peak at 205°C can be explained as the reduction of undecomposed $Co(NO_3)_2$. Mass Spectrometer analysis has shown that $Co(NO_3)_2$ decomposes completely at 220°C [22]. After the complete decomposition of the $Co(NO_3)_2$ the peak at 300°C can be ascribed to the reduction,

$$Co_3O_4 + H_2 \rightarrow 3CoO + H_2O$$

This assumption agrees with previous work reported by Baerns [27]. The peak at 362°C can be assigned to the reduction,

$$CoO + H_2 \rightarrow Co^0 + H_2O$$

The last broad feature can be explained as the reduction of small quantities of the interaction of cobalt oxide species and the support *e.g.*, "cobalt silicates". The catalyst 20Co/100SiO_2 exhibited similar behaviour as the 10Co/100SiO_2. The peaks assigned to cobalt oxide reductions shifted to 305 and 370°C. The TPR profile for the catalyst 30Co/100SiO_2 was similar to the TPR profiles of the catalyst mentioned above. The reduction of Co_3O_4 and CoO appeared at 315 and 375°C respectively. The reduction of the "silicate" occurred between 590 and 740°C. Overall it appeared that the cobalt oxide reduction peaks shifted toward higher temperatures as the cobalt loading was increased. The second peak for 10Co/100SiO_2 appeared at 300°C, for the 20Co/100SiO_2 at 305°C and for the 30Co/100SiO_2 this peak is shifted to 315°C. The same effect was observed for the third peak, the temperature maxima shifted from 362 to 370 and 375°C for the catalysts 10, 20 and 30Co/100SiO_2. From CO chemisorption the average diameter of each cobalt particle after reduction was calculated to be 39.5, 43.2 and 50.0nm for the catalysts with 10, 20 and 30Co/100SiO_2. A possible explanation is that reduction proceeds via the shrinking core model. However, the results contradict what has been reported elsewhere [29].

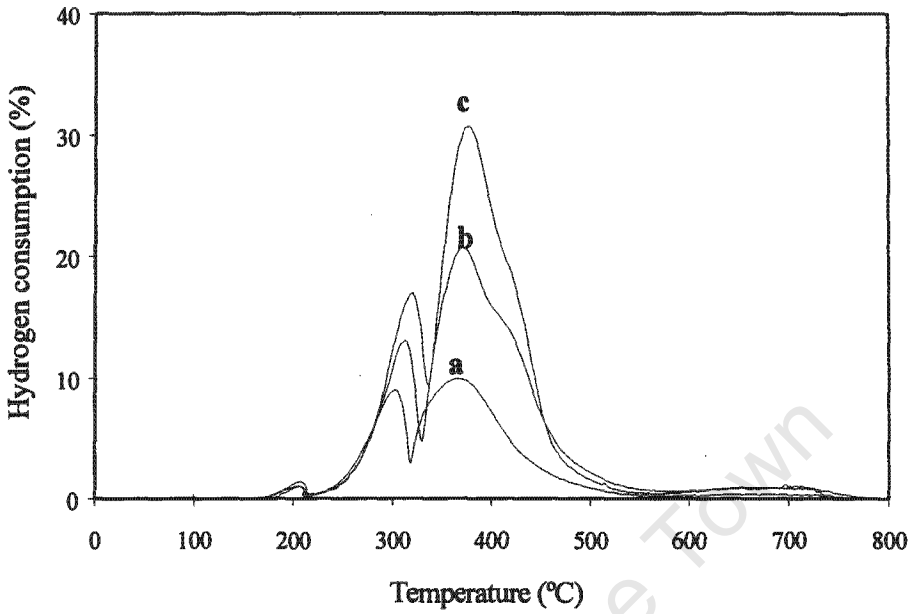

Figure 3.1.1: TPR profiles of catalysts with 10, 20 and 30gCo/100gSiO$_2$ 1SCN: **a.**-10gCo/100gSiO$_2$ catalyst. **b.**- 20gCo/100gSiO$_2$ catalyst. **c.**- 30gCo/100gSiO$_2$ catalyst.

According to the literature [29] the extent of reduction decreases with decreasing cobalt crystallite size. This was demonstrated using catalysts containing 3 and 9% Co on silica [29]. In the present studies the percentage of H_2 consumed for each peak related to the total H_2 consumption was similar for the three Co loading cases (see table 3.1.2). It was reported that after reduction well-dispersed cobalt catalysts contain a larger fraction of stable unreduced oxide phases [29]. From the present results it was observed that the H_2 consumption required to reduce the "silicate" peak for the three cases 10, 20 and 30Co/100SiO$_2$ was nearly the same. The percentage of H_2 consumed for the "silicate" peak over the total hydrogen consumed was 4.2, 5.0 and 3.5% for the three cases (see table 3.1.2).

Table 3.1.2 H_2 consumption of catalysts during reduction in TPR

Catalyst	Moles H_2 consumed x 10^{-3}/g.catalyst						% of H_2 consumed			
	peak				Total H_2 consumed measured	Total H_2 consumed expected	peak			
	1	2	3	4			1	2	3	4
10Co/100SiO$_2$ 1SCN	0.07	0.51	1.49	0.09	2.16	1.99	3.2	24	69	4.2
20Co/100SiO$_2$ 1SCN	0.06	0.97	2.76	0.20	3.99	3.56	1.5	24	69	5.0
30Co/100SiO$_2$ 1SCN	0.07	1.28	3.81	0.19	5.36	4.82	1.3	24	71	3.5
30Co/100SiO$_2$ (standard)	0.00	1.06	4.38	0.00	5.44	4.82	0.0	20	80	0.0

The total H_2 consumption expected was calculated on the assumption that all the cobalt was present as Co_3O_4 and that reduction to Co^0 was complete. XRD analyses confirmed that Co_3O_4 was the dominant phase present (see appendix III).

As expected the total H_2 consumption of catalysts 10, 20 and 30Co/100SiO_2 during reduction was proportional to the metal loading (see figure 3.1.2).

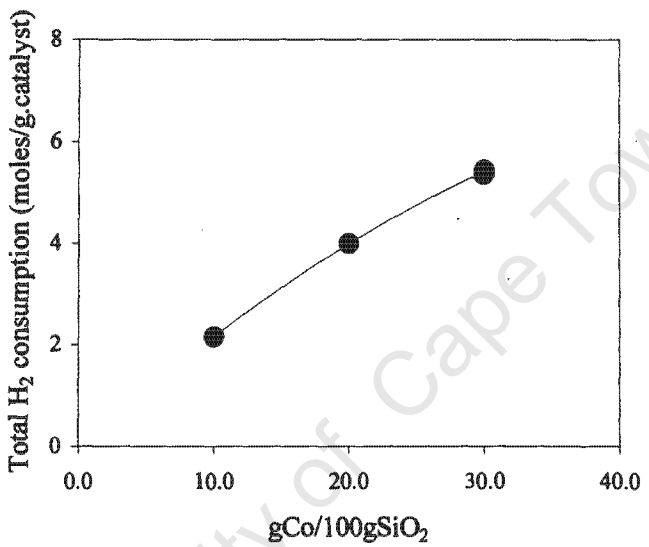

Figure 3.1.2: Correlation of total H_2 consumption and cobalt loading of catalysts 10, 20 and 30gCo/100gSiO_2.

3.1.3 CO Chemisorption

3.1.3.1 Metal Dispersion

The dispersion and the metal surface area were obtained after reduction in the chemisorption apparatus. The reduction conditions were similar as those in the FT reactor. The results obtained from the "strong" and "total" chemisorption gave a similar response. The results in table 3.1.3 are calculated from the "strong" chemisorption and those obtained from the "total" chemisorption analyses are listed in table 3.1.4. "Strong' and "total" chemisorption is discussed in section 2.2.5. Dispersion values were calculated as the percentage of the CO moles adsorbed over the moles of cobalt reduced. The metal surface area was calculated per gram of catalyst and also per gram of cobalt. The cobalt particle diameter was also calculated from the "strong" and "total" chemisorption data. Tables 3.1.3 and 3.1.4 summarise the strong and total chemisorption results of the 10, 20 and 30Co/100SiO_2 catalysts.

Table 3.1.3 Strong chemisorption of catalysts

Catalyst 1SCN	vol CO adsorbed (ml/g.reduced catalyst)	D (%)	m.s.a. (m^2/g.cat)	m.s.a. (m^2/g.Co)	p_d (nm)
$10Co/100SiO_2$	0.89	2.83	1.58	19.04	35.3
$20Co/100SiO_2$	1.27	2.30	2.26	15.59	43.2
$30Co/100SiO_2$	1.41	1.95	2.73	13.26	50.9

Table 3.1.4 Total chemisorption of catalysts

Catalyst 1SCN	vol CO adsorbed (ml/g.reduced catalyst)	D (%)	m.s.a. (m^2/g.cat)	m.s.a. (m^2/g.Co)	p_d (nm)
$10Co/100SiO_2$	1.25	3.97	2.22	26.75	25.2
$20Co/100SiO_2$	1.84	3.34	3.33	23.02	29.3
$30Co/100SiO_2$	2.06	2.72	3.80	18.38	36.7

D = Dispersion.
m.a.s. = Metallic surface area.
p_d = Cobalt average particle diameter.

From table 3.1.3 the dispersion values 2.83, 2.30 and 1.95% obtained form the "strong" chemisorption data decreased with increasing cobalt loading. A similar trend was also observed for dispersion values obtained from the "total" chemisorption data, see figure 3.1.3.

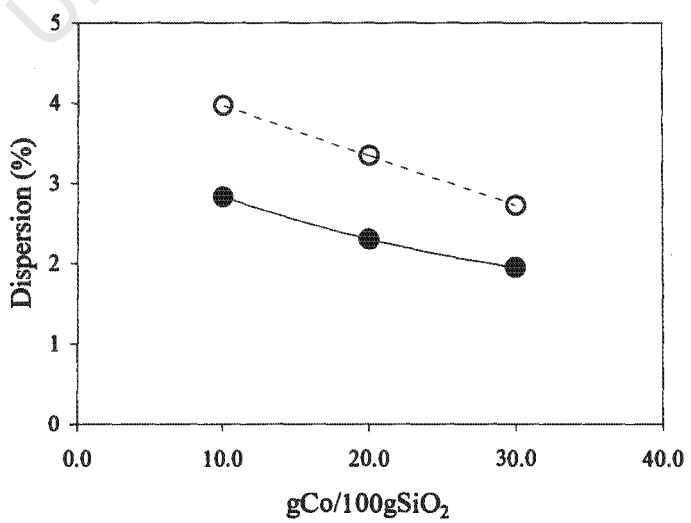

Figure 3.1.3: Dispersion of catalysts 10, 20 and $30gCo/100SiO_2$ as a function of cobalt content. Dispersion obtained from the "strong" (●) and "total" (○) chemisorption.

Backman reported that by preparing catalysts supported on silica with cobalt loadings of 5.9, 13.7 and 19.5%Co (wt%) the dispersion decreased from 15 to 2.6 to 1.7% [30]. Batholomew reported, using H_2 chemisorption measurements, that the dispersion did not change significantly on catalysts containing 3 and 10%Co (wt%). Dispersion values of 11 and 10% were found for catalysts containing 3 and 10%Co [29]. Using H_2 chemisorption a dispersion of 7.8% was obtained for silica supported catalyst containing 8%Co (wt%) [65]. Iglesia reported that from H_2 chemisorption at 100°C the dispersion decreases as the cobalt loading on silica was increased, see table 3.1.5 [12].

Table 3.1.5 Dispersion of catalysts [12].

Catalyst	Co (wt%)	Dispersion (%)
Co/SiO_2	32.1	0.45
	24.8	4.20
	23.1	3.20
	15.0	5.00
	14..0	1.90
	13.0	6.30
	10.3	9.50

The dispersions obtained in this thesis were lower than those found in the literature presumably due to different catalyst preparation and different chemisorption techniques. Bartholomew [29] prepared catalysts by impregnation, precipitation and by evaporative deposition. The catalysts used by Iglesia [12] were prepared by the incipient wetness impregnation technique. The catalyst with approximately 23 Co wt% [12] had similar dispersion percentage (3.2%) to our catalyst (D%=2.72) with more or less the same Co content, 20.7 Co wt% (see D% for catalyst $30Co/100SiO_2$ in table 3.1.4). The comments made previously (see page 50) regarding the calculations based on the CO chemisorption data should also be borne in mind.

3.1.3.2 Metal surface area

As expected the metallic surface areas per gram of reduced catalyst increased as the cobalt loading was increased. Using the "strong" chemisorption data the metal areas obtained were 1.58, 2.26 and 2.73 m^2/g.catalyst for the 10, 20 and $30Co/100SiO_2$ respectively. The metallic

areas per gram of cobalt however decreased with increasing cobalt loading, the resulting metallic areas were, 19.04, 15.59 and 13.26m^2/g.Co. As the dispersion decreased with increasing cobalt loading it means that the average cobalt particle size will increase and the metallic surface area per gram of cobalt will decrease as seen in tables 3.1.3 and 3.1.4.

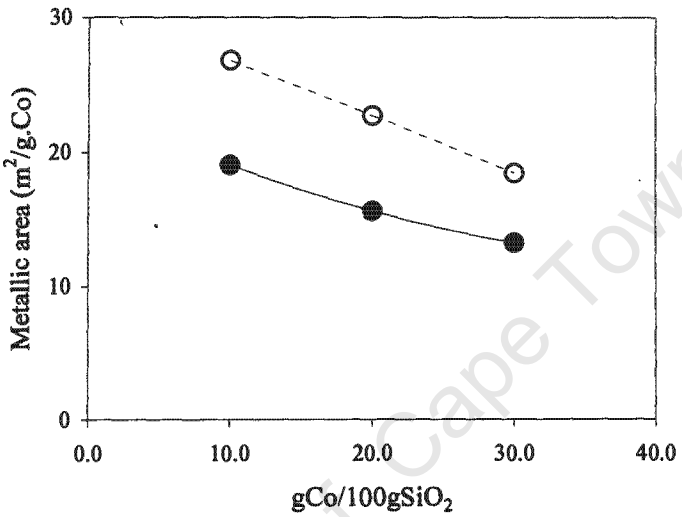

Figure 3.1.4: Metallic surface area/g.Co as a function of cobalt loading for the 10, 20 and 30gCo/100gSiO_2 catalysts. Dispersion obtained from the "strong" (●) and "total" (○) chemisorption.

3.1.3.3 Average particle diameter

The calculated average cobalt particle diameter increased as the cobalt loading increased. The particle diameter was calculated assuming that cobalt particles were spherical. The average particle diameters for the catalysts containing 10, 20 and 30gCo/100gSiO_2 were, 35.3, 43.2. and 50.9nm, calculated from the strong chemisorption data and from the total chemisorption data the values were, 25.2, 29.3 and 36.7nm respectively. Backman found that catalysts containing 5.9, 13.7 and 19.5%Co(wt%) had particle diameters in the order of 6.5, 36.0 and 56nm [30]. Kieneman [24] reported that catalysts supported on silica with cobalt loadings of 25, 39 and 64% (wt%) had Co_3O_4 particle sizes of 30.0, 28.0 and 40.5nm respectively. Iglesia [12] reported that catalysts supported on silica with Co loadings in the range of 10.2 to 32.1% (wt%) had average particle diameters from 10 to 210nm. Consequently, it was concluded that the average particle diameter of the cobalt will increase with increasing cobalt loadings [12].

3.1.4 BET Area

The measured BET surface areas of the unreduced catalysts are expressed as the area per gram of catalyst (table 3.1.6). The "expected" area per g. catalyst for each Co/SiO_2 catalyst were calculated on the assumption that the area of the Co_3O_4 was negligible (*i.e.*, expected area per g. catalyst is the area of 1.0g. SiO_2 multiplied by the $g.SiO_2/g.catalyst$ and the "expected" areas per $g.SiO_2$ were calculated from the "measured" surface areas (*i.e.*, the measured area of the catalyst divided by the g. SiO_2 per g. catalyst). The BET surface areas of the catalysts per gram of catalyst decreased as the cobalt content increased. This decrease in surface area is due to the fact that the content per gram of catalyst of the high area SiO_2 support decreases as the cobalt loading increases. The assumption that the area of the Co_3O_4 portion of the catalyst is low relative to that of the SiO_2 is supported by the finding that the calculated "expected" area is not markedly different for the measured areas and also by the finding that the calculated area per gram of SiO_2 component did also not change markedly. The small shift in area may, however, be explained as follows. As shown in figure 3.1.5b the surface area of the $catalyst/g.SiO_2$ for the 10 and $20gCo/SiO_2$ increased, this increment could be due to the extra surface area provided by cobalt oxides. The surface area of the silica support decreased from 286 to $269m^2/g.$ SiO_2 after loading the catalyst with 30g Co. This decrease in surface area per gram of silica could be attributed to pore blockages of the silica with cobalt oxides. This decrease in surface area is not dramatic, and possibly it is the starting point of blocking the silica pores with higher metal oxide loading. In agreement with the above findings Kienemmann [24] observed a loss of surface area after preparing SiO_2 supported catalysts with Co loadings of 25, 39 and 64Co% (wt%). The BET surfaces areas obtained for those catalysts were 293, 250 and $160m^2/g.$ catalyst.

Table 3.1.6 BET surface areas of catalysts

Catalyst	1 g. catalyst contains		BET Surface area measured ($m^2/g.cat$)	BET Surface area expected ($m^2/g.cat$)	BET surface area expected ($m^2/g.SiO_2$)
	Co_3O_4	SiO_2			
SiO_2 support (blank)	0.00	1.00	286	286	286
$10Co/100SiO_2$	0.11	0.89	265	254	298
$20Co/100SiO_2$	0.20	0.80	233	229	291
$30Co/100SiO_2$	0.28	0.72	194	206	269

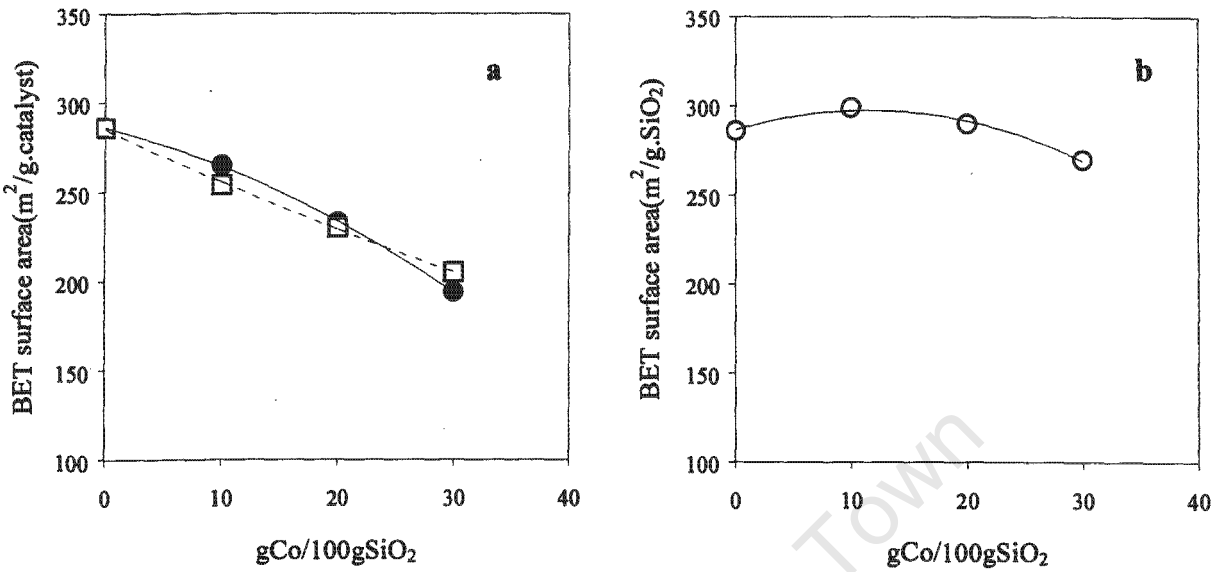

Figure 3.1.5: BET surface areas for the 10, 20 and 30gCo/100gSiO_2 catalysts. **a).-** BET surface area (m^2/g.catalyst). (●) Measured and (□) Expected. **b).-** BET surface area (m^2/g.SiO_2). (○) Measured.

3.1.5 FT Activity

3.1.5.1 Activity with time on stream (TOS)

The FT activity has been calculated from the CO converted during time on stream. Cobalt has a low activity for the water gas shift (WGS) reaction and hence CO_2 is not produced in large amounts as is the case for iron based catalysts. From the present studies, using 30Co/100SiO_2, CO_2 production was only detected at 2hrs on stream. The amount of CO_2 formed was only 0.05% of the total CO fed. The 10 and 20Co/100SiO_2 cases did not show production of CO_2 at any time. The FT reaction conditions were adjusted to 220°C, 15bar g and H_2/CO ratio =2, (H_2+CO) flow=28ml/min. From literature the specific activity of Co/SiO_2 catalysts prepared by impregnation methods increased with increasing metal loading from 3 to 10 wt%Co at operating conditions of 1bar, 225°C, H_2/CO=2 [29]. Bartholomew [29] observed that the larger the particle size, the higher the conversion was in a dispersion range between 0.25-86%. The supports used were, SiO_2, Al_2O_3, MgO and C. Kienemann [24] tested catalysts supported on silica with cobalt loadings of 25, 39 and 64wt%Co, the CO conversions increased from 10.8 to 23.4 to 38.5. The experimental conditions were 220°C,

20bar, H_2/CO ratio=2, syngas flowrate=2 *l* /h.g.catalyst. As expected from the above the present work showed that the FT activity was dependent on the metal loading, see figure 3.1.6 and table 3.1.7. Higher CO conversions were found for the catalysts containing higher metal loading. As can be seen from figure 3.1.6 there was a clear decline with TOS in all the cases.

Table 3.1.7 FT activity of catalysts

Catalyst	FT activity measured as CO converted (%)				
	Time on stream (hrs)				
	2	16	20	24	48
$10Co/100SiO_2$	17.1	14.2	9.1	12.5	7.6
$20Co/100SiO_2$	30.9	26.0	24.9	29.0	23.0
$30Co/100SiO_2$	39.4	41.4	37.0	39.7	29.0

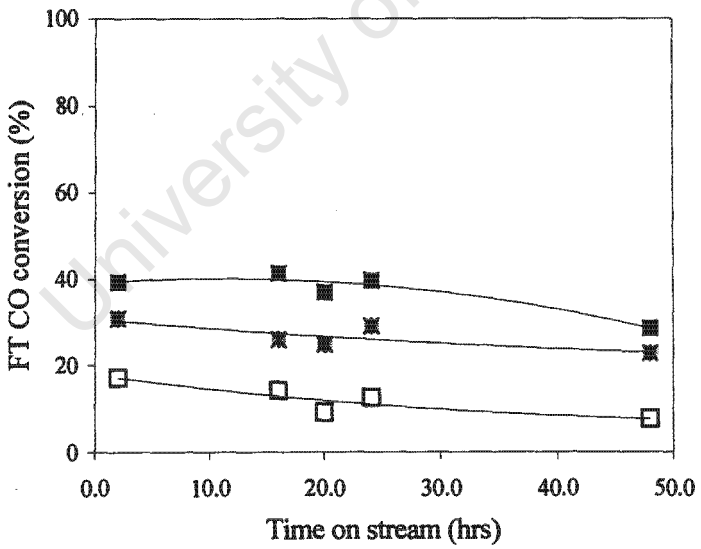

Figure 3.1.6: FT activities of 10, 20 and 30gCo/100gSiO2 catalysts. FT conditions, 220°C, 15bar g, $H_2/CO = 2$. Amount of metal area loaded in the reactor: 0.24, 0.50 and 0.71m^2.
(—□—)10gCo/100SiO_2, (—■—) 20gCo/100SiO_2 and (—■—)30gCo/100SiO_2

The loss in activity may be caused by the build up of liquid hydrocarbons in the pores which retards the "intraparticle" diffusion of H_2 and CO to the active Co metallic sites as well as by several other factors as discussed in section 1.2.4.

The FT activity of the above three catalysts correlated with the metal area exposed as shown in figure 3.1.7.

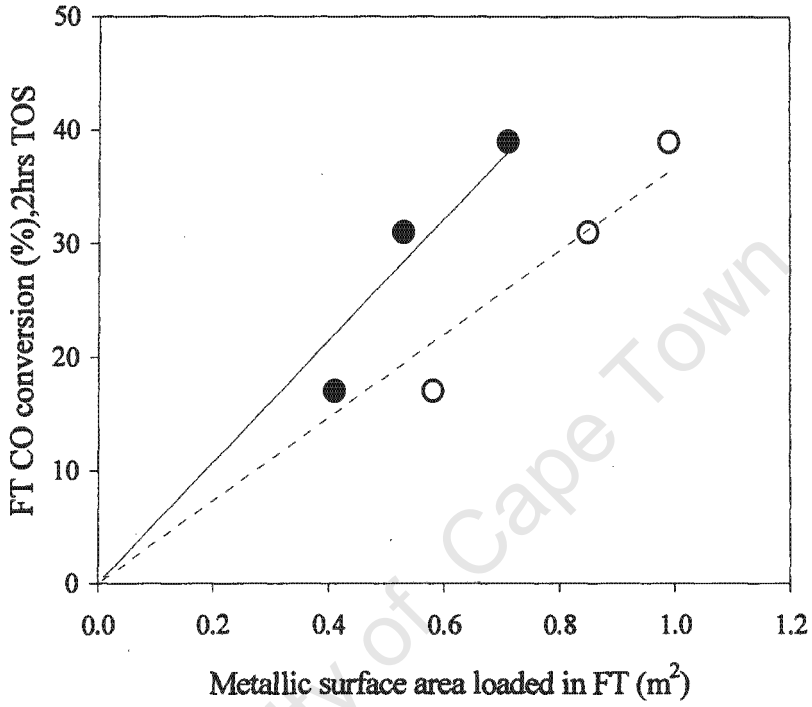

Figure 3.1.7: FT activity of catalysts 10, 20 and 30gCo/100gSiO_2 [measured as CO conversion (%)] at 2hrs on stream as a function of the metal area exposed, as quantified by "strong" (●) and "total" (○) CO chemisorption determination (see section 2.2.5).

There is a similar trend of the metal surface area loaded in the reactor calculated from the "strong" and "total" chemisorption data. For comparison purposes the FT conversion at 2hrs was plotted against the metallic area loaded in the FT reactor because the metallic area from CO chemisorption was measured straight after reduction. Iglesia [12] concluded that the FT rate per exposed Co atom depends only weakly on increasing cobalt loading and dispersion. This is not entirely unexpected because the surface structure does not change markedly in the dispersion range of 0.45-9.50% corresponding to catalysts supported on silica with cobalt loadings in the range of 10-54wt%Co [12]. Bartholomew [29] reported that the activity increased as the dispersion decreased, whereas Iglesia [12] reported the opposite. Iglesia [12] used catalysts with higher cobalt loading whereas Bartholomew [29] used catalysts with low cobalt loadings. Bartholomew suggested that when the cobalt crystallites are well dispersed Co is partially oxidised (poorly reduced).

3.1.5.2 Chain growth Probability

The chain growth probability was obtained from the slope of the plot of n against (logFn/n) for the hydrocarbon products between C_3 to C_{12} (see section 1.1.6). The α values obtained for the catalysts 10, 20 and 30Co/100SiO_2 are listed in table 3.1.8. The 10gCo/SiO_2 had lower alpha values but the 20 and 30gCo/SiO_2 catalysts appeared to have very similar alpha values. There were no significant changes in the H_2/CO ratios of the exit gases.

Table 3.1.8 Chain growth probability of catalysts.

Catalyst	Chain growth probability (α)				
	Time on stream (hrs)				
	2	16	20	24	48
10Co/100SiO_2	0.81	0.78	0.79	0.77	0.77
20Co/100SiO_2	0.84	0.83	0.84	0.85	0.84
30Co/100SiO_2	0.87	0.86	0.85	0.83	0.86

The finding that α increased with cobalt metal loading (table 3.1.8) is in keeping with previous studies by Batholomew who reported that the product selectivity of cobalt catalysts in CO hydrogenation was a function of metal loading [29]. The product selectivity shifted to higher molecular weight products as the metal loading was increased from 3 to 10%Co supported on silica. The product selectivity of the fraction C_1- C_3 was favoured with catalysts containing low cobalt loading (*e.g.,* 3%Co). The methane selectivity decreased with increasing cobalt loading and the C_5-C_{12} fraction selectivity increased from 15 to 42% with increasing Co loading from 3 to 10%. The FT reaction conditions were 225°C, 1bar, H_2/CO ratio=2 [29]. Chain growth probability was found to depend on the size and composition of Co crystallites *e.g.,* bigger crystallites gave higher molecular weight products [37]. Iglesia [12] studied Co/SiO_2 catalysts with cobalt loadings in the range 10.3 to 32.1 wt%Co. The catalysts were tested at 200°C, 20bar, H_2/CO ratio=2.1. CO conversions between 50-63%. The methane selectivity seemed to decrease with increasing metal loading. The C_5^+ selectivity did not show a significant variation [12].

Figure 3.1.8**a** gives a typical plot of selectivity against carbon number for the present study. Alpha (α) was obtained from the slope of log(Fn/n) against n as shown in figure 3.1.8b.

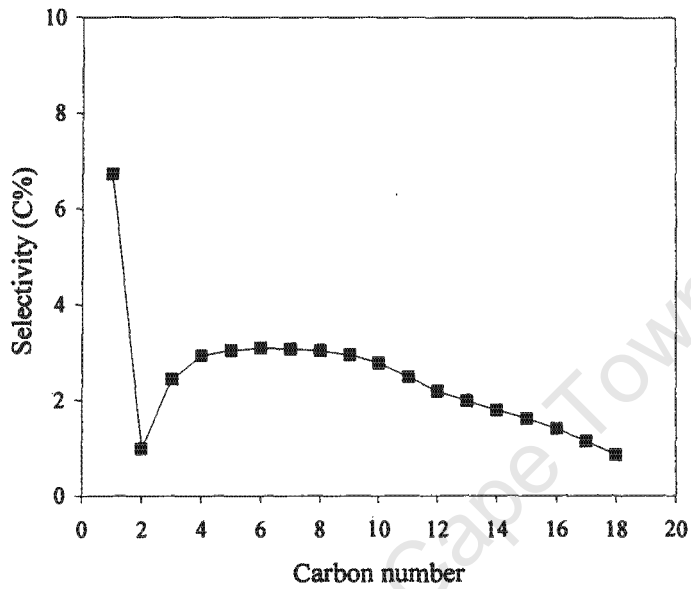

Figure 3.1.8. a: Selectivity of the 30gCo/100SiO_2 catalyst at 16-24hrs TOS. FT conditions, 220°C, 15bar g, $H_2/CO = 2$.

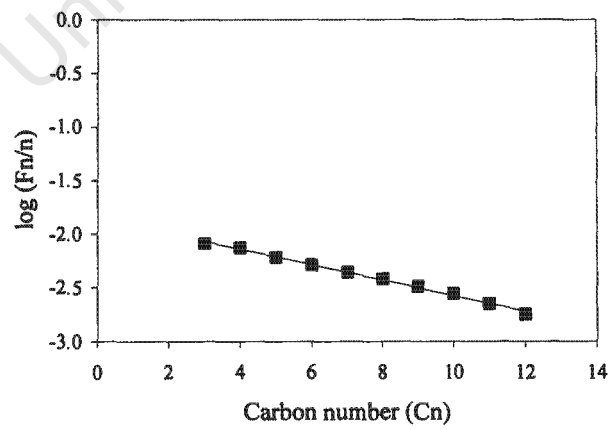

Figure 3.1.8. b: Chain Growth Probability of 30gCo/100SiO_2 catalyst at 16-24hrs TOS. FT conditions, 220°C, 15bar g, $H_2/CO = 2$.

The fraction of paraffins in the C_2 to C_7 hydrocarbons increased somewhat as the metal loading was increased, see table 3.1.9 and figure 3.1.9. In all cases the ratios also increased with increasing carbon number three and above (figure 3.1.9).

Table 3.1.9 Ratio of paraffins in the hydrocarbon fractions.

Catalyst	Paraffins/Total hydrocarbon					
	C_2	C_3	C_4	C_5	C_6	C_7
$10Co/100SiO_2$	0.49	0.24	0.25	0.31	0.30	0.40
$20Co/100SiO_2$	0.63	0.27	0.34	0.40	0.50	0.50
$30Co/100SiO_2$	0.63	0.32	0.39	0.42	0.50	0.50

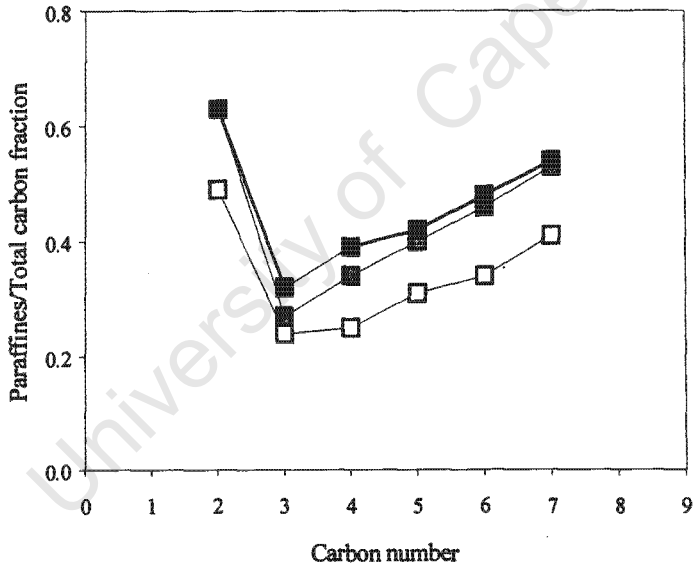

Figure 3.1.9: Ratio of paraffins over the total carbon fraction versus carbon number,. (—□—) $10gCo/100SiO_2$, (—■—) $20gCo/100SiO_2$ and (—■—)$30gCo/100SiO_2$ catalysts.

The increase in the paraffin ratios with increasing metal loadings implies that the system becomes more hydrogenating with increasing metal content. This appears to be in agreement with the findings of Bartholomew [29] who reported that the alcohol selectivity decreased with increasing metal loading using catalysts supported on silica with cobalt loadings of 3 and 10%. The alcohol selectivity decreased from 3.9 to 1.3%. From the present work, however, the alcohol selectivity expressed as the ratio of the alcohol over the total carbon fraction did not change significantly. For the C_2 the ratios encountered were 0.18, 0.19 and 0.16 for the catalysts containing 10, 20 and $30gCo/100g.SiO_2$.

3.2 Silica Supported Catalysts with Different Particle Sizes

3.2.1 Atomic Absorption Spectroscopy (AAS)

The catalysts composition of these samples prepared in a single step impregnation was measured using AAS analyses. The catalyst with particle sizes between 125-200μm was obtained by crushing the catalyst with particles sizes in the range of 250-400μm. The uncrushed catalyst was split into two portions, one portion was left uncalcined and the other one was subjected to calcination in nitrogen for 6 hrs at 270°C. The crushed sample was also calcined with the same conditions. The concentration of cobalt was expressed as weight percentage per mass of catalyst (see table 3.2.1). The measured weight percentage is slightly lower than the expected weight percentage. The hygrospcopic properties of the cobalt nitrate might have caused a decrease of cobalt content in the measured results or simply this difference was caused by experimental and systematic errors. The expected weight percentage was calculated on the assumption that the unreduced catalysts contained only Co_3O_4 species. The cobalt content should be the same for each case because the three catalysts were obtained from the same batch.

Table 3.2.1. Cobalt content of catalysts

Catalyst 1S	wt(%) Co expected	wt(%) Co measured (AAS)
30Co/100SiO$_2$		
125-200 μm calcined	21.3	20.6
250-400μm calcined	21.3	20.7
250-400μm uncalcined	21.3	20.7

3.2.2.- Temperature Programmed Reduction (TPR)

The catalyst reducibility was studied using temperature programmed reduction. The TPR measurements showed the reduction behaviour as a function of temperature. The total hydrogen consumption measured was obtained from the TPR spectrum. The total hydrogen

consumption expected was calculated on the assumption that Co was only present as Co_3O_4. The TPR measurements showed differences in the reduction behaviour of the calcined and the uncalcined samples (see figure 3.2.1). The uncalcined catalyst consumed more hydrogen during the reduction of the first peak at 205°C ascribed to the reduction of undecomposed cobalt nitrate (see table 3.2.2). The second peak probably attributed to the reduction of:

$$Co_3O_4 + H_2 \rightarrow 3CoO + H_2O$$

appeared at about 310°C for the uncalcined catalyst and at 315°C for the calcined catalyst. Hydrogen consumption during the reduction of the second peak was higher in the calcined sample. The reduction of the third peak ascribed to the reduction of:

$$CoO + H_2 \rightarrow Co^0 + H_2O$$

was seen at a maxima of 395°C for the uncalcined sample. For the calcined sample the peak shifted to a lower reduction temperature of about 375°C. The very small fourth peak suggested that the reduction of small amount of cobalt silicates appeared between 600-750°C for the calcined sample and from 600-775°C for the uncalcined sample. Backman [30] studied calcined and uncalcined Co/SiO_2 catalysts. On the calcined catalyst (19.5wt%Co) the peak assigned to the reduction of Co_3O_4 was seen at 325°C. The reduction of the "silicates" occurred at temperatures above 600°C. In the uncalcined catalyst the silicates started to reduce at temperatures higher than 650°C. Backman[30] suggested that the reductive decomposition of cobalt nitrate caused the formation of silicates. In the present work the TPR studies agreed with the observation seen by Backman, *e.g.*, the reductive decomposition of cobalt nitrate required more hydrogen consumption in the case of the uncalcined sample and the hydrogen consumed to reduce the "silicates" was also higher in the uncalcined sample (see table 3.2.2).

Backman [30] also found that the degree of reduction of the uncalcined catalyst was, in general higher than that of the corresponding calcined ones. In contradiction to this finding, in the present work, the calcined sample had a somewhat higher degree of reduction. Up to 550°C the degree of reduction of the uncalcined catalyst was 82.0% and that of the calcined catalyst was 96.5%.

Table 3.2.2. H_2 consumption of catalysts during reduction in TPR

Catalyst	Moles H_2 consumed x 10^{-3}/g.catalyst					% of H_2 consumed			
	peak				Total H_2 consumed measured	peak			
	1	2	3	4		1	2	3	4
30Co/100SiO$_2$									
250-400μm calcined	0.07	1.28	3.81	0.19	5.36	1.3	23.9	71.1	3.5
250-400μm uncalcined	0.28	1.19	3.61	0.44	5.52	5.0	21.6	65.4	8.0

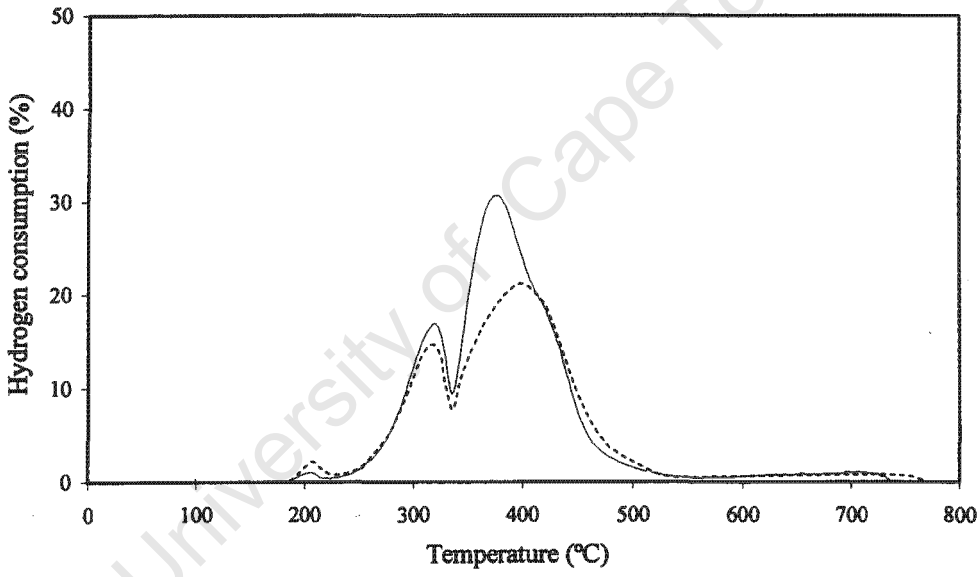

Figure 3.2.1: TPR profiles of 30gCo/100gSiO$_2$ catalysts. Hydrogen consumption (%) of the reducing mixture (6%H_2 in N_2) against temperature (°C). (————)250-400μm calcined and (- - - - - -)250-400μm uncalcined.

3.2.2 CO Chemisorption

3.2.2.1 Metal Dispersion

The dispersions and the metal surface areas were obtained after having reduced the catalysts in the chemisorption apparatus. The reduction in the chemisorption apparatus was carried out at 350°C for two hrs because the TPR profile (figure 3.2.2) of the 30gCo/100gSiO$_2$ calcined catalyst (250-400μm) showed complete reduction after 90min of the reduction procedure.

The temperature in the TPR system was raised from 100 to 350°C and kept at this temperature for about 2hrs.

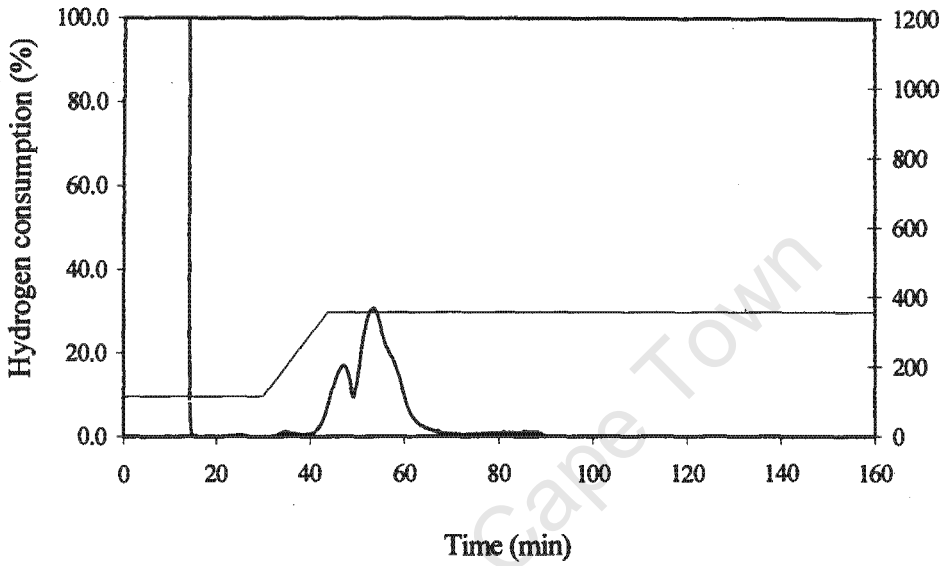

Figure 3.2.2: TPR profile of the 30gCo/100gSiO_2 calcined catalyst with particle sizes between 250 -400µm.

The results in table 3.2.3 were calculated from the "strong" chemisorption and those obtained from the "total" chemisorption analyses are listed in table 3.2.4. For more information "strong' and "total" chemisorption is discussed in section 2.2.5. Dispersion values were calculated as the percentage of the CO moles adsorbed over the moles of cobalt reduced. The metallic surface area was calculated per gram of catalyst and also per gram of cobalt. The cobalt particle diameter was also calculated from the "strong" and "total" chemisorption data.

Table 3.2.3 Strong chemisorption of catalysts

Catalyst	vol CO adsorbed (ml/g.reduced catalyst)	D (%)	m.s.a. (m^2/g.cat)	m.s.a. (m^2/g.Co)	p_d (nm)
30Co/100SiO_2					
125-200 µm calcined	0.63	0.80	1.13	5.44	123.9
250-400µm calcined	0.76	0.97	1.35	6.54	103.0
250-400µm uncalcined	0.58	0.74	1.04	5.00	134.8

Table 3.2.4 Total chemisorption of catalysts

Catalyst	vol CO adsorbed (ml/g.reduced catalyst)	D (%)	m.s.a. (m^2/g.cat)	m.s.a. (m^2/g.Co)	p_d (nm)
30Co/100SiO_2					
125-200 μm calcined	0.92	1.16	1.64	7.91	85.3
250-400μm calcined	1.09	1.39	1.94	9.38	71.9
250-400μm uncalcined	0.92	1.17	1.63	7.89	85.5

D = Dispersion.
m.a.s. = Metallic surface area.
p_d = Cobalt average particle diameter.

The calcined catalyst with particle sizes between 250-400μm showed the highest dispersion values. The calcined catalyst with particle sizes ranging from 125 to 200 μm and the uncalcined catalyst with particle sizes between 250-400μm had very similar dispersions. In general, the difference in dispersions between the three catalysts was not very marked.

It was reported in literature that when catalysts were prepared by incipient wetness impregnation with nickel nitrate and one sample was only dried at 120°C and the other one subsequently calcined at 400°C, the former appeared to have a higher dispersion than the calcined sample. From this, it could be suggested that, it is advantageous to use uncalcined samples [33]. In contradiction to this finding, in the present studies the uncalcined cobalt catalyst gave a somewhat lower dispersion than the calcined one. In keeping with the relatively small differences in the chemisorption data it was found that there was little, if any, difference in the FT activity of the two catalysts (see table 3.2.6 and figure 3.2.3).

3.2.2.2 Metal surface area

The metallic areas obtained from the "strong" chemisorption were 5.4 and 6.5 m^2/g.Co for the calcined catalysts (125-200μm and 250-400μm) and 5.0 m^2/g.Co for the uncalcined catalyst (250-400μm). The metallic areas calculated from the "total" chemisorption were 7.9, 9.4 and 7. 9m^2/g.Co in the same order for the catalysts mentioned above. Varying the catalysts preparation conditions, *e.g.,* making smaller particles sizes, calcining or not calcining the catalysts did not markedly affect the metal surface areas.

3.2.2.3 Average particle diameter

The particle diameter was calculated assuming that cobalt particles are spherical. The average particle diameters from the strong chemisorption corresponding to the calcined catalysts (125-200μm and 250-400μm) and to the uncalcined catalyst (250-400μm) were, 124, 103 and 134.8nm respectively. And the average particle diameters calculated from the total chemisorption were 85, 72 and 86 nm respectively.

Backman found that a catalyst containing 19.5wt%Co had a particle diameters of 56nm [30]. Kieneman [24] reported that a 25wt%Co catalyst supported on silica had Co_3O_4 particle sizes of 30nm. In the present studies the average particle diameters were larger than those catalysts reported in the literature.

In the present work, the 2hrs reduction in the chemisorption apparatus was apparently enough to reduce the catalysts. Later studies demonstrated that reducing the catalysts for 16 hrs more CO was adsorbed than when the reduction was only for 2 hrs. This might be one of the reasons why the average particle diameters of the metal were calculated to be greater than those reported in literature. It has to be pointed out that in the current studies, the comparison of the particle diameters was a relative comparison rather than an absolute one.

3.2.4 BET Area

The measured BET surface areas of the unreduced catalysts are expressed as the area per gram of catalyst and also as the area per gram of silica (table 3.2.5). The BET area per gram of catalyst and per gram of silica of both catalysts were practically the same. Obviously, the BET area per gram of silica is higher than that per gram of catalyst because in the latter case the high area silica is present in smaller quantities.

Table 3.2.5 BET surface areas of catalysts

Catalyst	1 g. catalyst contains		BET Surface area measured (m^2/g.cat)	BET Surface area expected (m^2/g.cat)	BET surface area expected (m^2/g.SiO_2)
	Co_3O_4	SiO_2			
SiO_2 support (blank)	0.00	1.00	286	286	286
30Co/100SiO_2					
125-200 μm calcined	0.28	0.72	193	206	268
250-400μm calcined	0.28	0.72	194	206	269

The measured as well as the two calculated expected areas were all the same. This is expected since the catalyst particles are from the same batch.

3.2.5 FT Activity

3.2.5.1 Activity with time on stream

The FT activity was calculated from the CO converted with time on stream. The FT reaction was performed at 220°C, 15bar g and H_2/CO ratio =2, (H_2+CO) flow= 28ml/min. From 2 to 24 hrs the FT activity of the 250-400μm calcined catalyst was higher than that of the 125-200μm calcined catalyst (see figure 3.2.3). If diffusion of the gases in and out of the catalyst particles were a factor then the activity of the smaller particles would have been expected to be higher. However since the opposite was the case the results show that diffusion rates were not a significant factor. At 48hrs the two calcined catalysts had similar activities. The small difference in the initial activities could be due to the differences in cobalt metal loaded and in the amount of cobalt metal area (see table 3.2.7).

The activity in each case declined with time on stream. The calcined catalyst with larger particle sizes deactivated faster than the one with smaller particle sizes. The deactivation of the 250-400μm calcined catalyst from 2 to 48hrs was about 26% whereas the deactivation of the 125-200μm calcined catalyst was about 14%. Similar FT activities were found for the uncalcined and calcined catalyst with particles sizes in the range of 250-400μm. Table 3.2.6 shows the catalysts FT activity.

Table 3.2.6 FT activity of catalysts

Catalyst	FT activity measured as CO converted (%)				
	Time on stream (hrs)				
	2	16	20	24	48
$30Co/100SiO_2$					
125-200 μm calcined	33.3	-----	34.1	33.9	30.4
250-400μm calcined	39.4	41.4	37.0	39.7	29.0
250-400μm uncalcined	38.9	40.2	36.8	38.6	29.3

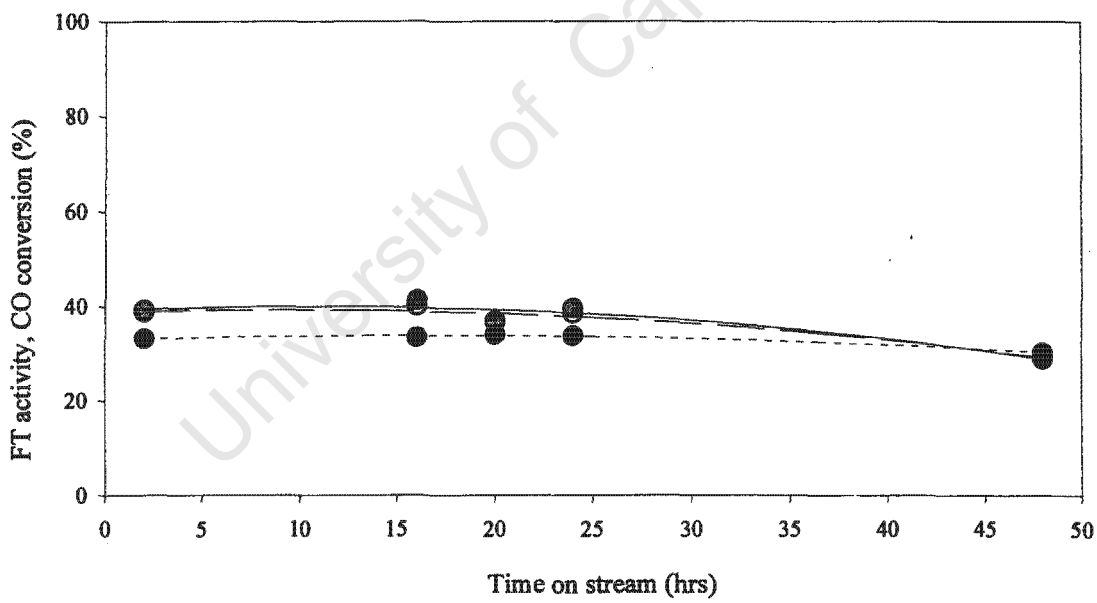

Figure 3.2.3: FT activities of $30gCo/100gSiO_2$ catalysts. FT conditions, 220°C, 15bar g, $H_2/CO = 2$.
(--●--)125-200 μm calcined, (—●—)250-400μm calcined and (---○---)250-400μm uncalcined.

The two cases with the same amount of cobalt metal loaded (56.8mg) had the same activity while the case with 53.6mg Co had a lower activity. Other things being equal these results are as one might expect. The chemisorption data for the 250-400μm uncalcined case, however, did not match the expectation that the lower the exposed Co metal area the lower the FT activity as was found for the first two cases in table 3.2.7.

Table 3.2.7 FT activity of catalysts

Catalyst	Metal loaded in FT reactor (mg)	FT activity measured as CO converted (%) at 2hrs TOS	Cobalt area loaded in the FT reactor (m^2)
$30Co/100SiO_2$			
125-200 μm calcined	53.6	33.3	0.29
250-400μm calcined	56.8	39.4	0.35
250-400μm uncalcined	56.8	38.9	0.27

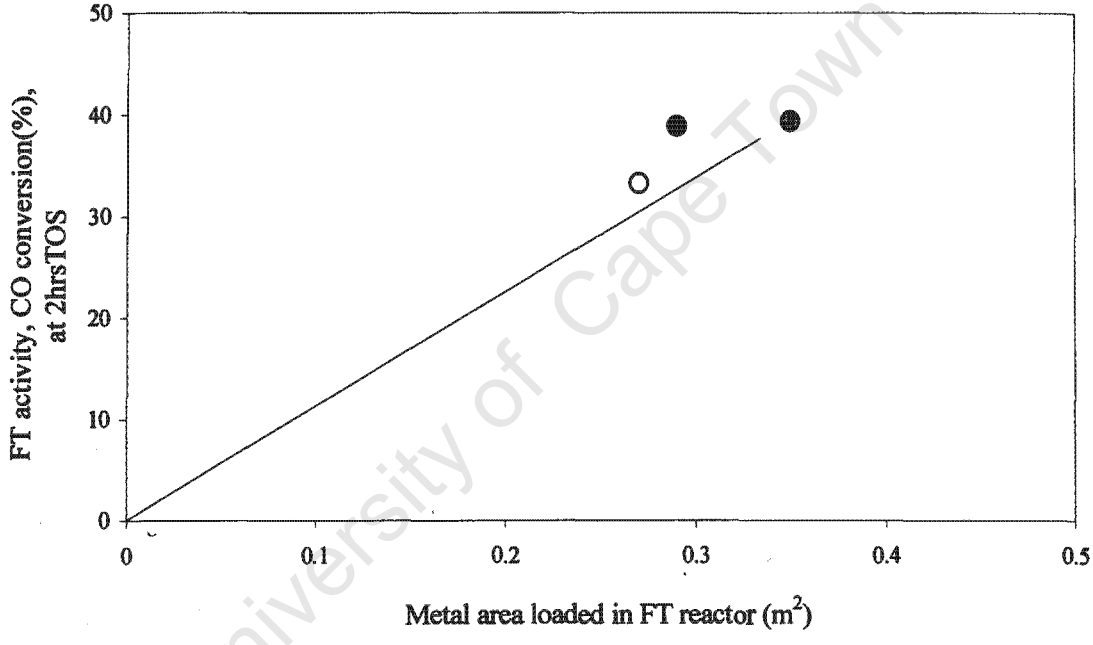

Figure 3.2.4: FT activity of $30gCo/100gSiO_2$ catalysts [measured as CO conversion (%) at 2hrs TOS as a function of the metal area exposed, as quantified by "strong" chemisorption. (--●--)125-200 μm calcined, (—●—)250-400μm calcined and (·····○·····)250-400μm uncalcined.

3.2.5.2 Chain growth Probability and Product Selectivity

The chain growth probability (α) was obtained from the slope of the plot of n against log(Fn/n) for the hydrocarbon products between C_3 to C_{12} (see section 1.1.6). The α values obtained for the calcined and uncalcined catalysts are listed in table 3.2.8. It was found that the α alpha value for the 250-400 μm uncalcined catalyst was lower than for the calcined

ones after two hours of FT synthesis but the data indicates that differences at longer TOS were not as marked.

Table 3.2.8 Chain growth probability of catalysts.

Catalyst	Chain growth probability (α)				
	Time on stream (hrs)				
	2	16	20	24	48
30Co/100SiO$_2$					
125-200 μm calcined	0.82	-----	-----	0.85	0.83
250-400μm calcined	0.87	0.86	0.85	0.83	0.86
250-400μm uncalcined	0.77	-----	0.83	0.81	-----

The fraction of paraffins in the C_2 to C_7 hydrocarbons were similar for the 125-200μm calcined catalyst and for the 250-400μm uncalcined catalyst. The 250-400μm calcined catalyst showed lower values of paraffins/total hydrocarbon ratios from the C_3 fraction onwards (see table 3.2.9 and figure 3.2.5). As can be seen in figure 3.2.5 the ratios from C_3 onwards increased constantly with carbon number for all three cases.

Table 3.2.9. Ratio of paraffins in the hydrocarbon fraction.

Catalyst	Paraffins/Total hydrocarbon					
	Carbon fraction					
	C_2	C_3	C_4	C_5	C_6	C_7
30Co/100SiO$_2$						
125-200 μm calcined	0.60	0.40	0.45	0.50	0.57	0.65
250-400μm calcined	0.63	0.32	0.39	0.42	0.48	0.54
250-400μm uncalcined	0.61	0.35	0.42	0.49	0.57	0.65

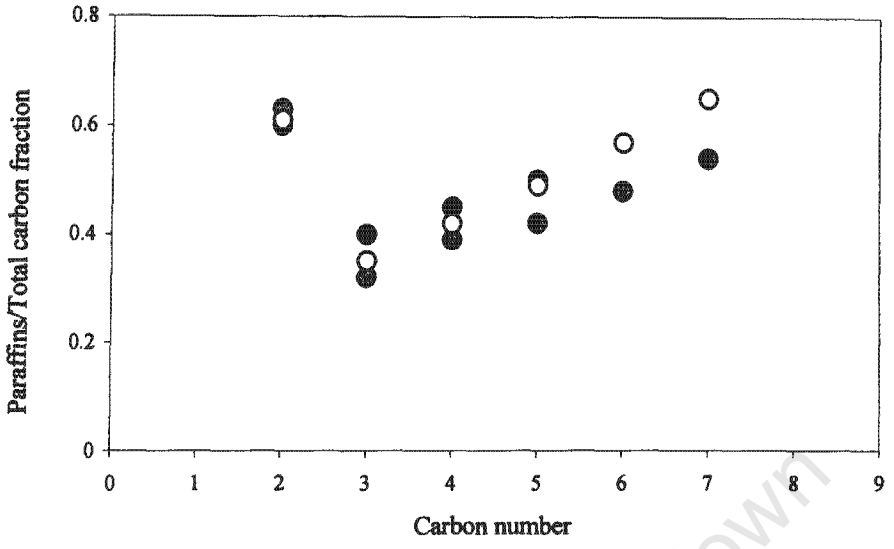

Figure 3.2.5: Ratio of paraffins over the total carbon fraction versus carbon number. (—●—)125-200 μm calcined. (—●—)250-400μm calcined and (—○—)250-400μm uncalcined.

The ratios of linear 1-Cn olefins over the total olefins produced per hydrocarbon fraction are shown in table 3.2.10. There appears to be no real differences between the three cases.

Table 3.2.10 Ratio of linear 1-Cn olefins over total olefins

Catalyst	Linear 1-Cn olefins/Total olefins					
	Carbon fraction					
	C_4	C_5	C_6	C_7	C_8	C_9
30Co/100SiO$_2$						
125-200 μm calcined	0.83	0.99	0.74	0.66	0.60	0.50
250-400μm calcined	0.91	0.89	0.87	0.83	0.69	0.52
250-400μm uncalcined	0.95	0.83	0.76	0.64	0.60	0.49

Ethanol and acetaldehyde were the most abundant alcohol and aldehyde species produced but there were no significant differences in the ratios of these compounds to the total C_2 hydrocarbons for the three catalysts tested. For ethanol the ratios were all 0.06 ± 0.01.

3.3 Single and Multi-step Cobalt Addition on Silica Supported Catalysts

3.3.1 Atomic Absorption Spectroscopy (AAS)

The metal content in the catalyst was measured using AAS. The concentration of cobalt was expressed as weight percentage per mass of catalyst. The expected wt%Co was calculated on the assumption that on the unreduced catalysts Co was present as Co_3O_4 species. The assumption was based on XRD analyses, which confirmed that Co_3O_4 was the most abundant phase present. The measured cobalt content is lower than the expected measurements for all cases. The difference between the expected and the measured concentrations were not of considerable extent. Table 3.3.1 lists the expected and the measured Co concentrations.

Table 3.3.1 Cobalt content of catalysts

Catalyst	wt(%) Co expected	wt(%) Co measured (AAS)
20Co/100SiO$_2$		
1-step	15.7	14.5
2-steps	15.7	14.6
30Co/100SiO$_2$		
1-step	21.3	20.7
3-steps	21.3	20.7
3-steps ®	21.3	20.7
6-steps	21.3	20.8

® = Repeat preparation

3.3.2 Temperature Programmed Reduction (TPR)

Table 3.3.2 and figure 3.3.1 show the hydrogen consumed and the reduction behaviour of two catalysts containing the same amount of cobalt, 30gCo/100gSiO_2. The first catalyst was prepared by impregnating the silica support with the Co precursor in a 1-step process and the

second one by impregnation of the support with a three fold diluted Co precursor in a 3-step impregnation process.

The total hydrogen consumed for both catalysts were almost identical. The catalyst prepared in 1-step consumed $5.36x10^{-3}$ moles of H_2/g.catalyst and the one impregnated in 3-steps $5.33x10^{-3}$ moles H_2/g.catalyst. The reduction profiles of both catalysts were fairly similar. The first peak ascribed to the reduction of cobalt nitrate appeared at 205°C for both cases. The second peak attributed to the reduction of:

$$Co_3O_4 + H_2 \rightarrow 3CoO + H_2O$$

was seen at about 320°C for both catalysts. The third peak assigned to the reduction of:

$$CoO + H_2 \rightarrow Co^0 + H_2O$$

was observed at 380°C for the catalyst prepared in 1-step. In the case of the 3-step catalyst the peak was broader and shifted to a lower reduction temperature of about 370°C. Finally the very small peak suggested to be the reduction of cobalt silicates appeared from 600 to 730°C.

Table 3.3.2 H_2 consumption of catalysts during reduction in TPR

Catalyst	Moles H_2 consumed x 10^{-3}/g.catalyst					% of H_2 consumed			
	peak				Total H_2 consumed measured	peak			
	1	2	3	4		1	2	3	4
30Co/100SiO$_2$									
1-step	0.07	1.28	3.81	0.19	5.36	1.3	23.9	71.1	3.5
3-step	0.08	1.24	3.74	0.27	5.33	1..5	23.3	70.2	5.1

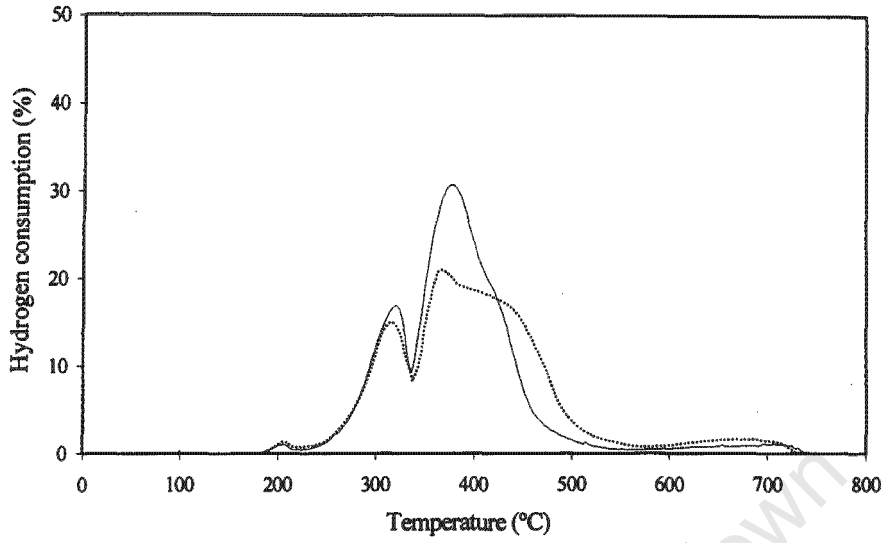

Figure 3.3.1: TPR profiles of 30gCo/100gSiO$_2$ catalysts. Hydrogen consumption (%) of the reducing mixture (6%H$_2$ in N$_2$) against temperature (°C). (——) 1-step 30gCo/100SiO$_2$ and (·····) 3-step 30gCo/100SiO$_2$.

3.3.2 CO Chemisorption

3.3.2.1 Metal Dispersion

The catalysts dispersions and the metal surface areas were obtained after reduction of the catalysts in the chemisorption apparatus. The reduction in the chemisorption apparatus was carried out at the same conditions as conducted in the FT reactor, 350°C for 16 hrs.

Tables 3.3.3 and 3.3.4 list the results obtained from the "strong" and "total" chemisorption measurements.

Dispersion values were calculated as the percentage of the CO moles adsorbed over the moles of cobalt reduced. The metallic surface areas were calculated per gram of catalyst and also per gram of cobalt.

In an attempt to study whether the catalysts prepared in multi-impregnation steps could give higher dispersions than the one prepared in a single step, a number of catalysts were prepared (see section 2.1.2.3). The 20gCo/100SiO$_2$ catalysts were prepared in a single and a double impregnation. The 30gCo/100SiO$_2$ catalysts were obtained by impregnation in 1, 3 and 6 steps.

Table 3.3.3 Strong chemisorption of catalysts

Catalyst	vol CO adsorbed (ml/g.reduced catalyst)	D (%)	m.s.a. (m^2/g.cat)	m.s.a. (m^2/g.Co)	p_d (nm)
20Co/100SiO$_2$					
1-step	1.27	2.30	2.26	15.59	43.2
30Co/100SiO$_2$					
1-step	1.41	1.79	2.51	12.11	55.7
3-steps	1.54	1.95	2.73	13.26	51.0
3-steps ®	1.28	1.65	2.31	11.16	60.4
6-steps	1.33	1.68	2.36	11.42	59.1

Table 3.3.4 Total chemisorption of catalysts

Catalyst	vol CO adsorbed (ml/g.reduced catalyst)	D (%)	m.s.a. (m^2/g.cat)	m.s.a. (m^2/g.Co)	p_d (nm)
20Co/100SiO$_2$					
1-step	1.85	3.34	3.34	23.02	29.3
30Co/100SiO$_2$					
1-step	2.06	2.72	3.67	17.73	38.0
3-steps	2.32	2.95	4.12	19.90	33.9
3-steps ®	1.88	2.39	3.34	16.16	41.7
6-steps	1.94	2.45	3.45	16.68	40.4

D = Dispersion.
m.a.s. = Metallic surface area.
p_d = Average particle diameter of cobalt metal.
® = Repeat preparation.

Of the 30Co/100SiO$_2$ catalysts the 3-step case appeared to be the most dispersed. To check this, the catalyst was prepared again and named the 3-step® 30gCo/100gSiO$_2$ catalyst. The dispersion for the repeat preparation was lower and more in line with the dispersions of the other preparations. The reason for the higher dispersion of the first 3-step preparation was unclear. Possibly the impregnation temperature was higher. The dispersion obtained for the 1- and 6-steps catalysts were expected but the one for the 3-step catalyst was not expected. The high dispersion of the 3-step catalyst was apparently due to the impregnation of the cobalt solution on heated alumina support (see section 3.8, dealing with the effect of the impregnation temperature).

3.3.3.2 Metal surface area

The metallic surface areas obtained for the $30Co/100SiO_2$ catalysts were not distinctly different. Values of 2.5, 2.7, 2.3 and 2.4 m^2/g.catalyst were calculated from the strong chemisorption data. The resulting metallic surface areas calculated in m^2/g. Co were 12.1, 13.3, 11.2 and 11.4 for the 1, 2, 3, 3® and 6 steps catalysts respectively. Comparing the metallic surface areas obtained from the "strong" and "total" chemisorption the catalyst prepared in 3-steps gave higher metallic surface areas than those prepared in 1, 3® and 6 steps (see tables 3.3.3 and 3.3.4). Note that the BET area of the 3-step case was also somewhat higher than the others (see 3.1.4). Except for the one unexplained 3-step case the catalysts prepared in a single or in multi-impregnation steps gave similar metallic surface areas.

3.3.3.3 Average particle diameter

Preparing the catalysts with different number of impregnation steps did not play an important role except for the catalyst prepared in a 3-step impregnation process. The average particle diameters calculated from the "strong" chemisorption for the 1-step, 3-step, 3-step® and 6-step catalysts were 56, 51, 60 and 59nm and those calculated from the "total" chemisorption 38, 34, 42 and 40 nm. Once again, the particle diameters are similar except for the one prepared in 3-steps.

3.3.4 BET Area

The BET areas of the unreduced catalysts are shown in table 3.3.5. The two sets of "expected" areas were as explained in 3.1.4.

Table 3.3.5 BET surface areas of catalysts

Catalyst	1 g. catalyst contains		BET Surface area measured (m^2/g.cat)	BET Surface area expected (m^2/g.cat)	BET surface area expected (m^2/g.SiO_2)
	Co_3O_4	SiO_2			
SiO_2 support (blank)	0.00	1.00	286	286	286
20Co/100SiO_2					
1-step	0.20	0.80	233	230	290
2-steps	0.20	0.80	235	230	293
30Co/100SiO_2					
1-step	0.28	0.72	194	205	269
3-steps	0.28	0.72	207	205	288
3-steps ®	0.28	0.72	196	205	273
6-steps	0.28	0.72	196	205	273

The "measured" BET areas (m^2/g.catalyst) of the 1-step and 2-step 20gCo/100SiO_2 catalysts were the same. The same conclusions were arrived at for the four 30Co/100SiO_2 preparations. Only the "3-step" case had a somewhat higher area. Overall it was concluded that the number of impregnation steps did not significantly influence the BET areas of the calcined catalysts. This is, as one would expect if the area of the Co oxide was low relative to that of the SiO_2 support.

3.3.5 FT Activity

3.3.5.1 Activity with time on stream TOS

The catalysts were evaluated in terms of their activity in a fixed bed reactor. The FT reaction was performed at 220°C, 15bar g and H_2/CO ratio =2, (H_2+CO) flow rate =28ml/min. The activity was calculated from the CO converted at different intervals. Table 3.3.6 summarises the FT activity of the 20 and 30Co/100SiO_2 catalysts prepared by impregnation in 1, 2 and 1, 3 and 6-steps respectively. The results are also plotted in figure 3.3.2. Assuming that the results at 24 h for the 1-step and at 48 h for the 2-step cases were suspect it appears that the performance of the 1 and 2 step cases were similar for the 20Co/100SiO_2 catalyst. For the

$30Co/100SiO_2$ series the activity of the 3-step case appeared to be markedly superior to those of the other preparations. In order to check this result another sample was prepared and named as 3-step® $30Co/100SiO_2$ catalyst. The obtained activity was lower than that of the previous preparation but was more in keeping with the other cases. The reason for the higher activity of the first 3-step case is probably due to its higher metal surface area (*i.e.* higher dispersion, see section 3.3.2.1).

Table 3.3.6 FT activity of catalysts

Catalyst	FT activity measured as CO converted (%)				
	Time on stream (hrs)				
	2	16	20	24	48
$20Co/100SiO_2$					
1-step	30.9	26.0	24.9	29.0	23.0
2-steps	32.3	27.1	25.5	24.9	18.8
$30Co/100SiO_2$					
1-step	39.4	41.4	37.0	39.7	29.0
3-steps	52.4	51.6	48.8	47.8	44.4
3-steps ®	34.8	32.0	30.2	28.5	------
6-steps	33.9	31.5	30.9	30.3	26.2

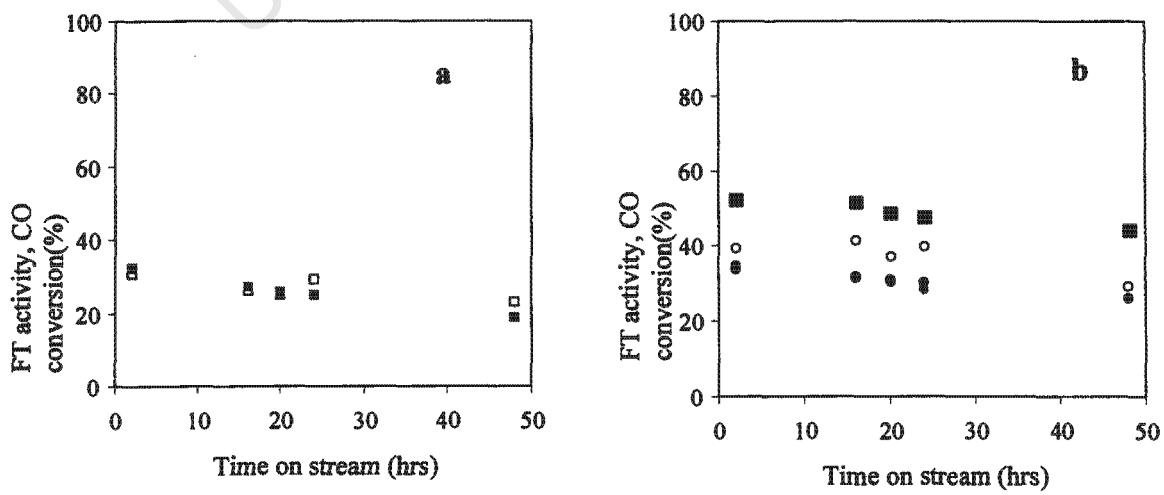

Figure 3.3.2 : FT activities of catalysts against time on stream TOS. FT conditions, 220°C, 15bar g, H_2/CO=2. **a)** (□) 1-step $20gCo/100gSiO_2$, (■) 2-step $20gCo/100gSiO_2$ **b)** (○) 1-step $30gCo/100gSiO_2$, (●) 3-step $30gCo/100gSiO_2$, (●) 3-step® $30gCo/100gSiO_2$, (●) 6-step $30gCo/100gSiO_2$.

Figure 3.3.3 shows that the catalysts' activities apparently were dependent on the metal area loaded in the FT reactor. The 3-step $30Co/SiO_2$ catalysts had the highest activity and the largest metal area available. In general these findings were as one would expect, namely that the activity of the catalysts would not only be dependent on the mass of cobalt on the catalyst but also on how effectively the metal was dispersed on the support.

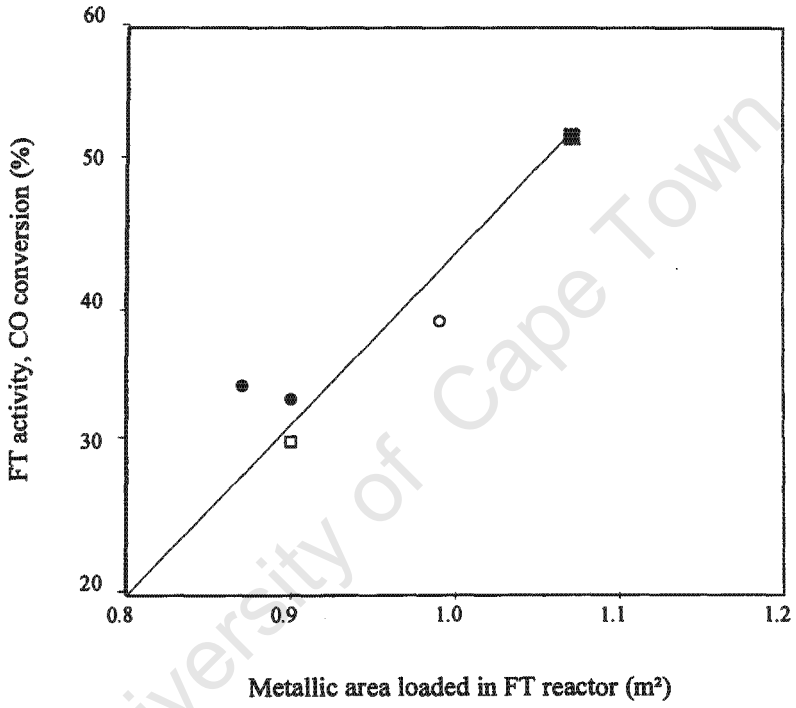

Figure 3.3.3: FT activity of catalysts measured as CO conversion(%) at 2hrs TOS as a function of metallic area exposed (obtained from the "total" chemisorption). (□) 1-step $20gCo/100gSiO_2$, (○) 1-step $30gCo/100gSiO_2$, (■) 3-step $30gCo/100gSiO_2$, (●) 3-step® $30gCo/100gSiO_2$ and (●) 6-step $30gCo/100gSiO_2$.

3.3.5.2 Chain growth Probability and Product Selectivity

The chain growth probability (α) was calculated from the slope of the ASF plot of n against log(Fn/n) for the hydrocarbon products between C_3 to C_{12} (see section 1.1.6). The α values obtained are given in table 3.3.7. The α alpha values for the 1-step and 2-step $20Co/100SiO_2$ catalysts were very similar. The α alpha values obtained for the 1-step, 3-step, 3step® and 6-step $30Co/100SiO_2$ catalysts are also generally similar except for the 3-step® at 2hrs TOS

and the 1-step catalyst at 24 hrs, which were slightly lower. Overall the impression gained is that the number of impregnation steps used had little effect if any influence in the α values, nor did the amount of exposed Co metal (or activity) have any influence.

Table 3.3.7 Chain growth probability of catalysts

Catalyst	Chain growth probability (α)				
	Time on stream (hrs)				
	2	16	20	24	48
20Co/100SiO$_2$					
1-step	0.84	0.83	0.84	0.85	0.84
2-steps	0.85	0.85	0.85	0.83	0.84
30Co/100SiO$_2$					
1-step	0.87	0.86	0.85	0.83	0.86
3-steps	0.85	0.86	0.86	0.85	0.86
3-steps ®	0.83	0.86	0.85	0.85	-----
6-steps	0.86	0.84	0.85	0.85	-----

The ratios of the paraffins over the total hydrocarbon fractions are shown in table 3.3.8 and plotted in figure 3.3.4. In the case of the 20Co/100SiO$_2$ catalysts the ratio of paraffins over the total hydrocarbon fraction of the C_2 to C_6 hydrocarbons were somewhat higher for the one prepared in 1-step compared to the one of 2-steps. For the 30gCo/100SiO$_2$ series the ratios decreased as the number of impregnation steps increased except for the one prepared in 3-steps. The latter catalyst yielded hydrocarbons, which were more paraffinic than the others containing the same amount of cobalt. This could be due to the fact that this catalyst was more active than the others (see 3.1.5.1) resulting in more extensive hydrogenation of the primary formed olefins. In support of this concept it can be seen that when comparing table 3.3.6 with table 3.3.8 there is a relation between the FT activity and the paraffin/total hydrocarbon ratio, *i.e.*, the higher the activity the more paraffinic the hydrocarbon. In turn, as expected, there is a correlation between the FT activity and the metal surface area loaded in the reactor (compare table 3.3.6 with table 3.3.4).

Table 3.3.8 Ratio of paraffins in the hydrocarbon fraction.

Catalyst	Paraffins/Total hydrocarbon (average 2-24 hrs TOS)					
	Carbon fraction					
	C_2	C_3	C_4	C_5	C_6	C_7
20Co/100SiO$_2$						
1-step	0.63	0.27	0.34	0.40	0.50	0.50
2-steps	0.58	0.23	0.32	0.37	0.42	0.50
30Co/100SiO$_2$						
1-step	0.63	0.32	0.39	0.42	0.48	0.54
3-steps	0.70	0.42	0.49	0.55	0.61	0.79
3-steps ®	0.63	0.29	0.31	0.33	0.38	0.45
6-steps	0.55	0.25	0.26	0.27	0.34	0.40

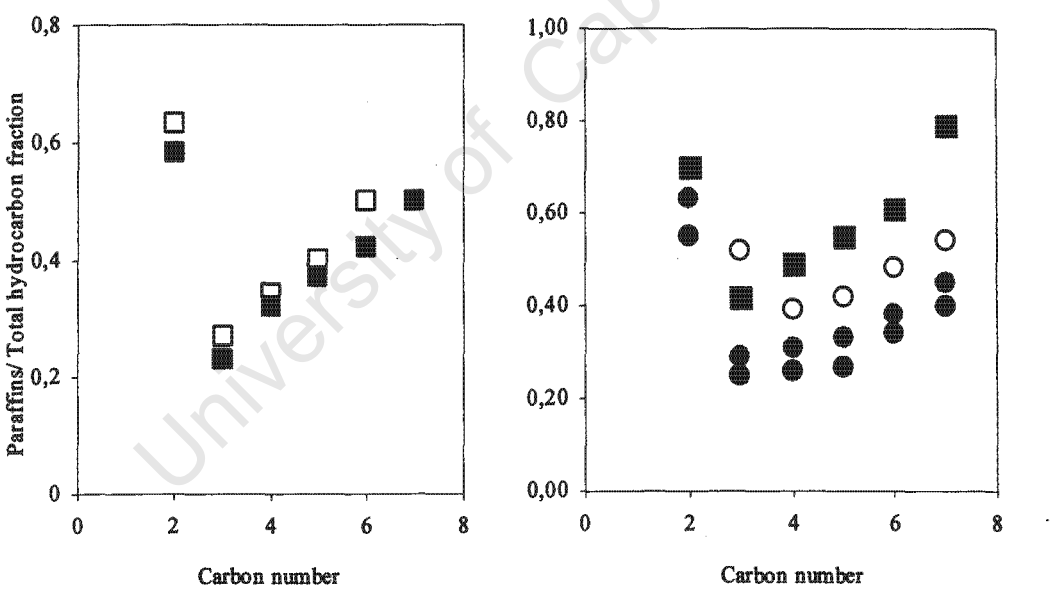

Figure 3.3.4: Ratio of paraffins over the total carbon fraction versus carbon number.
a) (□) 1-step 20gCo/100gSiO$_2$, (■) 2-step 20gCo/100gSiO$_2$, **b)** (○) 1-step 30gCo/100gSiO$_2$, (■) 3-step 30gCo/100gSiO$_2$, (●) 3-step® 30gCo/100gSiO$_2$, (●) 6-step 30gCo/100gSiO$_2$.

The ratios of the ethanol over the total C_2 hydrocarbon fraction were, 0.17 and 0.09 for the 1-step and 2-step 20Co/100SiO$_2$ catalysts. The ratios of the aldehydes over the total hydrocarbon fraction gave the same results. In the case of the 30Co/100SiO$_2$ catalysts ethanol was the main alcohol produced. The average ethanol/C_2 ratio was 0.08. Alcohols from C_3 to C_7 were negligible. The acetaldehyde fractions were also 0.08. Aldehydes with carbon atoms from 3 to 7 were hardly produced.

3.4 Modified catalysts by coating silica with MnO or ZnO

With the purpose of investigating whether the catalyst characteristic and FT activity are affected by coating the silica support, a number of catalysts were prepared by depositing 1 or 3 theoretical monolayers of MnO or ZnO onto the silica and subsequently impregnated with the cobalt precursor (see catalyst preparation in section 2.1.2.4).

3.4.1 Atomic Absorption Spectroscopy (AAS)

The concentrations of Co, Mn and Zn in the catalysts were measured using AAS. The measured concentrations were calculated as weight percentage per mass of catalyst. The "expected" concentrations of Co, Mn and Zn were calculated on the assumption that the metal oxides were present in the unreduced catalysts as Co_3O_4, MnO_2, Mn_2O_3 and ZnO. MnO_2 and Mn_2O_3 were assumed to be present in a molecular ratio of 1:1. The analyses of the XRD patterns revealed that those species were the most predominant phases. Table 3.4.1 shows the "expected" and the "measured" results. It is seen that in most of the cases the expected and the measured concentrations were close. If the exact concentrations of MnO_2 and Mn_2O_3, would have been known there might have been a better match between the expected and the measured calculations.

Table 3.4.1 Cobalt content of catalysts

Catalyst	wt(%) expected			wt(%) measured (AAS)		
	Co	Mn	Zn	Co	Mn	Zn
30gCo/100gSiO_2	21.3			20.7		
30gCo/27.9gMn/100gSiO_2	16.2	12.0		15.5	11.9	
30gCo/85.3gMn/100gSiO_2 1-step	11.0	30.6		12.0	31.7	
30gCo/29.3gZn/100gSiO_2	16.9		16.5	14.9		12.7
30gCo/87.7gZn/100gSiO_2 1-step	12.0		35.1	10.6		35.9

Concentrations of Mn and Zn were equivalent to:

27.9gMn/100gSiO_2 = 1 monolayer MnO coverage of the silica.
85.3gMn/100gSiO_2 = 3 monolayers MnO coverage of the silica.
29.2gZn/100gSiO_2 = 1 monolayer ZnO coverage of the silica.
87.7gZn /100gSiO_2 = 3 monolayers ZnO coverage of the silica.

3.4.2 Temperature programmed reduction (TPR)

Temperature programmed reduction was used to study the catalysts' reduction behaviour. The obtained TPR spectra were plotted as the percentage of H_2 consumed in the H_2 in N_2 mixture. As demonstrated in previous sections the $30gCo/100gSiO_2$ catalyst showed four reduction peaks. The first small peak at 205 was assigned to the reduction of undecomposed $Co(NO_3)_2$. The second peak at 315°C was assigned to the reduction of:

$$Co_3O_4 + H_2 \rightarrow 3CoO + H_2O$$

The third peak appeared at 375°C with the reduction of:

$$3CoO + 3H_2 \rightarrow 3Co^0 + 3H_2O$$

The fourth peak attributed to the reduction of possible cobalt silicates were represented by a small broad peak showed between 590 and 740°C.

In order to evaluate the reduction behaviour of Mn and Zn oxides two blank samples were prepared by coating silica with three theoretical monolayers of MnO or ZnO. The samples were subsequently reduced in the TPR apparatus. The spectrum of the Mn/SiO_2 blank sample showed two peaks at 358 and 478°C (see figure 3.4.1). The first peak was assumed to be the reduction of;

$$2MnO_2 + H_2 \rightarrow Mn_2O_3 + H_2O$$

and the second peak the reduction of;

$$Mn_2O_3 + H_2 \rightarrow 2MnO + H_2O$$

The reduction behaviour of the ZnO blank sample showed a small protuberance from 400 to 580°C as shown in figure 3.4.1. No hydrogen consumption was expected because ZnO should not reduce below 600°C.

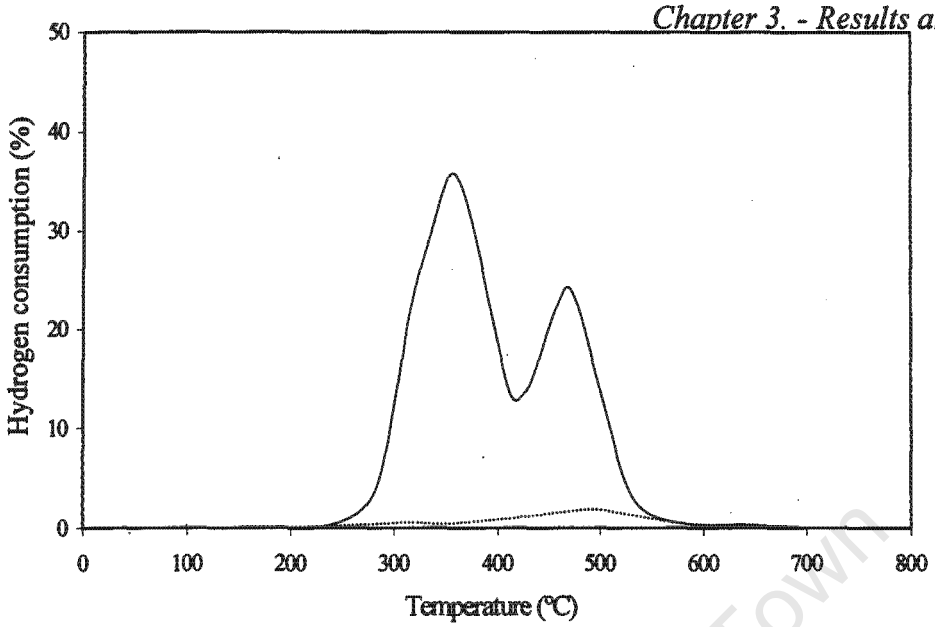

Figure 3.4.1: TPR profiles of the blank samples. (——) 83.5gMn/100gSiO_2, (·····) 87.7gZn/100gSiO_2. Hydrogen consumption (%) of the reducing mixture (6% H_2 in N_2) against temperature.

As expected the catalysts coated with 1 or 3 theoretical monolayers of MnO prior the deposition of the cobalt (see catalyst preparation in section 2.1.2.4) showed more complicated TPR profiles (see figure 3.4.2) than that of the 30gCo/100gSiO_2 catalyst. The first small peak for both catalysts can be suggested to be the reduction of undecomposed NO_x from the metal nitrates. The second peaks at 307 and 317°C could be assigned to the simultaneous reduction:

$$Co_3O_4 + H_2 \rightarrow 3CoO + H_2O$$

$$2MnO_2 + H_2 \rightarrow Mn_2O_3 + H_2O$$

The third peaks at 436 and 441°C could be attributed to the reduction of the following reaction:

$$CoO + H_2 \rightarrow Co^0 + H_2O$$

$$Mn_2O_3 + H_2 \rightarrow 2MnO + H_2O$$

The peaks at 646 and 663°C may be assigned to be the reduction of Co-Mn complexes such as spinels. From figure 3.4.2 it can be observed that the two first reduction peaks for the Zn catalysts have shifted to lower temperatures. It could be that Zn promotes reduction but this is not clear at this stage because the activity of these catalysts was inferior to the uncoated reference catalyst (30gCo/100SiO_2).

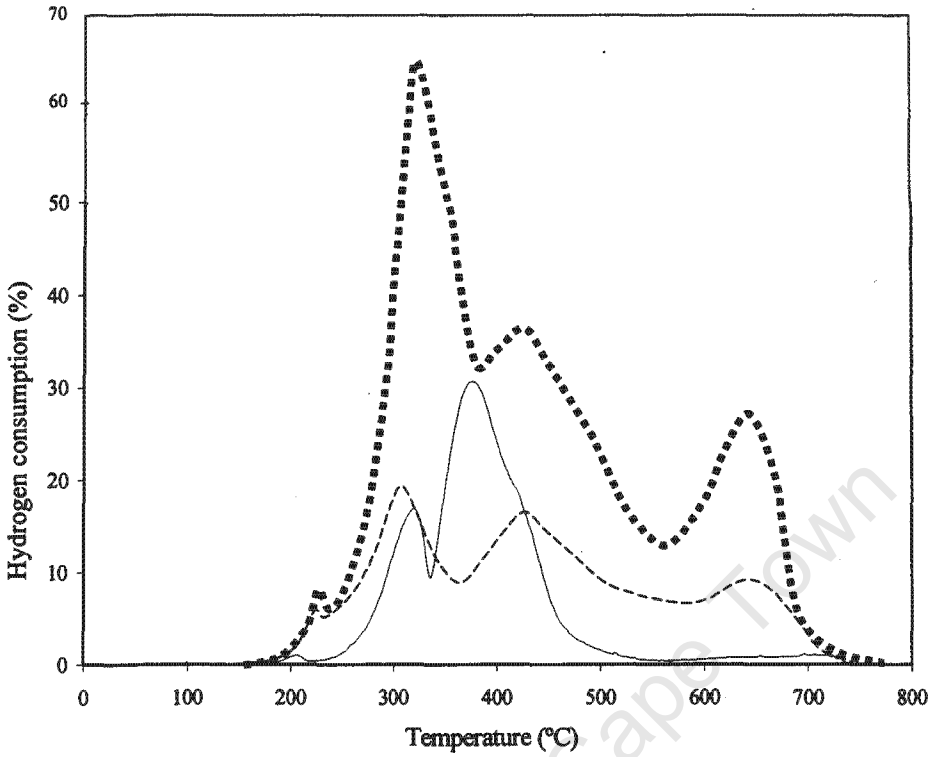

Figure 3.4.2: TPR profiles of the catalysts. (——) 30gCo/100gSiO_2, (– – –)30gCo/27.9gMn/100gSiO_2, (▪▪▪▪▪) 30gCo/83.5gMn/100gSiO_2. Hydrogen consumption (%) of the reducing mixture (6% H_2 in N_2) against temperature.

The catalysts coated with 1 or 3 theoretical monolayers of ZnO showed similar behaviours (see figure 3.4.3). The first peaks assigned to the reduction of undecomposed NO_x were hardly seen. The peaks at 240 and 283°C possibly represented the reduction of:

$$Co_3O_4 + H_2 \rightarrow 3CoO + H_2O$$

for the 29Zn and 88Zn cases respectively.

The peaks at 298 and 307°C probably corresponded to the reduction of:

$$CoO + H_2 \rightarrow Co^0 + H_2O$$

for the two Zn cases.

The broad peaks at 600 and 680°C might be suggested to the reduction of Co-Zn complexes.

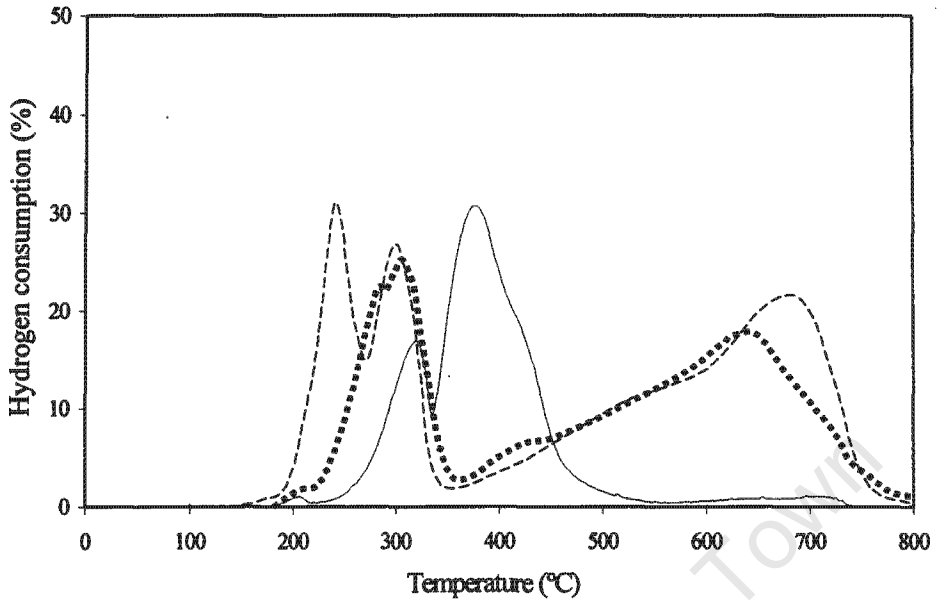

Figure 3.4.3: TPR profiles of the catalysts. (——) 30gCo/100gSiO$_2$, (---) 30gCo/29.2gZn/100gSiO$_2$, (▪▪▪▪▪)30gCo/87.7gZn/100gSiO$_2$. Hydrogen consumption (%) of the reducing mixture (6% H_2 in N_2) against temperature.

Table 3.4.2 shows the H_2 consumptions during the catalysts' reduction. There is a good agreement of the total "measured" and "expected" H_2 consumption for the catalysts coated with 1 or 3 layers of MnO. The "expected" H_2 consumption was calculated on the basis that equal amounts of MnO_2 and Mn_2O_3 were present in the unreduced catalysts. The total "measured" and "expected" H_2 consumption of the catalysts coated with 1 or 3 layers of ZnO were different. In both cases more H_2 was consumed experimentally. The possible reduction of Co-Zn complexes might have been responsible of the higher H_2 consumption. From figure 3.4.4 one could observe that for the Zn cases the two peaks attributed to the reduction of Co_3O_4 shifted to lower reduction temperatures than the pure Co_3O_4. This means that for the ZnO coated catalysts the Co_3O_4 crystallites are bigger than those of the pure Co_3O_4. Bigger cobalt crystallites reduce easier than the smaller ones. Smaller crystallites may "interact" more with the surface and so are more difficult to reduce. The larger cobalt crystallites of these catalysts produced smaller metal surface areas and hence inferior activities than that of the uncoated case.

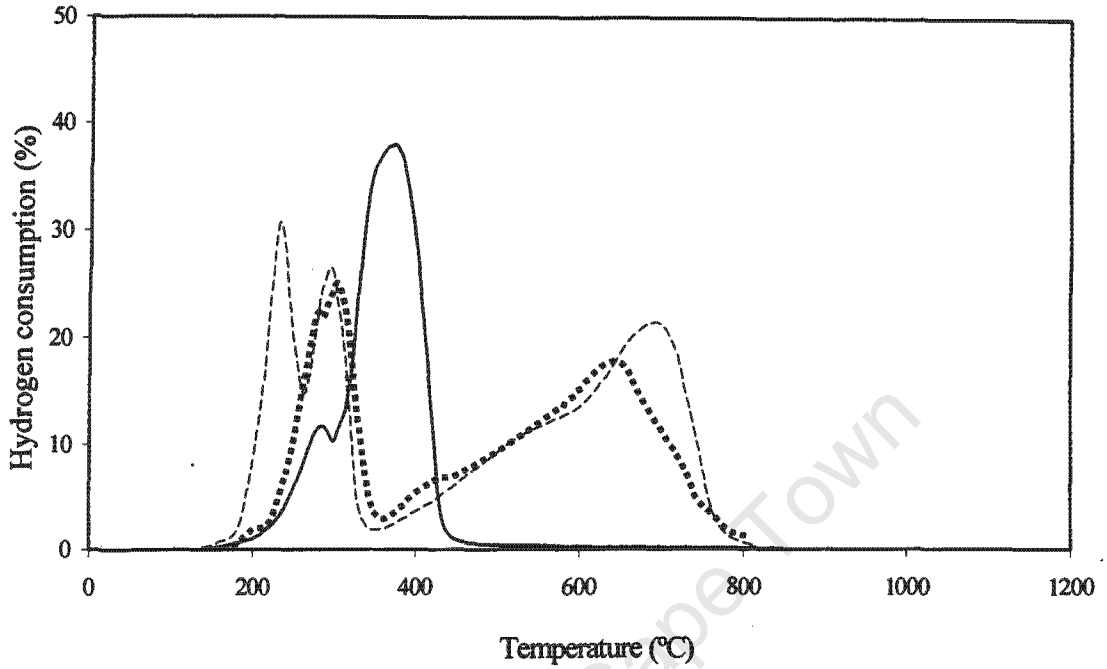

Figure 3.4.4: TPR profiles of the catalysts. (——) pure Co_3O_4 , (- - - -) 30gCo/29.2gZn/100gSiO_2, (▪▪▪▪▪) 30gCo/87.7gZn/100gSiO_2. Hydrogen consumption (%) of the reducing mixture (6% H_2 in N_2) against temperature.

Table 3.4.2 H_2 consumption of catalysts during reduction in TPR

Catalyst	Moles H_2 consumed x 10^{-3}/g.catalyst						% of H_2 consumed			
	peak				Total H_2 consumed measured	Total H_2 consumed expected	peak			
	1	2	3	4			1	2	3	4
30gCo/100gSiO_2	0.07	1.28	3.81	0.19	5.36	4.82	1.3	23.9	71.1	3.5
85.3gMn/100gSiO_2 (blank)		3.01	1.89		4.90	4.99		61.4	38.6	
30gCo/27.9gMn/100gSiO_2	0.61	1.90	2.69	0.78	5.98	6.21	10.2	31.8	45.0	13.0
30gCo/85.3gMn/100gSiO_2	0.27	5.47	3.04	1.66	10.44	9.91	2.6	52.4	29.1	15.9
87.7gZn/100gSiO_2 (blank)				0.29	0.29	0.00				100
30gCo/29.3gZn/100gSiO_2		1.79	1.32	3.76	6.87	3.97		26.0	19.3	54.7
30gCo/87.7gZn/100gSiO_2		0.66	0.90	2.14	3.70	2.96		17.8	24.4	57.8

3.4.3 CO Chemisorption

Reduction of the catalysts in the chemisorption apparatus was carried out at 350°C for 2 hrs. The results are shown in table 3.4.3. Dispersions were calculated from the "strong" and "total" chemisorption data (see tables 3.4.3 and 3.4.4). The metal dispersions were calculated on the basis of the total cobalt present on the catalysts. As it has been shown that not all the cobalt was in fact reduced at 350°C over 16 hrs the calculated dispersions here represent the amount of surface Co metal atoms as a percentage of the total cobalt present and not of the reduced Co present. It is clearly observed that by coating the silica support with 1 or 3 monolayers of MnO or ZnO the dispersion is decreased notably. The uncoated $30gCo/100SiO_2$ was 1.39% whereas the coated catalyst had dispersions between 0.08% to 1.25% for the "total" chemisorption data. The lower dispersions of Co for the Mn and Zn oxide coated samples could be due to pore blockage of the SiO_2 (see 3.4.4) thus leaving less area for the deposition of cobalt. This would lead to a greater extent of agglomeration of the cobalt and hence to lower dispersions.

Table 3.4.3 Strong chemisorption of catalysts

Catalyst	vol CO adsorbed (ml/g.reduced catalyst)	D (%)	m.s.a. (m^2/g.cat)	m.s.a. (m^2/g.Co)	p_d (nm)
$30gCo/100gSiO_2$	0.76	0.97	1.35	6.54	103
$30gCo/27.9gMn/100gSiO_2$	0.19	0.26	0.33	2.14	315
$30gCo/85.3gMn/100gSiO_2$ 1-step	0.12	0.27	0.22	1.81	372
$30gCo/85.3gMn/100gSiO_2$ 3-steps	0.06	0.13	0.11	0.90	749
$30gCo/29.2gZn/100gSiO_2$	0.05	0.08	0.08	0.54	1248
$30gCo/87.7gZn/100gSiO_2$ 1-step	0.08	0.22	0.15	1.41	478
$30gCo/87.7gZn/100gSiO_2$ 3-steps	0.18	0.44	0.31	2.97	227

Table 3.4.4 Total chemisorption of catalysts

Catalyst	vol CO adsorbed (ml/g.reduced catalyst)	D (%)	m.s.a. (m^2/g.cat)	m.s.a. (m^2/g.Co)	p_d (nm)
30gCo/100gSiO_2	1.09	1.39	1.94	9.38	72
30gCo/27.9gMn/100gSiO_2	0.37	0.52	0.66	4.28	158
30gCo/85.3gMn/100gSiO_2 1-step	0.27	0.60	0.48	4.01	168
30gCo/85.3gMn/100gSiO_2 3-steps	0.13	0.29	0.24	1.99	339
30gCo/29.2gZn/100gSiO_2	0.05	0.08	0.08	0.54	1248
30gCo/87.7gZn/100gSiO_2 1-step	0.19	0.50	0.34	3.19	211
30gCo/87.7gZn/100gSiO_2 3-steps	0.50	1.25	0.89	8.43	80

D = Dispersion.
m.a.s. = Metallic surface area.
p_d = Average particle diameter of cobalt metal.

The "strong" metal surface area of the uncoated 30gCo/100gSiO_2 decreased from 1.35 m^2/g.cat to 0.33 to 0.08 when the support was coated with 1-layer of MnO or ZnO respectively. Coating catalysts with 3 layers of MnO or ZnO gave metal surface areas of 0.22 and 0.15 m^2/g.cat. From the "strong" chemisorption data, the average crystallite size of uncoated 30gCo/100gSiO_2 catalyst was 103nm. In the coated cases with 1-layer of MnO or ZnO the Co crystallite sizes were larger, 315 and 1248nm were calculated for these catalysts. The coated catalysts with 3-layers of MnO or ZnO had Co particle sizes of 372 and 478nm respectively. Coating the catalysts with 3–layers of MnO or ZnO in 3-steps also resulted in larger crystallite sizes.

3.4.4 BET Area

The "expected" and the "measured" BET areas are given in table 3.4.5. The "measured" areas were in all cases smaller than the "expected" ones. From figure 3.4.5 it is observed that by depositing 1 or 3 monolayers of MnO or ZnO the catalyst surface areas decreased. The decrease in surface area could be due to pore blockage of the silica support by Mn or Zn oxides. Mn or Zn oxides might have had lower surface areas than that of silica and this could have resulted in inferior catalysts' surface areas.

Table 3.4.5 BET surface areas of catalysts

Catalyst	1 g. catalyst contains			BET Surface area		
	Co_3O_4	Mn_2O_3 or ZnO	SiO_2	measured (m^2/g.cat)	expected (m^2/g.cat)	expected (m^2/g.SiO_2)
Silica support			1.00	286		286
30gCo/100gSiO_2	0.28		0.72	194	206	269
85.3gMn/100gSiO_2 (blank)		0.56	0.44	117	127	266
30gCo/27.9gMn/100gSiO_2	0.21	0.17	0.62	139	177	224
30gCo/85.3gMn/100gSiO_2 1-step	0.16	0.46	0.38	93	109	245
30gCo/85.3gMn/100gSiO_2 3-steps	0.16	0.46	0.38	97	109	255
87.7gZn/100gSiO_2 (blank)		0.52	0.48	89	137	185
30gCo/29.3gZn/100gSiO_2	0.20	0.16	0.64	130	183	203
30gCo/87.7gZn/100gSiO_2 1-step	0.14	0.45	0.41	83	117	202

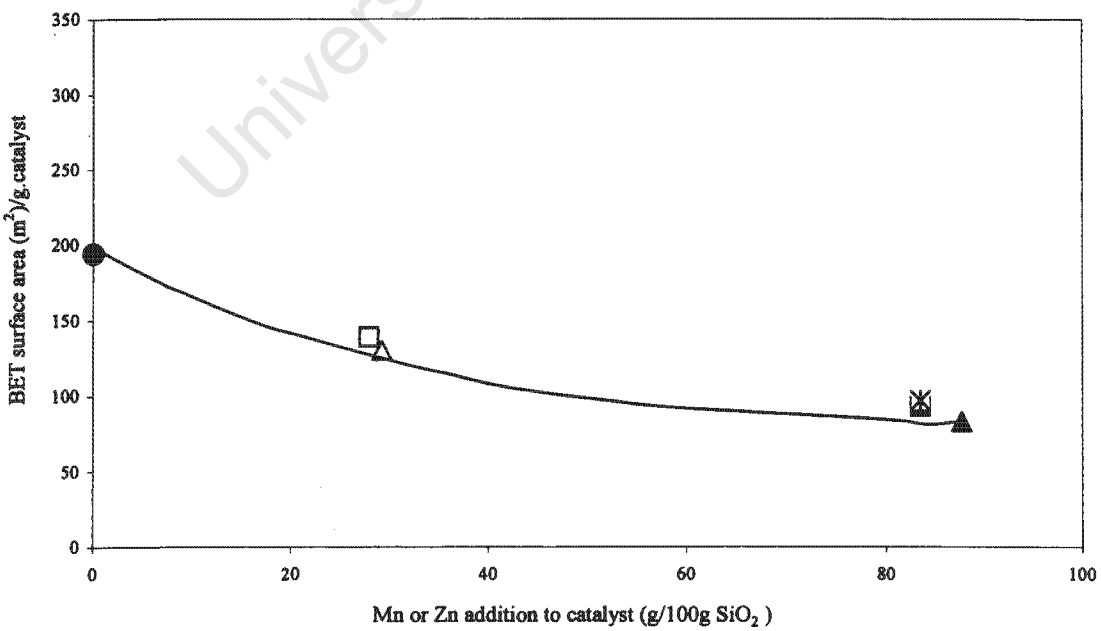

Figure 3.4.5: BET surface areas (m^2/g.cat) against Mn or Zn addition over silica(g/100g. SiO_2); (●) 30gCo/100gSiO_2, (□)30gCo/27.9gMn/100gSiO_2, (■)30gCo/83.5gMn/100gSiO_2 1-step, (✳) gCo/83.5gMn /100gSiO_2 3-steps. (△) 30gCo/29.2gZn/100gSiO_2, (▲)30gCo/87.7gZn/100gSiO_2 1-step.

3.4.5 FT Activity

3.4.5.1 Activity with time on stream (TOS)

The FT reaction was performed at reaction conditions of 220°C, 15 bar g H_2/CO = 2, total H_2+CO flow rate=28ml/min. The activity was calculated from the CO converted (%) during TOS. The FT activities of the uncoated and the coated catalysts were compared (table 3.4.6 and figure 3.4 6). Lower activities were found for the coated cases. The low metal surface areas of these catalysts matched to the lower activities. Figure 3.4.7 shows the catalysts' activities expressed as CO converted at 2hrs TOS against the metal area loaded in the reactor. The comparison of the catalysts' activities suggests that the activities were dependent on the metal areas available. It is important to note that in each case that the same amount of Co metal was loaded in the FT reactor, which consequently resulted in different metal surface areas.

Table 3.4.6 FT activity of catalysts

Catalyst	FT activity measured as CO converted (%)				
	Time on stream (hrs)				
	2	16	20	24	48
30gCo/100gSiO_2	39.4	41.4	37.0	39.7	28.6
30gCo/27.9gMn/100gSiO_2	30.1	21.5	20.9	20.9	
30gCo/85.3gMn/100gSiO_2 1-step	29.1	24.5	20.6	12.7	12.8
30gCo/85.3gMn/100gSiO_2 3-steps	27.8		10.4	8.1	
30gCo/29.3gZn/100gSiO_2	16.5	13.8	13.1	10.8	8.7
30gCo/87.7gZn/100gSiO_2 1-step	21.0	18.3	16.7	15.2	
30gCo/87.7gZn/100gSiO_2 3-steps	27.8	14.7	11.6	14.1	13.3

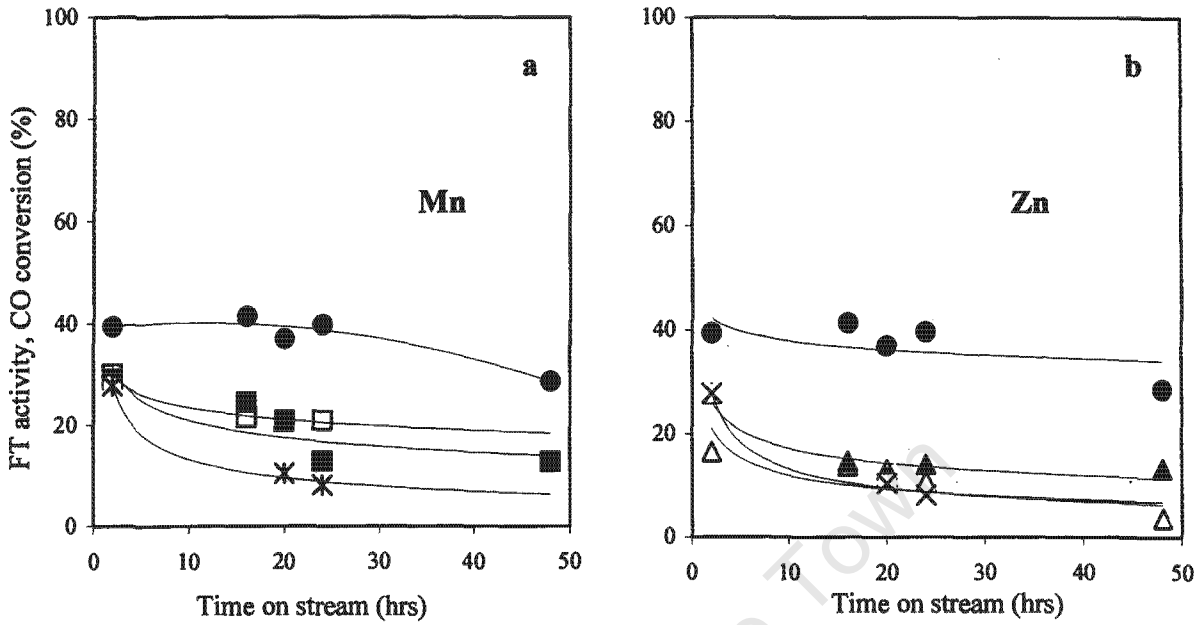

Figure 3.4.6. FT activities of catalysts against time on stream TOS. FT conditions, 220°C, 15bar g, H_2/CO= 2. **a)** (●)30gCo/100gSiO$_2$, (□)30gCo/27.9gMn/100gSiO$_2$, (■)30gCo/83.5gMn/100gSiO$_2$ 1-step,(✱) 30gCo/83.5gMn/100gSiO$_2$ 3-steps. **b)** (●)30gCo/100gSiO$_2$, (△)30gCo/29.2gZn/100gSiO$_2$, (▲) 30gCo/87.7gZn/100gSiO$_2$ 1-step, (✕) 30gCo/87.7gZn/100gSiO$_2$ 3-steps.

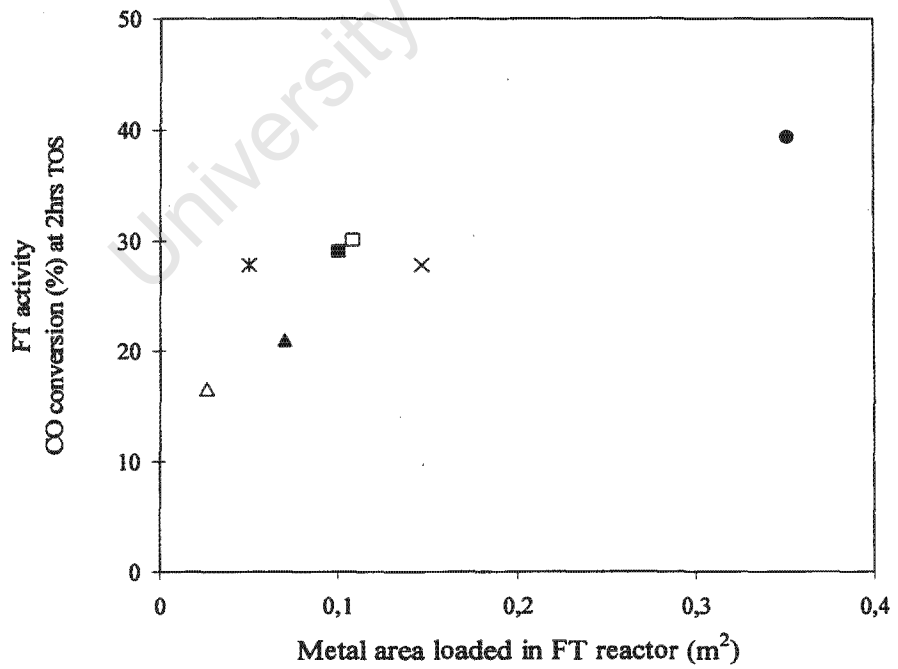

Figure 3.4.7: FT activity of catalysts measured as CO conversion (%)at 2hrs TOS as a function of the metal area loaded in the FT reactor (obtained from the "strong" chemisorption).

a) (●)30gCo/100gSiO$_2$, (□)30gCo/27.9gMn/100gSiO$_2$, (■)30gCo/83.5gMn/100gSiO$_2$ 1-step,(✱) 30gCo/83.5gMn/100gSiO$_2$ 3-steps. **b)** (●)30gCo/100gSiO$_2$, (△)30gCo/29.2gZn/100gSiO$_2$, (▲) 30gCo/87.7gZn/100gSiO$_2$ 1-step, (✕) 30gCo/87.7gZn/100gSiO$_2$ 3-steps.

3.4.5.2 Chain growth probability and selectivity

The chain growth probability (α) was obtained from the slope of the plot of n against (logFn/n) for the hydrocarbon products between C_3 to C_{12} (see 1.1.6). The uncoated catalyst showed the highest alpha values of about 0.86 whereas, the MnO coated catalysts showed lower initial alpha values at around 0.81 which, declined with TOS to around 0.77 (24hrsTOS). The ZnO coated catalysts had the lowest alpha values around 0.67 which, increased with TOS to about 0.72 at 24hrs.

Table 3.4.7 Chain growth probability of catalysts.

Catalyst	Chain growth probability (α)				
	Time on stream (hrs)				
	2	16	20	24	48
30gCo/100gSiO_2	0.87	0.86	0.85	0.83	0.86
30gCo/27.9gMn/100gSiO_2	0.81	0.82		0.77	0.65
30gCo/85.3gMn/100gSiO_2 1-step	0.81	0.80	0.79	0.77	
30gCo/85.3gMn/100gSiO_2 3-steps	0.83	0.83	0.78	0.76	
30gCo/29.3gZn/100gSiO_2	0.69	0.57	0.58	0.59	
30gCo/87.7gZn/100gSiO_2 1-step	0.67	0.75	0.75	0.76	
30gCo/87.7gZn/100gSiO_2 3-steps	0.62	0.72	0.72	0.72	0.73

The ratios of the paraffins over the total hydrocarbon fraction are summarised in table 3.4.8. The ratios were the average ratios between 16 to 48hrs TOS. It was unexpected that the catalysts coated with Mn gave more paraffinic products than the uncoated 30gCo/100SiO_2 catalyst (see table 3.4.8) because this appears to contradict the findings in the literature [26] where MnO supported Fe catalysts yielded a greater production of C_2-C_4 alkenes compared to Fe catalysts supported on either alumina or titania. In the present studies, the catalysts coated with Zn yielded less paraffins than the uncoated 30gCo/100SiO_2catalyst.

Table 3.4.8 Ratio of paraffins over total hydrocarbons

Catalyst	Paraffins/Total hydrocarbon					
	C_2	C_3	C_4	C_5	C_6	C_7
30gCo/100gSiO_2	0.63	0.32	0.39	0.42	0.50	0.50
30gCo/27.9gMn/100gSiO_2	0.62	0.37	0.43	0.47	0.51	0.57
30gCo/85.3gMn/100gSiO_2 1-step	0.59	0.34	0.38	0.43	0.46	0.53
30gCo/85.3gMn/100gSiO_2 3-steps	0.45	0.42	0.47	0.51	0.57	0.62
30gCo/29.3gZn/100gSiO_2	0.34	0.26	0.27	0.44	0.41	0.47
30gCo/87.7gZn/100gSiO_2 1-step	0.41	0.27	0.31	0.37	0.42	0.48
30gCo/87.7gZn/100gSiO_2 3-steps	0.47	0.21	0.30	0.35	0.44	0.52

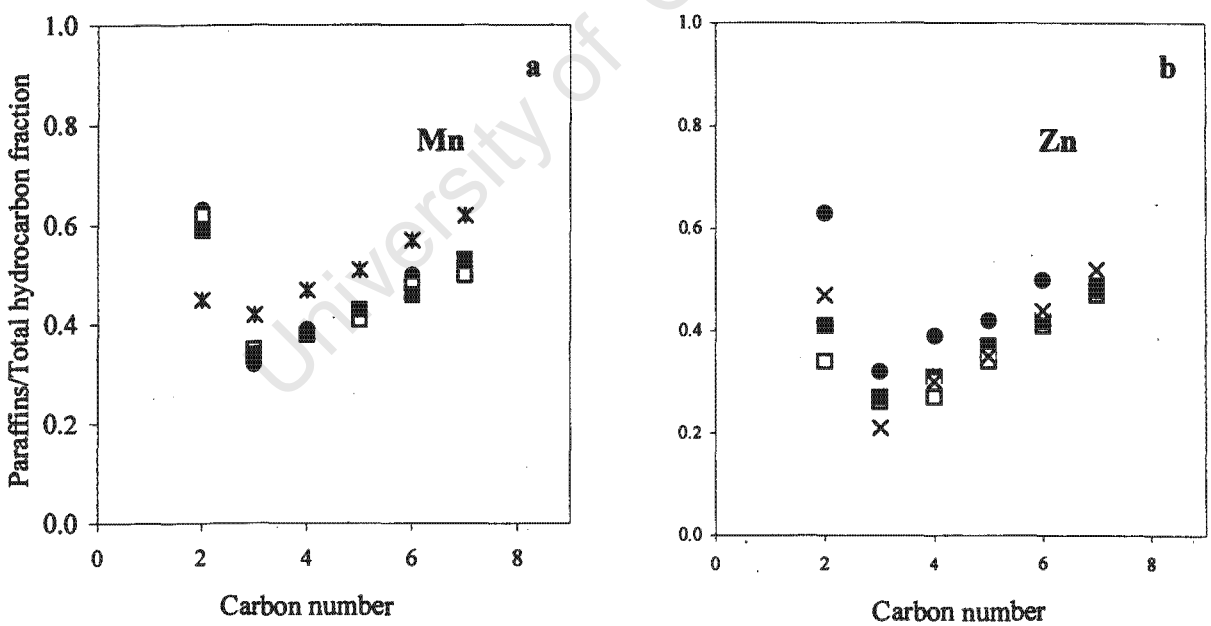

Figure 3.4.8: Ratio of paraffins over the total hydrocarbon fraction versus carbon number.
a) (●)30gCo/100gSiO_2, (□)30gCo/27.9gMn/100gSiO_2, (■)30gCo/83.5gMn/100gSiO_2 1-step,(✱) 30gCo/83.5gMn/100gSiO_2 3-steps. **b)** (●)30gCo/100gSiO_2, (△)30gCo/29.2gZn/100gSiO_2, (▲) 30gCo/87.7gZn/100gSiO_2 1-step, (✕) 30gCo/87.7gZn/100gSiO_2 3-steps.

Generally the paraffin/hydrocarbon ratios seemed to be dependant on the %CO conversion or metal area loaded (see page 74).

Ethanol and acetaldehyde were the most abundant oxygenated products (see table 3.4.9). The Zn coated catalysts gave more ethanol than the Mn coated and the uncoated catalysts. In all cases acetaldehyde was yielded in similar amounts.

Table 3.4.9 Ethanol/Total C_2 fraction and Acetaldehyde/Total C_2 fraction

Catalyst	Ethanol/Total C_2	Acetaldehyde/Total C_2
30gCo/100gSiO_2	0.07	0.01
30gCo/27.9gMn/100gSiO_2	0.02	0.02
30gCo/85.3gMn/100gSiO_2 1-step	0.03	0.02
30gCo/29.3gZn/100gSiO_2	0.17	0.02
30gCo/87.7gZn/100gSiO_2 1-step	0.34	0.02

3.5 Alumina supported catalysts using different solvents and different salts solutions

3.5.1 Atomic Absorption Spectroscopy (AAS)

AAS was employed to measure the concentration of cobalt in the samples calcined in N_2. The obtained concentrations were given as weight percentage per mass of catalyst. Since mainly Co_3O_4 was detected by XRD analyses in Co/SiO_2 catalysts the expected weight percentage of cobalt in Co/Al_2O_3 was calculated assuming that Co_3O_4 was the only oxide present. The measured concentrations of cobalt in the cobalt nitrate catalysts did not differ much from the expected concentrations. The difference in concentration might be due to the hygroscopic properties of the cobalt nitrate. The catalysts prepared with cobalt acetate and cobalt acetyl acetonate showed lower concentrations than the expected ones. Thermogravimetric analysis (TGA) showed that the calcination temperature of 270°C was not sufficient to decompose the C-C bonds of the acetate and acetylacetonate groups. Consequently, undecomposed "carbonaceous" material was still present in the calcined catalysts and this caused the lowering of cobalt content per mass of catalyst. The cobalt concentrations of the catalysts are given in table 3.5.1.

Table 3.5.1 Cobalt content of catalysts

Catalyst 4SCN	wt(%) Co expected	wt(%) Co measured (AAS)
30Co-nit(H_2O) /100Al_2O_3 (over calcined)	21.3	20.00
30Co-nit(H_2O) /100Al_2O_3	21.3	18.34
30Co-nit(CH_3OH) /100Al_2O_3	21.3	18.80
30Co-ace(H_2O) /100Al_2O_3	21.3	16.90
30Co-acac(CH_2Cl_2) /100Al_2O_3	21.3	13.90

4SCN = Catalyst impregnated in four steps and calcined in N_2 between each step.
Co-nit(H_2O) = Cobalt nitrate dissolved in water.
Co-nit(CH_3OH) = Cobalt nitrate dissolved in methanol.
Co-ace(H_2O) = Cobalt acetate dissolved in water.
Co-acac(CH_2Cl_2) = Cobalt acetylacetonate dissolved in dichloromethane.

3.5.2 Temperature Programmed Reduction (TPR)

First of all, the alumina support was used as a blank in the TPR apparatus. The profile showed no hydrogen consumption. Therefore all TPR peaks can be assigned to the reduction of cobalt species.

The hydrogen consumed during the catalyst reduction was calculated in moles of hydrogen required to reduce 1 gram of catalyst (see Appendix I). The reduction profiles of the catalysts prepared with different cobalt salts were different. One can observe that the reduction behaviour of the catalyst prepared with cobalt nitrate dissolved in water showed three peaks (see figure 3.5.1). The first peak at 258°C was assigned to the reduction of:

$$Co_3O_4 + H_2 \rightarrow 3CoO + H_2O$$

The second peak at 326°C was assigned to the reduction of:

$$3CoO + 3H_2 \rightarrow 3Co^0 + 3H_2O$$

The third peak at 630°C represented possibly the reduction of Co aluminates. Kogelbahuer [22] observed only two reduction peaks for Co/Al_2O_3 (20wt%Co) catalysts calcined at 300°C for 4hrs. The first peak appeared at 320°C and the second one between 400 and 800°C [22]. The author [22] also performed TPR scans on catalysts calcined only for 2 hrs where three peaks were observed at 230, 320°C and 400-800°C. The peak at 230°C was confirmed to be the reduction of undecomposed $Co(NO_3)_2$ [22]. In the present study it appears that $Co(NO_3)_2$ on Co/Al_2O_3 catalysts was decomposed completely because such peak was not observed on the TPR profile.

In previous sections of this thesis it was observed that TPR profiles of $30Co/100SiO_2$ catalysts showed a small protuberance corresponding to the reduction of cobalt silicates (see figure 3.5.1). The required hydrogen to reduce the cobalt silicate peak was only $0.19x10^{-3}$ moles/g.cat and to reduce the aluminate peak on $30Co/100Al_2O_3$ was $3.62x10^{-3}$ moles/g.cat (see table 3.5.2). It appears that the interaction of the metal oxide-alumina was stronger than the metal oxide-silica. A speculation that was considered in this thesis was that cobalt aluminates might have been formed while the catalyst was being reduced in the TPR

apparatus. To test this, the catalyst was reduced in two stages. At first the temperature was raised from 100 to 360°C and kept at this temperature for 16 hrs, then the temperature was elevated to 1000°C at a rate of 10°C/min. The measured hydrogen consumption to reduce the aluminate peak in two stages was $3.8x10^{-3}$ moles/g.cat whereas, the reduction of this peak in one stage consumed $3.6x10^{-3}$ moles/g.cat (see table 3.5.2.). Since the two results are similar it is probable that the aluminates were formed during the catalyst calcination step at 270°C.

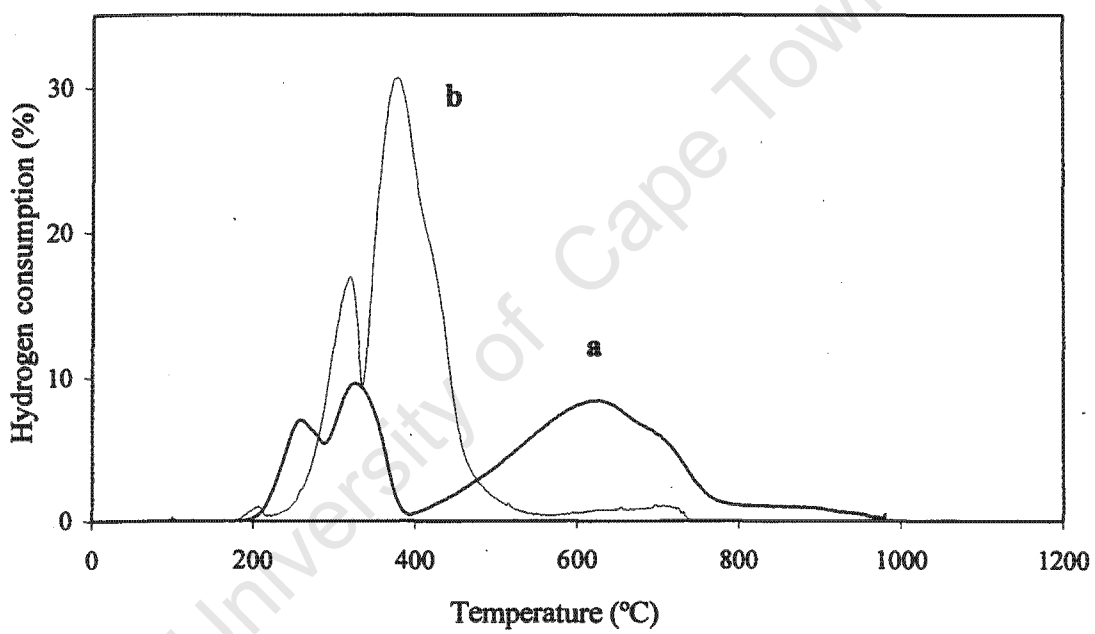

Figure 3.5.1: TPR profiles of: (**a**) 30gCo-nit (H_2O)/100g100Al_2O_3 and (**b**) 30gCo-nit (H_2O)/100g100SiO_2 catalysts. Hydrogen consumption (%) of the reducing mixture (6%H_2 in N_2) against temperature (°C).

The TPR profiles of the catalysts prepared with cobalt nitrate dissolved either in water or methanol were similar (see figure 3.5.2). The total hydrogen consumed during the reduction of the 30Co-nit(H_2O)/100Al_2O_3 and 30Co-nit(CH_3OH)/100Al_2O_3 catalyst was $5.5x10^{-3}$ and $5.3x10^{-3}$moles/g.cat respectively (see table 3.5.2).

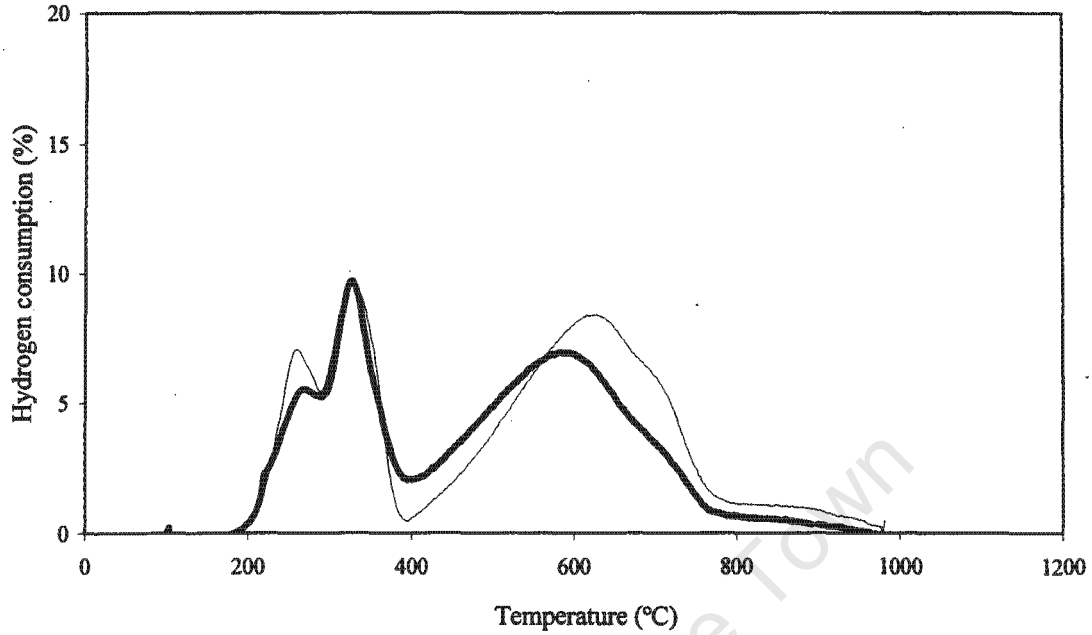

Figure 3.5.2: TPR profiles of: (——) 30gCo-nit (H_2O)/100g100Al_2O_3 and (▬▬) 30gCo-nit (CH_3OH)/100g100Al_2O_3 catalysts. Hydrogen consumption (%) of the reducing mixture (6%H_2 in N_2) against temperature (°C).

Table 3.5.2 H_2 consumption of catalysts during reduction in TPR

Catalyst 4SCN	Moles H_2 consumed$x10^{-3}$/g.catalyst						% of H_2 consumed			
	peak				Total H_2 consumed measured	Total H_2 consumed expected	peak			
	1	2	3	4			1	2	3	4
30Co-nit(H_2O)/100Al_2O_3	0.56	1.28	3.62		5.46	4.82	10.3	23.4	66.3	
30Co-nit(H_2O)/100Al_2O_3 (*)	0.72	1.01	3.77		5.50	4.82	13.1	18.4	68.5	
30Co-nit(CH_3OH)/100Al_2O_3	0.33	1.62	3.36		5.31	4.82	6.2	30.5	63.3	
30Co-ace(H_2O)/100Al_2O_3	0.65	1.16	1.62	0.49	3.92	3.84	16.6	29.6	41.3	12.5
30Co-acac(CH_2Cl_2)/100Al_2O_3	0.23	0.84	0.21		1.28	3.14	18.0	65.6	16.4	

(*) = Two stage reduction.

The "measured" hydrogen consumption to reduce 1 gram of 30Co-ace(H_2O)/100Al_2O_3 was very close to the "expected" hydrogen consumed/g.catalyst (see table 3.5.2). The catalyst prepared with cobalt acetate catalyst exhibited four peaks at 340, 500, 610 and 860°C (figure 3.5.3). The peak at 340°C could be the stepwise reduction of Co_3O_4 to Co as follows,

$$Co^{3+} \rightarrow Co^{2+} \rightarrow Co^{0}$$

Baerns found that alumina supported catalysts prepared with cobalt acetate showed only one peak at 387°C. The author proposed that this single peak is the overlap of two reduction steps from Co^{3+} to Co^{2+} to Co^0 because organic precursors do not show two separate peaks for the above reductions. In the TPR experiments reported by Baerns [27] the samples were heated during the reduction only to a maximum temperature of 400°C and hence no peak for the reduction of "cobalt aluminates" was observed. In the present work the reduction of the cobalt aluminates on the 30Co-ace(H_2O) /100Al_2O_3 catalyst was detected at 500, 610 and 860°C. Up to 420°C the degree of reduction of the 30Co-nit(H_2O) /100Al_2O_3 catalyst was 34% and that of the catalyst prepared with cobalt acetate was 17% (see table 3.5.2). From this one could expect that the cobalt nitrate catalyst would have more metal reduced and hence greater activity than the 30Co-ace(H_2O) /100Al_2O_3 catalyst but this is not the case. In sections 3.5.3 and 3.5.4 it will be shown that the 30Co-ace(H_2O) /100Al_2O_3 catalyst had a higher metallic surface area and greater activity than cobalt nitrate catalysts.

The TPR profile of the 30Co-acac(CH_2Cl_2) /100Al_2O_3 catalyst was different from that of the 30Co-nit(H_2O) /100Al_2O_3 catalyst, which was used as a reference catalyst. While 30Co-nit(H_2O) /100Al_2O_3 showed three reduction peaks the 30Co-acac(CH_2Cl_2) /100Al_2O_3 catalyst showed one shoulder and two peaks (see figure 3.5.3). At this stage it was unclear which reduction was occurring at 320°C (shoulder) but what is certainly possible is that at 380°C the following was happening:

$$Co_3O_4 + H_2 \rightarrow 3CoO + H_2O$$

$$3CoO + 3H_2 \rightarrow 3Co^0 + 3H_2O$$

The peak at 570°C could be the reduction of cobalt aluminates. Generally the measured hydrogen consumption was very low compared to the expected H_2 consumption (table 3.5.2). The negative peaks at 460 and at 800°C could be attributed to the decomposition of acetyl acetonate ligands, which could have a higher thermal conductivity than hydrogen. The acetyl acetonate ligands were not completely decomposed at the calcination temperature of 270°C employed in these studies. To investigate the complete decomposition temperature of this catalyst TGA analyses were performed and the scans are shown in section 3.6.2.

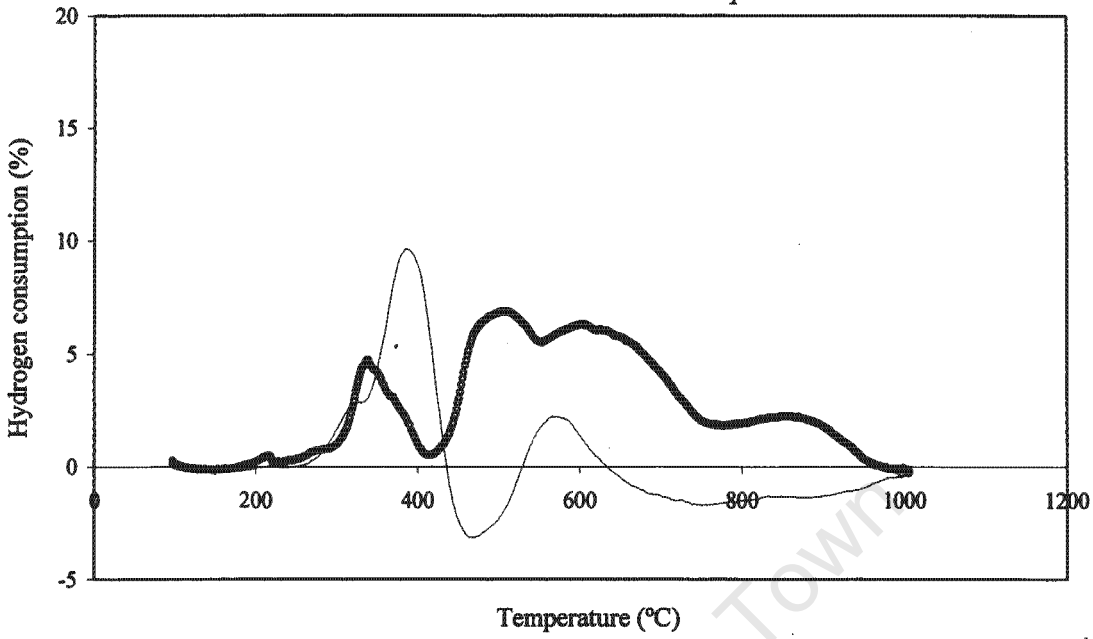

Figure 3.5.3: TPR profiles of: (∞∞∞∞∞) 30gCo-ace(H_2O)/100g100Al_2O_3 and (———) 30gCo-acac(CH_2CH_2) /100g100Al_2O_3 catalysts. Hydrogen consumption (%) of the reducing mixture (6%H_2 in N_2) against temperature (°C).

3.5.3 CO Chemisorption

3.5.3.1 Metal Dispersion, metal surface area and average particle diameter

The results obtained using CO chemisorption are summarised in table 3.5.3. The metal dispersions were calculated on the basis of the total cobalt present on the catalyst. As it has been shown that not all the cobalt was in fact reduced at 350°C over 16 hrs the calculated dispersions here represent the amount of surface Co metal atoms as a percentage of the total cobalt present and not of the reduced Co present. The reduction in the chemisorption apparatus was carried out at the same conditions as in the FT reactor. The catalysts to be investigated in this section were prepared as described in section 2.1.3.1. These catalysts were prepared in order to investigate whether catalysts prepared with different cobalt salts could lead to different dispersions and hence to different FT activities. Three cobalt salts were employed, cobalt nitrate, acetate and acetyl acetonate. The small pore volume of the alumina support was the main reason of choosing a solvent in which more cobalt salt would be dissolved. Cobalt nitrate was best dissolved in water and in methanol, cobalt acetate in

water and cobalt acetyl acetonate in trichloromethane. For comparison purposes with the literature Co acetyl acetonate was dissolved in CH_2Cl_2. The metal dispersions shown in table 3.5.3 were obtained from the "strong" chemisorption data [results from the total chemisorption (table 3.5.4) showed the same trend and are not discussed in the present section]. Accidentally a 30Co-nit(H_2O)/100Al_2O_3 catalyst was over calcined due to a thermocouple failure and so the actual calcination temperature was unknown. Nevertheless its dispersion was measured. The preparation of the 30Co-nit(H_2O)/100Al_2O_3 catalyst was repeated, the obtained dispersion this time was 0.90% against 0.57% for the over calcined catalyst. The obtained metal dispersions from these catalysts confirmed that over calcination leads to sintering and therefore to low dispersions. Previous work by Goodwin [69] on Co/Al_2O_3 catalysts calcined in a range of temperatures from 300 to 450°C showed that by increasing the calcination temperature the hydrogen uptake decreased. Ho *et.al.,* [72] also reported lower chemisorption values with increasing calcination temperature for Co/SiO_2 catalysts. The 30Co-nit(CH_3OH)/100Al_2O_3 catalyst gave a dispersion of 0.81%. This lower dispersion is not clear at this stage and will be further discussed in the following section. The highest dispersion of about 3.2% was obtained for the 30Co-ace(H_2O)/100Al_2O_3 catalyst. As expected from the low degree of reduction (see table 3.5.2), the 30Co-acac(CH_2Cl_2) /100Al_2O_3 catalyst had one of the lowest dispersions if one does not take into account the over calcined catalyst. In contradiction to this, work reported by Baerns [27] showed the highest dispersion on a Co-acac/TiO_2 catalyst calcined in oxygen.

Table 3.5.3 Strong chemisorption of catalysts

Catalyst 4SCN	vol CO adsorbed/g. reduced cat (ml)	D (%)	m.s.a. (m^2/g.cat)	Co loaded (mg)	Co^0 area loaded in FT (m^2)	p_d (nm)
30Co-nit(H_2O)/100Al_2O_3 (over calcined)	0.43	0.57	0.77	52	0.20	174
30Co-nit(H_2O)/100Al_2O_3	0.69	0.90	1.22	48	0.32	110
30Co-nit(CH_3OH)/100Al_2O_3	0.59	0.81	1.04	49	0.27	121
30Co-ace(H_2O)/100Al_2O_3	2.05	3.18	3.64	48	1.04	31
30Co-acac(CH_2Cl_2)/100Al_2O_3	0.91	1.70	1.61	48	0.56	58

D = Dispersion.
m.a.s. = Metallic surface area.
p_d = Average particle diameter of cobalt metal.

Table 3.5.4 Total chemisorption of catalysts

Catalyst 4SCN	vol CO adsorbed/g. reduced cat (ml)	D (%)	m.s.a. (m^2/g.cat)	Co loaded (mg)	Co loaded in FT (m^2)	p_d (nm)
30Co-nit(H_2O)/100Al_2O_3 (over calcined)	1.18	1.55	2.10	52	0.55	64
30Co-nit(H_2O)/100Al_2O_3	1.73	2.27	3.08	48	0.80	44
30Co-nit(CH_3OH)/100Al_2O_3	1.52	2.10	2.70	49	0.70	47
30Co-ace(H_2O)/100Al_2O_3	6.02	9.35	10.71	48	3.07	11
30Co-acac(CH_2Cl_2)/100Al_2O_3	2.06	3.87	3.66	48	1.27	26

D = Dispersion.

m.a.s. = Metallic surface area.

p_d = Average particle diameter of cobalt metal.

For the FT synthesis the reactor always was loaded with an amount of catalyst, which contained 48 mg of cobalt. The corresponding loaded metallic areas for the different catalysts varied in a range of 0.20 to 1.04 m^2. The lowest metallic area was observed when the 30Co-nit(H_2O)/100Al_2O_3 catalyst was over calcined. After the repeat preparation of the latter catalyst the metallic area showed an increment from 0.20 to 0.32m^2. The 30Co-nit(CH_3OH)/100Al_2O_3 had a lower metal area than the 30Co-nit(H_2O)/100Al_2O_3. In spite of its lower metal surface area this catalyst had a higher initial activity (2hr TOS) than the one dissolved in water. The highest metal surface area corresponded to the 30Co-ace(H_2O)/100Al_2O_3. The highest initial activity also corresponded to the 30Co-ace(H_2O)/100Al_2O_3. The lowest metal surface area corresponded to the 30Co-acac(CH_2Cl_2)/100Al_2O_3.

3.5.4 BET Area

The BET surface areas of the catalysts are given in table 3.5.5. The alumina support on its own had a BET surface area of 163m^2/g. The "expected" BET surface areas of the catalysts were calculated taking into account the alumina content in the catalyst. The "measured" surface area was expressed as the total surface area of the catalyst per 1 gram of catalyst. In

all cases the measured areas were smaller than the expected ones. The measured BET area of the 30Co-nit(H_2O)/100Al_2O_3 catalyst, which was over calcined was 91m^2/g.catalyst and the one calcined at 270°C had a surface area of 102 m^2/g.catalyst. It appears that over calcination causes alumina structure break down which results in lower alumina surface area and/or sintering of the cobalt particles which causes cobalt particle growth and these large particles then block the alumina pores making the alumina pores less accessible for N_2 adsorption. The measured catalyst surface area of the 30Co-nit(H_2O)/100Al_2O_3 and that of the 30Co-nit(CH_3OH)/100Al_2O_3 were the same namely 102 and 100 m^2/g.catalyst respectively. A slightly higher surface area of 108m^2/g.catalyst was obtained for the 30Co-ace(H_2O)/100Al_2O_3 catalyst. A large loss in catalyst surface area was observed on the 30Co-acac(CH_2Cl_2)/100Al_2O_3 catalyst. The surface area of this catalyst was only 20m^2/g.catalyst. The loss of catalyst surface area was attributed to the presence of large quantities of undecomposed carbonaceous material in the alumina pores.

Table 3.5.5 BET surface areas of catalysts

Catalyst 4SCN	1 g. catalyst contains g. Al_2O_3	BET Surface area expected (m^2/g.cat)	BET Surface area measured (m^2/g.cat)
SiO_2 support (blank)	1.00	163	163
30Co-nit(H_2O)/100Al_2O_3 (over calcined)	0.73	119	91
30Co-nit(H_2O)/100Al_2O_3	0.73	119	102
30Co-nit(CH_3OH)/100Al_2O_3	0.74	121	100
30Co-ace(H_2O)/100Al_2O_3	0.77	126	108
30Co-acac(CH_2Cl_2)/100Al_2O_3	0.81	132	20

3.5.5 FT Activity

3.1.5.1 Activity with time on stream

The FT activity was calculated from the CO converted with time on stream. The FT reaction was performed at 220°C, 15bar g and H_2/CO ratio =2, (H_2+CO) flow = 28ml/min. The FT activities of the catalysts are summarised in table 5.5.6 and shown in figure 3.5.4. The 30Co-

nit(H_2O)/100Al_2O_3 over calcined showed very low FT activity. Sintering was most probably the cause of the poor activity. As observed in table 3.5.6 the repeat preparation of the 30Co-nit(H_2O)/100Al_2O_3 gave higher FT activity. The 30Co-nit(CH_3OH)/100Al_2O_3 catalyst had higher initial activity than the 30Co-nit(H_2O)/100Al_2O_3 catalyst (used as a reference catalyst) but after 16 hrs of reaction this activity decreased and was lower than that of the standard catalyst activity. The lower activity of the Co-nit(CH_3OH)/100Al_2O_3 catalyst through out the run matches the lower metal surface area. It could be that the initial activity of the Co-nit(CH_3OH)/100Al_2O_3 was "out of line". The 30Co-ace(H_2O)/100Al_2O_3 catalyst gave the best initial FT performance and this is in accordance with the high metal surface area obtained for this particular catalyst. The activity of the latter catalyst declined rapidly and after 20 hrs TOS the CO converted was lower than that of the 30Co-nit(H_2O)/100Al_2O_3 catalyst. The decline in activity might have been caused by the re-oxidation of the small cobalt crystallites. Iglesia [20] reported that cobalt crystallites smaller than 5-6nm re-oxidise and deactivate rapidly in the presence of the water produced at typical FTS conditions. The 30Co-acac(CH_2Cl_2)/100Al_2O_3 catalyst showed the lowest activity except for the 30Co-nit(H_2O)/100Al_2O_3 catalyst over calcined. The low activity of the 30Co-acac(CH_2Cl_2)/100Al_2O_3 catalyst could be explained as a result of pore blockage of the alumina support by the carbonaceous deposits. From BET analyses this catalyst had a surface area around 20m^2/g.catalyst, which was very low compared to 102m^2 found for the 30Co-nit(H_2O)/100Al_2O_3 catalyst (table 3.5.5).

Table 3.5.6 FT activity of catalysts

Catalyst 4SCN	FT activity measured as CO converted (%)				
	Time on stream (hrs)				
	2	16	20	24	48
30Co-nit(H_2O)/100Al_2O_3 (over calcined)	7.1	5.6	3.9	4.1	4.1
30Co-nit(H_2O)/100Al_2O_3	57.8	56.2	55.6	53.3	44.0
30Co-nit(CH_3OH)/100Al_2O_3	64.8	41.3	41.3		42.5
30Co-ace(H_2O)/100Al_2O_3	82.2	54.5	48.4	49.9	43.0
30Co-acac(CH_2Cl_2)/100Al_2O_3	42.1	33.0	32.1	32.0	33.8

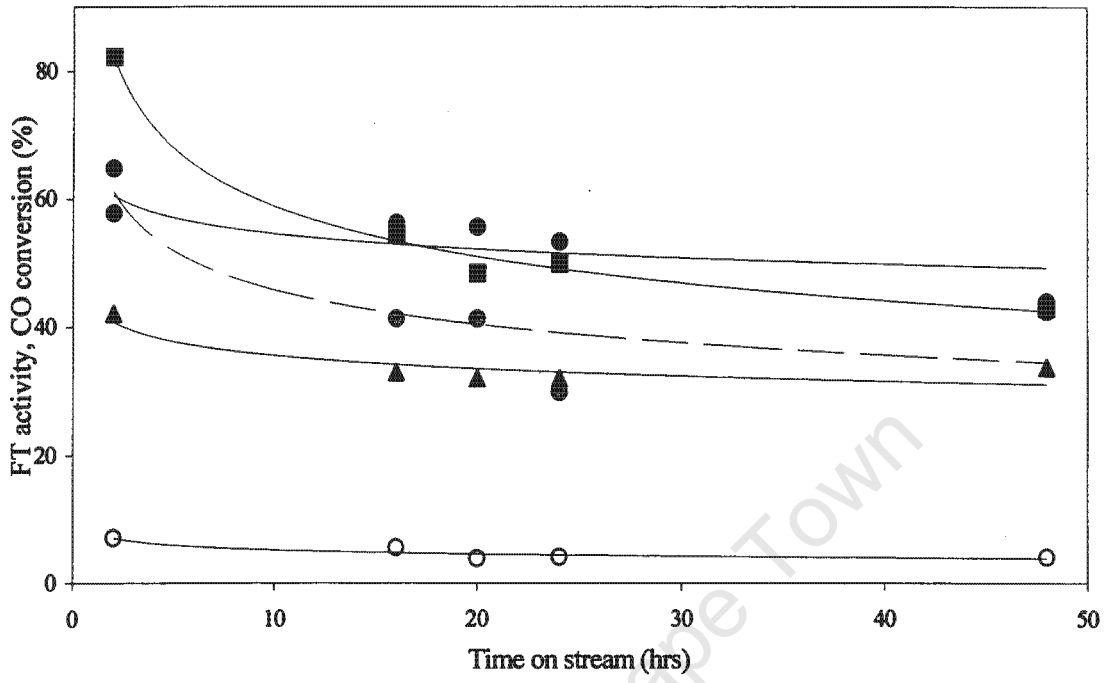

Figure 3.5.4: FT activities of, (○) 30gCo-nit(H_2O)/100gAl_2O_3 over calcined, (●) 30gCo-nit(H_2O)/100gAl_2O_3 repeat preparation , (●) 30gCo-nit(CH_3OH)/100gAl_2O_3, (■) 30gCo-ace(H_2O)/100gAl_2O_3, (▲) 30gCo-acac(CH_2Cl_2)/100gAl_2O_3 catalysts. FT conditions, 220°C, 15bar g, $H_2/CO = 2$.

The FT initial activities of the catalysts were plotted against the metal surface area loaded in the FT reactor. As seen in figure 3.5.5 there is some correlation of the catalysts' activities with the metallic surface areas. The activity of the catalysts prepared with cobalt nitrate did not quite fall within the trend. In further sections it will be shown that catalysts prepared with cobalt nitrate are out of the trend of activity versus metal area.

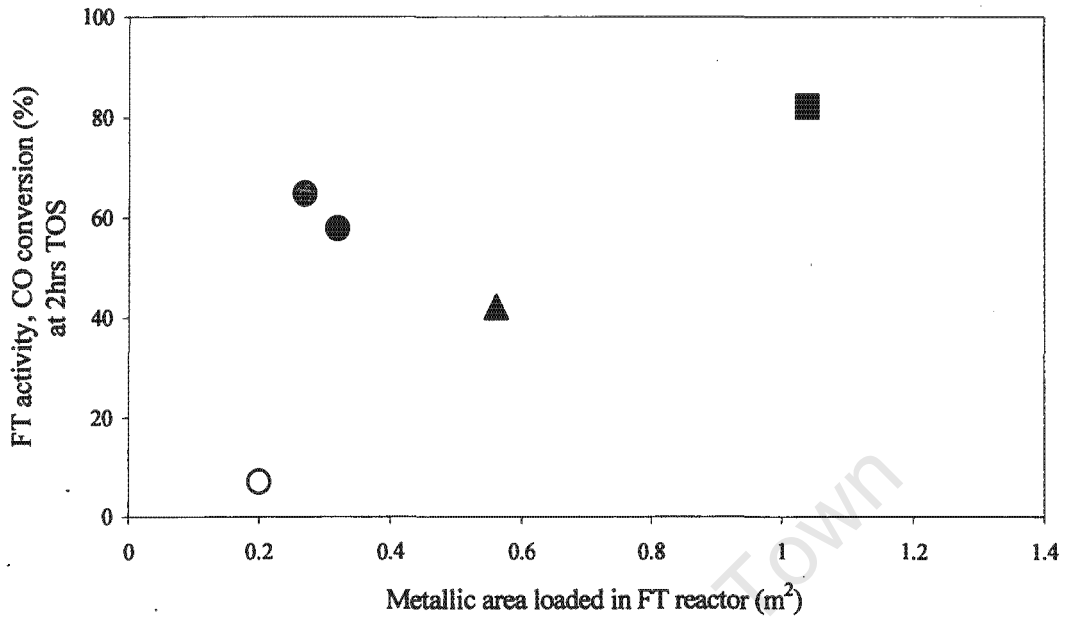

Figure 3.5.5: FT activities versus metallic area loaded in FT reactor, (○) 30gCo-nit(H_2O)/100gAl_2O_3 over calcined, (●) 30gCo-nit(H_2O)/100gAl_2O_3 repeat preparation , (●) 30gCo-nit(CH_3OH)/100gAl_2O_3, (■) 30gCo-ace(H_2O)/100gAl_2O_3, (▲) 30gCo-acac(CH_2Cl_2)/100gAl_2O_3 catalysts. FT conditions, 220°C, 15bar g, $H_2/CO = 2$.

3.5.5.2 Chain growth Probability and Product Selectivity

The chain growth probability (α) was obtained from the slope of the plot of n against log(Fn/n) for the hydrocarbon products between C_3 to C_{12} (see section 1.1.6). The obtained α values are listed in table 3.5.7. All the catalysts prepared with cobalt nitrate showed similar α values of about 0.84. A slightly decrease in α values were obtained for the 30Co-ace(H_2O)/100Al_2O_3 catalyst, which were around 0.81. The lowest α values corresponded to the 30Co-acac(CH_2Cl_2)/100Al_2O_3 catalyst. The average alpha values for the latter catalyst were estimated to be around 0.76.

Table 3.5.7 Chain growth probability of catalysts.

Catalyst 4SCN	Chain growth probability (α)				
	Time on stream (hrs)				
	2	16	20	24	48
30Co-nit(H_2O)/100Al_2O_3 (over calcined)	0.82	0.84	0.85	0.84	0.84
30Co-nit(H_2O)/100Al_2O_3	0.83	0.83	0.85	0.84	0.84
30Co-nit(CH_3OH)/100Al_2O_3	0.81	0.85	0.83	0.85	0.83
30Co-ace(H_2O)/100Al_2O_3	0.82	0.81	0.81	0.81	0.80
30Co-acac(CH_2Cl_2)/100Al_2O_3	0.73	0.74	0.79	0.73	0.82

The catalysts, which produced the lowest ratio of paraffins to total hydrocarbons was the over calcined 30Co-nit(H_2O)/100Al_2O_3 catalyst. Surprisingly the 30Co-nit(CH_3OH)/100Al_2O_3 catalyst appeared to produce the most paraffinic products of all the catalysts. Although the 30Co-ace(H_2O)/100Al_2O_3 initially was the most active catalyst the selectivity for paraffins was lower than the 30Co-nit(CH_3OH)/100Al_2O_3. On the other hand the 30Co-acac(CH_2Cl_2)/100Al_2O_3 catalyst showed low activity and also low paraffins selectivity, as was the case for the over calcined catalyst. Generally the high activity catalysts yielded higher paraffins' selectivities. This is not surprising, as from kinetics one would expect the more active catalyst to hydrogenate the olefins to a greater extent.

Table 3.5.8 Ratio of paraffins in the hydrocarbon fraction.

Catalyst	Paraffins/Total hydrocarbon										
	Carbon fraction										
	C_2	C_3	C_4	C_5	C_6	C_7	C_8	C_9	C_{10}	C_{11}	C_{12}
30Co-nit(H_2O)/100Al_2O_3 (over calcined)	0.63	0.21	0.31	0.32	0.38	0.45	0.52	0.61	0.67	0.73	0.78
30Co-nit(H_2O)/100Al_2O_3	0.59	0.44	0.51	0.57	0.65	0.72	0.79	0.81	0.85	0.90	0.95
30Co-nit(CH_3OH)/100Al_2O_3	0.78	0.69	0.70	0.75	0.80	0.85	0.89	0.95	0.94	0.97	0.98
30Co-ace(H_2O)/100Al_2O_3	0.63	0.56	0.55	0.60	0.66	0.72	0.76	0.79	0.84	0.90	0.94
30Co-acac(CH_2Cl_2)/100Al_2O_3	0.39	0.48	0.51	0.58	0.62	0.69	0.73	0.78	0.84	0.86	0.90

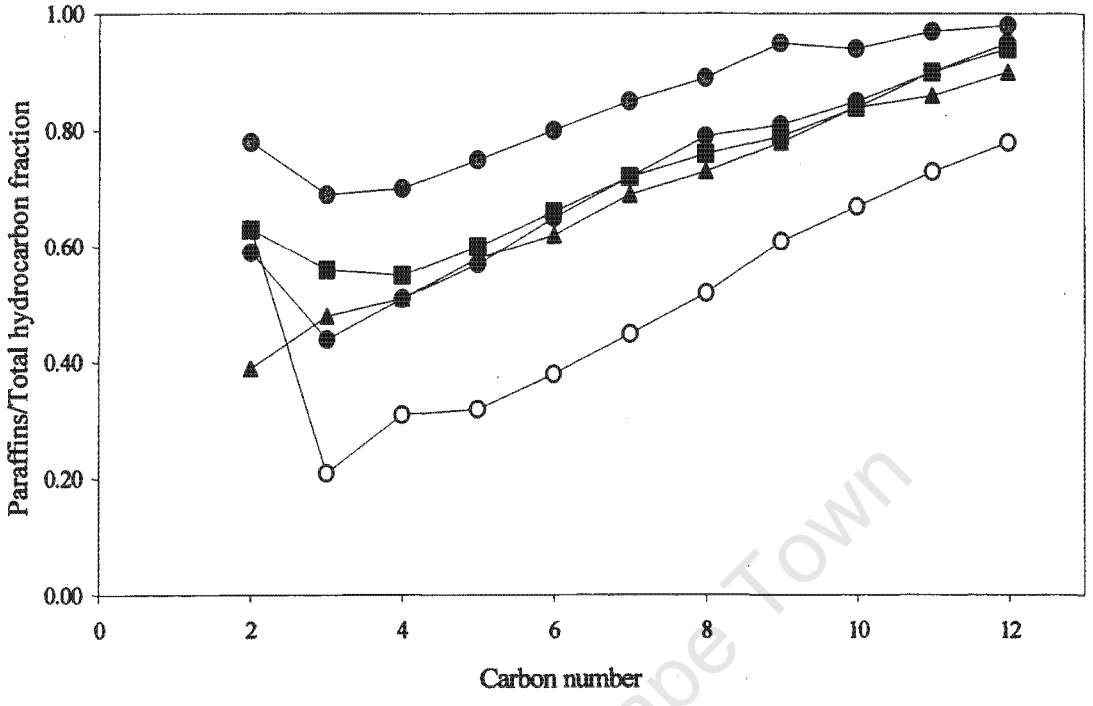

Figure 3.5.6: Ratio of paraffins over total carbon fraction versus carbon number for catalysts, (○) 30gCo-nit(H_2O)/100gAl_2O_3 over calcined, (●) 30gCo-nit(H_2O)/100gAl_2O_3 repeat preparation , (◉) 30gCo-nit(CH_3OH)/100gAl_2O_3, (■) 30gCo-ace(H_2O)/100gAl_2O_3, (▲) 30gCo-acac(CH_2Cl_2)/100gAl_2O_3 catalysts. FT conditions, 220°C, 15bar g, $H_2/CO = 2$.

The most abundant alcohol produced was ethanol. The ratio of ethanol over the total C_2 hydrocarbons using the 30Co-nit(H_2O)/100Al_2O_3 catalyst was 0.1. The 30Co-ace(H_2O)/100Al_2O_3 catalyst gave a ratio of 0.2 and the 30Co-acac(CH_2Cl_2)/100Al_2O_3 catalyst 0.5. The ratios of aldehydes over the total hydrocarbons were insignificant. In most of the cases the ratios were below 0.01. The more paraffinic the product the lower the $EtOH/C_2^+$ could be expected. The more active catalyst would hydrogenate the olefins and also the alcohols.

3.6 Different calcination procedures on alumina supported catalysts

The investigated catalysts in this section were prepared as explained in section 2.1.3.2. In this particular preparation all the catalysts were calcined in air rather than in nitrogen. The purpose of calcining the catalysts under different media was to investigate whether the calcining gas plays an important role during the catalysts' pre-treatment and this could result in different dispersions.

3.6.1 Atomic Absorption Spectroscopy (AAS)

The cobalt concentration of the air calcined catalysts was determined using an atomic adsorption spectrometer (AAS). The "expected" cobalt concentrations were calculated as if only Co_3O_4 was formed by calcination. Table 3.6.1 shows the cobalt concentrations of catalysts calcined in air and in N_2. It is evident that more material was burnt off by calcination in air than in N_2, particularly in the case of the acetyl acetonate sample. Evidently calcination under air facilitated the decomposition of the cobalt salt more efficiently than calcination under nitrogen. To prove this finding a couple of thermogravimetric analyses (TGA) were performed on the acetyl acetonate sample. The results confirmed that when calcining these samples in air there was a higher loss of carbonaceous material as shown in figure 3.6.3.

Table 3.6.1 Cobalt content of catalysts

Catalyst 4SCA	wt(%) Co expected	wt(%) Co measured (AAS)		
		Calcination in air (°C)		Calcination in N_2 at 270°C (table 3.5.1)
30Co-nit(H_2O) /100Al_2O_3,	21.3	270	21.9	18.3
30Co-nit(CH_3OH) /100Al_2O_3,	21.3	270	21.9	18.8
30Co-ace(H_2O) /100Al_2O_3,	21.3	270	18.6	16.9
30Co-acac(CH_2Cl_2) /100Al_2O_3, 300°C	21.3	300	14.7	13.9
30Co-acac(CH_2Cl_2) /100Al_2O_3, 350°C	21.3	350	19.5	13.9

Co-nit(H_2O) = Cobalt nitrate dissolved in water.
Co-nit(CH_3OH) = Cobalt nitrate dissolved in methanol.
Co-ace(H_2O) = Cobalt acetate dissolved in water.
Co-acac(CH_2Cl_2) = Cobalt acetylacetonate dissolved in dicloromethane.
4SCA = Impregnation in four steps and calcination under air.

3.6.2 Temperature Programmed Reduction (TPR)

The TPR profile of the 30Co-nit(H_2O) /100Al_2O_3, catalyst calcined in air was similar to that of the one calcined under nitrogen. The total hydrogen consumed was $5.5x10^{-3}$ and $5.4x10^{-3}$ moles H_2/g. cat respectively. As previously shown in section 3.5.2 the TPR profile of the 30Co-nit(H_2O) /100Al_2O_3, catalyst calcined under nitrogen showed reduction peaks at 258, 328 and 630°C. Similarly the TPR profile of the 30Co-nit(H_2O) /100Al_2O_3 catalyst calcined in air shows one shoulder at 300°C and two peaks at 350 and 640°C (see figure 3.6.1). The shoulder and the first peak that followed was assigned to be the reductions of:

$$Co_3O_4 + H_2 \rightarrow 3CoO + H_2O$$

and

$$3CoO + 3H_2 \rightarrow 3Co^0 + 3H_2O$$

The final peak was suggested to be the reduction of cobalt aluminates. Similar TPR reduction profiles were reported by Blekkan [66] with Co/Al_2O_3 (12wt%Co) catalysts calcined in air at 350°C. The TPR scans showed two peaks at 286, 397 and a broad peak between 507 and 767°C [64]. Goodwin [23] reported some TPR profiles corresponding to Co/Al_2O_3 (20wt%Co) catalysts previously calcined in air at 300°C. The TPR scans showed two peaks located at 260 and 480°C. Similarly, catalysts supported on alumina containing 20wt%Co calcined under air at 300°C were reduced in a TPR apparatus [45]. Three peaks were observed at 245, 355 and from 450 to 720°C [45]. The first two peaks were assigned to the reduction of Co_3O_4 and the third broad peak to the reduction of highly dispersed amorphous cobalt oxides interacting strongly with the alumina support [45]. Another evidence of TPR profiles of Co-nit/Al_2O_3 catalysts calcined under air showing three reduction peaks were reported by Hilmen [65]. The reduction of Co_3O_4 involved two peaks at 276 and 362°C and the broad peak at 627°C was due to the reduction of highly dispersed amorphous surface phases. The reduction of $CoAl_2O_4$ was reduced at about 930°C [65]. In the present work a small protuberance was observed from 800 to 970°C but it seems unlikely that this protuberance could only represent the reduction of $CoAl_2O_4$ and not the broad peak starting at about 640°C.

Table 3.6.2 H_2 consumption of catalysts during TPR

Catalyst 4SCA	Moles H_2 consumed x 10^{-3}/g.catalyst						% of H_2 consumed			
	peak				Total H_2 consumed measured	Total H_2 consumed expected	peak			
	1	2	3	4			1	2	3	4
30Co-nit(H_2O)/100Al_2O_3	0.74	1.11	3.58		5.43	4.82	13.6	20.5	65.9	
30Co-ace(H_2O)/100Al_2O_3	0.86	1.47	1.64	0.68	4.65	3.84	18.5	31.6	35.3	14.6
30Co-ace(H_2O)/100Al_2O_3 ®	0.80	1.35	1.44	1.09	4.68	3.84	17.1	28.8	30.8	23.3
30Co-acac(CH_2Cl_2)/100Al_2O_3										
300°C	1.09	0.37			1.46	3.14	74.7	25.3		
350°C	0.52	2.34	0.67	0.49	4.62	3.14	12.9	58.2	16.7	12.2

® = Repeat TPR scan.
4SCA = Four step impregnation, calcined in air.
300°C and 350°C = Calcination temperatures.

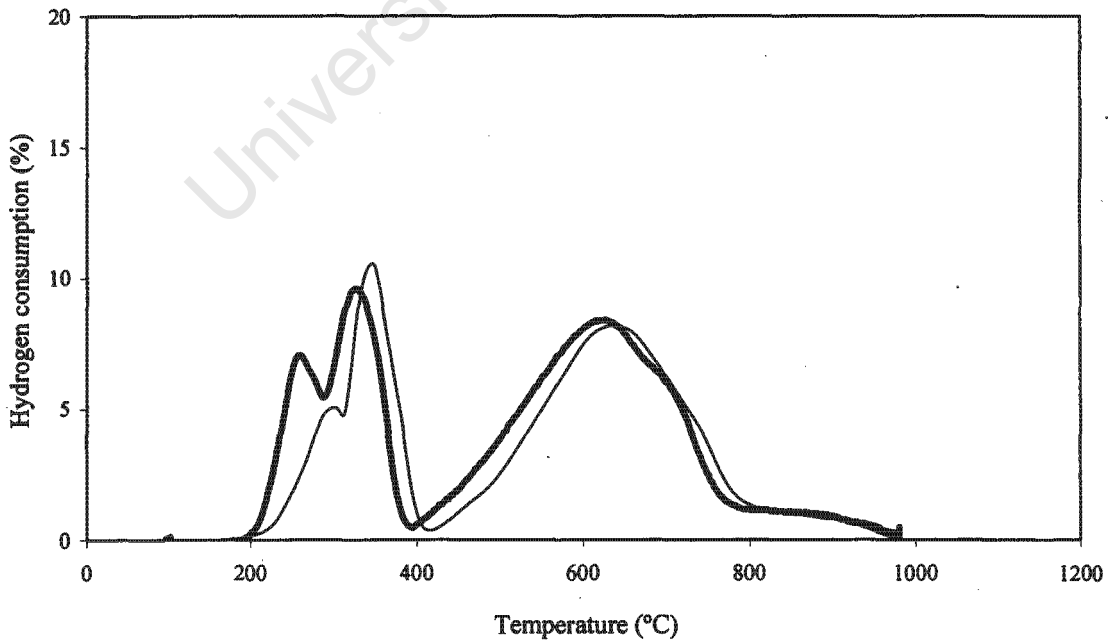

Figure 3.6.1: TPR profiles of: 30gCo-nit (H_2O)/100g100Al_2O_3 catalysts, (——)calcined in air and (▬) calcined in nitrogen. Hydrogen consumption (%) of the reducing mixture (6%H_2 in N_2) against temperature (°C).

The TPR scan of the 30Co-ace(H_2O) /100Al_2O_3, catalyst calcined in air showed a shoulder at 220°C and four peaks at 310, 345, 650 and 870°C (figure 3.6.2). The shoulder at 220°C can not be explained at present. The peaks at 310 and 345°C may represent the stepwise reduction:

$$Co_3O_4 + H_2 \rightarrow 3CoO + H_2O$$
$$3CoO + 3H_2 \rightarrow 3Co^0 + 3H_2O$$

The peak at 650°C may be due to the reduction of cobalt species interacting with the support. The peak at 870°C may involve the reduction of $CoAl_2O_4$ as pointed out in the literature [65]. It can be seen in figure 3.6.2 that the reduction peaks of the 30Co-ace(H_2O) /100Al_2O_3, 4SCA catalyst were shifted to lower temperatures by changing the calcining gas from nitrogen to air. In the literature [27, 66, 67] only two reduction peaks were found on TPR scans of Co-ace/SiO_2, catalysts calcined in air. Generally the first peak represented the reduction of:

$$Co^{3+} \rightarrow Co^{2+} \rightarrow Co^0$$

And the second peak was attributed to the reduction of the strong interaction of cobalt oxides with the silica support [27,66, 67]. The TPR studies carried out in this work have shown that the reduction of 30Co-ace(H_2O) /100Al_2O_3, 4SCA catalyst and the one calcined under nitrogen were reduced in a higher number of stages compared to Co-ace/SiO_2 catalyst reported in literature. The higher number of reduction stages may have been due to the formation of several Co-Al_2O_3 complexes with different reduction properties. From the TPR profiles for 30Co-ace(H_2O) /100Al_2O_3 catalysts obtained during the present work and those reported in the literature it appears that cobalt acetate interacted strongly with alumina as it did with silica.

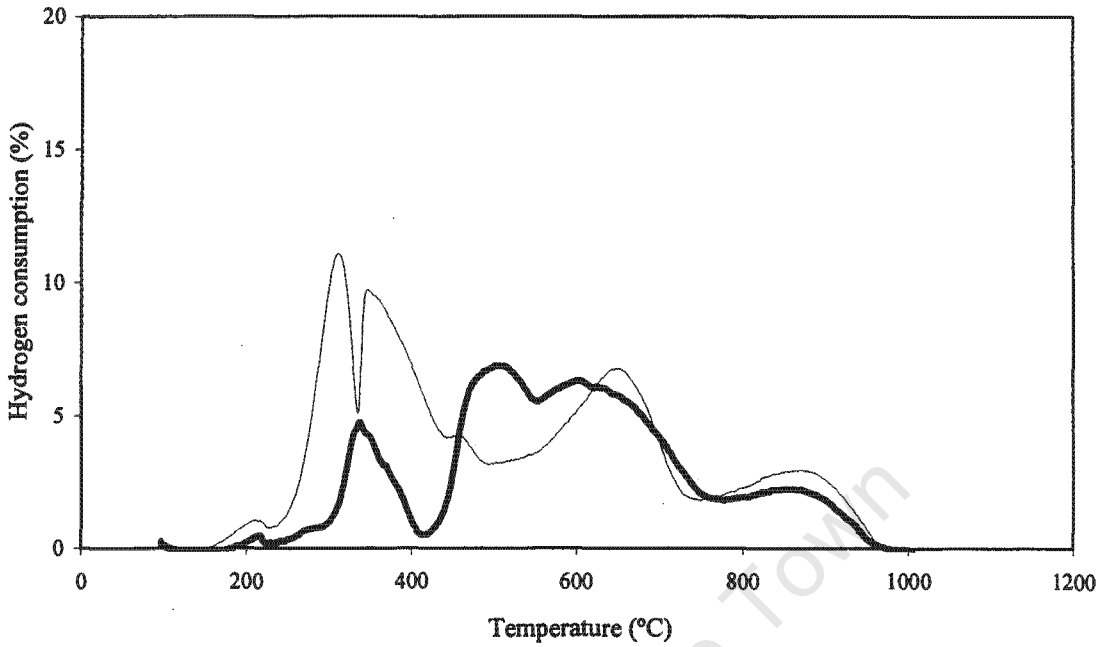

Figure 3.6.2: TPR profiles of: 30gCo-ace (H_2O)/100g100Al_2O_3 catalysts, (——)calcined in air and (▬) calcined in nitrogen. Hydrogen consumption (%) of the reducing mixture (6%H_2 in N_2) against temperature (°C).

The TPR scans of the 30Co-acac(CH_2Cl_2) /100Al_2O_3 catalysts calcined in N_2 and in air are shown in figure 3.5.3 and 3.6.4 respectively. The corresponding hydrogen consumptions are given in tables 3.5.2 and 3.6.2 respectively.

The TPR profile for the 30Co-acac(CH_2Cl_2) /100Al_2O_3 catalysts calcined in N_2 (discussed in section 3.5.2) showed two peaks above and two peaks below the baseline. The low calcination temperature was believed to be responsible for this result because acetyl acetonate groups were not removed at the calcination temperature of 270°C. At this stage a TGA analysis was conducted in order to observe the removal of acetyl acetonate groups, which is accompanied by loss of weight. The TGA results indicated loss of sample weight between about 310 and 330°C (see figure 3.6.3). Two separate TPR runs were performed after calcining the samples at 300 and 350°C in air. After calcining the catalyst at 300°C the TPR profile showed hydrogen consumption at two temperatures 380 and 560°C. The first peak was attributed to be the reduction of

$$Co^{3+} \rightarrow Co^{2+} \rightarrow Co^{0}$$

The second peak was assigned to the reduction of the strong interaction of cobalt oxides and the support. The negative peak at about 500°C possibly represented the decomposition of acetyl acetonate groups. The total hydrogen consumption was $1.5x10^{-3}$ moles H_2/g.cat, which was only about 50% of the expected hydrogen consumption. The TPR profile for the. 30Co-acac(CH_2Cl_2) /100Al_2O_3, 4SCA calcined at 350°C showed one shoulder at 320°C and three peaks at 370, 660 and around 840°C. The shoulder could indicate the reduction of:

$$Co^{3+} \rightarrow Co^{2+}$$

The peak at 370°C may be represented the reduction of:

$$Co^{2+} \rightarrow Co^{0}$$

The peaks at 660 and 840°C represent the reduction of strong metal –support interactions. The total hydrogen consumed for this particular catalyst was $4.0x10^{-3}$ moles H_2/g.cat., which is closer to the "expected" one of about $3.1x10^{-3}$ moles H_2/g.cat. In the literature [31] the TPR scans for Co-acac/SiO_2 calcined in air at 450°C showed two peaks at about 330°C and 800°C. The peak at 330°C represented the reduction of Co_3O_4 to Co^0 and the peak at 800°C was responsible for the reduction of CoO_x-SiO_2 species [34]. TPR studies conducted by Baerns [27] demonstrated that Co-acac/SiO_2 catalysts were reduced in only one single stage. The reduction peak appeared at 397°C [27]:

$$Co^{3+} \rightarrow Co^{2+} \rightarrow Co^{0}$$

The peak attributed to the strong interaction of cobalt oxides and the silica support was not observed because the maximum heating temperature during the catalyst reduction was set-up to only 400°C [27].

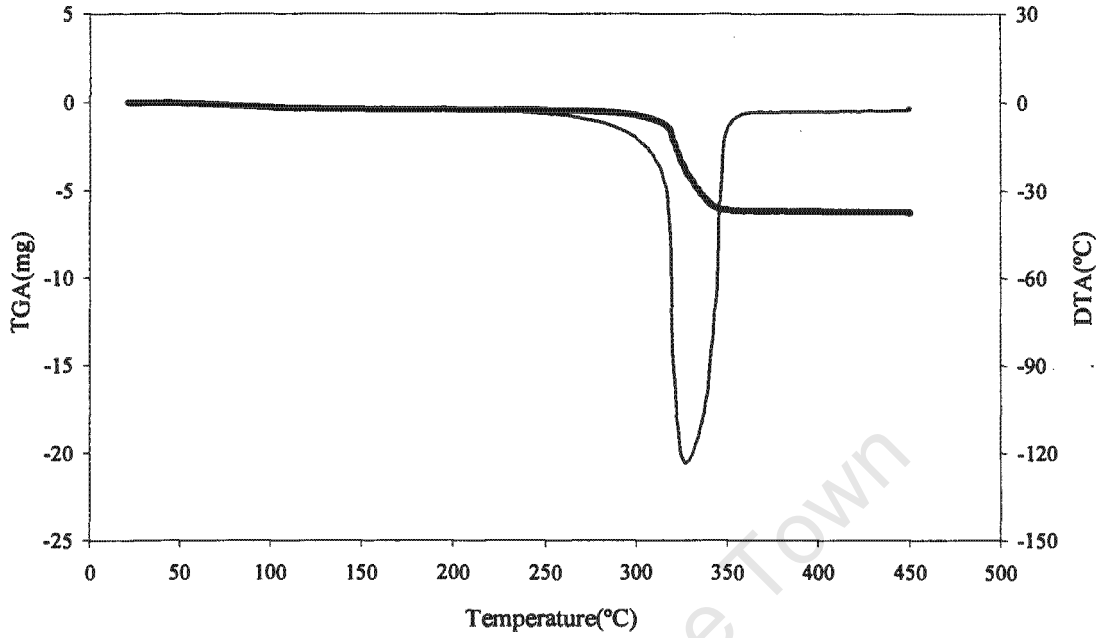

Figure 3.6.3: TGA (▬) and DTA (——) analyses of: 30gCo-acac (CH_2Cl_2)/100g100Al_2O_3 4SCA catalyst. Sample linearly heated at 5°C/min in air from 25°C to 500°C, kept at 500°C for 2hrs.

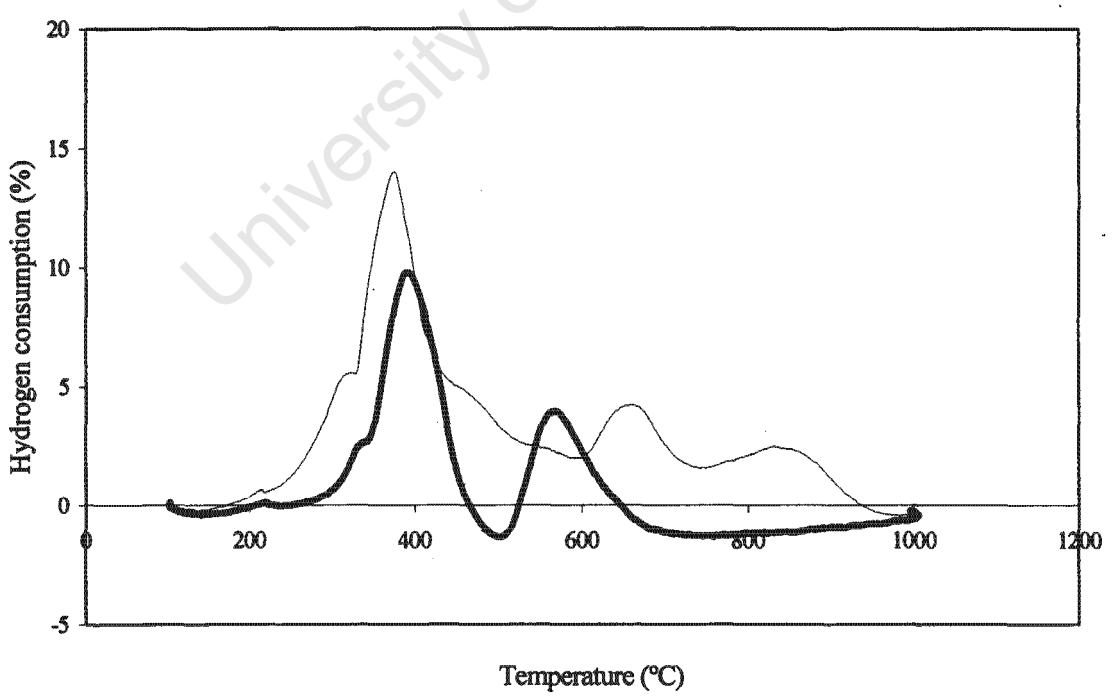

Figure 3.6.4: TPR profiles of: 30gCo-acac (CH_2Cl_2)/100g100Al_2O_3 catalysts calcined in air at , (▬) 300°C and (——) 350°C before reduction in TPR apparatus. Hydrogen consumption (%) of the reducing mixture (6%H_2 in N_2) against temperature (°C).

3.6.3 CO Chemisorption

3.6.3.1 Metal Dispersion, metal surface area and average particle diameter

The results of the catalysts tested for CO adsorption are given in table 3.6.3. The dispersion values obtained for the catalysts were calculated on the basis of the total Co present on the catalysts. As is has been shown that not all the cobalt was in fact reduced at 350°C over 16 hrs the calculated dispersions here represent the amount of surface Co atoms as a percentage of the total cobalt present and not of the reduced Co present. Generally, lower dispersions were achieved on catalysts calcined in air, an exception was the 30Co-acac(CH_2Cl_2) /100Al_2O_3 catalysts calcined in air, which now had the highest dispersion of all the catalysts investigated. The reason for the low dispersion of this catalyst when calcined in nitrogen was the incomplete removal of the organic material as explained in section 3.5.3. The high dispersion obtained when calcined in air is in agreement with Baerns' [27] who found higher dispersions on Co-acac(III)/TiO_2 catalysts compared to Co-acac(II)/TiO_2, Co-nit(II)/TiO_2 and Co-ace(II)/TiO_2 catalysts. The differences in dispersions using different cobalt precursors might be related to physical properties of the cobalt salts *e.g.,* melting point. It is relevant to evaluate the states of cobalt salts after impregnation and before calcination. The following could be the explanation of differences in catalysts' behaviour. After drying the catalyst at 120°C cobalt nitrate is present as liquid droplets since the melting point is 57°C. During calcination at 270°C under nitrogen or air nitrogen oxides are formed, which are strong oxidising agents. The formation of nitrogen oxides might have been favoured in the presence of air, which results in faster metal particle growth. Cobalt acetate on the other hand looses its crystal water during drying, thus under calcination conditions cobalt acetate is present as a solid. Calcination under nitrogen does not change the particle size significantly. During calcination under air the acetate group is burnt off in exothermic reaction resulting in higher temperatures, which causes sintering and hence larger particles. Cobalt acetyl acetonate under calcination conditions is liquid; the salt decomposes at 197°C. The rapid removal of carbonaceous material during calcination under air might cause agglomeration. Keeping the above in mind, the obtained catalysts prepared with different cobalt salts will show different cobalt surface areas and hence different activities.

Table 3.6.3 Strong chemisorption of catalysts

Catalyst 4SCA	vol CO adsorbed/g. reduced cat (ml)	D (%)	m.s.a. (m^2/g.cat)	Co loaded in FT (mg)	Co area loaded in FT (m^2)	p_d (nm)
30Co-nit(H_2O)/100Al_2O_3	0.39	0.46	0.70	51	0.18	213
30Co-nit(CH_3OH)/100Al_2O_3	0.39	0.46	0.69	51	0.18	215
30Co-ace(H_2O)/100Al_2O_3	1.73	2.44	3.08	48	0.80	41
30Co-acac(CH_2Cl_2)/100Al_2O_3 35	2.78	3.76	4.95	51	1.29	26

D = Dispersion.
m.a.s. = Metallic surface area.
p_d = Average particle diameter of cobalt metal.

The metal surface areas of the catalysts were given as m^2 per gram of catalyst. As expected the 30Co-ace(H_2O) /100Al_2O_3 catalyst showed higher metal surface area than the 30Co-nit(H_2O) /100Al_2O_3 catalysts. Unexpectedly, the 30Co-acac(CH_2Cl_2) /100Al_2O_3 catalyst, in spite of its high metal surface area had a low FT activity (see figure 3.6.5). This is a contradiction because it was usually found that the catalyst activity was a function of the metal surface area. TEM photographs showed that this catalyst had small cobalt oxide particles and the CO chemisorption results confirmed this but BET analyses showed that the surface area of the catalyst was very low compared to the cobalt nitrate and cobalt acetate catalysts (see table 3.6.4). The catalyst activity was expected to be proportional to the metal surface area and not to the decrease in the BET surface area. In the present studies it appears that the large decrease in BET surface area lowered the activity of the 30Co-acac(CH_2Cl_2) /100Al_2O_3 catalyst due to pore blockage by the undecomposed acetylacetonate groups, resulting in the reduced metal particles being less accessible during the FT reaction.
The average particle diameters of the catalysts were 26, 41, 213 and 215 nm for the 30Co-acac(CH_2Cl_2) /100Al_2O_3, 30Co-ace(H_2O) /100Al_2O_3, 30Co-nit(H_2O) /100Al_2O_3 and 30Co-nit(CH_3OH)/100Al_2O_3 catalysts respectively.

3.6.4 BET Area

The BET areas of the catalysts are listed in table 3.6.4. The "expected" surface areas of the catalysts were estimated according to their alumina contents. The expected surface areas

were higher than the measured ones per one gram of catalyst. The surface area of the 30Co-acac(CH_2Cl_2) /100Al_2O_3 catalyst calcined under air at 300°C was very low as it was when the same catalyst was calcined under nitrogen at 270°C (see table 3.5.5). Calcining the catalyst under air at 300°C did not facilitate to a greater extent the burn off the acetylacetonate groups, which were plugging the alumina support.

Table 3.6.4 BET surface areas of catalysts

Catalyst 4SCA	1 g. catalyst contains		BET surface area (m^2/g.cat)	
	Co_3O_4	Al_2O_3	expected	measured
Al_2O_3	0.00	1.00	163	163
30Co-nit(H_2O)/100Al_2O_3	0.30	0.70	114	99
30Co-nit(CH_3OH)/100Al_2O_3	0.30	0.70	114	96
30Co-ace(H_2O)/100Al_2O_3	0.25	0.75	122	134
30Co-acac(CH_2Cl_2)/100Al_2O_3	0.20	0.80	130	17

3.6.5 FT Activity

3.6.5.1 Activity with time on stream

The FT synthesis was carried out at 220°C, 15 bar g and H_2/CO ratio = 2. The total H_2+CO flow rate was 28ml/min. The activity of the 30Co-nit(H_2O)/100Al_2O_3 catalyst calcined in air (see table 3.6.5a) was throughout lower than the one calcined under nitrogen (see table 3.5.6). The initial activity of the 30Co-nit(CH_3OH)/100Al_2O_3 catalyst calcined in air was also slightly lower than that of the one calcined under nitrogen. Following this trend the activity of the 30Co-ace(H_2O)/100Al_2O_3 catalyst calcined in air was also lower throughout than the one calcined under nitrogen. Once again the high activity of the Co-ace catalyst decreases rapidly due possibly to re-oxidation of the small cobalt crystallites. The 30Co-acac(CH_2Cl_2)/100Al_2O_3 catalysts were calcined in air at 300 and 350°C in order to burn off the acetyl acetonate groups and have improved accessibility for CO hydrogenation. The results however indicated that the FT activities of the catalysts calcined at 300 and 350°C in air were not much better than the one calcined in nitrogen at 270°C. Although the metal surface area loaded for the catalyst calcined in air at 300°C (table 3.6.3) was twice as high as

the one calcined under nitrogen at 270°C (table 3.5.3) the activity of the catalyst calcined in air at 300°C was not enhanced. As seen in section 3.6.4 the BET area of the 30Co-acac(CH_2Cl_2)/100Al_2O_3 catalyst calcined in air was only 17m^2/g.catalyst. It could be that the FT activity was again lowered due to alumina pore blockage.

Table 3.6.5a FT activity of catalysts

Catalyst 4STCA	FT activity measured as CO converted (%)				
	Time on stream (hrs)				
	2	16	20	24	48
30Co-nit(H_2O)/100Al_2O_3	51.3	44.3	43.9	43.7	41.0
30Co-nit(CH_3OH)/100Al_2O_3	62.6	51.5		48.1	43.3
30Co-ace(H_2O)/100Al_2O_3	67.5	42.5	39.7	39.6	36.7
30Co-acac(CH_2Cl_2)/100Al_2O_3 300°C	42.4	38.8	39.1	36.2	32.3
30Co-acac(CH_2Cl_2)/100Al_2O_3 350°C	42.0	35.4	34.9	33.2	31.1

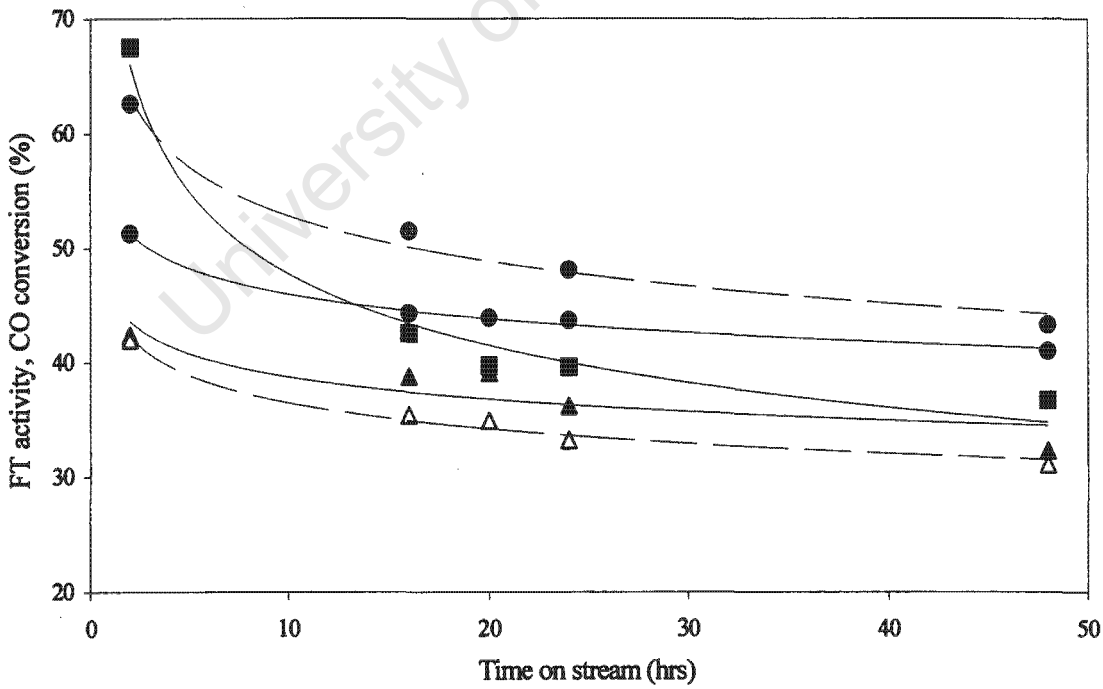

Figure 3.6.5: FT activities of, (●) 30gCo-nit(H_2O)/100gAl_2O_3, (●) 30gCo-nit(CH_3OH)/100gAl_2O_3, (■) 30gCo-ace(H_2O)/100gAl_2O_3, (▲) 30gCo-acac(CH_2Cl_2)/100gAl_2O_3 300°C and (△) 30gCo-acac (CH_2Cl_2)/100gAl_2O_3 350°C catalysts. FT conditions, 220°C, 15bar g, H_2/CO = 2.

The FT activities of the catalysts calcined in air were plotted against the metal surface area loaded in the FT reactor (figure 3.6.6a). The aim of this association was to see whether the catalysts' activities were dependent on the metal area exposed. From figures 3.6.6a and b one can see that the activities of the catalysts calcined under nitrogen or in air against the metal surface area followed different trends. The ones calcined under nitrogen appeared to have a reasonable correlation of the FT activities and the metal surface area loaded in the reactor. The ones calcined in air did not follow the same trend. In the case of the catalysts calcined in air the activities did not vary much as the loaded metal surface areas increased. It is possible that the small cobalt crystallites re-oxidised quite rapidly even before the 2 hrs TOS sampling, which means that right at the beginning of the FT reaction the activities were higher than the measured ones at 2hrs TOS.

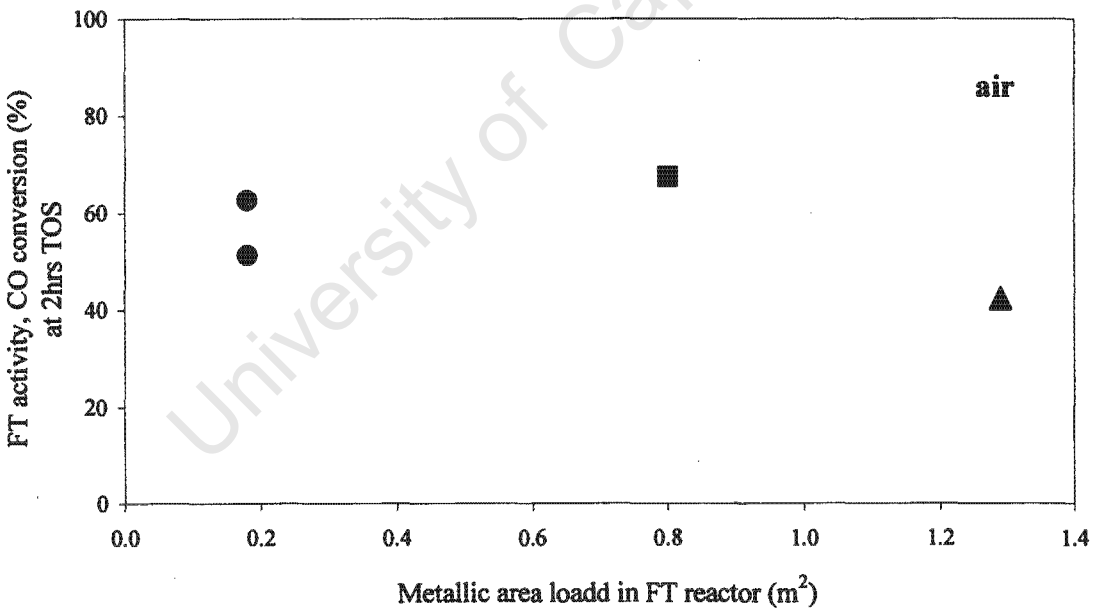

Figure 3.6.6 a: FT activities versus metallic area loaded in FT reactor of catalysts calcined in air, (●) 30gCo-nit (H_2O)/100gAl_2O_3, (●) 30gCo-nit(CH_3OH)/100gAl_2O_3, (■) 30gCo-ace(H_2O)/100gAl_2O_3 and (▲) 30gCo-acac(CH_2Cl_2)/100gAl_2O_3 300°C catalysts.

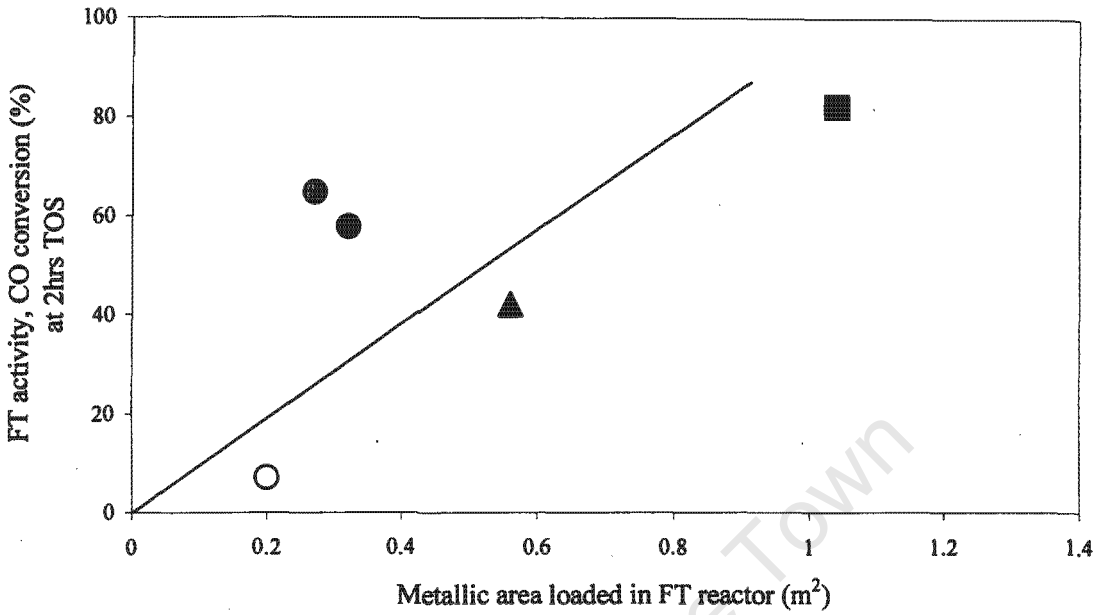

Figure 3.6.6 b: FT activities versus metallic area loaded in FT reactor of catalysts calcined in N_2, (●) 30gCo-nit(H_2O)/100gAl_2O_3 over calcined, (○) 30gCo-nit(H_2O)/100gAl_2O_3 repeat preparation , (●) 30gCo-nit(CH_3OH)/100gAl_2O_3, (■) 30gCo-ace(H_2O)/100gAl_2O_3, (▲) 30gCo-acac(CH_2Cl_2)/100gAl_2O_3 catalysts.

When reviewing the FT activity data of both tables 3.5.6 and 3.6.5a it appears that for each type of cobalt salt used the difference between nitrogen and air calcination was not large and possibly not very significant. In table 3.6.5b the combined averages of the FT activities of the air and nitrogen calcination cases for each of the different salts are shown at different TOS's.

Table 3.6.5b Average FT activities

Cobalt salt used	Average dispersion (%)	Average FT activities (%)CO converted)		
		TOS (hrs)		Decline % points
		2	16-24	
Nitrate	0.6	60	48	12
Acetate	2.2	75	45	30
Acetyl acetonate	2.3	42	37	7

From the table 3.6.5b it can be seen that under the preparation conditions used in the present investigation the nitrates produced the best catalyst in that the activity after 16 hrs TOS was the highest, followed by the acetate and acetyl acetonate. In keeping with its high dispersion

the acetate cases had the highest initial activity but they declined faster than the nitrate cases. The acetyl acetonate cases, despite their high conversions, were the least active at all TOS's. It must be born in mind that the CO chemisorption data (*i.e.*, % dispersions, metal areas, average crystal sizes) only reflect the situation of the freshly reduced catalyst. It is know that the smaller Co metal crystals can rapidly oxidised, *i.e.*, become catalytically inert, under FT conditions leaving only the remaining larger crystallites to do the FT work [20]. It is therefore not surprising that there is not always a simple correlation between FT activity and the dispersion or Co metal areas as determined by chemisorption techniques.

3.6.5.2 Chain growth Probability and Product Selectivity

From the slope of the plot of n against log(Fn/n) for the hydrocarbon products between C_3 to C_{12} the chain growth probability (α) was obtained (see section 1.1.6). The α values obtained for the catalysts calcined in air are listed in table 3.6.6. The catalyst prepared with cobalt nitrate and cobalt acetate showed basically the same alpha values around 0.84. The same cobalt nitrate and acetate catalysts calcined under nitrogen also gave alpha values around 0.84. The 30Co-acac(CH_2Cl_2)/100Al_2O_3 catalyst calcined under air at 300 or 350°C had lower alpha values around 0.75.

Table 3.6.6 Chain growth probability of catalysts.

Catalyst 4SCA	Chain growth probability (α)				
	Time on stream (hrs)				
	2	16	20	24	48
30Co-nit(H_2O)/100Al_2O_3	0.80	0.80	0.85	0.80	0.80
30Co-nit(CH_3OH)/100Al_2O_3	0.83	0.84	0.85	0.84	0.85
30Co-ace(H_2O)/100Al_2O_3	0.84	0.84	0.85	0.84	0.83
30Co-acac(CH_2Cl_2)/100Al_2O_3 300°C	0.72	0.73	0.85	0.73	0.74
30Co-acac(CH_2Cl_2)/100Al_2O_3 350°C	0.75	0.75	0.84	0.76	0.75

The fractions of paraffins of the total hydrocarbon products in the C_2 to C_{12} hydrocarbons are shown in table 3.6.7. For the 30Co-nit(H_2O)/100Al_2O_3 catalyst calcined under nitrogen (see table 3.5.7) the products were more paraffinic than for the catalyst calcined in air (see table

3.6.7). The same trend was observed for the 30Co-nit(CH_3OH)/100Al_2O_3 catalysts. On the other hand for the 30Co-ace(H_2O)/100Al_2O_3 catalyst the products were more paraffinic when it was calcined in air. The 30Co-acac(CH_2Cl_2)/100Al_2O_3 catalyst calcined in air at 300°C yielded products more paraffinic than the one calcined at 350°C (see figure 3.6.7).

Table 3.6.7 Ratio of paraffins in the hydrocarbon fraction.

Catalyst 4SCA	Paraffins/Total hydrocarbon										
	Carbon fraction										
	C_2	C_3	C_4	C_5	C_6	C_7	C_8	C_9	C_{10}	C_{11}	C_{12}
30Co-nit(H_2O)/100Al_2O_3	0.58	0.24	0.35	0.38	0.44	0.52	0.59	0.66	0.74	0.79	0.85
30Co-nit(CH_3OH)/100Al_2O_3	0.58	0.34	0.42	0.47	0.56	0.65	0.72	0.78	0.83	0.87	0.94
30Co-ace(H_2O)/100Al_2O_3	0.55	0.52	0.58	0.61	0.69	0.75	0.79	0.83	0.88	0.92	0.95
30Co-acac(CH_2Cl_2)/100Al_2O_3 300°C	0.30	0.54	0.56	0.63	0.68	0.74	0.78	0.82	0.88	0.91	0.95
30Co-acac(CH_2Cl_2)/100Al_2O_3 350°C	0.43	0.27	0.38	0.44	0.51	0.59	0.66	0.71	0.76	0.79	0.88

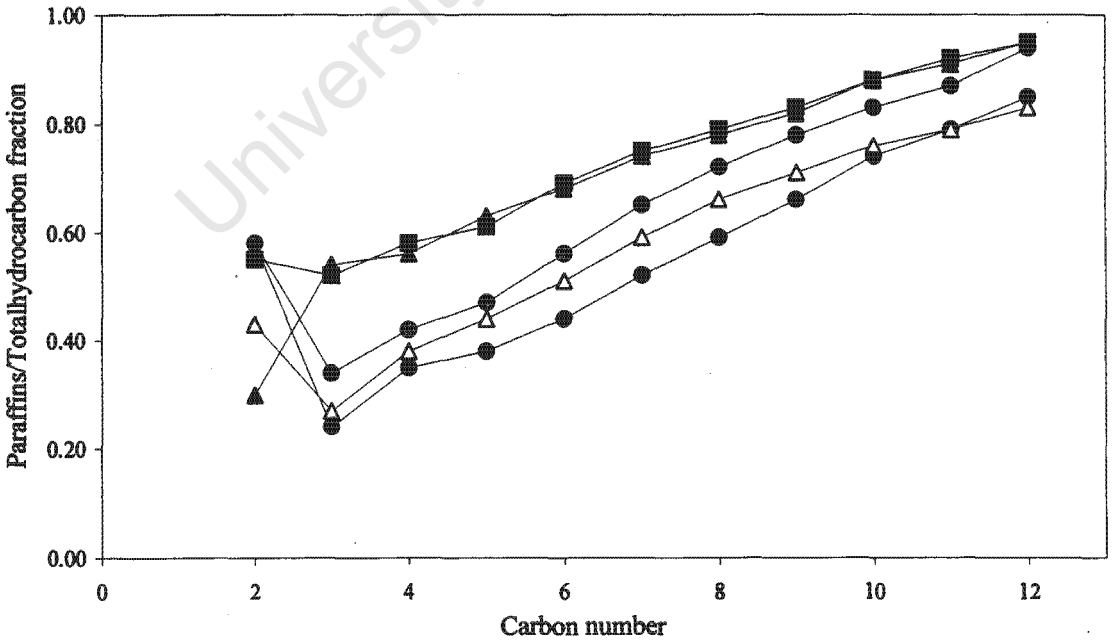

Figure 3.6.7: Ratio of paraffins over total carbon fraction versus carbon number for catalysts, (●) 30gCo-nit(H_2O)/100gAl_2O_3, (●) 30gCo-nit(CH_3OH)/100gAl_2O_3, (■) 30gCo-ace(H_2O)/100gAl_2O_3, (▲) 30gCo-acac(CH_2Cl_2)/100gAl_2O_3 300°C and (△) 30gCo-acac(CH_2Cl_2)/100gAl_2O_3 350°C catalysts. FT conditions, 220°C, 15bar g, $H_2/CO = 2$.

As before ethanol and acetaldehyde were found to be the most abundant alcohol and aldehyde species produced. The ratios of ethanol and the acetaldehyde to the total C_2 hydrocarbon products are shown in table 3.6.8. It appeared that more ethanol was yielded when the 30Co-acac(CH_2Cl_2)/100Al_2O_3 catalyst was used. For all the catalysts the acetaldehyde ratios over the total hydrocarbon products were around zero. The catalysts calcined under nitrogen also showed the same trend with regard to the ethanol yield.

Table 3.6.8 Ratios of ethanol and acetaldehyde over the total C_2 hydrocarbon products.

Catalyst 4SCA	Ratios of oxygenated compounds/Total C_2 hydrocarbon product	
	Ethanol	Acetaldehyde
30Co-nit(H_2O)/100Al_2O_3	0.20	0.00
30Co-nit(CH_3OH)/100Al_2O_3	0.22	0.00
30Co-ace(H_2O)/100Al_2O_3	0.27	0.00
30Co-acac(CH_2Cl_2)/100Al_2O_3 300°C	0.67	0.00
30Co-acac(CH_2Cl_2)/100Al_2O_3 350°C	0.46	0.00

3.7 Alumina supported catalysts using different drying variations

The idea of preparing catalysts dried by microwave heat was to see whether the rapid removal of water could result in a higher dispersion. This expectation was based on the simultaneous and rapid heat produced by microwaves [70]. For this purpose two catalysts were prepared, the first catalyst, 30Co-nit(H_2O)/100Al_2O_3 (c) was dried by microwaves without ageing after impregnation of the cobalt salt, and subsequently calcined under nitrogen. This procedure was repeated 4 times. The second catalyst 30Co-nit(H_2O)/100Al_2O_3 (d) was first aged in a dessicator for 5 days, then heated in a microwave oven and subsequently calcined in nitrogen. For more detailed information regarding to the preparation of this catalyst see section 2.1.3.3.

3.7.1 Atomic Absorption Spectroscopy (AAS)

The measured cobalt concentrations were lower than the expected ones as was usually found in this investigation. One can speculate in this case that drying the samples by conventional heat or by microwave heat the concentrations will not differ to a considerable extent.

Table 3.7.1 Cobalt content of catalysts

Catalyst 4SCN	wt(%) Co	
	expected	measured (AAS)
30Co-nit(H_2O) /100Al_2O_3 (a)	21.3	18.34
30Co-nit(H_2O) /100Al_2O_3 (b)	21.3	(---)
30Co-nit(H_2O) /100Al_2O_3 (c)	21.3	(---)
30Co-nit(H_2O) /100Al_2O_3 (d)	21.3	20.1

4SCN = Impregnation in four steps, calcination under nitrogen.
(a) = Reference catalyst. Aged in dessicator for 5 days, then dried at 120°C.
(b) = Not aged in dessicator, dried at 120°C straight after impregnation.
(c) = Not aged in dessicator, dried by microwaves straight after impregnation.
(d) = Aged in dessicator for 5 days, then dried by microwaves.
(---) = Not determined.

From the two determinations available it appeared that the cobalt concentration for the catalysts dried by microwaves was higher than the one dried by conventional heat. The difference, however, may not be significant.

3.7.2 Temperature Programmed Reduction (TPR)

The reduction profiles of the catalysts dried by microwave heat and that of the reference catalyst are shown in figure 3.7.1. As before the profiles showed three peaks. The three peaks have been discussed previously. In table 3.7.2 one can observe very low hydrogen consumption for the catalyst (d) aged for 5 days before microwaving. The percentage of hydrogen consumed during the reduction of cobalt aluminate was only 38.8 as against 77.5% when the catalyst was dried in microwave straight after impregnation (catalyst c). This could mean that when exposing the catalyst directly under microwaves after impregnation more aluminate species was formed. The activity of the catalyst aged for 5 days before microwaving was lower than the one dried by microwaving straight after impregnation.

Table 3.7.2 H_2 consumption of catalysts during reduction in TPR

Catalyst 4SCN	Moles H_2 consumed x 10^{-3}/g.catalyst						% of H_2 consumed			
	peak				Total H_2 consumed measured	Total H_2 consumed expected	peak			
	1	2	3	4			1	2	3	4
30Co-nit(H_2O)/100Al_2O_3 (a)	0.56	1.28	3.62	---	5.46	4.82	10.3	23.4	66.3	
30Co-nit(H_2O)/100Al_2O_3 (c)	0.46	0.63	3.76	---	4.85	4.82	9.5	13.0	77.5	
30Co-nit(H_2O)/100Al_2O_3 (d)	1.19	0.26	0.92	---	2.37	4.82	50.2	11.0	38.8	

(a) = Reference catalyst. Aged in dessicator for 5 days, then dried at 120°C.
(c) = Not aged in dessicator, dried by microwaves straight after impregnation.
(d) = Aged in dessicator for 5 days, then dried by microwaves.

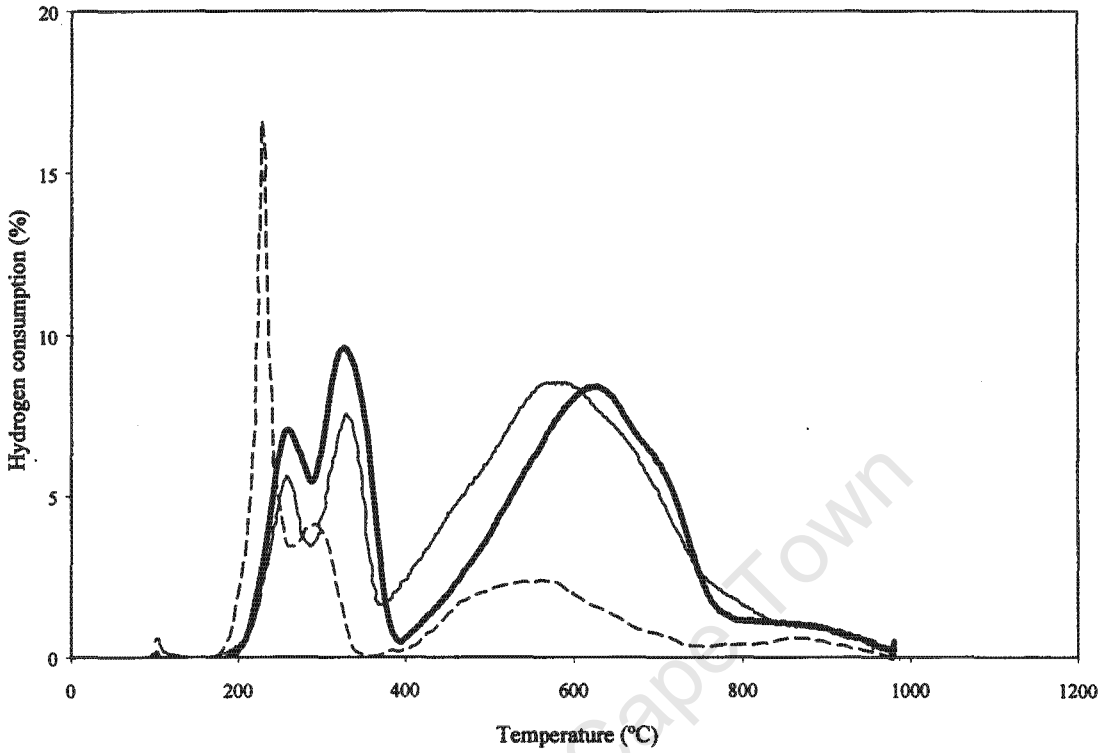

Figure 3.7.1: TPR profiles of $30gCo/100gAl_2O_3$ catalysts. **a.-** (▬▬); **c.-** (——) and **d.-** (– –). Hydrogen consumption (%) of the reducing mixture ($6\%H_2$ in N_2) against temperature (°C).

3.7.3 CO Chemisorption

3.7.3.1 Metal Dispersion, metal surface area and average particle diameter

The metal dispersion, the metal surface area and the average particle diameter are summarised in table 3.7.3. Section 2.1.3.3 describes in detail the preparation of the catalysts investigated in this section. Only two catalysts of this section were analysed and their dispersions compared, the reference catalyst (a) and the one aged in a dessicator and subsequently dried with microwaves (d). The reference catalyst had a dispersion of 0.9 % and the one dried with microwaves 1.5%. This result did not agree with the catalyst activity because the catalyst dried with microwaves was less active than the reference catalyst, which is opposite to expectation. In the literature it was reported that when drying with microwave heating the cobalt crystallites were much larger than when the catalysts were dried with conventional heating [28]. In the present studies the opposite was observed.

Table 3.7.3 Strong chemisorption of catalysts

Catalyst 4SCN	vol CO adsorbed/g. reduced cat (ml)	D (%)	m.s.a. (m^2/g.cat)	Co loaded (mg)	Co loaded in FT (m^2)	p_d (nm)
30Co-nit(H_2O)/100Al_2O_3 (a)	0.69	0.90	1.22	48	0.32	110
30Co-nit(H_2O)/100Al_2O_3 (d)	1.13	1.47	2.00	52	0.52	68

D = Dispersion.
m.a.s. = Metallic surface area.
p_d = Average particle diameter of cobalt metal.
(a) = Reference catalyst. Aged in dessicator for 5 days, then dried at 120°C.
(d) = Aged in dessicator for 5 days, then dried by microwaves.

3.7.4 FT Activity

3.7.4.1 Activity with time on stream

The FT reaction was performed at 220°C, 15bar g and H_2/CO ratio =2, (H_2+CO) flow = 28ml/min. The FT activities of the different catalysts are given in table 3.7.4. The reference catalyst (a) showed higher activity than those catalysts dried with different drying procedures. The initial activity of the reference catalyst was around 58%. The catalyst, which was dried straight after impregnation (catalyst b) showed an initial activity of about 54%, slightly lower than that the reference catalyst. This implies that maybe ageing plays an important role in the preparation of catalyst. During ageing the cobalt crystallites might be more evenly distributed on the alumina support due to slow evaporation of the water. Subjecting the catalyst to heat straight after impregnation might result in sintering and/or the presence of water during drying might facilitate the formation of cobalt aluminates. The latter agreed with TPR scans obtained for catalyst **c**. It was observed that 78% of H_2 was consumed during the reduction of the aluminate peak whereas in the case of the reference catalyst 66% of the total H_2 consumed was needed to reduce the aluminate peak (see table 3.7.2). The activity of the catalyst dried with microwaves after impregnation (catalyst c) was about 48%. If catalyst **b** and **c** are compared, one could conclude that drying with microwave heat resulted in larger cobalt crystallites. The activity of the catalyst aged for five days and subsequently dried with microwaves (catalyst d) had a very low activity around 14%. The latter catalyst can be

compared with the reference catalyst because they were similarly prepared with the only difference that catalyst d was dried with microwaves. As seen above the activity of catalyst **d** was lowered by microwave heat. The metal surface area of catalyst **d** was higher than that of catalyst **a** and this does not confirm that heating catalysts with microwaves results in cobalt particle growth and therefore in low catalyst activity. In the literature it was reported that lower metal surface area was obtained on silica supported catalysts dried with microwaves than when the catalysts were dried with conventional heat [28]. Catalysts **c** and **d** were dried with microwaves; the difference was that one of them was dried straight after impregnation and the other one first aged in a dessicator for 5 days. Both of them showed different catalyst activities. In the case of catalyst **c**, the microwaves heated the catalyst when it was wetted with cobalt nitrate. It could be that during drying mainly water was removed out of the catalyst. Drying catalyst **d** the picture was a slightly different. Catalyst **d** was almost dried after ageing and before drying with microwaves. It appears that wetted and dried catalysts react differently to microwaves. It seems that larger cobalt crystallites were formed when the dryer catalyst was exposed to microwaves. This was confirmed with TPR scans where it was seen that catalyst **d** consumed more hydrogen to reduce the first two peaks attributed to the reduction of free Co_3O_4. This means that catalyst **d** had more free cobalt oxides than catalyst **c** but catalyst **d** had a higher metal surface area and low activity. This could imply that catalyst **d** had larger cobalt crystallites than catalyst **c**. The results for catalyst d may however be suspect but overall it appears that drying with microwaves is deleterious.

Table 3.7.4 FT activity of catalysts

Catalyst 4SCN	FT activity measured as CO converted (%)				
	Time on stream (hrs)				
	2	16	20	24	48
30Co-nit(H_2O) /100Al_2O_3 (a)	57.8	56.2	55.6	53.3	44.0
30Co-nit(H_2O) /100Al_2O_3 (b)	53.8	48.4	43.4	43.1	39.9
30Co-nit(H_2O) /100Al_2O_3 (c)	47.5	36.6	36.0	35.4	33.0
30Co-nit(H_2O) /100Al_2O_3 (d)	13.8	12.2	12.1	11.2	11.0

4SCN = Impregnation in four steps, calcination in N_2 between each step.
(a) = Reference catalyst. Aged in dessicator for 5 days, then dried at 120°C.
(b) = Not aged in dessicator, dried at 120°C straight after impregnation.
(c) = Not aged in dessicator, dried by microwaves straight after impregnation.
(d) = Aged in dessicator for 5 days, then dried by microwaves.

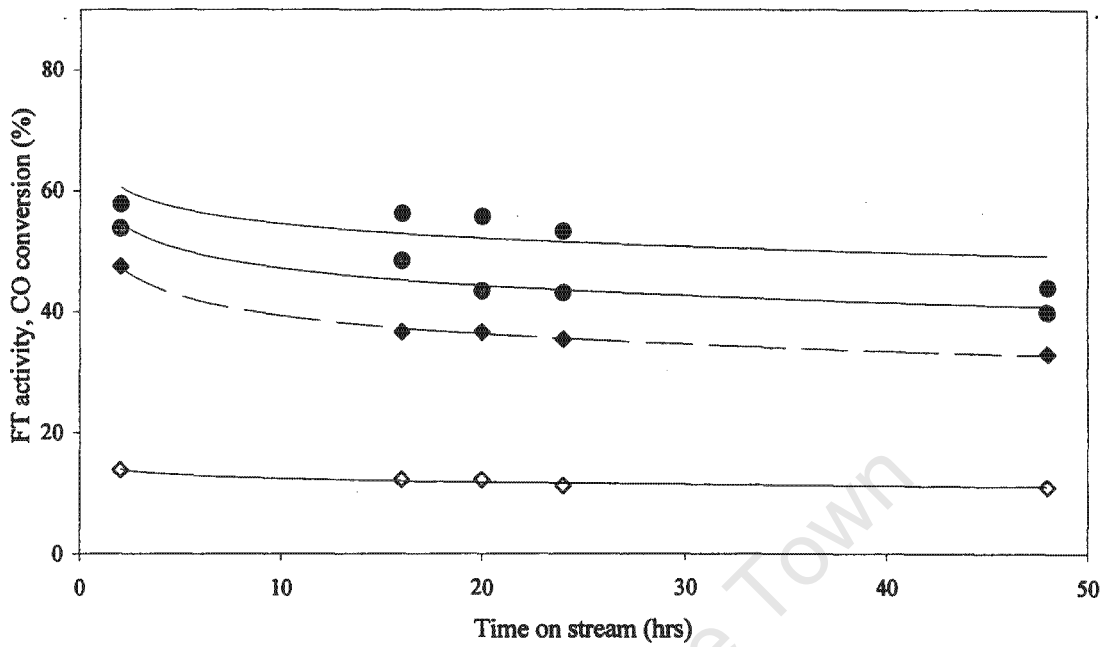

Figure 3.7.2: FT activities of 30gCo-nit(H_2O)/100gAl_2O_3 catalysts, a.- (●)Reference catalyst. Aged in dessicator for 5 days, then dried at 120°C, b.- (●)Not aged in dessicator, dried at 120°C straight after impregnation, c.- (◆) Not aged in dessicator, dried by microwaves straight after impregnation, d.-(◇)Aged in dessicator for 5 days, then dried by microwaves.

3.7.4.2 Chain growth Probability and Product Selectivity

The α values obtained for this group of catalysts are shown in table 3.7.5. Most of the catalysts had alpha values around 0.84 except for catalyst **d**, which gave alpha values around 0.75.

Table 3.7.5. Chain growth probability of catalysts.

Catalyst 4SCN	Chain growth probability (α)				
	Time on stream (hrs)				
	2	16	20	24	48
30Co-nit(H_2O) /100Al_2O_3 (a)	0.83	0.83	0.85	0.84	0.84
30Co-nit(H_2O) /100Al_2O_3 (b)	0.86	0.84	0.85	0.84	0.84
30Co-nit(H_2O) /100Al_2O_3 (c)	0.83	0.84	0.85		0.84
30Co-nit(H_2O) /100Al_2O_3 (d)	0.74		0.85	0.74	0.75

(a) = Reference catalyst. Aged in dessicator for 5 days, then dried at 120°C.
(b) = Not aged in dessicator, dried at 120°C straight after impregnation.
(c) = Not aged in dessicator, dried by microwaves straight after impregnation.
(d) = Aged in dessicator for 5 days, then dried by microwaves.

The fraction of paraffins in the C_2 toC_{12} hydrocarbons were very similar for catalysts **a** and **b**. (see table 3.7.6 and figure 3.7.3). Catalyst **c** was less active than catalysts **a** and **b** and therefore the paraffins' yield was lower. Similarly, catalyst **d** had low activity and also low paraffins' yield. From this it could be concluded that more paraffins were produced when the activity was higher.

Table 3.7.6 Ratio of paraffins in the hydrocarbon fraction.

Catalyst	Paraffins/Total hydrocarbon										
	Carbon fraction										
	C_2	C_3	C_4	C_5	C_6	C_7	C_8	C_9	C_{10}	C_{11}	C_{12}
30Co-nit(H_2O) /100Al_2O_3 (a)	0.59	0.44	0.51	0.57	0.65	0.72	0.79	0.81	0.85	0.90	0.95
30Co-nit(H_2O) /100Al_2O_3 (b)	0.70	0.40	0.52	0.57	0.65	0.71	0.76	0.80	0.84	0.90	0.94
30Co-nit(H_2O) /100Al_2O_3 (c)	0.70	0.29	0.40	0.43	0.52	0.59	0.66	0.72	0.77	0.83	0.93
30Co-nit(H_2O) /100Al_2O_3 (d)	0.63	0.35	0.40	0.37	0.42	0.46	0.52	0.61	0.69	0.75	0.79

(a) = Reference catalyst. Aged in dessicator for 5 days, then dried at 120°C.
(b) = Not aged in dessicator, dried at 120°C straight after impregnation.
(c) = Not aged in dessicator, dried by microwaves straight after impregnation.
(d) = Aged in dessicator for 5 days, then dried by microwaves.

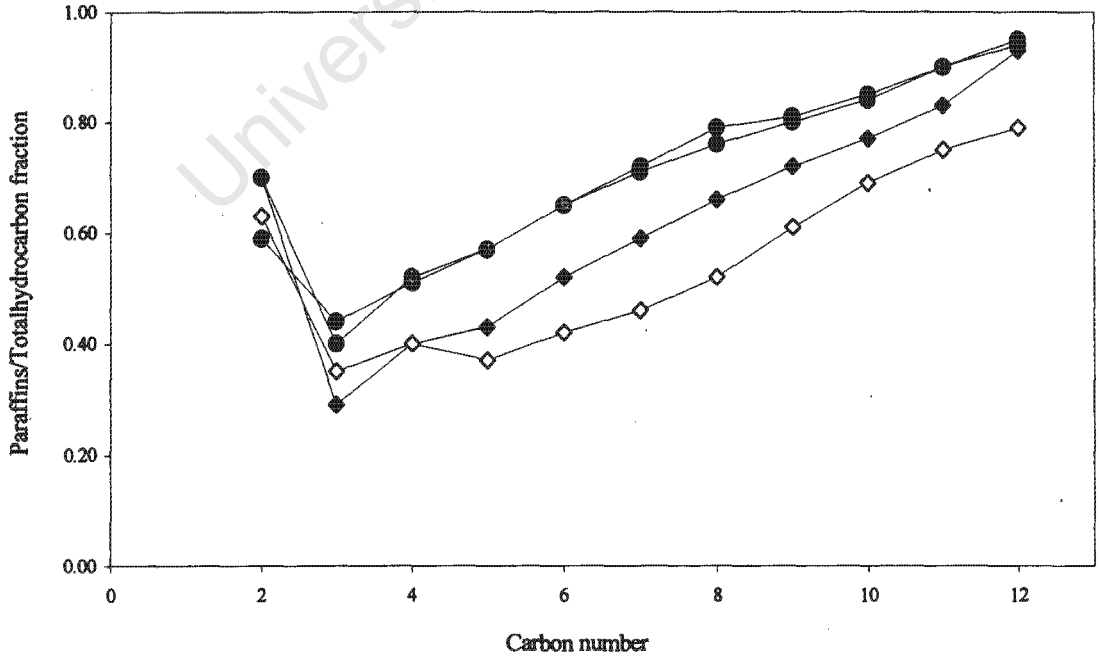

Figure 3.7.3: Ratio of paraffins over the total carbon fraction versus carbon number of, 30gCo-nit(H_2O)/100gAl_2O_3 catalysts, **a**.- (●)Reference catalyst. Aged in dessicator for 5 days, then dried at 120°C, **b**.- (●)Not aged in dessicator, dried at 120°C straight after impregnation, **c**.- (◆) Not aged in dessicator, dried by microwaves straight after impregnation, **d**.-(◇)Aged in dessicator for 5 days, then dried by microwaves.

3.8 Different impregnation temperatures

3.8.1 Atomic Absorption Spectroscopy (AAS)

A number of catalysts were prepared by impregnating the metal salt onto the alumina support at temperatures around 80°C (see experimental section 2.1.3.4). The catalysts were prepared in two impregnation steps with calcination between each step or simply without calcination. The cobalt content of each catalyst was measured using AAS analysis. The obtained concentrations indicated that the measured concentrations were lower than the expected ones as it is usually obtained by reasons explained in sections 3.1.1 and 3.2.1.

Table 3.8.1 Cobalt content of catalysts

Catalyst 2S	wt(%) Co	
	expected	measured (AAS)
30Co-nit(H_2O) /100Al_2O_3 calcined (1)	21.3	20.3
30Co-nit(H_2O) /100Al_2O_3 uncalcined (2)	21.3	20.0
30Co-nit(H_2O) /100Al_2O_3, uncalcined 80°C (3)	21.3	20.6
30Co-nit(H_2O) /100Al_2O_3 calcined 80°C (4)	21.3	18.4
30Co-nit(H_2O) /100Al_2O_3 calcined 80°C (5)	21.3	18.7

2S = Impregnation in two steps.

Catalyst:
(1) = Impregnation at room temperature, calcined catalyst.
(2) = Impregnation at room temperature, **uncalcined** catalyst.
(3) = impregnation on heated Al_2O_3 at around 80°C, calcined catalyst.
(4) = impregnation on heated Al_2O_3 at around 80°C, **uncalcined** catalyst.
(5) = impregnation on heated Al_2O_3 and cobalt nitrate at 80°C, calcined catalyst.

3.8.2 Temperature Programmed Reduction (TPR)

Figure 3.8.1 shows the TPR profiles of the catalysts with and without calcination in nitrogen at 270°C. It was found that the TPR profiles of the catalysts looked similar. All TPR profiles exhibited three peaks. As discussed in previous sections, the first two peaks represented the reduction of:

$$Co_3O_4 + H_2 \rightarrow 3CoO + H_2O$$

$$3CoO + 3H_2 \rightarrow 3Co^0 + 3H_2O$$

The third peak was attributed to be the reduction of the metal-support interaction. The reduction profile of Catalyst 1 showed peaks at around 253, 308 and 580°C. Catalyst 2 showed peaks at 205, 305 and 580°C. For the uncalcined catalyst the first peak occurred at higher temperature than the one corresponding to the calcined catalyst. The first peak of catalyst 1 was smaller than that of catalyst 2, which means that probably more Co^{3+} was formed on the uncalcined catalyst 2 (see table 3.8.2 and figure 3.8.1). Catalyst 2 also showed low percentage of H_2 consumption (56%) on the third peak (aluminate peak) compared to that of the catalyst 1 (70%). Similarly, the uncalcined catalyst 3 and the calcined catalyst 5 followed the same trend as those prepared by impregnation at room temperature. The uncalcined catalyst 3 exhibited three peaks at 230, 342 and 570°C while the calcined catalyst 5 showed reduction peaks at 301, 350 and 637°C. For the uncalcined catalyst 3 the first peak assigned to the reduction of Co^{3+} to Co^{2+} consumed 17.6% of the total H_2 consumption and the same peak for the calcined catalyst 5 consumed 11.5% (see table 3.8.2 and figure 3.8.2). Again it appears that Co^{3+} was more predominant in the uncalcined samples than in the calcined ones. The H_2 consumed to reduce the aluminate peak for the uncalcined and calcined catalysts were 60.3 and 66.2% respectively. Both uncalcined catalysts prepared at room temperature and at 80°C showed more H_2 consumption for the reduction of Co^{3+} to Co^{2+} and also for the reduction of the aluminate peak. As could be expected the latter finding indicated that calcination caused higher metal-support interaction. These metal-support species are non-reducible at FT conditions and this lowers the availability of cobalt metal in the catalyst and more importantly lowers the catalyst activity. This is in agreement with literature [33] where it was shown that uncalcined Ni/SiO_2 catalysts had greater dispersions than calcined Ni/SiO_2 catalysts.

Table 3.8.2 H_2 consumption of catalysts during reduction in TPR

Catalyst ST	Moles H_2 consumed x 10^{-3}/g.catalyst					% of H_2 consumed			
	peak				Total H_2 consumed measured	peak			
	1	2	3	4		1	2	3	4
30Co-nit(H_2O) /100Al_2O_3 (1)	0.26	0.97	2.91		4.14	6.3	23.4	70.3	
30Co-nit(H_2O) /100Al_2O_3 (2)	1.25	0.87	2.70		4.82	25.9	18.1	56.0	
30Co-nit(H_2O)/100Al_2O_3 (3)	0.88	1.11	3.02		5.01	17.6	22.1	60.3	
30Co-nit(H_2O) /100Al_2O_3 (5)	0.59	1.15	3.41		5.15	11.5	22.3	66.2	

Catalyst: (1) = Impregnation at room temperature, calcined catalyst.
(2) = Impregnation at room temperature, **uncalcined** catalyst.
(3) = impregnation on heated Al_2O_3 at around 80°C , **uncalcined** catalyst.
(5) = impregnation on heated Al_2O_3 and cobalt nitrate at 80°C, calcined catalyst.

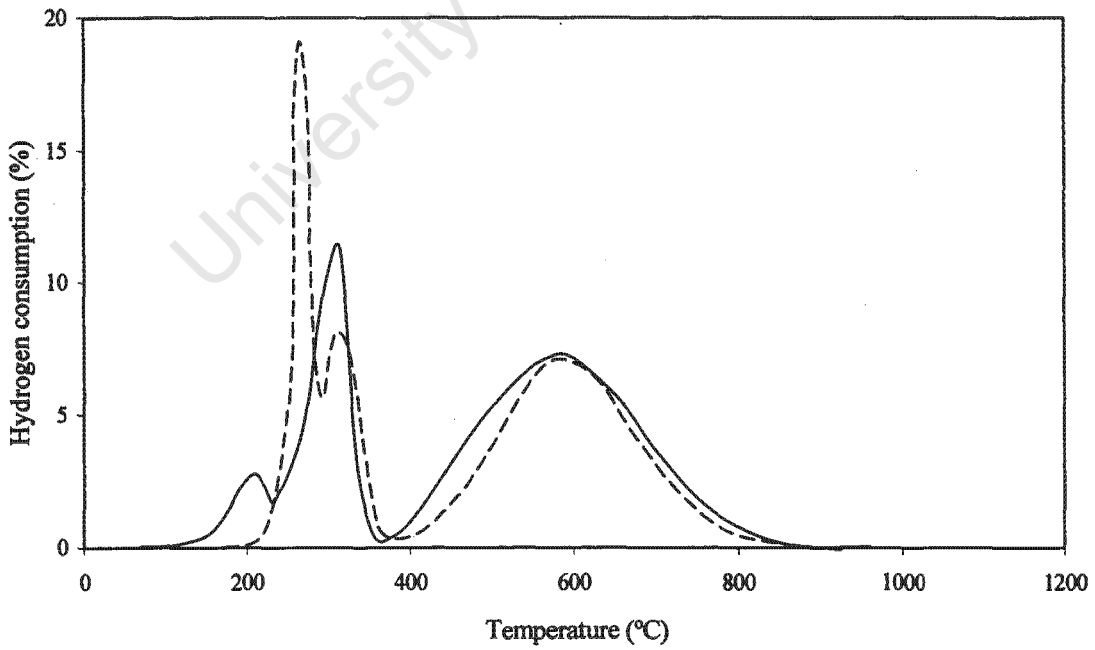

Figure 3.8.1: TPR profiles of: 30gCo-nit (H_2O)/100g100Al_2O_3 2S catalysts,.(——) Calcined catalyst **1**, (- - -) Uncalcined catalyst **2**. H_2 consumption (%) of the reducing mixture (6%H_2 in N_2) against temperature (°C).

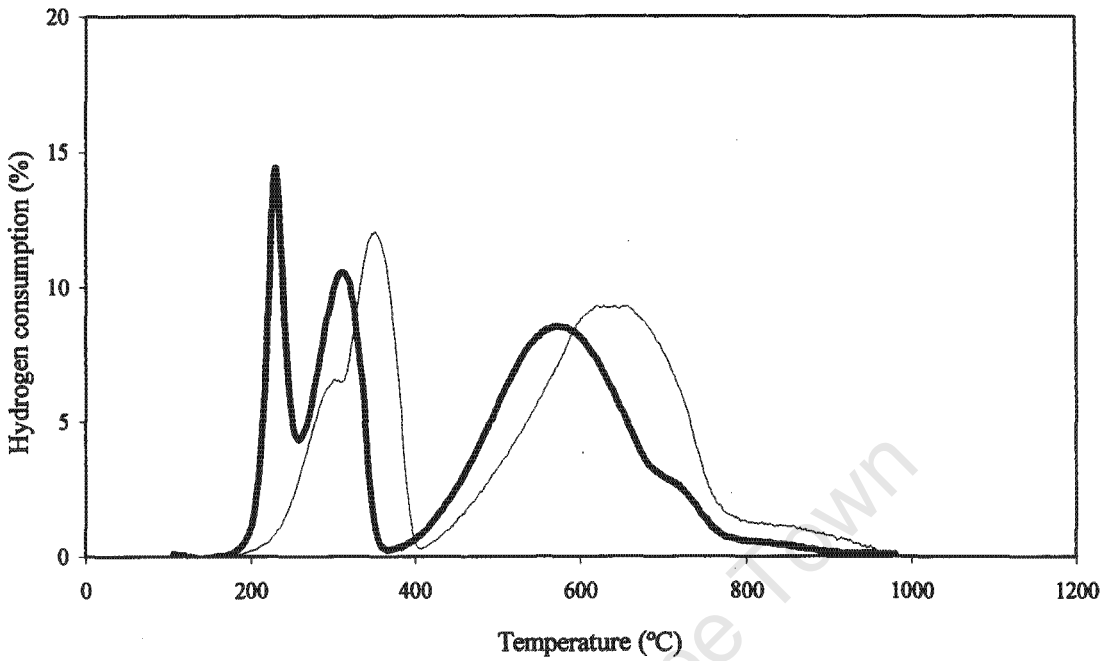

Figure 3.8.2: TPR profiles of,: 30gCo-nit (H_2O)/100g100Al_2O_3 2S catalysts impregnated at 80°C, (▬▬) Uncalcined catalyst **3**, (——)Calcined catalyst **5**. H_2 consumption (%) of the reducing mixture (6%H_2 in N_2) against temperature (°C).

3.8.3 CO Chemisorption

3.8.3.1 Metal Dispersion, metal surface area and average particle diameter

The metal dispersions, metal surface areas and the average pore diameters are listed in table 3.8.3. The "strong" metal dispersions were calculated as described in section 3.5.3.1. The reduction in the chemisorption apparatus was carried out at the same conditions as in the FT reactor. The investigated catalysts in this section were prepared as described in section 2.1.3.4. The aim of the preparation of these catalysts was to investigate whether by varying the impregnation temperature the catalysts would have different dispersions. In the present work the impregnation was commonly done at room temperature. The catalysts to be studied in this section were prepared by impregnating cobalt nitrate solution on heated alumina at around 80°C. The cobalt impregnation was carried out in two steps with calcination between each step. In order to compare the activities of the catalysts prepared at 80°C, catalyst 1 was prepared in a two-step impregnation process at room temperature.

Table 3.8.3 Strong chemisorption of catalysts

Catalyst 2ST	vol CO adsorbed/g. reduced cat (ml)	D (%)	m.s.a. (m^2/g.cat)	Co Loaded In FT (mg)	Co area loaded in FT (m^2)	p_d (nm)
30Co-nit(H_2O) /100Al_2O_3 uncalcined, (2)	0.56	0.72	0.99	48	0.26	138
30Co-nit(H_2O) /100Al_2O_3 uncalcined, 80°C (3)	0.61	0.78	1.09	53	0.28	127
30Co-nit(H_2O) /100Al_2O_3 calcined, 80°C (4)	0.80	1.14	1.42	48	0.41	87
30Co-nit(H_2O) /100Al_2O_3 calcined, 80°C (5)	0.64	0.90	1.15	49	0.30	110

D = Dispersion.
m.a.s. = Metallic surface area.
p_d = Average particle diameter of cobalt metal.

It is observed in table 3.8.3 that dispersion values for the catalysts prepared by impregnating the cobalt nitrate on alumina heated to 80°C (catalysts 3, 4 and 5) were higher than the dispersion of the catalyst prepared by impregnating cobalt nitrate at room temperature (catalyst 2). The obtained dispersion for catalyst 2 was 0.72% and for catalysts 3, 4 and 5 were 0.78, 1.14 and 0.90% respectively. Although more or less the same amount of cobalt metal was loaded in the FT reactor, the metal areas loaded were different. Catalyst 2 had a metal area around 0.26 m^2 and catalysts 3, 4 and 5 had metal areas around 0.28, 0.41 and 0.30m^2 in that order. Obviously, the metal particle sizes for the catalysts of this group depended on the degree of dispersion. The particle diameter of the metal decreased when the catalysts were prepared by impregnating cobalt nitrate on heated alumina. The better dispersion at the higher temperature might have been due possibly to a better attachment of the cobalt nitrate onto the alumina support and this would inhibit sintering to some extent during calcination. Impregnation at room temperature may cause a weak attachment of the cobalt nitrate onto the alumina support. Calcination may enhance the mobility of these cobalt particles because they are weakly attached to the support.

3.8.4 BET area

The BET surface areas of the catalysts are given in table 3.8.4. The alumina support on its own had a BET surface area around 163m^2/g. The "expected" BET surface areas of the

catalysts were calculated taking into consideration the alumina content in the catalyst. The "measured" surface area was expressed as the total surface area of the catalyst per 1 gram of catalyst. The uncalcined catalyst prepared by impregnation when the support was at room temperature and at 80°C showed similar BET surface areas. It is evident that after impregnating the support, the alumina will loose surface area because of the occupancy of cobalt oxides, which seemed to have lower surface areas than the alumina.

Table 3.8.4 BET surface areas of catalysts

Catalyst 2ST	1 g. catalyst contains Al_2O_3	BET Surface area (m^2/g.cat)	
		expected	measured
Al_2O_3 support (blank)	1.00	163	163
30Co-nit(H_2O) /100Al_2O_3 uncalcined (2)	0.72	117	91
30Co-nit(H_2O) /100Al_2O_3 uncalcined, 80°C (3)	0.72	117	93

3.8.5 FT Activity

3.8.5.1 Activity with time on stream

The FT reaction was performed at 220°C, 15bar g and H_2/CO ratio =2, (H_2+CO) flow = 28ml/min. The FT activities of the catalysts are summarised in table 3.8.5. The FT activity of catalyst 2, which was prepared by impregnating cobalt nitrate at room temperature-showed FT activities of 79% at 2hrs (see table 3.8.5). Catalyst 3 had high initial activity of 90% at 2hrs TOS but the activity declined quite rapidly with TOS. The reason of the initial high activity might be due to this catalyst's somewhat higher dispersions (see table 3.8.3). The decline of activity might have been due to the re-oxidation of the smaller cobalt crystallites during the FT synthesis, which in the long run deactivated the catalyst activity. Catalyst 4 was prepared in a similar manner to catalyst 3 but it was calcined and catalyst 3 was not. The catalyst 4 showed a lower initial activity than catalyst 3 despite the higher dispersion of catalyst 4 (see table 3.8.3). The activities of catalyst 4, however, were subsequently higher than those of catalyst 3, which does match with the higher dispersions of catalyst 4. The

initial activity of catalyst 4 therefore maybe suspect. Catalyst 5 was prepared having both cobalt nitrate and alumina at the same temperature, around 80°C. Catalyst 5, despite having a lower dispersion than catalyst 4, was more active than catalyst 4 throughout the duration of the runs. Figure 3.8.3 does not show a correlation of dispersion which activity, either at 2hrs TOS or later.

Table 3.8.5 FT activity of catalysts

Catalyst 2S	FT activity measured as CO converted (%)				
	Time on stream (hrs)				
	2	16	20	24	48
30Co-nit(H_2O) /100Al_2O_3 uncalcined (2)	79.4	56.4	53.3	54.6	48.5
30Co-nit(H_2O) /100Al_2O_3 uncalcined 80°C (3)	89.5	37.1	35.0	36.2	32.0
30Co-nit(H_2O) /100Al_2O_3 calcined 80°C (4)	73.8	51.1	51.1	50.2	49.9
30Co-nit(H_2O) /100Al_2O_3 calcined 80°C (5)	76.5	64.1	62.1	60.1	54.7

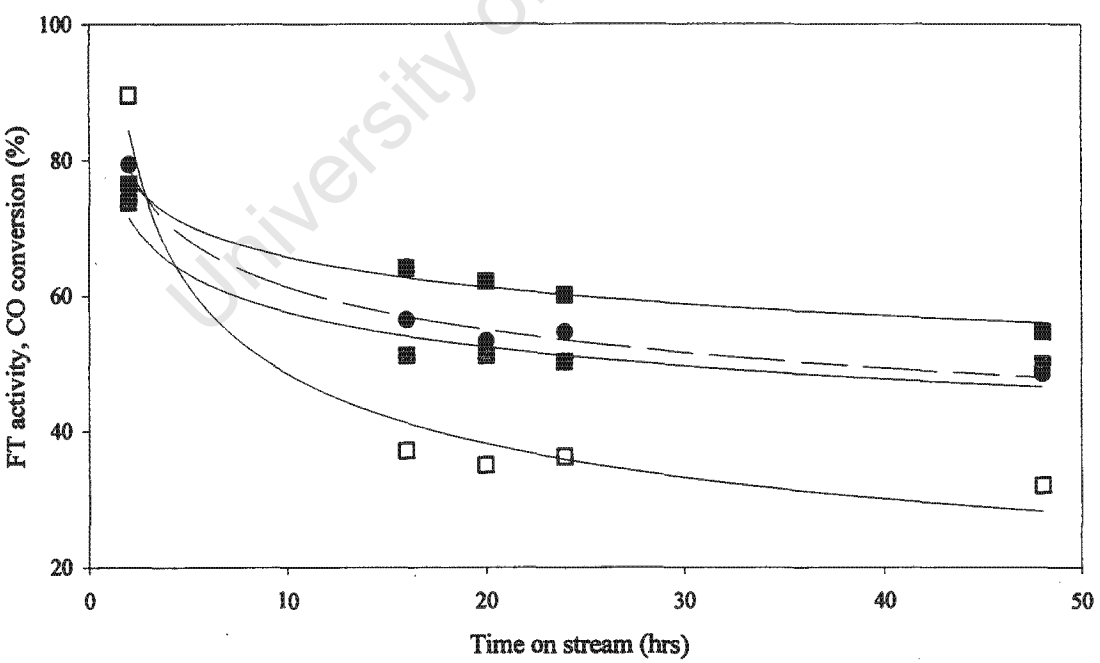

Figure 3.8.3: FT activities of catalysts prepared in two-impregnation steps, catalyst 2.-(●)30gCo-nit(H_2O)/100gAl_2O_3 uncalcined, impregnation at room temperature; 3.- (□) 30gCo-nit(H_2O)/100gAl_2O_3 uncalcined, impregnation at 80°C; 4.- (■)30gCo-nit(H_2O)/100gAl_2O_3 calcined, impregnation at 80°C; 5.-(■). 30gCo-nit(H_2O)/100gAl_2O_3 calcined, impregnation at 80°C, cobalt nitrate and alumina at 80°C. FT conditions, 220°C, 15bar g, $H_2/CO = 2$.

In figure 3.8.4 the activities at 20 hrs TOS of the four catalysts are plotted against the metallic surface area loaded in the FT reactor. Overall there is no clear correlation and so for this set of catalysts no satisfactory explanation of the differences in activity can be offered.

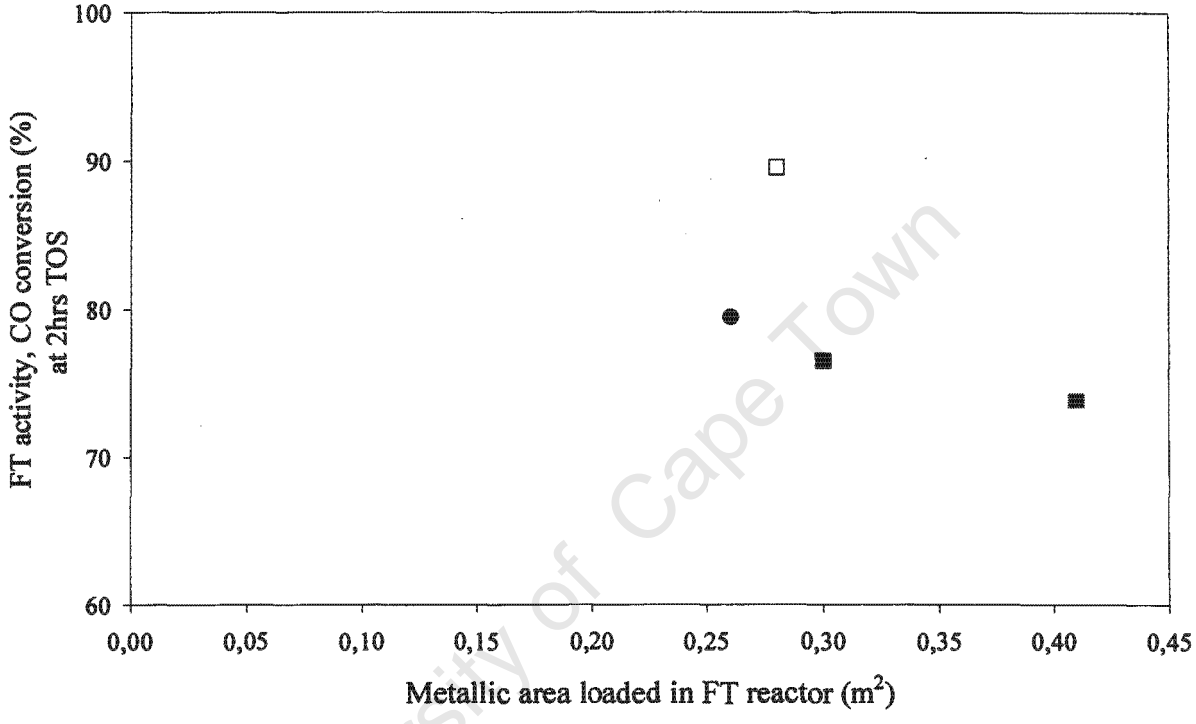

Figure 3.8.4: FT activities at 20hrs TOS of catalysts prepared in two-impregnation steps versus metallic area loaded in FT reactor. Catalyst 2.-(●)30gCo-nit(H_2O)/100gAl_2O_3 uncalcined, impregnation at room temperature; 3.- (□) 30gCo-nit(H_2O)/100gAl_2O_3 uncalcined, impregnation at 80°C; 4.- (■)30gCo-nit(H_2O)/100gAl_2O_3 calcined, impregnation at 80°C; 5.-(■). 30gCo-nit(H_2O)/100gAl_2O_3 calcined, impregnation at 80°C, cobalt nitrate and alumina at 80°C.

3.8.5.2 Chain growth Probability and Product Selectivity

The obtained α values are listed in table 3.8.6. The alpha values were obtained as explained in section 1.1.6. Generally, the alpha values for the catalysts of this group were very similar. A slightly lower alpha value was found for catalyst 5.

Table 3.8.6 Chain growth probability of catalysts.

Catalyst 2S	Chain growth probability (α)				
	Time on stream (hrs)				
	2	16	20	24	48
30Co-nit(H_2O) /100Al_2O_3 uncalcined (2)	0.84	0.86	0.85	0.85	0.87
30Co-nit(H_2O) /100Al_2O_3 uncalcined 80°C(3)	0.84	0.89	0.85	0.85	0.85
30Co-nit(H_2O) /100Al_2O_3 2SCN 80°C (4)	0.84	0.85	0.85	0.84	0.84
30Co-nit(H_2O) /100Al_2O_3 2SCN 80°C (5)	0.85	0.80	0.85	0.82	0.82

The ratios of paraffins over the total hydrocarbon products corresponding to the C_2 to C_{12} hydrocarbon fractions are summarised in table 3.8.7. The products from using catalyst 5 appeared to be more paraffinic than those from using catalysts 2, 3 and 4 (see figure 3.8.5). This was in agreement with the higher activity of catalyst 5.

Table 3.8.7 Ratio of paraffins in the hydrocarbon fraction.

Catalyst	Paraffins/Total hydrocarbon										
	Carbon fraction										
	C_2	C_3	C_4	C_5	C_6	C_7	C_8	C_9	C_{10}	C_{11}	C_{12}
30Co-nit(H_2O) /100Al_2O_3											
uncalcined (2)	0.70	0.48	0.51	0.59	0.66	0.72	0.77	0.80	0.84	0.90	0.94
uncalcined 80°C (3)	0.72	0.34	0.46	0.50	0.57	0.65	0.71	0.76	0.84	0.90	0.94
80°C (4)	0.69	0.43	0.45	0.51	0.58	0.67	0.73	0.78	0.82	0.91	0.94
80°C (5)	0.81	0.73	0.72	0.79	0.83	0.88	0.91	0.93	0.96	0.98	0.99

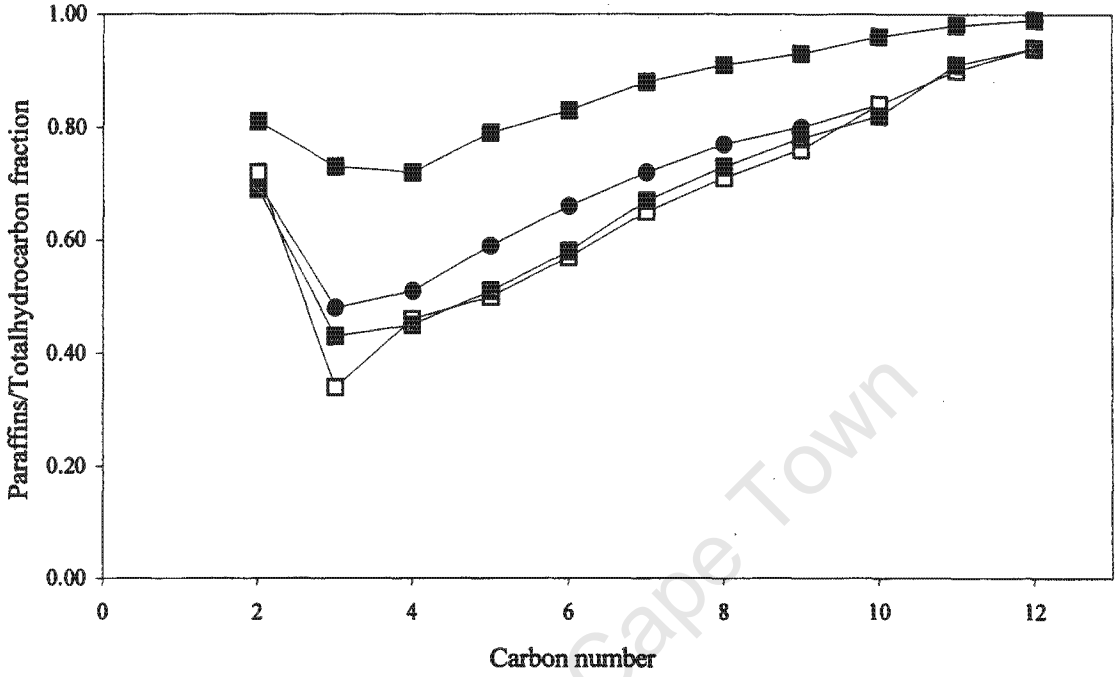

Figure 3.8.5: Ratio of paraffins over total carbon fraction versus carbon number for catalysts, 2.-(●)30gCo-nit(H_2O)/100gAl_2O_3 uncalcined, impregnation at room temperature; 3.- (□) 30gCo-nit(H_2O)/100gAl_2O_3 uncalcined, impregnation at 80°C; 4.- (■)30gCo-nit(H_2O)/100gAl_2O_3 calcined, impregnation at 80°C; 5.-(■). 30gCo-nit(H_2O)/100gAl_2O_3 calcined, impregnation at 80°C, cobalt nitrate and alumina at 80°C.

As before ethanol was found to be the most abundant oxygenated compound. The obtained ratios of ethanol to the total C_2 hydrocarbon product was about 0.18 ± 0.04.

3.9 Modified alumina support

From TPR scans it was observed that while cobalt oxides reacted strongly with the alumina support, cobalt oxides apparently did not readily form cobalt silicates (see section 3.1.2). It was thus believed that the preparation of a catalyst using silinized alumina as a support would hopefully result in a lower metal-support interaction. The surface of alumina is often known to be somewhat acidic in nature. It was hence decided to impregnate the alumina with a base such as KOH to eliminate any support acidity and then to see what effect this had on the cobalt's performance in the FT process. For more information of the preparation of these catalysts see section 2.1.3.5.

3.9.1 Atomic Absorption Spectroscopy (AAS)

A few catalysts were prepared by impregnating the cobalt salt onto the "modified" support. The detailed preparation of these catalysts was explained in the experimental section 2.1.3.5. The cobalt concentrations of these catalysts were measured using AAS analyses. In the catalyst supported on silinized Al_2O_3, the "measured" cobalt concentration was somewhat lower than the unmodified 30Co-nit(H_2O)/100Al_2O_3 4SCN catalyst. A lower cobalt concentration was also measured in the KOH impregnated catalyst. Obviously, the catalyst supported on "cobalt aluminates" had a high cobalt concentration because the AA analysis detects all the cobalt. Cobalt in this case formed part of the support as well as being present as Co_3O_4.

Table 3.9.1 Cobalt content of catalysts

Catalyst 4SCN	wt(%) Co	
	expected	measured (AAS)
30Co-nit(H_2O) /100Al_2O_3 (a)	21.30	18.34
30Co-nit(H_2O) /100(Al_2O_3 + SiO_2)	21.30	17.70
30Co-nit(H_2O), 4KOH /100Al_2O_3	20.71	16.90
30Co-nit(H_2O) /100Al_2O_3 ($CoAl_2O_4$)	33.02	31.10

30Co-nit(H_2O) /100Al_2O_3 (a) = Reference catalyst.
30Co-nit(H_2O) /100Al_2O_3 + SiO_2 = Silinized catalyst.
30Co-nit(H_2O), 4KOH /100Al_2O_3 = KOH catalysts.
30Co-nit(H_2O) /100Al_2O_3 ($Co_2Al\ O_4$) = catalyst supported on aluminates.

3.9.2 Temperature Programmed Reduction (TPR)

The TPR profile of the silinized catalyst exhibited two peaks at 220 and 330°C and the reference catalyst showed these peaks at 260 and 328°C (see figure 3.9.1a). These two were attributed to the following reactions;

$$Co_3O_4 + H_2 \rightarrow 3CoO + H_2O$$
$$3CoO + 3H_2 \rightarrow 3Co^0 + 3H_2O$$

The third peak was assigned to the reduction of cobalt aluminate. Contrary to the objective silinizing the alumina support did not prevent the interaction cobalt-alumina. Since, the quantities of cobalt aluminates in this catalyst were similar to the reference catalyst, it could be expected that the activity would also be similar. Figure 3.9.1a clearly shows that the performances of the two catalysts were indeed similar.

The TPR profiles of the reference and of the KOH catalysts are shown in figure 3.9.1b. The TPR profiles showed a three-peak pattern. The first peak corresponding to the reference catalyst was detected at 260°C and for the KOH catalyst at 322°C. The latter peak represented the reduction of:

$$Co^{3+} \rightarrow Co^{2+}$$

The second peak occurred at 330 for the reference catalyst and at390°C for the KOH catalyst. This peak was attributed to the reduction of:

$$Co^{2+} \rightarrow Co^0$$

As before the peak at 622°C was assigned to be the reduction of the metal-support interaction. It is seen clearly that both peaks for the KOH catalyst appeared at higher temperatures than those of the reference catalyst. The percentage of hydrogen consumption for the metal-support interaction of the KOH and the reference catalysts were 63 and 66% respectively. Note that the sum of the H_2 consumed for peaks 1 and 2 in the case of the "KOH" catalyst was greater than that of the reference catalyst and so the "KOH" catalyst was well reduced.

The total hydrogen consumption for the reference and KOH catalyst were close, 5.1 and $5.4x10^{-3}$ moles/g. catalyst respectively. The "KOH" catalyst is obviously well reduced (table 3.9.2), but it does have somewhat lower dispersion than that of the reference catalyst (table 3.9.3). However the activity is much lower than expected from the difference in metal area.

Table 3.9.2 H_2 consumption of catalysts during reduction in TPR

Catalyst 4SCN	Moles H_2 consumed x 10^{-3}/g.catalyst					% of H_2 consumed			
	peak				Total H_2 consumed measured	peak			
	1	2	3	4		1	2	3	4
30Co-nit(H_2O) /100Al_2O_3 (a)	0.56	1.28	3.62		5.46	10.3	23.4	66.3	
30Co-nit(H_2O)/100(Al_2O_3 + SiO_2)	0.33	1.44	3.59		5.36	6.1	26.9	67.0	
30Co-nit(H_2O), 4KOH /100Al_2O_3	1.34	1.08	2.72		5.14	26.1	21.0	52.9	

30Co-nit(H_2O) /100Al_2O_3 (a) = Reference catalyst.
30Co-nit(H_2O) /100(Al_2O_3 + SiO_2) = Silinized catalyst.
30Co-nit(H_2O), 4KOH /100Al_2O_3 = KOH catalyst.

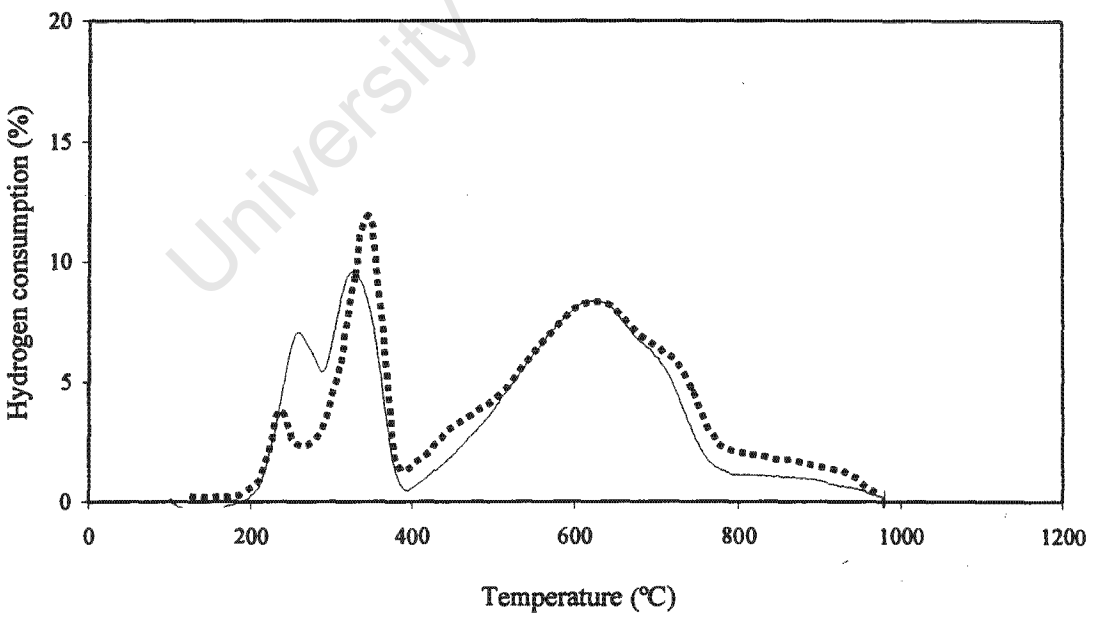

Figure 3.9.1a: TPR profiles of: (——) 30gCo-nit (H_2O)/100g100Al_2O_3 Reference catalyst and the (▪▪▪▪) 30gCo-nit (H_2O)/100g100(Al_2O_3+SiO_2) silinized catalyst. H_2 consumption (%) of the reducing mixture (6%H_2 in N_2) against temperature (°C).

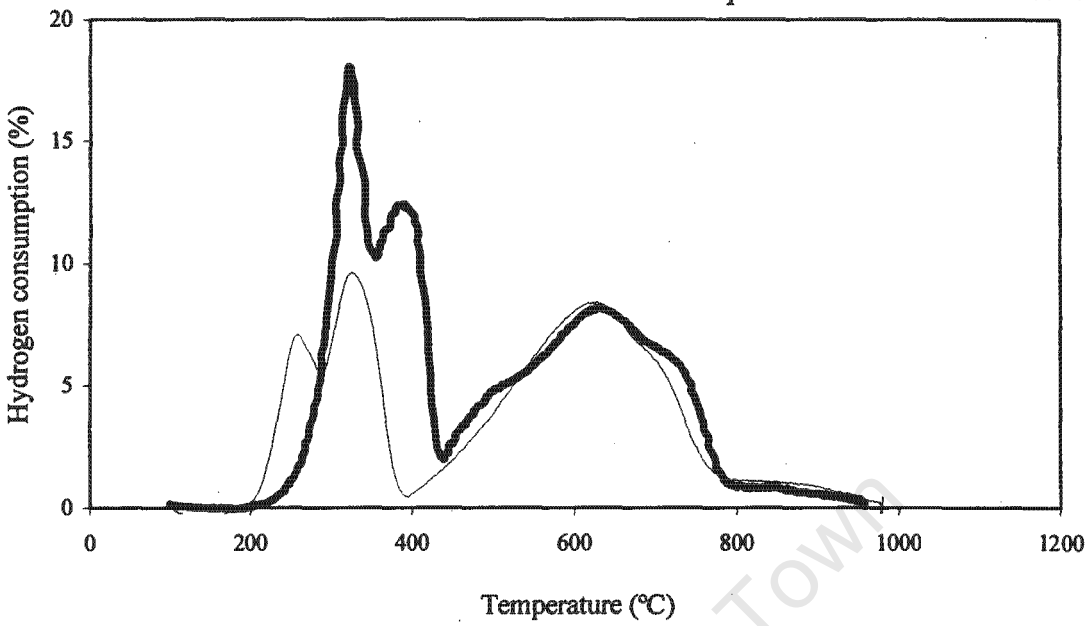

Figure 3.9.1b: TPR profiles of: (——) 30gCo-nit (H_2O)/100g100Al_2O_3 Reference catalyst and (▬) 30gCo-nit (H_2O),4KOH/100g100Al_2O_3. H_2 consumption (%) of the reducing mixture (6%H_2 in N_2) against temperature (°C).

3.9.3 CO Chemisorption

3.9.3.1 Metal Dispersion, metal surface area and average particle diameter

Table 3.9.3 shows the results for the strong chemisorption. The results for the total chemisorption followed the pattern of the strong chemisorption and for this reason the total chemisorption results are omitted in this section. The metal dispersion obtained for the silinized alumina catalyst was similar than that of the reference catalyst. The catalyst prepared with KOH had a dispersion not much different from that of the reference catalyst. The metal area loaded in the reactor corresponding to the reference catalyst was 0.32 m^2/g.catalyst, whereas the metal area loaded using the KOH catalyst was about 0.28 m^2/g.catalyst. Nevertheless, the activity of the KOH catalyst was very low compared to the reference catalyst. The possible explanation of the low activity of this catalyst is given in section 3.9.5.

The metal surface area of the catalyst supported on cobalt aluminate was much higher than the one obtained for the reference catalyst. The metal area loaded in the FT reactor was

around $0.3m^2$, for the reference catalyst and for the catalyst supported on cobalt aluminate the metal area loaded was around 1.0 m^2. Obviously, the activity of the catalyst supported with cobalt aluminate was much greater than that of the reference catalyst.

The average particle diameters of the cobalt particles were 110, 88, 108 and 35 nm, for the reference, silinized, KOH and the cobalt aluminate supported catalyst respectively. The most active catalyst appeared to be the one prepared using cobalt aluminate as support and this in fact was the one with the smallest average particle diameter.

Table 3.9.3 Strong chemisorption of catalysts

Catalyst 4SCN	vol CO adsorbed/g. reduced cat (ml)	D (%)	m.s.a. (m^2/g.cat)	Co loaded (mg)	Co loaded in FT (m^2)	p_d (nm)
30Co-nit(H_2O) /100Al_2O_3 (a)	0.69	0.90	1.22	48	0.32	110
30Co-nit(H_2O) /100(Al_2O_3 + SiO_2)	0.76	1.12	1.35	46	0.35	88
30Co-nit(H_2O), 4KOH /100Al_2O_3	0.59	0.91	1.05	45	0.28	108
30Co-nit(H_2O) /100Al_2O_3 ($CoAl_2O_4$)	1.78	2.84	3.17	49	1.01	35

D = Dispersion.
m.a.s. = Metallic surface area.
p_d = Average particle diameter of cobalt metal.

3.9.4 BET Area

The BET areas of three of the catalysts were measured and are given in table 3.9.4. The BET surface area of the support on its own was around $163m^2$/g.catalyst. The reference catalyst had a surface area of $102m^2$/g.catalyst. The KOH catalyst's area was only $81m^2$/g.catalyst. The amount of KOH present was not enough to cause much blocking of the alumina pores. It seems likely that as the result of a chemical interaction of the KOH with the alumina the area of the support was lowered. The catalyst prepared using cobalt aluminate as support had an area of $62m^2$/g.catalyst. This decrease of surface area was probably due to the high content of cobalt oxides and cobalt aluminate on the catalyst surface, which would block the alumina pores and so lower the area of the catalyst.

Table 3.9.4 BET surface areas of catalysts

Catalyst 4SCN	1 g. catalyst contains Al_2O_3	BET Surface area (m^2/g.cat)	
		expected	measured
Al_2O_3 support (blank)	1.00	163	163
30Co-nit(H_2O) /100Al_2O_3 (a)	73	119	102
30Co-nit(H_2O), 4KOH /100Al_2O_3	77	126	81
30Co-nit(H_2O) /100Al_2O_3 ($CoAl_2O_4$)	59	96	62

3.9.5 FT Activity

3.9.5.1 Activity with time on stream

The FT reaction was performed at 220°C, 15bar g and H_2/CO ratio =2. The FT activity of the silinized catalyst throughout the run was slightly higher than that of the reference catalyst. Initially the silinized alumina catalyst showed higher activity (70%) than the reference catalyst (58%). After 16 hrs TOS the activity declined and was lower than the reference catalyst. At 48 hrs TOS the silinized alumina catalyst showed slightly higher activity (49%) than the reference catalyst (44%). Overall, except for the initial activity there was not a market difference between the two catalysts (see figure 3.9.2). The silinization of the alumina support with five cycles of tetraetoxisilane seemed not to be sufficient to cover a large part of the alumina surface. To confirm this, TPR scans of the silinized catalyst showed that the aluminate peak consumed 67% of the total hydrogen consumption as against 66% for the reference catalyst. From this it can be concluded that more or less the same amount of cobalt aluminates were formed when the alumina support was silinized as when the alumina was used as such.

The catalyst prepared with KOH had very low FT performance. The initial activity at 2hrs TOS was below 1% and after 20hrs TOS the average conversion was only about 3%. In very general terms the initial activity trends of the four catalysts matched the amount of cobalt

metal area loaded (see table 3.9.3). However, for the KOH case the actual activity was much lower than would be expected from the cobalt metal area of this catalyst. For iron catalysts as well as for supported cobalt catalysts it is known that high levels of alkali result in lower FT activities [16]. In agreement with this the present study showed a dramatic decrease in activity as the result of the addition of KOH. The activity of this catalyst may also have been influenced by the decrease in BET surface area of the catalyst, which was around 81m^2/g.catalyst as against 102 m^2/g. for the reference catalyst. Despite the above possible explanations it is probable that some other unknown factor contributed to the very poor performance of this catalyst.

The catalyst on "cobalt aluminate" showed high FT activity. It started at 99% at 2hrs TOS. The activity declined to 56% at 20hrs TOS and at 48hrs the activity was 50%. This catalyst showed superior activity to the reference catalyst at all times. The high activity of this particular catalyst might have been due to a higher dispersion of the cobalt (see table 3.9.3). To make sure that the support was converted to cobalt aluminates the catalyst had to be calcined previously at 700°C. A TPR scan conducted on this support showed no peaks corresponding to Co_3O_4, *i.e.*, all the cobalt species had been converted to the aluminate.

Table 3.9.5 FT activity of catalysts

Catalyst 4SCN	FT activity measured as CO converted (%) Time on stream (hrs)				
	2	16	20	24	48
30Co-nit(H_2O) /100Al_2O_3 (a)	57.8	56.2	55.6	53.3	44.0
30Co-nit(H_2O) /100(Al_2O_3 + SiO_2)	70.2	53.0	47.2	51.9	49.2
30Co-nit(H_2O), 4KOH /100Al_2O_3	0.9		4.3	3.2	1.6
30Co-nit(H_2O) /100Al_2O_3 ($CoAl_2O_4$)	98.9		56.8	59.1	50.0

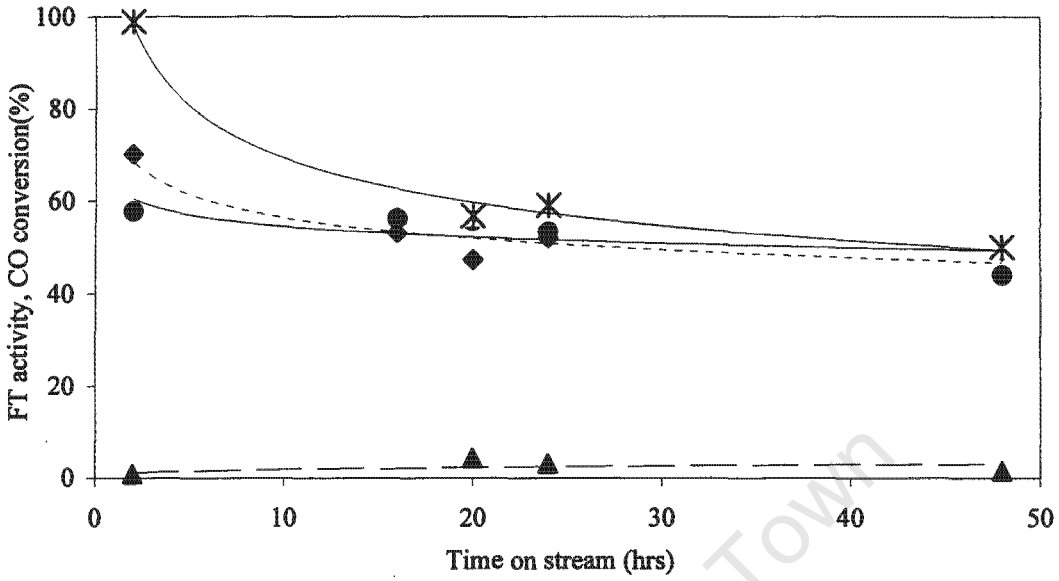

Figure 3.9.2: FT activities of: (●)30gCo-nit(H_2O)/100gAl_2O_3 Reference catalyst. (◆)30gCo-nit(H_2O) /100g(Al_2O_3+SiO_2)silinized catalyst; (▲) 30gCo-nit(H_2O),4KOH/100gAl_2O_3 KOH catalyst and (✳) 30gCo-nit(H_2O)/100gAl_2O_3 ($CoAl_2O_4$) catalyst supported on aluminates.

The FT activities of the catalysts and the metal surface area loaded in the FT reactor were plotted in order to see whether there was a correlation as shown in figure 3.9.3 where the trends in the activities did roughly match the trends in the cobalt metal area, however, the activity of the KOH case was much lower than expected from the metal area of this catalyst.

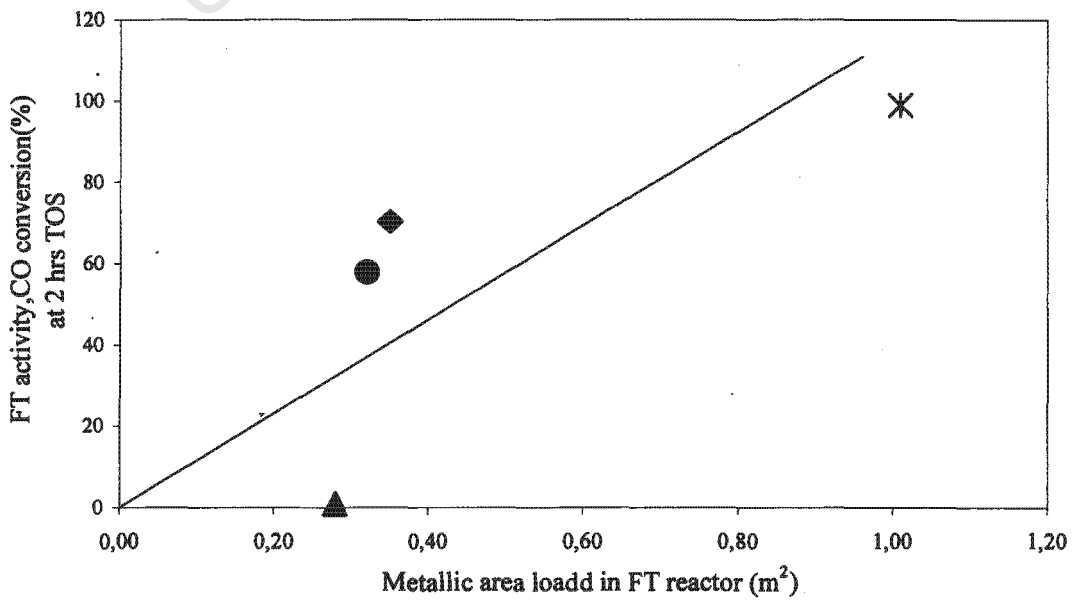

Figure 3.9.3: FT activities versus metal area loaded in the reactor. FT conditions, 220°C, 15bar g, $H_2/CO = 2$.

3.9.5.2 Chain growth Probability and Product Selectivity

The chain growth probability (α) was obtained from the slope of the plot of n against log(Fn/n) for the hydrocarbon products between C_3 to C_{12} (see section 1.1.6). The obtained α values are listed in table 3.9.6. The alpha values corresponding to two catalysts only are described in this section. The organic products of the KOH catalyst were usually not detected and hence the alpha values could not be calculated. The reference catalyst and the one supported on cobalt aluminate had similar alpha values. Throughout the results of this thesis, the alpha values were similar for the catalysts prepared with cobalt nitrate (*e.g.*, 0.86, 0.85) and slightly lower for those prepared from Co acetate (*e.g.*, 0.83) and much lower when prepared with cobalt acetyl acetonate (*e.g.*, 0.74).

Table 3.9.6 Chain growth probability of catalysts.

Catalyst 4SCN	Chain growth probability (α) Time on stream (hrs)				
	2	16	20	24	48
30Co-nit(H_2O) /100Al_2O_3 (a)	0.83	0.83	0.85	0.84	0.84
30Co-nit(H_2O) /100Al_2O_3 ($CoAl_2O_4$)	0.83		0.85	0.82	0.83

The ratios of the paraffins over the total hydrocarbon products are given in table 3.9.7. Overall, it was observed that the reference catalyst produced less paraffins than the catalyst supported on cobalt aluminate. Generally, the high activity of the catalyst resulted in high paraffin selectivity.

Table 3.9.7 Ratio of paraffins in the hydrocarbon fraction.

Catalyst 4SCN	Paraffins/Total hydrocarbon Carbon fraction										
	C_2	C_3	C_4	C_5	C_6	C_7	C_8	C_9	C_{10}	C_{11}	C_{12}
30Co-nit(H_2O) /100Al_2O_3 (a)	0.54	0.44	0.51	0.57	0.65	0.72	0.79	0.81	0.85	0.90	0.95
30Co-nit(H_2O)/100Al_2O_3(Co_2AlO_4)	0.82	0.51	0.58	0.63	0.70	0.76	0.81	0.84	0.88	0.92	0.94

Very small quantities of ethanol and acetaldehyde were detected. The ratios of ethanol over the total C_2 hydrocarbon product were 0.13 and 0.17 for the reference and for the catalyst supported on aluminate.

Chapter IV

4.- Conclusions

Silica supported catalysts with different Co loadings were studied. TPR scans were conducted on catalysts with 10, 20 and 30g.Co per 100g.silica. From CO chemisorption the average diameter of the cobalt particles after reduction were 40, 43 and 50nm for the catalysts with 10, 20 and 30gCo/100gSiO_2 respectively. It appears that the resistance to reduction of the catalysts is proportional to the oxide particle diameter and this resulted in the shift of the peaks to higher temperatures. The percentage of H_2 consumed for the cobalt silicate peak of the total H_2 consumed was low at only about 4% for the three cases. Using the "strong" chemisorption data the metallic surface areas for these catalysts were 1.6, 2.3 and 2.7 m^2/g.catalyst respectively. The dispersion decreased with increasing cobalt loading. The 20 and 30gCo/SiO_2 had similar dispersions to those reported by Iglesia (12). The 10gCo/SiO_2 catalyst when expressed in wt% would have around 8.8%Co and a dispersion percentage of 2.97%. Iglesia reported a catalyst 10.3(wt%)Co with a dispersion percentage of 9.5. The BET surface areas of the 10 and 20gCo/100gSiO_2 catalysts per 1 g. SiO_2 increased due to the extra surface area provided by the cobalt oxides particles. The BET area per 1g.SiO_2 for the 30gCo/100gSiO_2 case, however, decreased probably due to pore blockage of the silica by the higher level of cobalt oxide. The FT activity of the catalysts mentioned above was dependent on the metal loading. As expected higher conversions were found for the catalysts containing higher metal loading. The alpha value increased with cobalt metal loading *i.e.,* the selectivity shifted to higher molecular weight products. This is in agreement with Bartholomew [29].

Catalysts with different particle sizes ranging from 125 to 200μm and from 250 to 400μm (both calcined and uncalcined) were investigated. Dispersion of the calcined 250-400μm catalyst was higher than the uncalcined one. In the literature [33] it was reported that uncalcined Ni/SiO_2 catalysts gave better dispersions than calcined samples. This finding seemed not to apply to cobalt catalysts investigated in the present work.

A number of catalysts were prepared by impregnating the cobalt solution in a 1, 2, 3 or 6 step process. The TPR profiles of the catalysts were similar, as were the degrees of reduction and the dispersion. Generally, the FT activity of all the catalysts prepared in 1, 2, 3 or 6 steps were not significantly different. The number of impregnation steps had little if any effect in the alpha values. The ratios of the paraffins over the total hydrocarbon fraction of the C_2 to

C_6 hydrocarbons increased with catalyst activity. This could have been due to the fact that when the catalysts were more active it resulted in more extensive hydrogenation of the primary formed olefins.

A number of catalysts were prepared by depositing 1 or 3 theoretical monolayers of MnO or ZnO on to the silica support prior to impregnation of the cobalt precursor. It was observed that by coating the silica support the dispersions were decreased notably. The low dispersions in the coated cases could be due to pore blockage of the SiO_2 support. Pore blockage resulted in less available area for the deposition of the cobalt and this resulted in agglomeration of the cobalt and hence in lower dispersions. The FT activities of the coated catalysts were inferior to that of the uncoated catalyst $30gCo/100gSiO_2$. The lower metal surface areas of the coated catalysts matched the lower activities. The catalyst coated with MnO gave higher ratios of the paraffins over the total hydrocarbon fraction from C_2 to C_7 than the uncoated Co/SiO_2 catalyst. However, it was reported in the literature that MnO supported Fe catalysts yielded more C_2-C_4 alkenes than Fe catalysts supported on alumina or titania [26]. On the other hand the catalyst coated with ZnO yielded less paraffins than the uncoated catalyst. From the obtained metal surface areas it can be deduced that coating silica with 1 or 3 layers of MnO or ZnO does not enhance the formation of small cobalt crystallites and consequently the achievement of higher metal surface areas.

Different cobalt salts *i.e.,* cobalt nitrate, acetate and acetyl acetonate were dissolved in different solvents *i.e.,* H_2O, CH_3OH and CH_2Cl_2 and subsequently impregnated onto the Al_2O_3 support. These catalysts were calcined in N_2 at 270°C after each of the 4-impregnation steps. TPR profiles of these catalysts showed stronger cobalt-support interaction than silica supported catalysts whereas for the Co/SiO_2 cases only about 4% of the H_2 consumed in TPR runs was assigned to the reduction of cobalt-silicate complexes, the percentage of H_2 consumed in the reduction of cobalt-alumina complexes were much higher, typically 65%. The cobalt metal areas were different for each catalyst prepared with different cobalt salts and hence the activities were also different. The BET surface areas of the catalysts were lower than the expected ones, which were calculated according to the alumina content in the catalyst. The $30gCo\text{-}acac(CH_2Cl_2)/100gAl_2O_3$ had a much lower BET surface area compared to those prepared using cobalt nitrate or acetate. This was ascribed to the presence of undecomposed acetyl acetonate deposits, which presumably blocked the pores of the Al_2O_3 support. Although the initial activity of the $30gCo\text{-}ace(H_2O)/100gAl_2O_3$ was higher than the

30gCo-nit(H_2O)/100gAl_2O_3 catalyst the most active and stable catalyst over longer times on streams appeared to be the one prepared with cobalt nitrate. The lowest activity corresponded to the one prepared with cobalt acetyl acetonate. The catalysts' activities showed some correlation with the metallic surface areas. The cobalt nitrate cases did not fall within the trend. The catalysts prepared with cobalt nitrate dissolved either in H_2O or in CH_3OH gave similar alpha values. The 30gCo-ace(H_2O)/100gAl_2O_3 showed slightly lower alpha values than the nitrate cases. The lowest alpha values were obtained using the 30gCo-acac(CH_2Cl_2)/100gAl_2O_3 catalyst. Generally, the high activity catalysts yielded higher paraffins' selectivities.

The preparation of the catalysts mentioned above were repeated but this time the calcination took place in air. The objective was to investigate whether the calcination medium could affect the distribution of the cobalt particles. AAS and TGA analyses confirmed that calcination of the samples in air showed higher loss of carbonaceous material than when the catalysts were calcined in N_2. TPR profiles indicated that the 30gCo-acac(CH_2Cl_2)/ 100gAl_2O_3 catalyst showed a lower percentage of H_2 consumption for the reduction of the metal-support interaction peak than those prepared with cobalt nitrate or acetate. Except for the 30gCo-nit(H_2O)/100gAl_2O_3 catalyst H_2 consumption required to reduce the metal-support interaction peak was higher when the catalysts were calcined in air. The "measured" BET surface areas of the catalysts calcined in air were lower than the "expected" ones and were not much different from those obtained for the catalysts calcined in N_2. The FT activities of the catalysts calcined in air were lower than those calcined in N_2. Calcination in air appeared to decrease the metal dispersion and hence the catalysts' activities. The initial activity of the 30gCo-ace(H_2O)/100gAl_2O_3 catalyst was higher than that of the 30gCo-nit(H_2O)/100gAl_2O_3 and 30gCo-acac(CH_2Cl_2)/100gAl_2O_3 catalysts. The activities and the metallic areas of the catalysts calcined in air did not show that the activities were dependent on the metal surface area available. The 30gCo-acac(CH_2Cl_2)/100gAl_2O_3 catalyst had the highest dispersion but the lowest activity. For this catalyst the rapid re-oxidation of the small cobalt crystallites was possibly the cause of the decrease in activity of the freshly reduced catalysts before the CO conversion was measured after 2hrs.

Two 30gCo-nit(H_2O)/100gAl_2O_3 catalysts were dried by microwave heating prior to calcination in N_2. Drying catalysts with microwaves resulted in lower FT activities compared to the reference catalyst dried by conventional heat. The catalyst dried with microwaves

prior to ageing in a dessicator for 5 days showed a higher dispersion than the reference catalyst. Generally, the fractions of paraffins over the total hydrocarbon product in the fractions C_2-C_{12} were higher when the FT activity was higher.

Several catalysts were prepared by impregnating the metal salt onto the alumina support at temperatures around 80°C in two impregnation steps. TPR scans confirmed that the uncalcined catalysts showed lower metal-support interaction than the calcined catalysts. This is in agreement with the literature [33] where in that case uncalcined Ni/SiO_2 catalysts were more dispersed than calcined catalysts. The dispersion % of the catalyst impregnated at around 80°C was higher than that of the one impregnated at room temperature. The FT activity and the metal area loaded in the FT reactor of these catalysts, however, did not show a clear correlation. It was observed that the higher ratios of paraffins over the total hydrocarbon in the fractions from C_2-C_{12} were related to the high catalysts' activities.

The alumina support was modified in order to investigate whether the performance of the catalysts would be influenced by such alterations. One catalyst was modified by silinizing the alumina and the other by impregnating the alumina with KOH solution prior to impregnation of the cobalt nitrate solution. In another preparation a Co/Al_2O_3 catalyst was first calcined to convert all the cobalt present to cobalt aluminate and this was then subsequently impregnated with cobalt nitrate. The FT activity of the latter catalyst was superior to the reference catalysts at all TOS's. The silinized alumina catalyst had similar activity to the reference catalyst and the KOH catalyst showed very poor activity. In the silinized case TPR profiles showed that more or less the same amount of H_2 was required to reduce the metal-support interaction phase. The KOH sample showed similar dispersion to that of the reference catalyst but the activity corresponding to the former catalyst was nevertheless poor.

Comparing silica and alumina as supports (using the preparation techniques employed in this work) it was found that alumina was the better support. At 30gCo/100 support the alumina catalyst typically had a FT activity of 55% CO conversion as against about 40% for the silica catalysts. This was in spite of the fact that about 65% of the Co was present as unreducible "Co-aluminate" as against about 4% unreducible "CO-silicate" (this refers to the standard H_2 reduction carried out at 360°C for 14 hrs prior to the FT reactor runs).

References

1. Storch, Golumbic and Anderson., "The Fischer- Tropsch and Related Synthesis", (1951)233, 283.
2. H. Schulz., *Appl. Catal.*, **186** (1999)3.
3. A. Cybulski and J.A. Moulijn., "Structured Catalysis and Reactors" (1998).
4. M. E. Dry., *Appl. Catal., A: Gen.*, **138** (1996) 319.
5. R.L. Espinoza, A.P. Steynberg, B. Jager, A.C. Vooslo., *Appl. Catal., A: Gen.*, **186** (1999) 13.
6. S.T. Sie, R. Krishna., *Appl. Catal., A Gen.*, **186** (1999) 55.
7. A.P. Steynberg, R.L. Espinoza, B. Jager, A.C. Vooslo., *Appl. Catal., A: Gen.*, **186** (1999) 41.
8. M.E. Dry., "The Sasol Fischer-Tropsch Process", Vol 2, Chapter 5 (1983). Academic Press Inc.
9. H.C. Long, M.L. Turner, P. Fornasiero, J. Kaspar, M. Graziani, P.M. Maitlis., *J. Catal.*, **167** (1997) 172.
10. M. E. Dry and H.B. Erasmus, "Annual Rev. Energy" (1987)1.
11. R. Quyoum, V. Berdini, M.L. Turner, H. Long and P.M. Maitlis, *J. Catal.*, **173** (1998)355.
12. E. Iglesia, S.C. Reyes, R.J. Madon and S.L. Soled., *Advances in Catal.*, **39** (1993)224.
13. S.A. Eliason and C.H. Bartholomew., *Appl. Catal., A: Gen.*, **186** (1999)229.
14. A.P. Rage and B.H. Davis., *Catal. Today*, **36** (1997)335.
15. M.E. Dry., *Catal., Today,* **71** (2002)227.
16. M.E. Dry., Encyclopedia of Catalysis., Jonh Wiley and Sons ., N.Y. USA. Vol **3**, (2003) 347.
17. H. Schulz and M. Claeys., *Appl . Catal., A: Gen.*, **186** (1999)91.
18. G.A. Huff and C.N. Satterfield., *J. Catal.*, **85** (1984)370.
19. M.Vannice., *J. Catal.*, **37** (1975)449.
20. E. Iglesia., *Appl. Catal., A:Gen.*, **161** (1997)59.
21. R.C. Reuel and C.H. Bartholomew., *J. Catal.*, **85** (1984)63.
22. A. Kogelbauer, J.G. Goodwin and R. Oukaci., *J. Catal.*, **160** (1996)125.

23. Y. Zhang, D. Wei, S. Hammache and J.G. Goodwin., *J. Catal.*, **188** (1999)281.
24. B. Ernst, S. Libs, P. Chaumette and A. Kiennemann., *Appl . Catal., A: Gen.*, **186** (1999)145.
25. G.J. Haddad, B. Chen and J. G. Goodwin., *J. Catal.*, **161** (1996)274.
26. A. Adesina, *Appl . Catal., A: Gen.*, **138** (1996)345.
27. M. Kraum and M. Baerns, *Appl . Catal., A: Gen.*, **186** (1999)189.
28. F.J. Berry, L.R. Smart, P.S. Sai Prasad, N. Lingaiah, P. kaota Rao., *Appl . Catal., A: Gen.*, **204** (2000)191
29. R.C. Reuel and C.H. Bartholomew., *J. Catal.*, **85** (1984)78.
30. L.B. Backman, A. Rautiainen, M. Lindblad and A.O.I. Krause, *Appl . Catal., A: Gen.*, **191** (2000)55
31. L.B. Backman, A. Rautiainen, M. Lindblad and A.O.I. Krause, *Appl . Catal., A: Gen.*, **43** (1998)11.
32. P. van Berge, J. van de Loosdrecht, S. Barradas and A.M. van der Kraan, *Catal., Today,* **58** (2000)321.
33. "Handbook of Heterogeneous Catalysis", vol 1, Ed., G. Ertl, H. Knozinger, J. Weitkamp., A. Wiley Company. Authors M.Che, O. Clause, Ch. Marcilly. Weinheim-Germany(1997)191
34. E. van Steen, G.S. Sewell, R.A. Makhothe, C. Micklethwaite, H. Manstein, M. de Lange and C.T. O'Connor, *J. Catal.*, **162** (1996)220.
35. A. Yu Khodakov, J. Lynch, D. Bazin, B. Rebours, N. Zanter, B. Moisson and P. Chaumette., *J. Catal.*, **168** (1997)16.
36. E. Iglesia, S.L. Soled, R. A. Fiato and H. Grayson, *J. Catal.*, **143** (1993)345.
37. E. Iglesia., *Appl. Catal., A: Gen* **161** (1997)59.
38. J.G. Goodwin., *J. Catal.*, **160** (1996)125.
39. E. Iglesia, S. L. Soled and R.A. Fiato,, *J. Catal.*, **137** (1992)212.
40. R. Oukaci, A.H. Singleton and J.G. Goodwin., *Appl. Catal., A: Gen* **186** (1999)129.
41. N. Tsubaki, S. Sun and K. Fujimoto., *J. Catal.*, **199** (2001)236.
42. J. Li and N.J. Coville., *Appl. Catal., A: Gen* **181** (1999)201.
43. C. H. Bartholomew., *J. Catal.*, **92** (1985)376.
44. V. Curtis, C.P. Nicolaides, N.J. Coville, D. Hildrebrandt and D. Glasser., *Catal., Today*, **49** (1999) 33.

45. D. Schanke, A.M. Hilmen, E. Bergene, K. Kinnari, E. Rytter, E. Adnanes, and A. Holmen., *J. Energy and Fuels.,* **10** N° 4 (1996)867.

46. A.M. Hilmen, D. Schanke, K.F. Hanssen, and A. Holmen., *Appl. Catal., A: Gen* **186** (1999)169.

47. M. Rothaemel, K. Firing Hanssen, E.A. Blekkan, D. Schanke and Anders Holmen., *Catal., Today.,* **38** (1997)79.

48. G.F. Froment., *Appl. Catal., A: Gen* **212** (2001)117.

49. J.A. Moulijn, A.E. van Diepen and F. Kapteijn., *Appl. Catal., A: Gen* **212** (2001)3.

50. M. Guisnet and P. Magnoux., *Appl. Catal., A: Gen* **212** (2001)83.

51. M.E. Dry, T. Shingles and L.J. Boshoff., *J. Catal.,* **25** (1972)105.

52. C.H. Bartholomew., *Appl. Catal., A: Gen* **212** (2001)17.

53. L.B. Backman, A. Rautiainen, M. Lindblad, O. Jylha and A.O.I. Krause., *Appl. Catal., A: Gen* **208** (2001)223.

54. T. Matsuzaki, K. Takeuchi, T. Hanaoka, H. Arakawa and Y. Sugi., *Catal., Today* **28** (1996)251.

55. C.H. Bartholomew., *Catal., Today.,* **6** (1989)81.

56. M.K. Niemela and A.O.I. Krause., *Catal., Letters,* **42** (1996)161.

57. B. Jager and R. Espinoza., *Catal., Today.,* **23** (1995)17.

58. D.R. Milburn, K.V.R. Chary, R.J.O'Brien and B.H. Davis., *Appl. Catal., A: Gen* **144** (1996)133.

59. R. Bechara, D.Balloy and D. Vanhove., *Appl. Catal., A: Gen* **207** (2001)343.

60. P.J. van Berge., *Stu., Surf., Science and Catal.*, **107** (1997)207.

61. H. Schulz and M. Claeys., *Stu., Surf., Science and Catal.*, **107** (1997)183.

62. H. Schulz., *Appl. Catal., A: Gen* **186** (1999)71.

63. J.R. Anderson, K.C. Pratt, "Introduction to Characterization and Testing of Catalyst", Academic Press, Australia (1985) 8.

64. I.M. Ciobica., PhD Thesis., Technische Universiteit Eindhoven., The Netherlands (2002).

65. Michael Claeys,, *J. Catal.*, **185**(1999)120.

66. F. Rohr, O.A. Lindvag, A. Holmen and E.A. Blekkan., *Catal., Today.,* **58**(2001)247.

67. A.H. Hilmen, D, Schanke and A. Holmen., *Catalysis Letters*, **38** (1996) 143.

68. S. Sun, N. Tsubaki and Kaoru Fujimoto, *Appl Catal., A: Gen*, **202**(2000) 121.

69. Master Thesis of Richard Waals. University of Cape Town (1998).
70. Introduction to Microwave sample preparation. Theory and Practice, Edited by H.M. Kingston and Lois B. Jossie, ACS Professional Reference Book. American Chemical Society, Washington DC, 1988.
71. R. Belambe, R. Oukaci and J.G. Goodwin., *J. Catal.*, **166** (1997)8.
72. S. Ho, M. Hualla and D.M. Hercules., *J. Phys. Chem.* **94**(1990) 6396-6399.
73. G. Fierro, M. Locajono, M. Inversi, P. Porta, R. Lavecchia and F. Cioci, *J. Catal* **148** (1994) 709.

APPENDICES

APPENDIX I. Temperature programmed reduction, TPR

The required H_2 consumption was measured using a mixture of H_2 in N_2 and a separate flow of N_2 used as a reference gas. The difference between the two gases was the total flow of H_2 used as a reducing gas. The flows were set to 60 ml/min. The thermal conductivity of the H_2 in N_2 gas was recorded by a thermal conductivity detector (TCD) and measured relative to the reference gas.

The hydrogen consumption was measured using the trapezoidal equation:

$$H_2 consumption = \sum_n \frac{[(t_{n+1} - t_n) \times (c_{n+1} - c_n)]}{2}$$

Where:

c	=	H_2 consumption in mmol/min.
t	=	Time elapsed in minutes.

1.1 TPR calibration

The concentration of H_2 in N_2 was calculated when a sample of CuO was reduced in the TRP apparatus. CuO was chosen to calibrate the TPR because Fierro at al., [33, 73] have demonstrated that CuO gave a narrow single reduction peak. To quantify the amount of hydrogen used, it has being assumed that the reduction stoichiometry of CuO is:

$$CuO + H_2 \rightarrow Cu^0 + H_2O$$

It is clearly seen that in the above reaction 1 mol of H_2 is required for the reduction of CuO to Cu^0, *i.e.*,

S	=	Sample weight, 0.2011g CuO.
MW_{CuO}	=	Molecular weight of CuO, 79.55 g.

First, it is necessary to calculate the number of CuO moles present in the sample.

1mol CuO ——————— 79.55g. CuO

xmol CuO ——————— 0.2011g. CuO

x = 0.002528 moles CuO

If, 1 mol of CuO requires 1 mol of H_2 to be reduced to Cu^0 so, 0.002528 moles of CuO would need 0.002528 moles of H_2 to be reduced to CuO. In this thesis, the H_2 consumed was given in H_2 moles per 1 gram of catalyst. So, the next step is to recalculate the moles of H_2 required to reduce 1 gram of sample, *i.e.*,

1mol CuO ——————— 79.55g. CuO

xmol CuO ——————— 1.00g. CuO

x = 0.01257 moles CuO

From the relation above it is expected that 0.01257 moles of H_2 would be needed to reduce 1 g. of CuO to Cu^0.

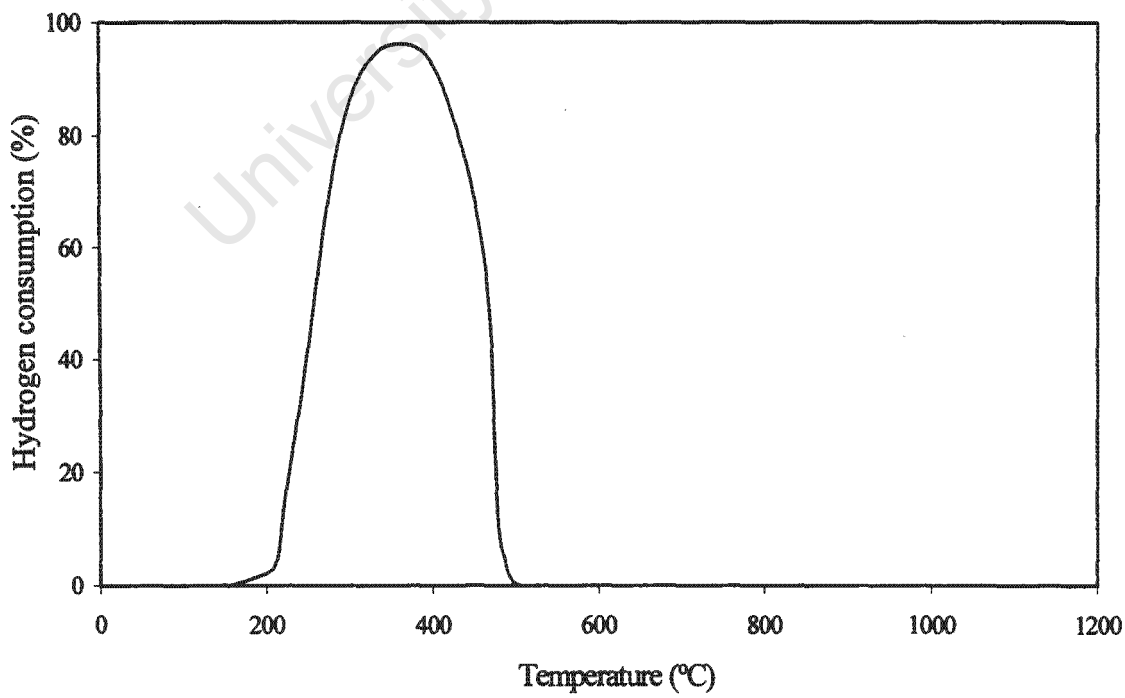

Figure 1.1: TPR profile of: CuO. H_2 consumption (%) of the reducing mixture (6%H_2 in N_2) against temperature (°C).

After the calibration of the TPR a catalyst sample was reduced in the TPR. The sample was the 30gCo/100gSiO_2 (figure 1.2). The H_2 consumption was calculated assuming that only Co_3O_4 was present after calcination. The Co_3O_4 then would reduce to Co^0 in the following reaction:

$$Co_3O_4 + 4H_2 \rightarrow 3Co^0 + 4H_2O$$

$MW_{Co_3O_4}$ = Molecular weight of Co_3O_4, 240.79g.
M_{Co} = Atomic weight of cobalt, 58.93g.
$M_{[O]}$ = Atomic weight of oxygen, 16.00g.

First, it is necessary to calculate the amount of cobalt in the unreduced sample per 1 gram of catalyst. One gram of unreduced catalyst contains 0.2130g Co. For this we make the following relation:

240.79g. Co_3O_4 ——— 176.79g Co
x g. Co_3O_4 ——— 0.2130g Co
x = 0.2901 g. Co_3O_4

Then, the number of moles of Co_3O_4 in 0.2901 g of Co_3O_4 is calculated;

1 mol Co_3O_4 ——— 240.79g Co
x moles. Co_3O_4 ——— 0.2901g Co
x = 0.001205 moles. Co_3O_4

The stoichiometric reduction of Co_3O_4 requires 4 moles of H_2 to be reduced to Co^0. Finally, the H_2 required to reduce 0.001205 moles of Co_3O_4 will be:

1 mol Co_3O_4 ——— 4molesH_2
0.001205moles. Co_3O_4 ——— x molesH_2
x = 0.00482 moles. H_2

The H_2 consumption will then be 0.00482moles H_2 per 1 gram of 30gCo/100gSiO_2 catalyst.

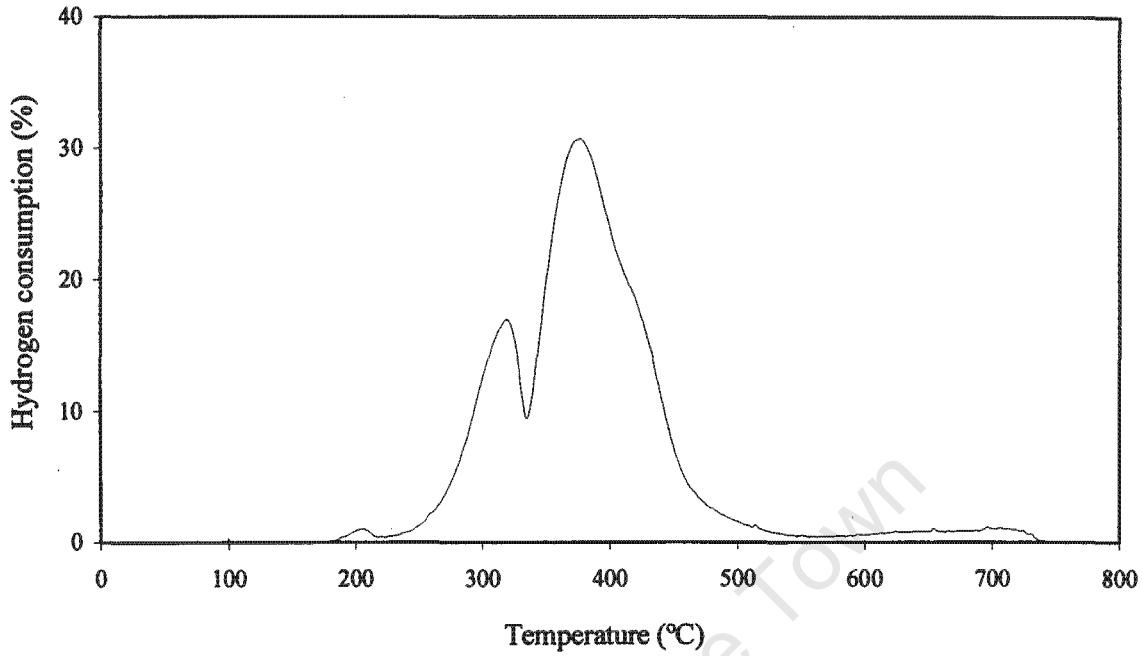

Figure 1.2: TPR profile of: 30gCo/100gSiO_2. H_2 consumption (%) of the reducing mixture (6%H_2 in N_2) against temperature (°C).

The reducibility of the 30gCo/100gSiO_2 catalyst was shown in section 3.1.2. The small shoulder was assigned to be the reduction of undecomposed cobalt nitrate. The first peak at 300°C was attributed to the reduction,

$$Co_3O_4 + H_2 \rightarrow 3CoO + H_2O$$

The peak at 362°C can be assigned to the reduction,

$$CoO + H_2 \rightarrow Co^0 + H_2O$$

The reactions above indicate that the reduction of 3 atoms of Co in Co_3O_4 require 1 mol of H_2 to be reduced to Co^0. And that 1 atom of Co in CoO requires one mol of H_2 to be reduced to Co^0. This means that the first peak attributed to the reduction of Co_3O_4 to 3CoO would have an area of about 1/3 of the peak assigned to the reduction of CoO to Co^0. From figure 1.2 it can be observed that the first peak is approximately 1/3 of the second peak.

APPENDIX II. CO chemisorption

2.1. Metal dispersion

The "strong" metal dispersion was calculated using the equation:

$$D_s = \frac{V_m}{22414}\frac{M}{wt} \times 100$$

Where,

D_s	=	"Strong" dispersion (%).
M	=	Atomic mass of the metal.
Vm	=	Volume of Co chemisorbed (ml/g.cat).
wt	=	mass of metal per 1 gram of catalyst (g/g.cat).

As an example the "strong" dispersion of the $30gCo/100SiO_2$ was calculated as follows:

M_{Co}	=	58.93g.
V_m	=	1.5390 ml/g.cat
wt	=	0.2070g/g.cat.

$$D_s = \frac{1.5390(ml/g.cat)}{22414ml} \times \frac{58.93(g)}{0.2070(g/g.cat)} \times 100$$

D_s = 1.95%

The "total" dispersion was obtained from the difference of the first isotherm and the support isotherm at 250°C as shown in figure 2.1.

$$V_t = V_a - V_{support}$$

V_t	=	Total volume adsorbed (ml/g.cat).
V_a	=	Volume adsorbed by the first isotherm (ml/g.cat).
$V_{support}$	=	Volume adsorbed by the silica support (ml/g.SiO_2).

V_t = 2.1382 - 0.3000

V_t = 1.8382ml/g.cat

Then the total dispersion (D_t) was adjusted to:

$$D_t = \frac{V_t \times D_s}{V_m}$$

$$D_t = \frac{1.8382 \times 1.95}{1.5390}$$

D_t = 2.72%

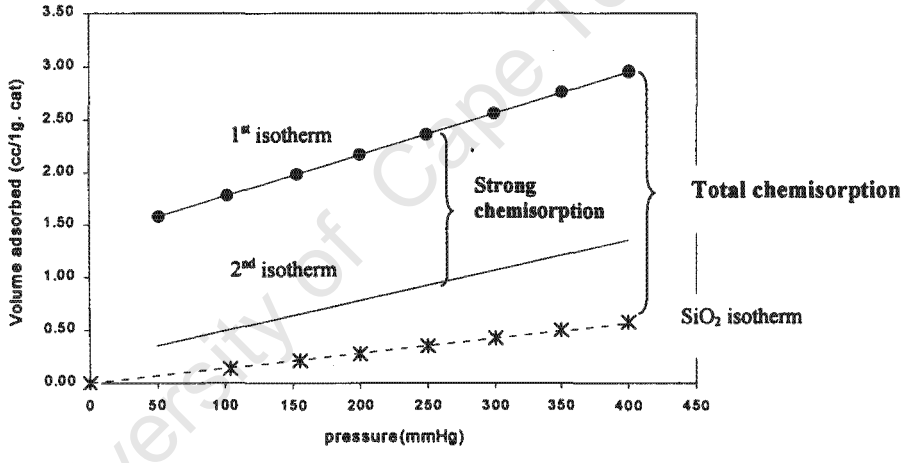

Figure 2.1: Chemisorption isotherms of the 30gCo/100gSiO_2.

2.2. Metallic surface area

The metallic area from the "**strong**" chemisorption was calculated using the following equation:

$$A_s = \frac{V_m}{22414} \times N \times a_m$$

Where:

A_s	=	Total metallic surface area (m^2/g.catalyst) from"strong" chemisorption.
Vm	=	Volume of CO chemisorbed (ml/g.cat).
N	=	Avogadro's number (6.03×10^{-23} molecules/mol).
a_m	=	Cross sectional area occupied by 1 atom of metal (6.62×10^{-20} m^2).

$$A_s = \frac{1.5390}{22414} \times (6.03 \times 10^{-23}) \times (6.62 \times 10^{-20})$$

$A_s = 2.74\ m^2/g.cat.$

The "strong"metallic area per 1 g. of cobalt can be re-calculated as follows;

$$\frac{2.7439 m^2}{g.cat} \times \frac{1.00 g.cat}{0.2070 g.Co} = 13.26 m^2 / g.Co$$

The "**total**" metallic surface area was calculated using the next equation:

$$A_t = \frac{V_t \times A_s}{V_m}$$

$$A_t = \frac{2.1382(ml / g.cat) \times 2.7439(m^2 / g.cat)}{1.5390(ml / g.cat)}$$

$A_t = 3.80\ m^2/g.cat$

The "total" metallic area per 1 g. of cobalt can be re-calculated in the following manner;

$$\frac{3.80 m^2}{g.cat} \times \frac{1.00 g.cat}{0.2070 g.Co} = 18.36 m^2 / g.Co$$

The metallic surface area in the FT reactor from the "strong" chemisorption data was obtained by multiplying the metallic area per g. catalyst times the weight of catalyst loaded in the FT reactor.

$$A_{FT} = A \times wt$$

A_{FT}	=	Metallic surface loaded in FT reactor (m^2).
A	=	Metallic surface are (m^2/g.cat).
wt	=	Weight of cobalt loaded in FT reactor (g).

$A_{FT_t} = 2.7439(m^2 / g.cat) \times 0.26(g.cat)$

$A_{FT\,t} = 0.71 m^2$

The metallic surface area in the FT reactor from the "total" chemisorption data was obtained by multiplying the "total" metallic area per g. catalyst times the mass of catalyst loaded in the FT reactor,

$A_{FT_t} = A_t \times wt$

$A_{FT\,t} = 3.80 m^2/g.cat \times 0.26g$

$A_{FT\,t} = 0.99 m^2$

2.3. Average particle diameter of cobalt metal

The average particle diameter of the cobalt metal from the "**strong**" chemisorption was calculated using the following relation;

$$\frac{A_{Co}(m^2)}{M_{Co}(g)} = \frac{A_{Co}(m^2)}{V_{Co}(ml) \times \delta_{Co}(g/ml)}$$

Where:

A_{Co}	=	Metallic surface area of cobalt (m^2).
M_{Co}	=	mass of cobalt (g).
V_{Co}	=	Volume of cobalt (ml).
δ_{Co}	=	Density of cobalt metal (g/ml).

Assuming that the cobalt particles were spherical the above equation can be substitute by the area and the volume for a sphere.

$A_{Co} = \pi d^2$

And

$V_{Co} = \pi d^3/6$

So, we can have,

$$\frac{A_{Co}(m^2)}{vol.Co \times \delta_{Co}} = \frac{\pi d^2}{\frac{\pi d^3}{6} \times \delta_{Co}}$$

Then, the cobalt diameter d is:

$$d_s = \frac{6}{A(m^2/g.Co) \times \delta_{Co}}$$

For example, the 30gCo/100g SiO_2 has a metallic area and a density of:

A_{Co} = 13.26m^2Co/g.Co
δ_{Co} = 8.9 (g/ml)

$$d_s = \frac{6}{A_s(m^2/g.Co) \times \delta_{Co}}$$

$$d_s = \frac{6}{13.26\left(\frac{m^2 Co}{g.Co}\right) \times 8.9\frac{(g.Co)}{cc}}$$

$$d_s = 0.05086\frac{cc}{m^2} \times \frac{10^{-6} m^3}{1cc}$$

$$d_s = 5.86 \times 10^{-9} m \times \frac{10^9\ nm}{1m}$$

$$d_s = 50.9\ nm$$

The average particle diameter of the cobalt metal from the "**total**" chemisorption was calculated using the metallic area per gram of Co from the "strong" chemisorption data.

$$d_t = \frac{6}{A_t(m^2/g.Co) \times \delta_{Co}}$$

$$d_t = \frac{6}{18.38(m^2/g.Co) \times 8.9(ml/cc)}$$

d_t = 36.7nm

APPENDIX III. X - rays diffractometry analysis, XRD

XRD analysis was carried out in order to identify the oxide species formed on the support prior to reduction. The XRD spectra of the catalyst $30Co/SiO_2$ catalyst shown in figure 3.1 showed that the most predominant oxide phase was Co_3O_4 followed by two peaks assumed to correspond to Co_2SiO_4 and a single peak, which confirmed the presence of CoO. The peaks, which confirmed the presence of Co_3O_4, Co_2SiO_4 and CoO are summarised in table 3.1.

Table 3.1 Table of XRD data for $30gCo/100gSiO_2$

d-spacing (nm)	Relative intensity (%)	Angle (°2Theta)	Detected Co oxide specie
0.464918	17.59	19.07358	Co_3O_4
0.243693	100.00	36.85277	Co_3O_4
0.213429	19.22	42.31185	CoO
0.203474	31.03	44.48952	Co_2SiO_4
0.155356	21.44	59.44697	Co_3O_4
0.142889	25.17	65.24140	Co_3O_4

The XRD scan for the coated catalyst with MnO, $30gCo/108gMnO/100gSiO_2$ is seen in figure 3.2. The XRD scan detected five peaks for Co_3O_4, four peaks for Mn_2O_3, two peaks for MnO_2 and one peak for MnO. The °2Theta angles are summarised in table 3.2. No peaks corresponding to Mn or Co silicates were observed.

Table 3.2 Table of XRD data for the $30gCo/108gMnO/100gSiO_2$ catalyst

d-spacing (nm)	Relative intensity (%)	Angle (°2Theta)	Detected Co oxide specie
0.309486	27.89	28.82369	Mn_2O_3
0.286616	16.97	31.17981	Co_3O_4
0.271493	48.34	32.96473	Mn_2O_3
0.243477	100.00	36.88673	Co_3O_4
0.222863	6.24	40.44049	MnO
0.211402	28.93	42.73726	MnO_2
0.202425	22.28	44.73244	Co_3O_4
0.184242	13.57	49.42685	Mn_2O_3
0.165979	26.38	55.30165	Mn_2O_3
0.162126	62.88	56.73337	MnO_2
0.155619	54.00	59.33675	Co_3O_4
0.142744	48.88	65.31576	Co_3O_4

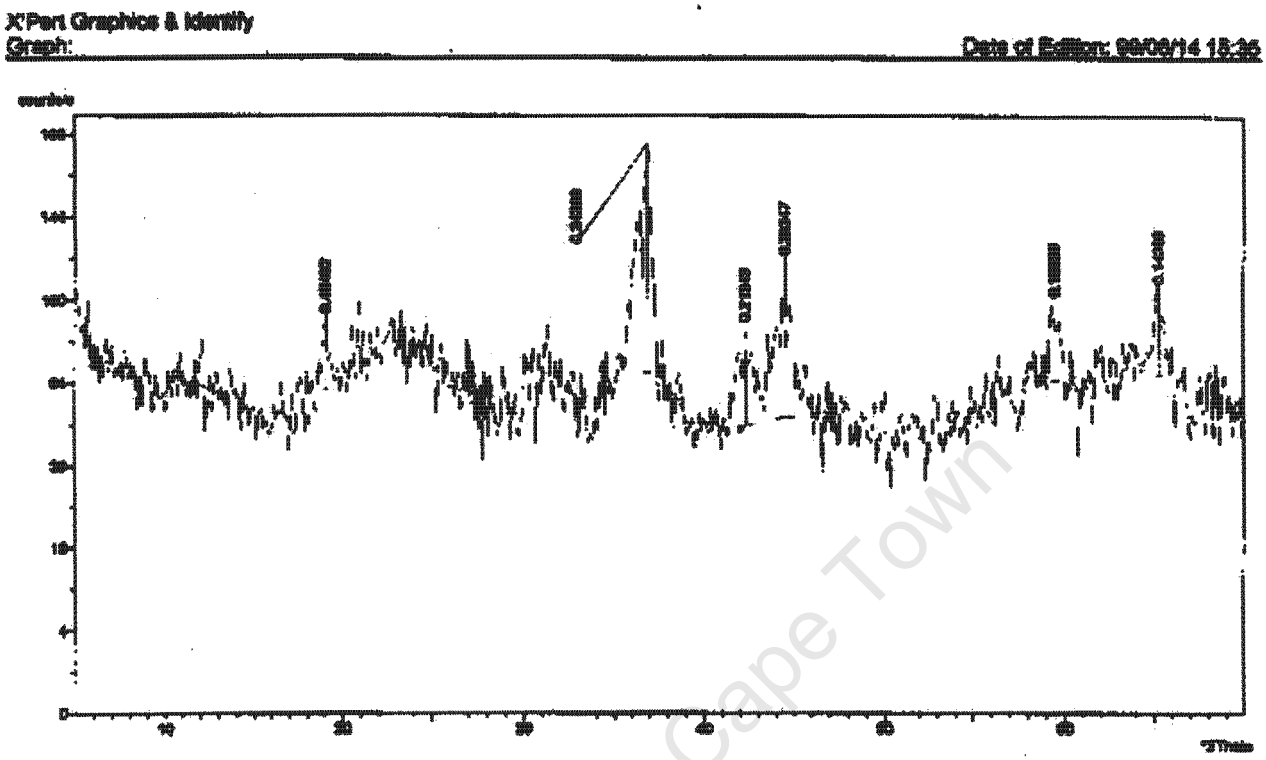

Figure 3.1: XRD spectra of the catalyst 30gCo/100g.SiO_2

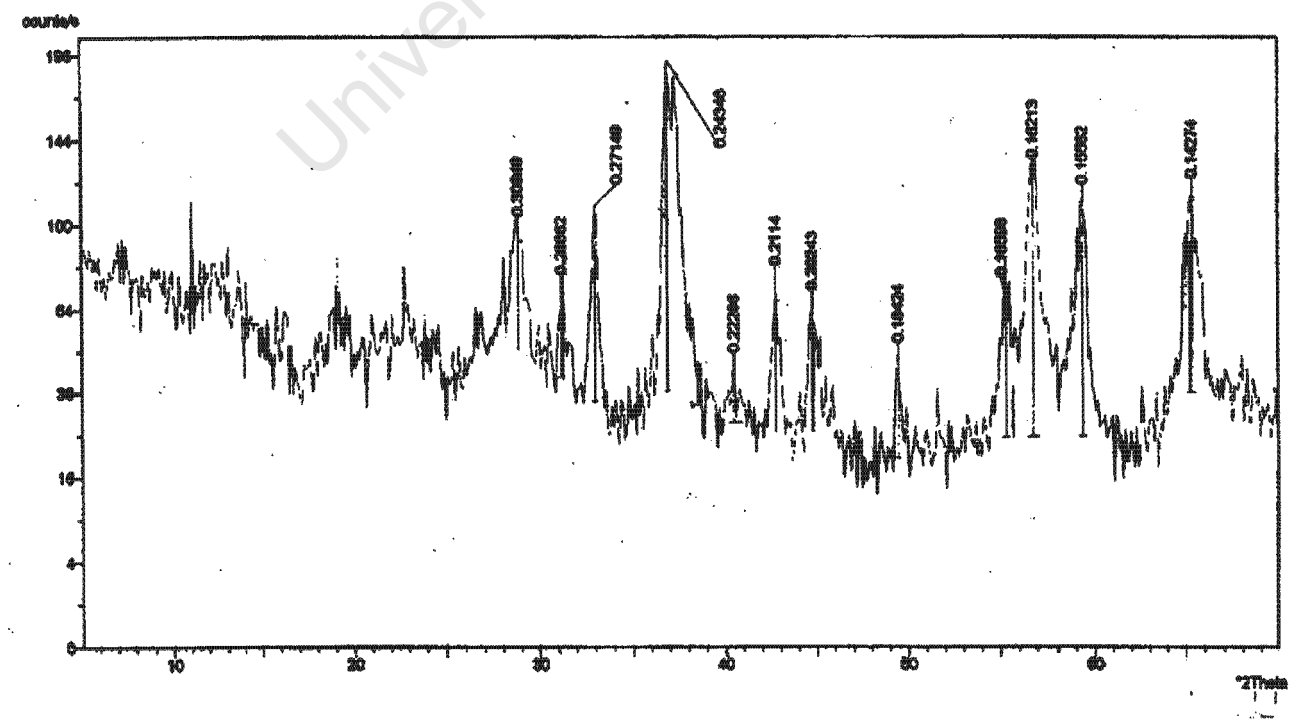

Figure 3.2: XRD spectra of the 30gCo/108gMnO/100gSiO_2.

APPENDIX IV. CO Conversion and Selectivity

4.1. CO Conversion

The CO converted was calculated from the difference of the CO gas feed and CO exiting the reactor according to the following equation:

$$\%\,\text{Conversion} = \frac{\left(\left(\frac{(A_{CO})}{(A_{N_2})}\right)_{in} - \left(\frac{(A_{CO})}{(A_{N_2})}\right)_{out}\right)}{\left(\frac{A_{CO}}{A_{N_2}}\right)_{in}} * 100$$

$$\%\,\text{Conversion} = \frac{\left(\left(\frac{(877149)}{(59670)}\right)_{in} - \left(\frac{(60599)}{60381}\right)_{out}\right)}{\left(\frac{877149}{59670}\right)_{in}} * 100$$

% Conversion = 32.0%

The CO feed was 9ml/min, which at standard conditions would be;

$T^{o} = 20^{o}C = 295^{o}K$, where 1molC = 12g occupies 22.41ℓ

$$= \frac{9ml}{min} \cdot \frac{12g.C}{1molC} \cdot \frac{1molC}{22414ml} \cdot \frac{273^{o}K}{295^{o}K}$$

= 0.00446 g.C/min

4.2. Selectivity

$N_2 + C_6H_{12}$ Feed = 5ml/min

Flow C_6H_{12} = 0.00586 ml C_6H_6 /min

At standard conditions

$$\frac{0.0586ml}{min} \cdot \frac{72g.C(C_6H_{12})}{1mol} \cdot \frac{1molC_6H_{12}}{22414ml} x \frac{273^{o}K}{295^{o}K}$$

= 1.74×10^{-4} gC C_6H_6 /min.

Cyclohexane area from chromatograms = 50020, which is $\cong 1.74 \times 10^{-4}$gC/min.

CH_4 Selectivity

CH_4 area from chromatogram $\cong 50020$
C_6H_{12} area from chromatogram $\cong 35003$

$$= \frac{35003}{50020} \cdot \frac{1.74 \times 10^{-4}\ \text{g.C}}{\text{min}}$$
$$= 1.22 \times 10^{-4}\ \text{gCH}_4/\text{min}$$

%CO conversion = 32.0%
C Converted = 0.32 x 0.00446 g.C/min
$= 1.43 \times 10^{-3}$ g.C/min

$$CH_4\ \text{Selectivity} = \frac{1.22 \times 10^{-4}}{1.43 \times 10^{-3}} * 100$$

$$= 8.5\ \%$$

The FID chromatograms of the organic products are shown in figures, 4.2.1a, b and c.

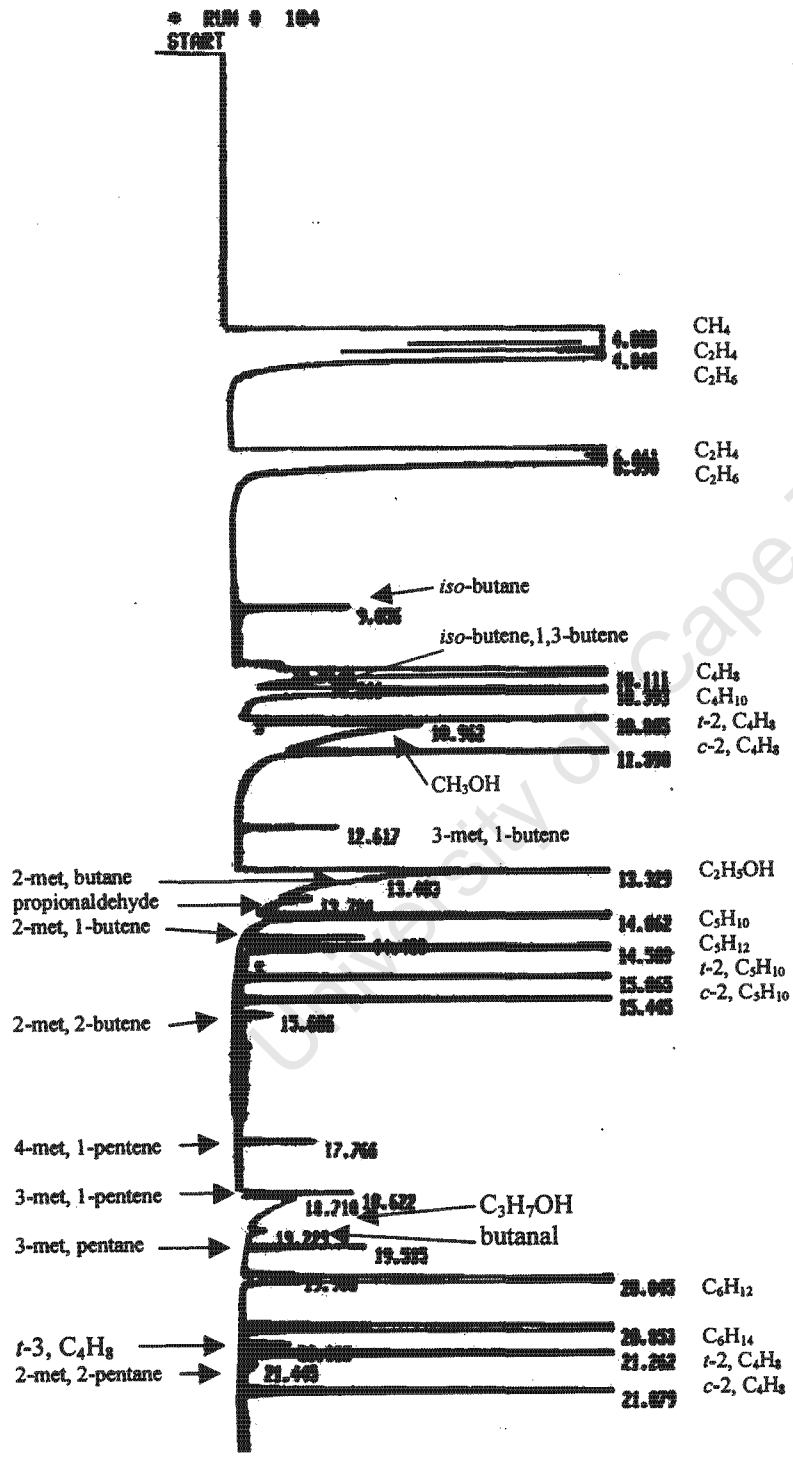

Figure 4.2.1a: FID chromatogram of the FT products

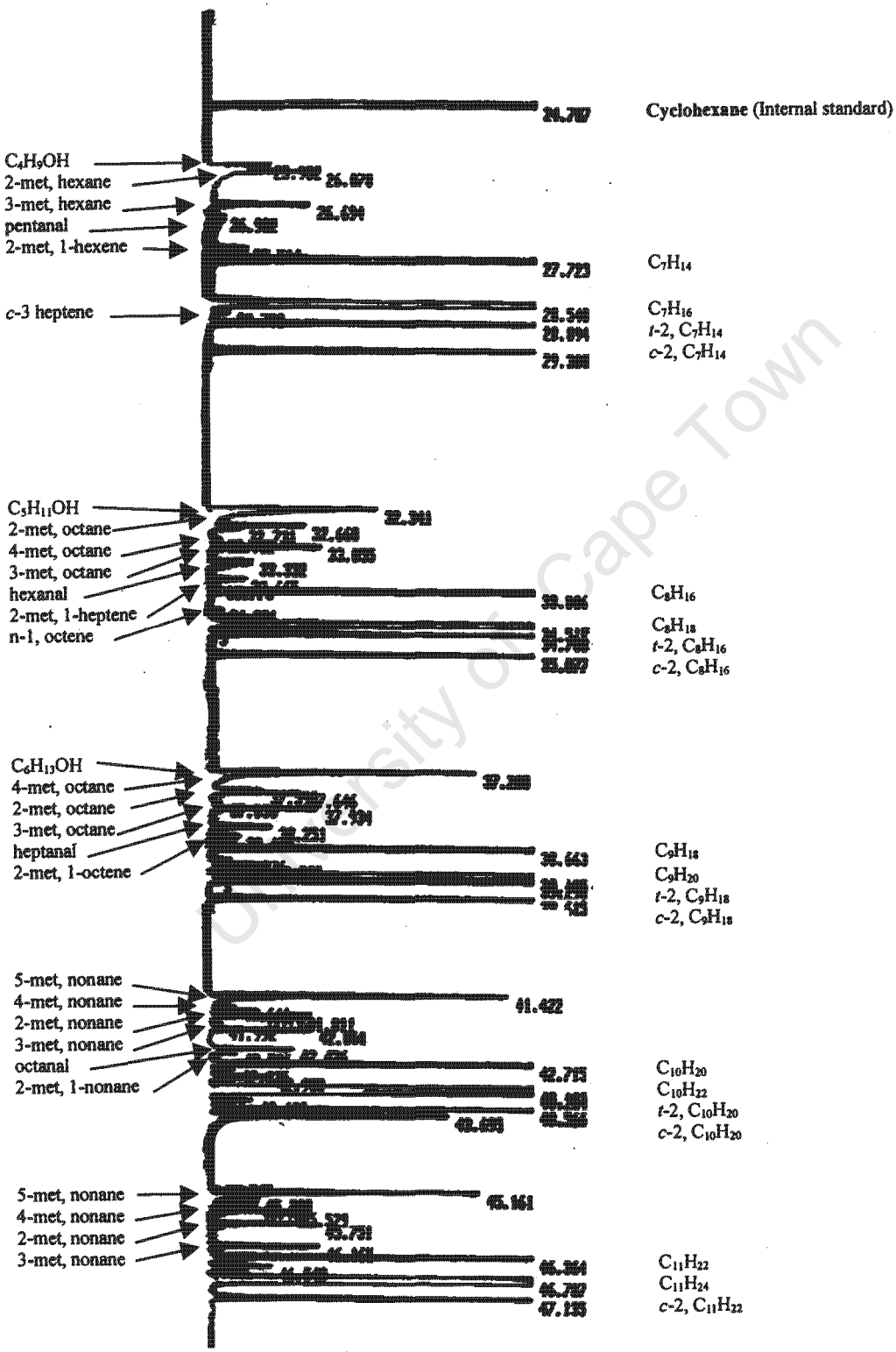

Figure 4.2.1b: FID chromatogram of the FT products

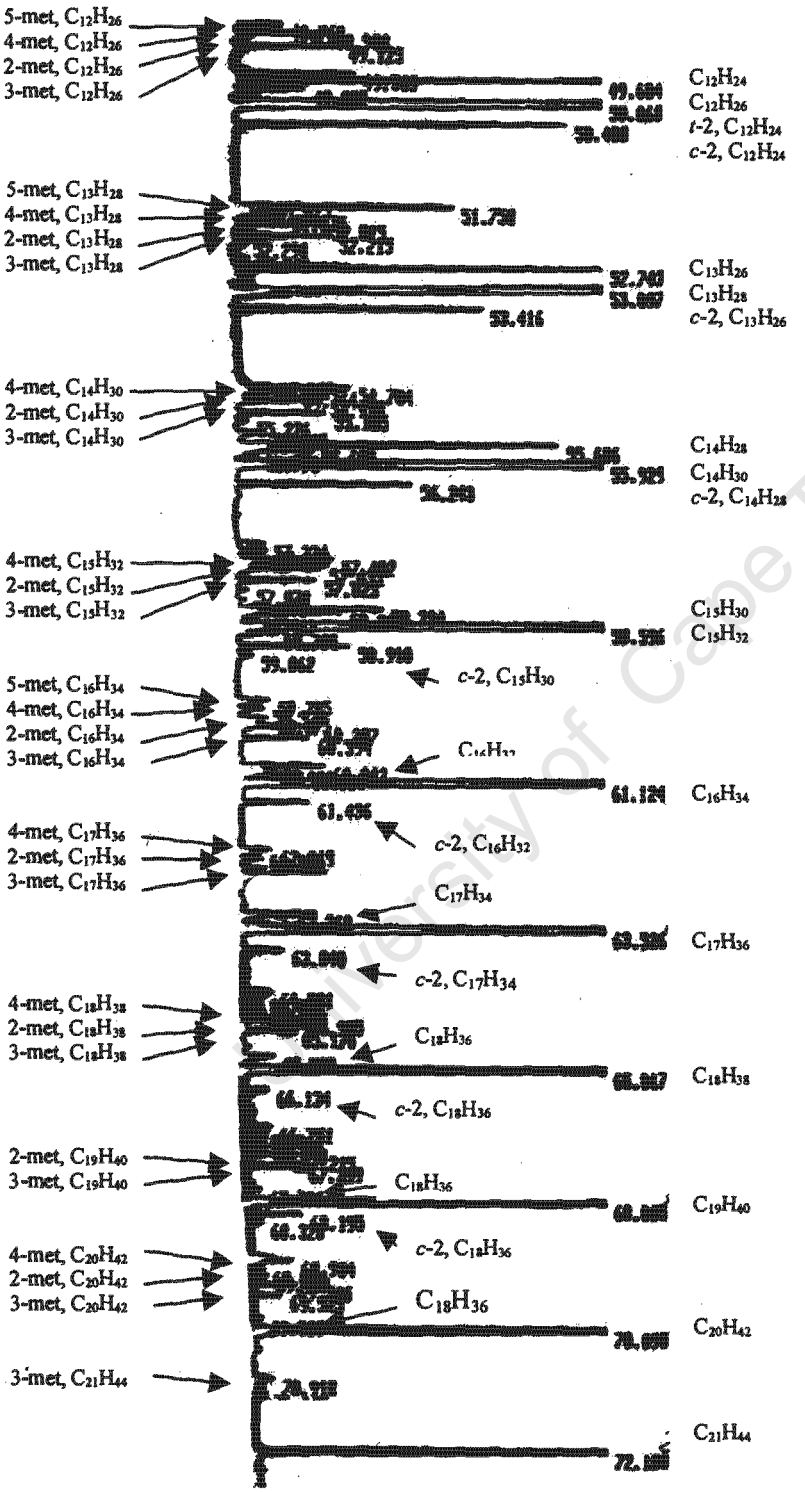

Figure 4.2.1c: FID chromatogram of the FT products